CONTENTS

Section 2. Physiology

1.	GENERAL ASPECTS	-
2.	CELL AND MEMBRANE PHYSIOLOGY	67
3.	FETAL AND NEONATAL PHYSIOLOGY	70
4.	NEUROPHYSIOLOGY	70
	4.1. Sensory physiology	79
	4.2. Motor physiology	85
	4.3. Psychophysiology	88
5.	MUSCLE PHYSIOLOGY	93
6.	CIRCULATION	98
7.	RESPIRATION	107
8.	DIGESTION	111
9.	EXCRETION	111
10.	REPRODUCTION	116
11.	METABOLISM AND ENERGY BALANCE	117
12.	THERMOREGULATION AND SWEATING	121
13.	BODY FLUIDS	123
14.	ALTITUDE, AVIATION AND SPACE PHYSIOLOGY	123
15.	WORK AND SPORT	124

Copyright © 2006, Elsevier B.V., Amsterdam. All rights reserved. No part of this publication may be reproduced, stored in a retrieval system or transmitted, in any form or by any means, electronic, electrostatic, magnetic tape, mechanical, photocopying, recording or otherwise, without the prior written permission of the Publisher, Elsevier B.V., Radarweg 29, 1043 NX Amsterdam, The Netherlands.

No responsibility is assumed by the Publisher for any injury and/or damage to persons or property as a matter of products liability, negligence or otherwise, or from any use or operation of any methods, products, instructions or ideas contained in the material herein. Because of rapid advances in the medical sciences, we recommend that independent verification of diagnosis and drug dosages should be made.

Although all advertising material is expected to conform to ethical (medical) standards, inclusion in this publication does not constitute a guarantee or endorsement of the quality of such product or of the claims made of it by its manufacturer.

SUBSCRIPTION INFORMATION

The Americas:

Rest of World:

Customer Service Department

Elsevier Customer Service Department 6277 Sea Harbor Drive Orlando, FL 32887-4800

USA

US Customers: Toll Free: +1 (877) 839-7126

Fax: +1 (407) 363-1354

Customers Outside US:

Tel: +1 (407) 345-4020 Fax: +1 (407) 363-1354 E-mail: usinfo-f@elsevier.com

Tel.: +31-20-485-3757 7) 839-7126 Fax: +31-20-485-3432 7) 363-1354 E-mail: nlinfo-f@elsevier.com

Elsevier

P.O. Box 211

The Netherlands

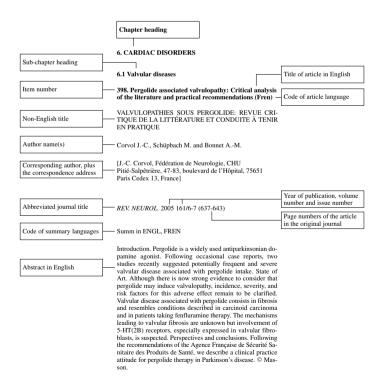
1000 AE Amsterdam

Orders may also be placed through any bookseller or subscription agency. Changes of address and claims for missing issues should be sent directly to the nearest Elsevier office. Claims for issues not received should be made within six months of publication. After this period, claims cannot be honored free of charge.

2006 subscription price for Section 2. Physiology

EURO 4,198/US\$ 4,696 for 3 volumes of 10 issues, 30 issues total, including postage and handling. Full-set subscriptions available at discount.

RECORD FORMAT



2. CELL AND MEMBRANE PHYSIOLOGY

321. Copper in Helix pomatia (Gastropoda) is regulated by one single cell type: Differently responsive metal pools in rhogocytes - Dallinger R., Chabicovsky M., Hödl E. et al. [R. Dallinger, Institut für Zoologie und Limnologie, Universität Innsbruck, Technikerstrasse 25, A-6020 Innsbruck, Austria] - AM. J. PHYSIOL. REGUL. INTEGR. COMP. PHYSIOL. 2005 289/4 58-4 (R1185-R1195) - summ in ENGL

Like all other animal species, terrestrial pulmonate snails require Cu as an essential trace element. On the other hand, elevated amounts of Cu can exert toxic effects on snails. The homeostatic regulation of Cu must therefore be a pivotal goal of terrestrial pulmonates to survive. Upon administration of Cu, snails accumulate the metal nearly equally in most of their organs. Quantitative studies in connection with HPLC and electrospray ionization mass spectrometry reveal that a certain fraction of Cu in snails is bound to a Cu-metallothionein (Cu-MT) isoform that occurs in most organs at constant concentrations, irrespective of whether the animals had been exposed to physiological or elevated amounts of Cu. In situ hybridization demonstrates that at the cellular level, the Cu-binding MT isoform is exclusively expressed in the so-called pore cells (or rhogocytes), which can be found in all major snail organs. The number of pore cells with Cu-MT mRNA reaction products remains unaffected by Cu exposure. Rhogocytes also are major storage sites of Cu in a granular form, the metal quickly entering the snail tissues upon elevated exposure. The number of rhogocytes with granular Cu precipitations strongly increases upon Cu administration via food. Thus, whereas Cu-MT in the rhogocytes represents a stable pool of Cu that apparently serves physiological tasks, the granular Cu precipitations form a second, quickly inducible, and more easily available pool of the metal that serves Cu regulation by responding to superphysiological metal exposure. Copyright © 2005 the American Physiological Society.

322. The granule pathway of programmed cell death - Ashton-Rickardt P.G. [P.G. Ashton-Rickardt, University of Chicago, Department of Pathology, Ben May Institute for Cancer Research, 924 E. 57th Street, Chicago, IL 60637, United States] - *CRIT. REV. IMMUNOL.* 2005 25/3 (161-182) - summ in ENGL

The exocytosis of death-inducing granzymes stored in the granules of cytotoxic lymphocytes allows the immune system to rapidly eliminate intracellular pathogens and transformed cells. The membrane-disrupting protein perform allows the entry of granzymes into a cell, where they induce apoptosis by cleaving target substrates in the cytoplasm and nucleus. Granzymes kill cells in a variety of ways. Recent work has demonstrated that granzymes induce mitochondrial dysfunction through caspase and caspase-independent pathways and destroy DNA and the integrity of the nucleus. Cytotoxic lymphocytes are susceptible to self-inflicted damage. Mice and humans defective in perform and granzymes point to a role for self-inflicted damage in downregulating lymphocyte responses. Given the propensity for the granule pathway to inflict cellular damage, cytotoxic lymphocytes have developed a variety of mechanisms to protect themselves. In this regard, endogenous serine protease inhibitors have been suggested to protect cytotoxic lymphocytes from granzyme B. It would appear that certain viruses and possibly even tumor cells also use the same mechanism to escape destruction from the exocytosis pathway of programmed cell death. © 2005 by Begell House, Inc.

323. Regulation of cell survival by lipid phosphate phosphatases involves the modulation of intracellular phosphatidic acid and sphingosine 1-phosphate pools - Long J., Darroch P., Wan K.F. et al. [S. Pyne, Department of Physiology and Pharmacology, Strathclyde Institute for Biomedical Sciences, University of Strathclyde, 27 Taylor Street, Glasgow G4 0NR, United Kingdom] - *BIOCHEM. J.* 2005 391/1 (25-32) - summ in ENGL

We have shown previously that LPPs (lipid phosphate phosphatases) reduce the stimulation of the p42/p44 MAPK (p42/p44 mitogen-activated protein kinase) pathway by the GPCR (G-protein-coupled receptor) agonists S1P (sphingosine 1-phosphate) and LPA (lysophosphatidic acid) in serum-deprived HEK-293 cells [Alderton, Darroch, Sambi, McKie, Ahmed, N. J. Pyne and S. Pyne (2001) J. Biol. Chem. 276, 13452-13460]. In the present

study, we now show that this can be blocked by pretreating HEK-293 cells with the caspase 3/7 inhibitor, Ac-DEVD-CHO [Nacetyl-Asp-Glu-Val-Asp-CHO (aldehyde)]. Therefore LPP2 and LPP3 appear to regulate the apoptotic status of serum-deprived HEK-293 cells. This was supported further by: (i) caspase 3/7catalysed cleavage of PARP [poly(ADP-ribose) polymerase] was increased in serum-deprived LPP2-overexpressing compared with vector-transfected HEK-293 cells; and (ii) serum-deprived LPP2and LPP3-overexpressing cells exhibited limited intranucleosomal DNA laddering, which was absent in vector-transfected cells. Moreover, LPP2 reduced basal intracellular phosphatidic acid levels, whereas LPP3 decreased intracellular S1P in serum-deprived HEK-293 cells. LPP2 and LPP3 are constitutively co-localized with SK1 (sphingosine kinase 1) in cytoplasmic vesicles in HEK-293 cells. Moreover, LPP2 but not LPP3 prevents SK1 from being recruited to a perinuclear compartment upon induction of PLD1 (phospholipase D1) in CHO (Chinese-hamster ovary) cells. Taken together, these data are consistent with an important role for LPP2 and LPP3 in regulating an intracellular pool of PA and S1P respectively, that may govern the apoptotic status of the cell upon serum deprivation. © 2005 Biochemical Society.

324. Human Rhesus B and Rhesus C glycoproteins: Properties of facilitated ammonium transport in recombinant kidney cells - Zidi-Yahiaoui N., Mouro-Chanteloup I., D'Ambrosio A.-M. et al. - *BIOCHEM. J.* 2005 391/1 (33-40) - summ in ENGL

The mammalian Rh (Rhesus) protein family belongs to the Amt/Mep (ammonia transporter/methylammonium permease)/Rh superfamily of ammonium transporters. Whereas RhCE, RhD and RhAG are erythroid specific, RhBG and RhCG are expressed in key organs associated with ammonium transport and metabolism. We have investigated the ammonium transport function of human RhBG and RhCG by comparing intracellular pH variation in wildtype and transfected HEK-293 (human embryonic kidney) cells and MDCK (Madin-Darby canine kidney) cells in the presence of ammonium (NH₄/NH₃) gradients. Stopped-flow spectrofluorimetry analysis, using BCECF [2',7'-bis-(2- carboxyethyl)-5(6)-carboxyfluorescein] as a pH-sensitive probe, revealed that all cells submitted to inwardly or outwardly directed ammonium gradients exhibited rapid alkalinization or acidification phases respectively, which account for ammonium movements in transfected and native cells. However, as compared with wild-type cells known to have high NH₃ lipid permeability, RhBG- and RhCG-expressing cells exhibited ammonium transport characterized by: (i) a five to six times greater kinetic rate-constant; (ii) a weak temperature-dependence; and (iii) reversible inhibition by mercuric chloride (IC₅₀: 52 μ M). Similarly, when subjected to a methylammonium gradient, RhBGand RhCG-expressing cells exhibited kinetic rate constants greater than those of native cells. However, these constants were five times higher for RhBG as compared with RhCG, suggesting a difference in substrate accessibility. These results, indicating that RhBG and RhCG facilitate rapid and low-energy-dependent bi-directional ammonium movement across the plasma membrane, favour the hypothesis that these Rh glycoproteins, together with their erythroid homologue RhAG [Ripoche, Bertrand, Gane, Birkenmeier, Colin and Cartron (2005) Proc. Natl. Acad. Sci. U.S.A. 101, 17222-17227] constitute a family of NH3 channels in mammalian cells. © 2005 Biochemical Society.

325. AS160, the Akt substrate regulating GLUT4 translocation, has a functional Rab GTPase-activating protein domain - Mîinea C.P., Sano H., Kane S. et al. [G.E. Lienhard, Department of Biochemistry, Dartmouth Medical School, Hanover, NH 03755, United States] - *BIOCHEM. J.* 2005 391/1 (87-93) - summ in ENGL

Recently, we described a 160 kDa protein (designated AS 160, for Akt substrate of 160 kDa) with a predicted Rab GAP (GTPase-activating protein) domain that is phosphorylated on multiple sites by the protein kinase Akt. Phosphorylation of AS160 in adipocytes is required for insulin-stimulated translocation of the glucose transporter GLUT4 to the plasma membrane. The aim of the present study was to determine whether AS160 is in fact a GAP for Rabs, and, if so, what its specificity is. We first identified a group of 16 Rabs in a preparation of intracellular vesicles containing GLUT4 by MS. We then prepared the recombinant GAP domain of AS 160 and examined its activity against many of these Rabs, as well as several

others. The GAP domain was active against Rabs 2 A, 8A, 10 and 14. There was no significant activity against 14 other Rabs. GAP activity was further validated by the finding that the recombinant GAP domain with the predicted catalytic arginine residue replaced by lysine was inactive. Finally, it was found by immunoblotting that Rabs 2A, 8A and 14 are present in GLUT4 vesicles. These results indicate that AS160 is a Rab GAP, and suggest novel Rabs that may participate in GLUT4 translocation. © 2005 Biochemical Society.

326. Mechanisms of hypotonicity-induced calcium signaling and integrin activation by arachidonic acid-derived inflammatory mediators in B cells - Zhu P., Liu X., Labelie E.F. and Freedman B.D. [Dr. B.D. Freedman, University of Pennsylvania, School of Veterinary Medicine, Department of Pathobiology, 3800 Spruce Street, Philadelphia, PA 19104, United States] - *J. IMMUNOL*. 2005 175/8 (4981-4989) - summ in ENGL

We previously characterized the initial steps in the activation of novel (calcium-permeant) nonselective cation channels (NSCCs)and calcium release-activated calcium channels in primary murine B lymphocytes. Phospholipase C products, namely diacylglycerol and D-myo-inositol 1,4,5-trisphosphate, were identified as proximal intracellular agonists of these respective channels following mechanical stimulation of B cells. However, neither the distal steps in NSCC activation nor the contribution of these channels to sustained mechanical signaling were defined in these previous studies. In this study, single cell measurements of intracellular Ca ²⁺ were used to define the mechanisms of NSCC activation and demonstrate a requirement for arachidonic acid liberated from diacylglycerol. Several arachidonic acid-derived derivatives were identified that trigger Ca2+ entry into B cells, including the lipoxygenase product 5-hydroperoxyeicosatetranenoic acid and the cytochrome P450 hydroxylase product 20-hydroxyeicosatetraenoic; however, the cytochrome P450 epoxygenase product 5,6-epoxyeicosatrienoic acid is primarily responsible for hypotonicity-induced responses. In addition to regulating calcium entry, our data suggest that eicosanoid-activated NSCCs have a separate and direct role in regulating the avidity of integrins on B cells for extracellular matrix proteins, including ICAM-1 and VCAM-1. Thus, in addition to defining a novel osmotically activated signal transduction pathway in B cells, our results have broad implications for understanding how inflammatory mediators dynamically and rapidly regulate B cell adhesion and trafficking. Copyright © 2005 by The American Association of Immunologists, Inc.

327. Expression of stromelysin-3 (matrix metalloproteinase-11) in macrophages of murine thymus following thymocyte apoptosis - Odaka C. and Izumiyama S. [C. Odaka, Department of Safety Research on Blood and Biological Products, National Institute of Infectious Diseases, Tokyo, Japan] - CELL. IMMUNOL. 2005 235/1 (21-28) - summ in ENGL

High expression of stromelysin-3 (ST-3), also known as matrix metalloproteinase-11, has been implicated in tumor progression and intense tissue remodeling. Nonetheless, details of the cell type(s)expressing ST-3 are less well defined. Here, we report that ST-3 expression was elevated in mouse thymus following thymocyte apoptosis after administration of anti-CD3 Ab. TUNEL analysis revealed that many thymocytes in the cortical region were induced to apoptotic cell death 14 h after the injection. After an additional 2-6 h, ST-3 expression in the thymus was more apparent. Costaining analysis by anti-ST-3 and F4/80 Abs showed that most F4/80-positive macrophages were also positive for ST-3. Murine peritoneal macrophages were found to constitutively express ST-3, and exposure to apoptotic cells hardly affected ST-3 expression in the macrophages. Taken together, our results indicate that ST-3 is not involved in the execution process of thymocyte apoptosis, and the increased levels of ST-3 in the thymus may be due to the presence of macrophages responsible for clearance of apoptotic cells. © 2005 Elsevier Inc. All rights reserved.

328. Pathways for K+ efflux in isolated surface and crypt colonic cells. Activation by calcium - Del Castillo J.R. and Burguillos L. [J.R. Del Castillo, Laboratorio de Fisiología Gastrointestinal, Centro de Biofísica Y Bioquímica, Institute Venezolano de Investigaciones Cientificas (IVIC), P.O. Box 21827, Caracas 1020-A,

Venezuela] - *J. MEMBR. BIOL.* 2005 205/1 (37-47) - summ in ENGL.

K+-conductive pathways were evaluated in isolated surface and crypt colonic cells, by measuring 86 Rb efflux. In crypt cells, basal K+ efflux (rate constant: 0.24 ± 0.044 min-1, span: $24\pm1.3\%$) was inhibited by 30 mM TEA and 5 mM Ba2+ in an additive way, suggesting the existence of two different conductive pathways. Basal efflux was insensitive to apamin, iberiotoxin, charybdotoxin and clotrimazole. Ionomycin ($\frac{1}{5} \mu M$) stimulated K+ efflux, increasing the rate constant to $0.65 \pm 0.007 \, \mathrm{min^{-1}}$ and the span to $83 \pm 3.2\%$ Ionomycin-induced K+ efflux was inhibited by clotrimazole (IC 50 of 25 \pm 0.4 μ M) and charybdotoxin (IC $_{50}$ of 65 \pm 5.0 nM) and was insensitive to TEA, Ba 2+, apamin and iberiotoxin, suggesting that this conductive pathway is related to the Ca²⁺-activated intermediate-conductance K + channels (IKca). Absence of extracellular Ca 2+ did neither affect basal nor ionomycin-induced K+ efflux. However, intracellular Ca²⁺ depletion totally inhibited the ionomycin-induced K+ efflux, indicating that the activation of these K+ channels mainly depends on intracellular calcium liberation. K+ efflux was stimulated by intracellular Ca²⁺ with an EC $_{50}$ of 1.1 \pm 0.04 μ M. In surface cells, K+ efflux (rate constant: 0.17 \pm 0.027 min⁻¹; span: $25 \pm 3.4\%$) was insensitive to TEA and Ba²⁺. However, ionomycin induced K + efflux with characteristics identical to that observed in crypt cells. In conclusion, both surface and crypt cells present IK_{Ca} channels but only crypt cells have TEA- and Ba²⁺-sensitive conductive pathways, which would determine their participation in colonic K+ secretion. © Springer Science+Business Media, Inc.

329. Leukemia inhibitory factor regulates glucocorticoid receptor expression in the hypothalamic-pituitary-adrenal axis - Kariagina A., Zonis S., Afkhami M. et al. [V. Chesnokova, Dept. of Medicine, Div. of Endocrinology, Cedars-Sinai Medical Center, 8700 Beverly Blvd., Los Angeles, CA 90048, United States] - *AM. J. PHYSIOL. ENDOCRINOL. METAB.* 2005 289/5 52-5 (E857-E863) - summ in ENGL

Leukemia inhibitory factor (LIF) is a pleiotropic cytokine belonging to the gp130 family. LIF is induced peripherally and within the brain during inflammatory or chronic autoimmune diseases and is a potent stimulator of the hypothalamic-pituitary-adrenal (HPA) axis. Here we investigated the role of LIF in mediating glucocorticoid receptor (GR) expression in the HPA axis. LIF treatment (3 μ g/mouse, ip) markedly decreased GR mRNA levels in murine hypothalamus (5-fold, P < 0.01) and pituitary (1.7-fold, P < 0.01) and downregulated GR protein levels. LIF decreased GR expression in murine corticotroph cell line AtT20 within 2 h, and this effect was sustained for 8 h after treatment. LIF-induced GR mRNA reduction was abrogated in AtT20 cells overexpressing dominant-negative mutants of STAT3, indicating that intact JAK-STAT signaling is required to mediate LIF effects on GR expression. Conversely, mice with LIF deficiency exhibited increased GR mRNA levels in the hypothalamus and pituitary (3.5- and 3.5-fold, respectively; P < 0.01 for both) and increased GR protein expression when compared with wild-type littermates. The suppressive effects of dexamethasone on GR were more pronounced in LIF-null animals. These data suggest that LIF maintains the HPA axis activation by decreasing GR expression and raise the possibility that LIF might contribute to the development of central glucocorticoid resistance during inflammation. Copyright © 2005 the American Physiological Society.

330. Identification of novel cAMP responsive element modulator (CREM) isoforms expressed by osteoblasts - Liu F., Huang Y.-F. and Kream B.E. [B.E. Kream, Department of Medicine, University of Connecticut Health Center, 263 Farmington Avenue, Farmington, CT 06030, United States] - *CALCIF. TISSUE INT.* 2005 77/2 (91-95) - summ in ENGL

CREM, the cyclic adenosine monophosphate (cAMP) responsive element modulator, belongs to a multigene family of cAMP-responsive transcription factors. CREM encodes a variety of different isoforms by utilizing four promoters and a complex pattern of alternative messenger ribonucleic acid (mRNA) splicing. We showed previously that parathyroid hormone induces the CREM P2 promoter products known as ICER (inducible cAMP early repressor) in osteoblasts. Herein we report that osteoblasts also express at least 15 CREM transcripts initiated from the P1 promoter, including 7 novel

transcripts that result from alternative splicing. It is of interest that we found that CREM-X contains both $\mathsf{exon}\,\theta\,1$, previously identified only in P3 promoter products, and a new exon termed L, which is located upstream of exon $\theta\,1$. © 2005 Springer Science+Business Media, Inc.

331. Inhibitory effect of thiopental on ultra-rapid delayed rectifier K * current in H9c2 cells - Suzuki H., Momoi N., Ono T. et al. [J. Kimura, Department of Pharmacology, Fukushima Medical University, School of Medicine, Fukushima 960-1295, Japan] - J. PHARMACOL. SCI. 2005 99/2 (177-184) - summ in ENGL

Using the whole-cell voltage clamp technique, we investigated the effects of thiopental on membrane currents in H9c2 cells, a cell line derived from embryonic rat heart. Thiopental blocked a rapidly activating, very slowly-inactivating ultra-rapid type I_{Kur} like outward K⁺ current in a concentration-dependent manner. The half-maximal concentration (IC50) of thiopental was 97 $\mu\mathrm{M}$ with a Hill coefficient of 1.2. The thiopental-sensitive current was also blocked by high concentrations of nifedipine (IC₅₀ = 9.1 μ M) and 100 uM chromanol 293B, a blocker of slowly activating delayed rectifier K+ current (I_{Ks}), but was insensitive to E-4031, an inhibitor of rapidly activating delayed rectifier $K^{\scriptscriptstyle +}$ current (I $_{Kr}$). TEA (tetraethylammonium) at 5 mM and 4-AP (4-aminopiridine) at 1 mM reduced the K+ current to $30.8 \pm 12.2\%$ and $20.5 \pm 6.5\%$ of the control, respectively. Using RT-PCR, we detected mRNAs of Kv2.1, Kv3.4, Kv4.1, and Kv4.3 in H9c2 cells. Among those, Kv2.1 and Kv3.4 have I_{Kur} -type kinetics and are therefore candidates for thiopental-sensitive K^+ channels in H9c2 cells. This is the first report showing that thiopental inhibits I_{Kur}. This effect of thiopental may be involved in its reported prolongation of cardiac action potentials. ©2005 The Japanese Pharmacological Society.

332. Opioid elevation of intracellular free calcium: Possible mechanisms and physiological relevance - Samways D.S.K. and Henderson G. - *CELL. SIGNAL.* 2006 18/2 (151-161) - summ in ENGL

Opioid receptors are seven transmembrane domain G_i/G₀ proteincoupled receptors, the activation of which stimulates a variety of intracellular signalling mechanisms including activation of inwardly rectifying potassium channels, and inhibition of both voltage-operated N-type Ca ²⁺ channels and adenylyl cyclase activity. It is now apparent that like many other G_i/G₀-coupled receptors, opioid receptor activation can significantly elevate intracellular free Ca2+ ([Ca²⁺]_i), although the mechanism underlying this phenomenon is not well understood. In some cases opioid receptor activation alone appears to elevate [Ca²⁺]_i, but in many cases it requires concomitant activation of G_q-coupled receptors, which themselves stimulate Ca²⁺ release from intracellular stores via the inositol phosphate pathway. Given the number of Ca²⁺-sensitive processes known to occur in cells, there are therefore a myriad of situations in which opioid receptor-mediated elevations of [Ca²⁺]_i may be important. Here, we review the literature documenting opioid receptor-mediated elevations of [Ca²⁺]i, discussing both the possible mechanisms underlying this phenomenon and its potential physiological relevance. © 2005 Elsevier Inc. All rights reserved.

333. Nitric oxide stimulates a large-conductance Ca²⁺-activated K+ channel in human skin fibroblasts through protein kinase G pathway - Lim I., Yun J., Kim S. et al. [Dr. I. Lim, Department of Physiology, College of Medicine, Chung-Ang University, Heukseok-Dong, Dongjak-Gu, Seoul, 156-756, South Korea] - *SKIN PHARMACOL. PHYSIOL.* 2005 18/6 (279-287) - summ in ENGL

In order to investigate the large-conductance Ca^{2+} -activated K^+ (BK_{Ca}) channel and determine the effects of nitric oxide (NO) on the channel in human skin fibroblasts, we performed electrophysiological patch clamp recordings on 5th-passage cells of human genital skin cultures. The whole-cell outward K^+ current was increased with depolarization, and proved to be sensitive to NS1619 (a selective BK_{Ca} channel activator) and iberiotoxin (a specific BK_{Ca} channel inhibitor). The single-channel currents showed 226 pS of mean conductance in symmetrical K^+ . Sodium nitroprusside (SNP; an NO donor) significantly increased the K^+ current amplitude in the whole-cell mode, and open probability of the channel (NPo) in the cell-attached mode, but not in the inside-out mode. S-nitroso-N-acetylpenicillamine (an NO donor) and 8-Br-cGMP

(a membrane-permeant cGMP analogue) also increased the BK_{Ca} channel activity. The stimulatory effect of SNP on BK_{Ca} channels was inhibited by pretreatment with 1H-[1,2,4]- oxadiazolo[4,3-a]-quinoxalin-1-one (a soluble guanylyl cyclase inhibitor), or KT5823 [a specific protein kinase G (PKG) inhibitor]. Cytoplasmic PKG also increased the channel activity in inside-out patches. In conclusion, the present data indicate that BK_{Ca} channels constitute a significant fraction of K^+ current in human skin fibroblasts, and that NO increases NPo of BK_{Ca} channels, which are mediated via the cGMP/PKG pathway, without direct effects on the channel. Copyright $\ensuremath{\textcircled{@}}$ 2005 S. Karger AG.

334. The role of canonical transient receptor potential 7 in B-cell receptor-activated channels - Lievremont J.-P., Numaga T., Vazquez G. et al. [J.W. Putney Jr., NIEHS, National Institutes of Health, P.O. Box 12233, Research Triangle Park, NC 27709, United States] - *J. BIOL. CHEM.* 2005 280/42 (35346-35351) - summ in ENICI

Phospholipase C signaling stimulates Ca2+ entry across the Ca2+ store plasma membrane through multiple mechanisms. depletion stimulates store-operated Ca²⁺-selective channels, or alternatively, other phospholipase C-dependent events activate Ca²⁺-permeable non-selective cation channels. Transient receptor potential 7 (TRPC7) is a non-selective cation channel that can be activated by both mechanisms when ectopically expressed, but the regulation of native TRPC7 channels is not known. We knocked out TRPC7 in DT40 B-cells, which expresses both forms of Ca 24 entry. No difference in the store-operated current I crac was detected between TRPC7-/- and wild-type cells. Wild-type cells demonstrated non-store-operated cation entry and currents in response to activation of the B-cell receptor or protease-activated receptor 2, intracellular dialysis with GTP γ S, or application of the synthetic diacylglycerol oleyl-acetyl-glycerol. These responses were absent in TRPC7 -/- cells but could be restored by transfection with human TRPC7. In conclusion, in B-lymphocytes, TRPC7 appeared to participate in the formation of ion channels that could be activated by phospholipase C-linked receptors. This represents the first demonstration of a physiological function for endogenous TRPC7

335. The impact of electrical charge on the viability and physiology of dendritic cells - Hilpert F., Heiser A., Wieckhorst W. et al. [Dr. F. Hilpert, Klinik für Gynäkologie und Geburtshifte, Universitätsklinikum Schleswig-Holstein Campus Kiel, Michaelisstr. 16, D-24105 Kiel, Germany] - SCAND. J. IMMUNOL. 2005 62/4 (399-406) - summ in ENGL

The use of electrical charge for electroporation or electrofusion is widely applied to customize dendritic cells (DC) and their immunological properties as anticancer vaccines. The aim of this study was to evaluate the influence of various electrical field strengths on the recovery, viability and physiology of DC. Immature DC were transferred into low-conductive medium and electrically charged within a range of 0-1500 V/cm. Viability was assessed by Trypan Blue dye exclusion or staining with impermeant nucleic acid stains and fluorescence-activated cell sorter analysis. Additionally, apoptosis was determined by flow cytometry after staining with Annexin-V, endocytosis by uptake of fluorescein isothiocyanate-dextran and metabolic activity by a standardized fluorescent live/ dead assay. There was a strong correlation between the electrical field strength and the viability and physiology of DC. Field strengths ≥ 1000 V/cm significantly impaired viability, metabolism and endocytotic activity. Dual fluorescence with 7-7-amino-actinomycin D and Annexin-V demonstrated that loss of viability was predominantly due to necrosis rather than apoptosis. Field strengths ≤500 V/cm allowed to maintain good cell viability and recovery of DC and did not cause alterations of metabolism and endocytosis. Therefore, the frequently used amplification of field strengths to improve the efficacy of electroporation and electrofusion requires critical reevaluation. © 2005 Blackwell Publishing Ltd.

See also: 338, 339, 346, 358, 359, 360, 361, 362, 364, 365, 366, 367, 369, 380, 399, 400, 402, 403, 404, 405, 406, 408, 413, 422, 424, 425, 426, 432, 433, 437, 456, 463, 464, 465, 466, 468, 469, 470, 472, 474, 475, 478, 481, 484, 485, 486, 487, 488, 494, 495, 496, 497, 502, 503, 504, 510, 512, 516, 517, 518, 526, 527, 528,

532, 535, 536, 537, 538, 539, 540, 541, 542, 543, 544, 545, 546, 547, 548, 549, 550, 551, 555, 556, 558, 562, 563, 566, 567, 570, 572, 573, 586, 618, 627, 629.

3. FETAL AND NEONATAL PHYSIOLOGY

See: 338, 479, 504, 533, 538.

4. NEUROPHYSIOLOGY

336. Who's on first? What's on second? The time course of learning in corticostriatal systems - Laubach M. [M. Laubach, John B. Pierce Laboratory, Department of Neurobiology, Yale University School of Medicine, 290 Congress Avenue, New Haven, CT 06519, United States] - TRENDS NEUROSCI. 2005 28/10 (509-511) - summ in ENGL

The prefrontal cortex and basal ganglia are known to be crucial for learning arbitrary sensorimotor associations (e.g. knowing to stop at red traffic lights). However, little is known about the timing of learning-related activity in these brain systems. Conventional wisdom suggests that the prefrontal cortex should drive learning-related changes in the basal ganglia. However, it is possible that the basal ganglia are instead responsible for the development of learning-related activity in prefrontal cortex. Indeed, recent work using methods for recording in the prefrontal cortex and basal ganglia simultaneously suggests that learning-related activity emerges first in the basal ganglia. Here, these studies are reviewed and integrated with the known anatomy of corticostriatal connections. Testable hypotheses regarding corticostriatal interactions during learning are proposed. © 2005 Elsevier Ltd. All rights reserved.

337. Inhibiting change: Effects of memory on auditory selective attention - Melara R.D., Chen S. and Wang H. [R.D. Melara, Department of Psychological Sciences, Purdue University, 703 Third Street, West Lafayette, IN 47907, United States] - *COGN. BRAIN RES.* 2005 25/2 (431-442) - summ in ENGL

Two experiments investigated the behavioral and electrophysiological effects on human auditory selection of the psychophysical discriminability of a distractor channel in memory. Participants performed a set of baseline (single distractor) and filtering (multiple distractors) tasks, classifying the pitch of targets, while ignoring pitch variation in temporally distinct distractors, which differed from targets in timbre (Experiment 1) or loudness (Experiment 2). Increased distractor change progressively disrupted target accuracy and reaction time, and fostered confusion in distinguishing target from distractor channels. Physiologically, relative discriminability only affected distractor waveforms, whether or not distractor values physically differed across tasks, enhancing the N1 response while reducing an inhibitory slow-wave component. The results suggest that inhibition fails as distractors activate a wider range of the taskrelevant continuum in working memory. © 2005 Elsevier B.V. All rights reserved.

338. Constitutive neuronal expression of CCR2 chemokine receptor and its colocalization with neurotransmitters in normal rat brain: Functional effect of MCP-1/CCL2 on calcium mobilization in primary cultured neurons - Banisadr G., Gosselin R.-D., Mechighel P. et al. [S.M. Parsadaniantz, INSERM U732, UPMC, Hôpital Saint-Antoine, 184 rue du Faubourg Saint-Antoine, 75571 Paris Cedex 12, France] - *J. COMP. NEUROL.* 2005 492/2 (178-192) - summ in ENGL

Chemokines and their receptors are well described in the immune system, where they promote cell migration and activation. In the central nervous system, chemokine has been implicated in neuroinflammatory processes. However, an increasing number of evidence suggests that they have regulatory functions in the normal nervous system, where they could participate in cell communication. In this work, using a semiquantitative immunohistochemistry approach, we provide the first neuroanatomical mapping of constitutive neuronal CCR2 localization. Neuronal expression of CCR2 was observed in the anterior olfactory nucleus, cerebral cortex, hippocampal formation, caudate putamen, globus pallidus, supraoptic

and paraventricular hypothalamic nuclei, amygdala, substantia nigra, ventral tegmental area, and in the brainstem and cerebellum. These data are largely in accordance with results obtained using quantitative autoradiography with [125 I]MCP-1/CCL2 and RT-PCR CCR2 mRNA analysis. Furthermore, using dual fluorescent immunohistochemistry we studied the chemical phenotype of labeled neurons and demonstrated the coexistence of CCR2 with classical neurotransmitters. Indeed, localization of CCR2 immunostaining is observed in dopaminergic neurons in the substantia nigra pars compacta and in the ventral tegmental area as well as in cholinergic neurons in the substantia innominata and caudate putamen. Finally, we show that the preferential CCR2 ligand, MCP-1/CCL2, elicits Ca2+ transients in primary cultured neurons from various rat brain regions including the cortex, hippocampus, hypothalamus, and mesencephalon. In conclusion, the constitutive neuronal CCR2 expression in selective brain structures suggests that this receptor could be involved in neuronal communication and possibly associated with cholinergic and dopaminergic neurotransmission and related disorders. © 2005 Wiley-Liss, Inc.

339. The electrophysiological effects of neurotensin on spontaneously active neurons in the nucleus accumbens: An in vivo study - Stowe Z.N., Landry J.C., Tang Z. et al. [Dr. C.B. Nemeroff, Department of Psychiatry and Behavioral Sciences, Emory University School of Medicine, 101 Woodruff Circle, Atlanta, GA 30322, United States] - *SYNAPSE* 2005 58/3 (165-172) - summ in ENGL

Considerable evidence obtained from neuroanatomical and neurochemical studies suggests an interaction between the endogenous tridecapeptide neurotensin (NT) and central nervous system dopamine (DA) neurons. Centrally administered NT blocks many of the actions of synaptic DA in limbic brain areas; the specific mechanism and receptors involved remain under investigation. The electrophysiological effects of NT were studied using extracellular recording techniques and iontophoretic application in 243 spontaneously active neurons in the nucleus accumbens (NAc), with a positive/negative waveform. NT was directly applied to 208 neurons in a pulsatile fashion by iontophoresis (21 \pm 1 nA). NT had no effect on the firing rate of 120 neurons ((0.31 \pm 0.72)%), decreased the firing rate in 51 neurons ((-27.87 \pm 1.52)%), and increased the firing rates of 37 neurons ((33.38 \pm 2.6)%). One hundred ninety nine (81.9%) of the neurons studied were sensitive to iontophoretically applied DA (>15% decrease in firing rate). The effects of continuous NT application on DA-induced inhibitions were studied in 169 neurons. NT attenuated neuronal responses to directly applied DA by $(49.95 \pm 4.52)\%$, with antagonism in the "core" subregion (n = 96) of $(33.41 \pm 7.75)\%$ when compared with antagonism in the "shell" subregion (n = 71) of $(61.39 \pm 5.2)\%$. The effects of NT on DA were consistent and independent of the effects of NT alone. These data provide further evidence that NT functions as a true neuromodulator in the NAc, exerting minimal direct effects, but blocking the actions of DA. © 2005 Wiley-Liss, Inc.

340. Connexon connexions in the thalamocortical system - Cruikshank S.J., Landisman C.E., Mancilla J.G. and Connors B.W. [B.W. Connors, Department of Neuroscience, Division of Biology and Medicine, Brown University, Providence, RI 02912, United States] - *PROG. BRAIN RES.* 2005 149/- (41-57) - summ in ENGL

Electrical synapses are composed of gap junction channels that interconnect neurons. They occur throughout the mammalian brain, although this has been appreciated only recently. Gap junction channels, which are made of proteins called connexins, allow ionic current and small organic molecules to pass directly between cells, usually with symmetrical ease. Here we review evidence that electrical synapses are a major feature of the inhibitory circuitry in the thalamocortical system. In the neocortex, pairs of neighboring inhibitory interneurons are often electrically coupled, and these electrical connections are remarkably specific. To date, there is evidence that five distinct subtypes of inhibitory interneurons in the cortex make electrical interconnections selectively with interneurons of the same subtype. Excitatory neurons (i.e., pyramidal and spiny stellate cells) of the mature cortex do not appear to make electrical synapses. Within the thalamus, electrical coupling is observed in the reticular nucleus, which is composed entirely of GABAergic neurons. Some pairs of inhibitory neurons in the cortex

and reticular thalamus have mixed synaptic connections: chemical (GABAergic) inhibitory synapses operating in parallel with electrical synapses. Inhibitory neurons of the thalamus and cortex express the gap junction protein connexin36 (C×36), and knocking out its gene abolishes nearly all of their electrical synapses. The electrical synapses of the thalamocortical system are strong enough to mediate robust interactions between inhibitory neurons. When pairs or groups of electrically coupled cells are excited by synaptic input, receptor agonists, or injected current, they typically display strong synchrony of both subthreshold voltage fluctuations and spikes. For example, activating metabotropic glutamate receptors on coupled pairs of cortical interneurons or on thalamic reticular neurons can induce rhythmic action potentials that are synchronized with millisecond precision. Electrical synapses offer a uniquely fast, bidirectional mechanism for coordinating local neural activity. Their widespread distribution in the thalamocortical system suggests that they serve myriad functions. We are far from a complete understanding of those functions, but recent experiments suggest that electrical synapses help to coordinate the temporal and spatial features of various forms of neural activity. Copyright © 2005 Elsevier BV. All rights reserved.

341. Spike timing and synaptic dynamics at the awake thalamocortical synapse - Swadlow H.A., Bezdudnaya T. and Gusev A.G. [H.A. Swadlow, Department of Psychology, University of Connecticut, Storrs, CT 06269, United States] - *PROG. BRAIN RES.* 2005 149/- (91-105) - summ in ENGL

Thalamocortical (TC) neurons form only a small percentage of the synapses onto neurons of cortical layer 4, but the response properties of these cortical neurons are arguably dominated by thalamic input. This discrepancy is explained, in part, by studies showing that TC synapses are of high efficacy. However, TC synapses display activity-dependent depression. Because of this, in vitro measures of synaptic efficacy will not reflect the situation in vivo, where different neuronal populations have widely varying levels of "spontaneous' activity. Indeed, TC neurons of awake subjects generate high rates of spontaneous activity that would be expected, in a depressing synapse, to result in a chronic state of synaptic depression. Here, we review recent work in the somatosensory thalamocortical system of awake rabbits in which the relationship between TC spike timing and TC synaptic efficacy was examined during both thalamic "relay mode" (alert state) and "burst mode" (drowsy state). Two largely independent methodological approaches were used. First, we employed cross-correlation methods to examine the synaptic impact of single TC "barreloid" neurons on a single neuronal subtype in the topographically aligned layer 4 "barrel" - putative fast-spike inhibitory interneurons. We found that the initial spike of a TC burst, as well as isolated TC spikes with long preceding interspike intervals (ISIs) elicited postsynaptic action potentials far more effectively than did TC impulses with short ISIs. Our second approach took a broader view of the postsynaptic impact of TC impulses. In these experiments we examined spike-triggered extracellular field potentials and synaptic currents (using current source-density analysis) generated through the depths of a cortical barrel column by the impulses of single topographically aligned TC neurons. We found that (a) closely neighboring TC neurons may elicit very different patterns of monosynaptic activation within layers 4 and 6 of the aligned column, (b) synaptic currents elicited by TC impulses with long preceding ISIs were greatly enhanced in both of these layers, and (c) the degree of this enhancement differed reliably among neighboring TC neurons but, for a given neuron, was very similar in layers 4 and 6. Thus, results generated by both methodological approaches are consistent with the presence of a chronic depression at the awake TC synapse that is relieved by long ISIs. Since long ISIs necessarily precede TC "bursts", our results are consistent with the notion that these events powerfully activate cortical circuits. Copyright © 2005 Elsevier BV. All rights reserved.

342. Thalamic relays and cortical functioning - Sherman S.M. [S.M. Sherman, Department of Neurobiology, Pharmacology and Physiology, University of Chicago, Chicago, IL 60637, United States] - *PROG. BRAIN RES.* 2005 149/- (107-126) - summ in ENGL

Studies on the visual thalamic relays, the lateral geniculate

nucleus and pulvinar, provide three key properties that have dramatically changed the view that the thalamus serves as a simple relay to get information from subcortical sites to cortex. First, the retinal input, although a small minority (7%) in terms of numbers of synapses onto geniculate relay cells, dominates receptive field properties of these relay cells and strongly drives them; 93% of input thus is nonretinal and modulates the relay in dynamic and important ways related to behavioral state, including attention. We call the retinal input the driver input and the nonretinal, modulator input, and their unique morphological and functional differences allow us to recognize driver and modulator input to many other thalamic relays. Second, much of the modulation is related to control of a voltagegated, low threshold Ca2+ conductance that determines response properties of relay cells - burst or tonic - and this, among other things, affects the salience of information relayed. Third, the lateral geniculate nucleus and pulvinar (a massive but generally mysterious and ignored thalamic relay), are examples of two different types of relay: the LGN is a first order relay, transmitting information from a subcortical driver source (retina), while the pulvinar is mostly a higher order relay, transmitting information from a driver source emanating from layer 5 of one cortical area to another area. Higher order relays seem especially important to general corticocortical communication, and this view challenges the conventional dogma that such communication is based on direct corticocortical connections. In this sense, any new information reaching a cortical area, whether from a subcortical source or another cortical area, benefits from a thalamic relay. Other examples of first and higher order relays also exist, and generally higher order relays represent the majority of thalamus. A final property of interest emphasized in chapter 17 by Guillery (2005) is that most or all driver inputs to thalamus, whether from a subcortical source or from layer 5 of cortex, are axons that branch, with the extrathalamic branch innervating a motor or premotor region in the brainstem, or in some cases, spinal cord. This suggests that actual information relayed by thalamus to cortex is actually a copy of motor instructions (Guillery, 2005). Overall, these features of thalamic relays indicate that the thalamus not only provides a behaviorally relevant, dynamic control over the nature of information relayed, it also plays a key role in basic corticocortical communication. Copyright © 2005 Elsevier BV. All rights reserved.

343. Identifying brain regions for integrative sensorimotor processing with ankle movements - Ciccarelli O., Toosy A.T., Marsden J.F. et al. [O. Ciccarelli, Department of Headache, Brain Injury and Rehabilitation, Institute of Neurology, University College London, Queen Square, London, WC1N 3BG, United Kingdom] - *EXP. BRAIN RES.* 2005 166/1 (31-42) - summ in ENGL

The objective of this study was to define cortical and subcortical structures activated during both active and passive movements of the ankle, which have a fundamental role in the physiology of locomotion, to improve our understanding of brain sensorimotor integration. Sixteen healthy subjects, all right-foot dominant, performed a dorsi-plantar flexion task of the foot using a custommade wooden manipulandum, which enabled measurements of the movement amplitude. All subjects underwent a training session, which included surface electromyography, and were able to relax completely during passive movements. Patterns of activation during active and passive movements and differences between functional MRI (fMRI) responses for the two types of movement were assessed. Regions of common activation during the active and passive movements were identified by conjunction analysis. We found that passive movements activated cortical regions that were usually similar in location to those activated by active movements, although the extent of the activations was more limited with passive movements. Active movements of both feet generated greater activation than passive movements in some regions (such as the ipsilateral primary motor cortex) identified in previous studies as being important for motor planning. Common activations during active and passive movements were found not only in the contralateral primary motor and sensory cortices, but also in the premotor cortical regions (such as the bilateral rolandic operculum and contralateral supplementary motor area), and in the subcortical regions (such as the ipsilateral cerebellum and contralateral putamen), suggesting that these regions participate in sensorimotor integration for ankle movements. In future, similar fMRI studies using passive

movements have potential to elucidate abnormalities of sensorimotor integration in central nervous system diseases that affect motor function. © Springer-Verlag 2005.

344. Evidence from opsin genes rejects nocturnality in ancestral primates - Tan Y., Yoder A.D., Yamashita N. and Li W.-H. [W.-H. Li, Department of Ecology and Evolution, University of Chicago, 1101 East 57th Street, Chicago, IL 60637, United States] - *PROC. NATL. ACAD. SCI. U. S. A.* 2005 102/41 (14712-14716) - summ in ENGL

It is firmly believed that ancestral primates were nocturnal, with nocturnality having been maintained in most prosimian lineages. Under this traditional view, the opsin genes in all nocturnal prosimians should have undergone similar degrees of functional relaxation and accumulated similar extents of deleterious mutations. This expectation is rejected by the short-wavelength (S) opsin gene sequences from 14 representative prosimians. We found severe defects of the S opsin gene only in lorisiforms, but no defect in five nocturnal and two diurnal lemur species and only minor defects in two tarsiers and two nocturnal lemurs. Further, the nonsynonymous-to-synonymous rate ratio of the S opsin gene is highest in the lorisiforms and varies among the other prosimian branches, indicating different time periods of functional relaxation among lineages. These observations suggest that the ancestral primates were diurnal or cathemeral and that nocturnality has evolved several times in the prosimians, first in the lorisiforms but much later in other lineages. This view is further supported by the distribution pattern of the middle-wavelength (M) and long-wavelength (L) opsin genes among prosimians. © 2005 by The National Academy of Sciences of the

345. Pattern-dependent, simultaneous plasticity differentially transforms the input-output relationship of a feedforward circuit - Smith S.L. and Otis T.S. [S.L. Smith, Department of Neurobiology, School of Medicine, University of California, Los Angeles, CA 90095, United States] - *PROC. NATL. ACAD. SCI. U. S. A.* 2005 102/41 (14901-14906) - summ in ENGL

Memories are believed to be encoded by changes in the synaptic connections between neurons. Although many forms of synaptic plasticity have been identified, it remains unknown how such changes affect local circuits. Feedforward inhibitory networks are a common type of local circuitry and occur when principal neurons and their afferent inhibitory interneurons receive the same input. Using slices of cerebellar cortex, we explored how synaptic plasticity at multiple sites within a feedforward inhibitory network consisting of parallel fibers, interneurons, and Purkinje neurons alters the output of this circuit. We found that stimuli resembling baseline activity potentiated feedforward excitatory and simultaneously depressed feedforward inhibitory pathways. In contrast, stimuli resembling sensory-evoked patterns of firing potentiated both types of feedforward connections. These distinct forms of ensemble plasticity change the way Purkinje neurons subsequently respond to inputs. Such concerted changes in the circuitry of cerebellar cortex may contribute to certain forms of sensorimotor learning. © 2005 by The National Academy of Sciences of the USA.

346. Sex differences in estrogenic regulation of neuronal activity in neonatal cultures of ventromedial nucleus of the hypothalamus - Zhou J., Pfaff D.W. and Chen G. [G. Chen, Department of Biology, Pennsylvania State University, University Park, PA 16802, United States] - *PROC. NATL. ACAD. SCI. U. S. A.* 2005 102/41 (14907-14912) - summ in ENGL

Estrogenic effects have been implicated in sexual differentiation of brain and behavior, in part by affecting neuronal activity in the ventromedial nucleus of the hypothalamus (VMN). We report here a remarkable sex difference in estrogenic regulation of neuronal activity in male vs. female neural networks. Spontaneous synaptic currents originating from a population of neurons were recorded in primary VMN cultures using the whole-cell patch-clamp technique. Treatment with 17β -estradiol (E2, 10 nM) for 24 h induced opposite effects in the two sexes: the frequency of spontaneous synaptic events decreased significantly in neurons derived from males but increased in those from females. Interestingly, the 24-hour E2 effect was partially reversed by an acute application (5 min) of a second dose of E2 (10 nM), suggesting an interaction between extended

(24-hr) and acute (5-min) effects of E2 in VMN neurons. To understand the underlying mechanism of this sexually dimorphic action of E2, we analyzed the E2 effect on GABAergic neurotransmission by recording miniature inhibitory postsynaptic currents. After 24-hour E2 treatment, both the amplitude and frequency of miniature inhibitory postsynaptic currents increased in neurons derived from males but decreased in those from females. These results suggest that E2-induced changes in GABAergic inhibition could at least partially explain E2 effects on neuronal activity. We conclude that E2 may have sexually dimorphic effects on the synaptic output of VMN neurons by modulating GABAergic neurotransmission. © 2005 by The National Academy of Sciences of the USA.

347. Procedure for minimizing stress for fMRI studies in conscious rats - King J.A., Garelick T.S., Brevard M.E. et al. [J.A. King, Center for Comparative Neuroimaging, Department of Psychiatry, University of Massachusetts Medical Center, Worcester, MA 01655, United States] - *J. NEUROSCI. METHODS* 2005 148/2 (154-160) - summ in ENGL

Functional magnetic resonance imaging (fMRI) in conscious animals is evolving as a critical tool for neuroscientists. The present study explored the effectiveness of an acclimation procedure in minimizing the stress experienced by the animal as assessed by alterations in physiological parameters including heart rate, respiratory rate, and serum corticosterone levels. Results confirm that as the stress of the protocol is minimized, there is a significant decrease in head movements and enhancement in data quality. The feasibility of improving the quality of fMRI data acquired in alert rats by utilizing a relatively simple technique is presented. © 2005 Elsevier B.V. All rights reserved.

348. Building excitatory and inhibitory synapses: Balancing neuroligin partnerships - Levinson J.N. and El-Husseini A. [A. El-Husseini, Department of Psychiatry, Brain Research Centre, University of British Columbia, Vancouver, BC V6T 1Z3, Canada] - NEURON 2005 48/2 (171-174) - summ in ENGL

Processing of neural information is thought to occur by integration of excitatory and inhibitory synaptic inputs. As such, precise control mechanisms must exist to maintain an appropriate balance between each synapse type. Recent findings indicate that neuroligins and their synaptic binding partners modulate the development of both excitatory and inhibitory synapses. Here we highlight these finings and discuss a mechanism potentially involved in controlling the balance between excitation and inhibition. Copyright ©2005 by Elsevier Inc.

349. Integration of touch and sound in auditory cortex - Kayser C., Petkov C.I., Augath M. and Logothetis N.K. [C. Kayser, Max Planck Institute for Biological Cybernetics, Spemannstrasse 38, 72076 Tübingen, Germany] - *NEURON* 2005 48/2 (373-384) - summ in ENGL

To form a coherent percept of the environment, our brain combines information from different senses. Such multisensory integration occurs in higher association cortices; but supposedly, it also occurs in early sensory areas. Confirming the latter hypothesis, we unequivocally demonstrate supra-additive integration of touch and sound stimulation at the second stage of the auditory cortex. Using high-resolution fMRI of the macaque monkey, we quantified the integration of auditory broad-band noise and tactile stimulation of hand and foot in anaesthetized animals. Integration was found posterior to and along the lateral side of the primary auditory cortex in the caudal auditory belt. Integration was stronger for temporally coincident stimuli and obeyed the principle of inverse effectiveness: greater enhancement for less effective stimuli. These findings demonstrates that multisensory integration occurs early and close to primary sensory areas and - because it occurs in anaesthetized animals - suggests that this integration is mediated by preattentive bottom-up mechanisms. Copyright ©2005 by Elsevier Inc.

350. Inhibition of acetylcholine-induced activation of extracellular regulated protein kinase prevents the encoding of an inhibitory avoidance response in the rat - Giovannini M.G., Pazzagli M., Malmberg-Aiello P. et al. [M.G. Giovannini, Dipartimento di Farmacologia, Università di Firenze, Viale Pieraccini 6, 50139

Firenze, Italy] - NEUROSCIENCE 2005 136/1 (15-32) - summ in ENGL

It has been demonstrated that the forebrain cholinergic system and the extracellular regulated kinase signal transduction pathway are involved in the mechanisms of learning, encoding, and storage of information. We investigated the involvement of the cholinergic and glutamatergic systems projecting to the medial prefrontal cortex and ventral hippocampus and of the extracellular regulated kinase signal transduction pathway in the acquisition and recall of the step-down inhibitory avoidance response in the rat, a relatively simple behavioral test acquired in a one-trial session. To this aim we studied by microdialysis the release of acetylcholine and glutamate, and by immunohistochemistry the activation of extracellular regulated kinase during acquisition, encoding and recall of the behavior. Cholinergic, but not glutamatergic, neurons projecting to the medial prefrontal cortex and ventral hippocampus were activated during acquisition of the task, as shown by increase in cortical and hippocampal acetylcholine release. Released acetylcholine in turn activated extracellular regulated kinase in neurons located in the target structures, since the muscarinic receptor antagonist scopolamine blocked extracellular regulated kinase activation. Both increased acetylcholine release and extracellular regulated kinase activation were necessary for memory formation, as administration of scopolamine and of extracellular regulated kinase inhibitors was followed by blockade of extracellular regulated kinase activation and amnesia. Our data indicate that a critical function of the learning-associated increase in acetylcholine release is to promote the activation of the extracellular regulated kinase signal transduction pathway and help understanding the role of these systems in the encoding of an inhibitory avoidance memory. © 2005 IBRO. Published by Elsevier Ltd. All rights reserved.

351. Visual and haptic representations of scenes are updated with observer movement - Pasqualotto A., Finucane C.M. and Newell F.N. [F.N. Newell, Department of Psychology, Institute of Neuroscience, University of Dublin, Dublin 2, Ireland] - *EXP. BRAIN RES.* 2005 166/3-4 (481-488) - summ in ENGL

Scene recognition has been found to be sensitive to the orientation of the scene with respect to the stationary observer. Recent studies have shown, however, that observer movement can compensate for changes in visual scene orientation, through a process of spatial updating. Here we investigated whether spatial updating in scene recognition is affected by the encoding or learning modality by examining whether observer movement can also compensate for orientation changes in haptic scene recognition. In experiment 1, we replicated previously reported effects of observer movement on visual scene recognition. In experiment 2, we used the same apparatus as in experiment 1 but here participants were required to learn and recognize the scenes using touch alone. We found a cost in recognition performance with changes in scene orientation relative to the stationary observer. However, when participants could move around the scene to recognize the new orientation, then this cost in recognition performance disappeared. Thus, we found that spatial updating applies to recognition in both the visual and haptic modalities, both of which intrinsically encode the spatial properties of a scene. © Springer-Verlag 2005.

352. Visual bias of unseen hand position with a mirror: spatial and temporal factors - Holmes N.P. and Spence C. [N.P. Holmes, Department of Experimental Psychology, Oxford University, Oxford, OX1 3UD, United Kingdom] - *EXP. BRAIN RES.* 2005 166/3-4 (489-497) - summ in ENGL

Two experiments examined the integration of visual and proprioceptive information concerning the location of an unseen hand, using a mirror positioned along the midsagittal plane. In experiment 1, participants tapped the fingers of both hands in synchrony, while viewing the mirror-reflection of their left hand. After 6 s, participants made reaching movements to a target with their unseen right hand behind the mirror. Reaches were accurate when visually and proprioceptively specified hand positions were congruent prior to the reach, but significantly biased by vision when the visual location conflicted with the real location. This effect was independent of the target location and depended strongly upon the relative position of the mirror-reflected hand. In experiment 2, participants made reaching movements following 4, 8, or 12 s active visuomotor or

passive visual exposure to the mirror, or following passive exposure without the mirror. Reaching was biased more by the visual location following active visuomotor compared to passive visual exposure, and this bias increased with the duration of visual exposure. These results suggest that the felt position of the hand depends upon an integrated, weighted sum of visual and proprioceptive information. Visual information is weighted more strongly under active visuomotor than passive visual exposure, and with increasing exposure duration to the mirror reflected hand. © Springer-Verlag 2005.

353. Effect of posture change on tactile perception: impaired direction discrimination performance with interleaved fingers - Zampini M., Harris C. and Spence C. [M. Zampini, Department of Experimental Psychology, University of Oxford, South Parks Road, Oxford, OX1 3UD, United Kingdom] - *EXP. BRAIN RES.* 2005 166/3-4 (498-508) - summ in ENGL

We report a series of experiments in which participants had to judge the direction in which a pair of vibrotactile stimuli presented to two adjacent digits of either the same or different hands were stimulated (left-to-right or vice versa in experiments 1 and 2; nearto-far or vice versa in experiment 3, at stimulus onset asynchronies varying between 100 and 600 ms). When the participant's hands were placed side-by-side (anatomical posture), with their fingers either pointing away from them or else pointing toward the midline, directional discrimination performance was generally accurate. By contrast, when the fingers of the two hands were interleaved in either of these postures, performance deteriorated significantly for certain specific combinations of digits, with a more pronounced impairment seen when the fingers pointed away from the participant than when they pointed toward the midline. This decline in tactile direction discrimination performance in the interleaved fingers posture appears to reflect a failure to represent the position of tactile stimuli correctly when the fingers of the two hands are interleaved. © Springer-Verlag 2005.

354. Integration of visual and tactile stimuli: top-down influences require time - Shore D.I. and Simic N. [D.I. Shore, Multisensory Perception Laboratory, Department of Psychology Neuroscience and Behaviour, McMaster University, 1280 Main Street West, Hamilton, Ont. L8S 4K1, Canada] - *EXP. BRAIN RES.* 2005 166/3-4 (509-517) - summ in ENGL

In a visuotactile congruency task, a distracting flash of light presented near a tactile target can influence speeded judgments of tactile location. Localization of the tactile target is more rapid when the elevation of the visual distractor is congruent with the tactile stimulus than when it is incongruent. The goal of the present study was to examine the degree of control that can be exerted on the process proposed to integrate the visual and tactile stimuli. To this end, the proportion of spatially congruent items was manipulated across blocks of trials. A robust congruency effect was observed across three experiments. There was no effect of proportion congruency (varied between 75 and 11% congruent) when the visual event was presented only 30 ms prior to the tactile event. When this leadtime was increased to 100 ms there was a significant increase in the congruency effect, for errors, in the high proportion congruent conditions (experiment 3). We conclude that with sufficient leadtime, top-down influence can be exerted in this task, however, when presented at near simultaneity, visuotactile integration is independent of top-down effects. © Springer-Verlag 2005.

355. Long-lasting capture of tactile attention by body shadows - Galfano G. and Pavani F. [G. Galfano, DPSS, University of Padua, Via Venezia 8, 35131 Padua, Italy] - *EXP. BRAIN RES.* 2005 166/3-4 (518-527) - summ in ENGL

Four experiments addressed the role of cast shadows of the body in orienting tactile spatial attention to the body itself. We used a modified spatial-cueing paradigm to examine whether viewing of the cast shadow of a hand can elicit spatial shifts of tactile attention to that very same hand. Participants performed a speeded tactile-discrimination task (thumb versus index finger, regardless of touched hand), while viewing the shadow of either the touched or untouched hand cast in front of them by a lateral light-source. The hand casting the shadow changed either between blocks (expt 1) or unpredictably within each block (expts 2-4). In experiments 1 and 2 tactile targets were preceded by central non-informative visual cues delivered near

the shadow of the index finger and thumb. Despite the fact that cast shadows were always task-irrelevant and non-predictive of which hand was stimulated, tactile discrimination was consistently faster at the hand casting the shadow than at the other hand. This effect was not modulated by the duration of cue-target asynchrony, nor did it depend on whether the visual cue was present or not (expt 3). In addition, it was still reliable when vision of the hands was precluded, whereas it became inconsistent when the cast shadow of the hand was replaced by the cast shadow of an object (expt 4). Our results suggest that body shadows can induce a long-lasting capture of tactile attention for stimuli at the body itself. © Springer-Verlag 2005

356. Audiotactile interactions in near and far space - Kitagawa N., Zampini M. and Spence C. [N. Kitagawa, NTT Communication Science Laboratories, NTT Corporation, 3-1 Morinosato Wakamiya, Atsugi, Kanagawa 243-0198, Japan] - *EXP. BRAIN RES.* 2005 166/3-4 (528-537) - summ in ENGL

In this study we investigated audiotactile spatial interactions in the region behind the head. In experiment 1, participants made unspeeded temporal order judgments (TOJs) regarding pairs of auditory and tactile stimuli presented at varying stimulus onset asynchronies (SOAs) using the method of constant stimuli. Electrocutaneous stimuli were presented to the left or right earlobe while auditory stimuli were presented from just behind the participant's head on either the same or opposite side. Participants responded significantly more accurately when the stimuli were presented from different sides rather than from the same side. In experiment 2, we used a distractor interference task to show that speeded left/right discrimination responses to electrocutaneous targets were also modulated by the spatial congruency of auditory distractors presented behind the head. Performance was worse (i.e. response latencies were slower and error rates higher) when the auditory distractors were presented on the opposite side to the electrocutaneous target than when they were presented on the same side. This crossmodal distractor interference effect was larger when white noise distractors were presented from close to the head (20 cm) than when they were presented far from the head (70 cm). By contrast, pure tone distractors elicited a smaller crossmodal distractor interference effect overall, and showed no modulation as a function of distance. Taken together, these results suggest that the spatial modulation of audiotactile interactions occurs predominantly for complex auditory stimuli (for example, white noise) originating from the region close to the back of the head. © Springer-Verlag 2005.

357. Amygdala responsiveness is modulated by tryptophan hydroxylase-2 gene variation - Canli T., Congdon E., Gutknecht L. et al. [Dr. K.P. Lesch, Molecular and Clinical Psychobiology, Department of Psychiatry and Psychotherapy, University of Würzburg, Füchsleinstrasse 15, 97080 Würzburg, Germany] - *J. NEURAL TRANSM.* 2005 112/11 (1479-1485) - summ in ENGL

The tryptophan hydroxylase-2 gene (TPH2) codes for the enzyme of serotonin (5-HT) synthesis in the brain and variation of TPH2 has been implicated in disorders of emotion regulation. Here, we used functional magnetic resonance imaging (fMRI) to demonstrate that a potentially functional variant of TPH2 modulates amygdala responsiveness to emotional stimuli of both negative and positive valence. © Springer-Verlag 2005.

358. Centrally administered adrenomedullin 2 activates hypothalamic oxytocin-secreting neurons, causing elevated plasma oxytocin level in rats - Hashimoto H., Hyodo S., Kawasaki M. et al. [Y. Ueta, Dept. of Physiology, School of Medicine, Univ. of Occupational and Environmental Health, 1-1 Iseigaoka, Yahatanishi-ku, Kitakyushu 807-8555, Japan] - AM. J. PHYSIOL. ENDOCRINOL. METAB. 2005 289/5 52-5 (E753-E761) - summ in ENGL

We examined the effects of intracerebroventricular (ICV) administration of adrenomedullin 2 (AM2) on plasma oxytocin (OXT) and arginine vasopressin (AVP) levels in conscious rats. Plasma OXT levels were markedly increased 5 min after ICV administration of AM2 (1 nmol/rat) compared with vehicle and remained elevated in samples taken at 10, 15, 30, and 60 min. By contrast, plasma AVP levels were not significantly elevated in samples taken between 5 and 180 min after ICV administration of AM2 except at the 30-min time point. Fos-like immunoreactivity (Fos-LI) was observed

in various brain areas, including the paraventricular (PVN) and the supraoptic nuclei (SON) after ICV administration of AM2 (2 nmol/rat) in conscious rats (measured at 90 min post-AM2 infusion). Dual immunostaining for OXT/Fos and AVP/Fos showed that OXT-LI neurons predominantly exhibited nuclear Fos-LI compared with AVP-LI neurons in the PVN and the SON. In situ hybridization histochemistry showed that ICV administration of AM2 (0.2, 1, and 2 nmol/rat) caused marked induction of the expression of the c-fos gene in the PVN and the SON. This induction was significantly reduced by pretreatment with both the calcitonin gene-related peptide (CGRP) antagonist CGRP-(8-37) (3 nmol/rat) and the AM receptor antagonist AM-(22-52) (27 nmol/rat). These results suggest that centrally administered AM2 mainly activates OXT-secreting neurons in the PVN and the SON, at least in part through the CGRP and/or AM receptors with marked elevation of plasma OXT levels in conscious rats. Copyright © 2005 the American Physiological Society.

359. Properties of mouse spinal lamina I GABAergic interneurons - Dougherty K.J., Sawchuk M.A. and Hochman S. [S. Hochman, Whitehead Biomedical Research Bldg., Emory University School of Medicine, 615 Michael St., Atlanta, GA 30322, United States] - *J. NEUROPHYSIOL.* 2005 94/5 (3221-3227) - summ in ENGL

Lamina I is a sensory relay region containing projection cells and local interneurons involved in thermal and nociceptive signaling. These neurons differ in morphology, sensory response modality, and firing characteristics. We examined intrinsic properties of mouse lamina I GABAergic neurons expressing enhanced green fluorescent protein (EGFP). GABAergic neuron identity was confirmed by a high correspondence between GABA immunolabeling and EGFP fluorescence. Morphologies of these EGFP+/GABA+ cells were multipolar (65%), fusiform (31%), and pyramidal (4%). In whole cell recordings, cells fired a single spike (44%), tonically (35%), or an initial burst (21%) in response to current steps, representing a subset of reported lamina I firing properties. Membrane properties of tonic and initial burst cells were indistinguishable and these neurons may represent one functional population because, in individual neurons, their firing patterns could interconvert. Single spike cells were less excitable with lower membrane resistivity and higher rheobase. Most fusiform cells (64%) fired tonically while most multipolar cells (56%) fired single spikes. In summary, lamina I inhibitory interneurons are functionally divisible into at least two major groups both of which presumably function to limit excitatory transmission. Copyright © 2005 The American Physiological Society.

360. Enhancement of asynchronous and train-evoked exocytosis in bovine adrenal chromaffin cells infected with a replication deficient adenovirus - Thiagarajan R., Wilhelm J., Tewolde T. et al. [K.L. Engisch, Dept. of Neuroscience, Cell Biology, and Physiology, Wright State University, 014 M and M Bldg., 3640 Colonel Glenn Hwy., Dayton, OH 45435, United States] - *J. NEU-ROPHYSIOL*. 2005 94/5 (3278-3291) - summ in ENGL

Bovine adrenal chromaffin cells share many characteristics with neurons and are often used as a simple model system to study ion channels and neurotransmitter release. We infected bovine adrenal chromaffin cells with a replication deficient adenovirus that induces expression of the common reporters β -galactosidase and Green Fluorescent Protein via a bicistronic sequence. In perforated-patch recordings performed 48-h postinfection, peak calcium currents were reduced 32%, primarily due to loss of ω -conotoxin-GVIAsensitive current. In contrast, sodium currents were increased 17%. Exocytosis, detected as an increase in membrane capacitance immediately after a single step depolarization, was reduced in proportion to the decrease in calcium influx. However, capacitance continued to increase for seconds after the depolarization. The amplitude of this poststimulus drift, or asynchronous exocytosis, was approximately three times that which occurred in a small fraction of control cells. Exocytosis evoked by repetitive stimulation with a train of brief depolarizations was increased 50%. Intracellular calcium levels measured during and after stimulation were lower, not higher, in adenovirus-infected cells. Electroporated cells showed reduced calcium currents but no enhancement of exocytosis. Cells infected

with UV-irradiated virus showed reduced calcium currents and enhancement of exocytosis, but the changes were smaller than those caused by intact virus. Our results are consistent with the idea that adenovirus capsid and adenoviral DNA contribute to a $\rm Ca^{2+}$ in-flux- and [Ca $^{2+}$]_i-independent enhancement of exocytosis in bovine chromaffin cells. Copyright © 2005 The American Physiological Society.

361. Otolith deprivation induces optokinetic compensation - Andreescu C.E., De Ruiter M.M., De Zeeuw C.I. and De Jeu M.T.G. [M.T.G. De Jeu, Department of Neuroscience, Erasmus University Medical Center Rotterdam, Dr. Molewaterplein 50, 3000 DR, Rotterdam, Netherlands] - *J. NEUROPHYSIOL.* 2005 94/5 (3487-3496) - summ in ENGL

According to the multisensory integration theory vestibular, optokinetic and proprioceptive inputs act in concert to maintain a stable retinal image of the visual world. Yet, it remains elusive to what extent the otolith organs contribute to this process and whether a specific loss of otolith input is compensated for. Here we investigated the compensatory eye movements in tilted mice, which lack otoconia because of a mutation in otopetrin 1. Tilted mice showed very small displacements of the eyes in the orbit during static roll paradigms, suggesting the absence of functional otolith organs. Independent of head position with respect to gravity, the gain and phase lead of angular vestibuloocular reflex of tilted mice were decreased and increased, respectively (frequencies 0.2 to 1 Hz and peak accelerations 8 to 197°/s², respectively). Furthermore, lack of otolith input increases the dependency of the vestibular system on stimulus frequency. In contrast, the gain of optokinetic reflex in tilted mice was significantly higher in the low-frequency range than in control mice, regardless of the position of the mice in space or the plane of the eve movements. To explain these results, a simple model was used in which a multisensory integration unit was embedded. With this model, we were able to simulate all the behaviors observed. Thus our data and the model support the presence of the multisensory integration system and revealed a compensatory enhanced optokinetic reflex in tilted mice, indicating an adaptive synergism in the processing of otolith and visually driven signals. Copyright © 2005 The American Physiological Society.

362. Neural mechanisms of stimulus velocity tuning in the superior colliculus - Razak K.A. and Pallas S.L. [S.L. Pallas, Department of Biology, Georgia State University, 24 Peachtree Center Ave., Atlanta, GA 30303, United States] - *J. NEUROPHYSIOL.* 2005 94/5 (3573-3589) - summ in ENGL

Superior colliculus (SC)-mediated control of visuomotor behavior depends on neuronal selectivity for stimulus velocity. However, the mechanism responsible for velocity tuning in SC neurons is unclear. It was shown in a previous study of anesthetized, decorticate hamsters that the number and distribution of feed-forward retinal inputs are not critical for velocity tuning. Here the alternate hypothesis that inhibition from the surround determines velocity tuning of SC neurons was tested. Surround inhibition was present in 65% (43/66) of SC neurons recorded in the superficial gray layer. Neurons within this group that were selective for slowly moving stimuli exhibited spatially asymmetric surround inhibition, and their velocity tuning arose by preferential suppression of responses to rapidly moving stimuli. In the other 35% (23/66) of SC neurons recorded, surround inhibition was weak or absent and did not play a role in velocity tuning. Most neurons with surround inhibition were nonselective for the duration of stationary flashed stimuli, whereas neurons without surround inhibition were selective for stimulus duration. The majority of neurons that preferred intermediate or rapidly moving stimuli exhibited spatially symmetric surround inhibition. In these neurons, occluding the surround reduced velocity selectivity by enhancing responses to slowly moving stimuli. Based on these data, a model is proposed suggesting spatiotemporal interactions between inhibition and excitation that could underlie velocity tuning. Copyright © 2005 The American Physiological Society.

363. Light induces c-fos and per1 expression in the suprachiasmatic nucleus of arrhythmic hamsters - Barakat M.T., O'Hara B.F., Cao V.H. et al. [M.T. Barakat, Dept. of Biological Sciences, 371 Serra Mall, Stanford Univ., Stanford, CA 94305-5020, United

States] - AM. J. PHYSIOL. REGUL. INTEGR. COMP. PHYSIOL. 2005 289/5 58-5 (R1381-R1386) - summ in ENGL

Locomotor activity rhythms in a significant proportion of Siberian hamsters (Phodopus sungorus sungorus) become arrhythmic after the light-dark (LD) cycle is phase-delayed by 5 h. Arrhythmia is apparent within a few days and persists indefinitely despite the presence of the photocycle. The failure of arrhythmic hamsters to regain rhythms while housed in the LD cycle, as well as the lack of any masking of activity, suggested that the circadian system of these animals had become insensitive to light. We tested this hypothesis by examining light-induced gene expression in the suprachiasmatic nucleus (SCN). Several weeks after the phase delay, arrhythmic and reentrained hamsters were housed in constant darkness (DD) for 24 h and administered a 30-min light pulse 2 h after predicted dark onset because light induces c-fos and per1 genes at this time in entrained animals. Brains were then removed, and tissue sections containing the SCN were processed for in situ hybridization and probed with c-fos and per1 mRNA probes made from Siberian hamster cDNA. Contrary to our prediction, light pulses induced robust expression of both c-fos and per1 in all reentrained and arrhythmic hamsters. A separate group of animals held in DD for 10 days after the light pulse remained arrhythmic. Thus, even though the SCN of these animals responded to light, neither the LD cycle nor DD restored rhythms, as it does in other species made arrhythmic by constant light (LL). These results suggest that different mechanisms underlie arrhythmicity induced by LL or by a phase delay of the LD cycle. Whereas LL induces arrhythmicity by desynchronizing SCN neurons, phase delay-induced arrhythmicity may be due to a loss of circadian rhythms at the level of individual SCN neurons. Copyright © 2005 the American Physiological Society.

364. Hindlimb unloading and female gender attenuate baroreflex-mediated sympathoexcitation - Foley C.M., Mueller P.J., Hasser E.M. and Heesch C.M. [C.M. Foley, Univ. of Missouri-Columbia, Dalton Cardiovascular Research Center, 134 Research Park Drive, Columbia, MO 65211, United States] - *AM. J. PHYSIOL. REGUL. INTEGR. COMP. PHYSIOL.* 2005 289/5 58-5 (R1440-R1447) - summ in ENGL

Exposure to a period of microgravity or bed rest produces several physiological adaptations. These changes, which include an increased incidence of orthostatic intolerance, have an impact when people return to a IG environment or resume an upright posture. Compared with males, females appear more susceptible to orthostatic intolerance after exposure to real or simulated microgravity. Decreased arterial baroreflex compensation may contribute to orthostatic intolerance. We hypothesized that female rats would exhibit a greater reduction in arterial baroreflex function after hindlimb unloading (HU) compared with male rats. Mean arterial pressure (MAP), heart rate (HR), and renal sympathetic nerve activity (RSNA) were recorded in conscious animals after 13-15 days of HU. Baseline HR was elevated in female rats, and HU increased HR in both genders. Consistent with previous results in males, baroreflex-mediated activation of RSNA was blunted by HU in both genders. Maximum RSNA in response to decreases in MAP was reduced by HU (male control $513 \pm 42\%$, n = 11; male HU $346 \pm 38\%$, n = 13; female control 359 ± 44%, n = 10; female HU 260 \pm 43%, n = 10). Maximum baroreflex increase in RSNA was lower in females compared with males in both control and HU rats. Both female gender and HU attenuated baroreflex-mediated increases in sympathetic activity. The combined effects of HU and gender resulted in reduced baroreflex sympathetic reserve in females compared with males and could contribute to the greater incidence of orthostatic intolerance in females after exposure to spaceflight or bed rest. Copyright © 2005 the American Physiological Society.

365. NMDA channels control meal size via central vagal afferent terminals - Gillespie B.R., Burns G.A. and Ritter R.C. [G.A. Burns, Dept. of Veterinary Comparative Anatomy Physiology Pharmacology, College of Veterinary Medicine, Washington State Univ., Pullman, WA 99164-6520, United States] - *AM. J. PHYSIOL. REGUL. INTEGR. COMP. PHYSIOL.* 2005 289/5 58-5 (R1504-R1511) - summ in ENGL

The N-methyl-D-aspartate (NMDA) ion channel blocker MK-801 administered systemically or as a nanoliter injection into the nucleus of the solitary tract (NTS), increases meal size. Furthermore, we

have observed that ablation of the NTS abolishes increased meal size following systemic injection of dizocilpine (MK-801) and that MK-801-induced increases in intake are attenuated in rats pretreated with capsaicin to destroy small, unmyelinated, primary afferent neurons. These findings led us to hypothesize that NMDA receptors on central vagal afferent terminals or on higher-order NTS neurons innervated by these vagal afferents might mediate increased food To evaluate this hypothesis, we examined 15% sucrose intake after 50-nl MK-801 injections ipsilateral or contralateral to unilateral nodose ganglion removal (ganglionectomy). On the side contralateral to ganglionectomy, vagal afferent terminals would be intact and functional, whereas ipsilateral to ganglionectomy vagal afferent terminals would be absent. Three additional control preparations also were included: 1) sham ganglionectomy and 2) subnodose vagotomy either contralateral or ipsilateral to NTS cannula placement. We found that rats with subnodose vagotomies increased their sucrose intake after injections of MK-801 compared with saline, regardless of whether injections were made contralateral (12.6 \pm 0.2 vs. 9.6 \pm 0.3 ml) or ipsilateral (14.2 \pm 0.6 vs. 9.7 \pm 0.4 ml) to vagotomy. Rats with NTS cannula placements contralateral to nodose ganglionectomy also increased their intake after MK-801 $(12.2 \pm 0.9 \text{ and } 9.2 \pm 1.1 \text{ ml for MK-801}$ and saline, respectively). However, rats with placements ipsilateral to ganglionectomy did not respond to MK-801 (8.0 \pm 0.5 ml) compared with saline (8.3 \pm 0.4 ml). We conclude that central vagal afferent terminals are necessary for increased food intake in response to NMDA ion channel blockade. The function of central vagal afferent processes or the activity of higher-order NTS neurons driven by vagal afferents may be modulated by NMDA receptors to control meal size. Copyright © 2005 the American Physiological Society.

366. Hippocampal CA1 circuitry dynamically gates direct cortical inputs preferentially at theta frequencies - Ang C.W., Carlson G.C. and Coulter D.A. [Dr. D.A. Coulter, Abramson Pediatrics Research Center, 3516 Civic Center Boulevard, Philadelphia, PA 19104-4318, United States] - *J. NEUROSCI.* 2005 25/42 (9567-9580) - summ in ENGL

Hippocampal CA1 pyramidal neurons receive intrahippocampal and extrahipppocampal inputs during theta cycle, whose relative timing and magnitude regulate the probability of CA1 pyramidal cell spiking. Extrahippocampal inputs, giving rise to the primary theta dipole in CA1 stratum lacunosum moleculare, are conveyed by the temporoammonic pathway. The temporoammonic pathway impinging onto the CA1 distal apical dendritic tuft is the most electrotonically distant from the perisomatic region yet is critical in regulating CA1 place cell activity during theta cycles. How does local hippocampal circuitry regulate the integration of this essential, but electrotonically distant, input within the theta period? Using whole-cell somatic recording and voltage-sensitive dye imaging with simultaneous dendritic recording of CA1 pyramidal cell responses, we demonstrate that temporoammonic EPSPs are normally compartmentalized to the apical dendritic tuft by feedforward inhibition. However, when this input is preceded at a one-half theta cycle interval by proximally targeted Schaffer collateral activity, temporoammonic EPSPs propagate to the soma through a joint, codependent mechanism involving activation of Schaffer-specific NMDA receptors and presynaptic inhibition of GABAergic terminals. These afferent interactions, tuned for synaptic inputs arriving one-half theta interval apart, are in turn modulated by feedback inhibition initiated via axon collaterals of pyramidal cells. Therefore, CA1 circuit integration of excitatory inputs endows the CA1 principal cell with a novel property: the ability to function as a temporally specific "AND" gate that provides for sequence-dependent readout of distal inputs. Copyright © 2005 Society for Neuroscience.

367. The translation repressor 4E-BP2 is critical for eIF4F complex formation, synaptic plasticity, and memory in the hippocampus - Banko J.L., Poulin F., Hou L. et al. [Dr. E. Klann, Department of Molecular Physiology and Biophysics, Baylor College of Medicine, Houston, TX 77030, United States] - J. NEUROSCI. 2005 25/42 (9581-9590) - summ in ENGL

Long-lasting synaptic plasticity and memory requires mRNA translation, yet little is known as to how this process is regulated. To explore the role that the translation repressor 4E-BP2 plays in hippocampal long-term potentiation (LTP) and learning

and memory, we examined 4E-BP2 knock-out mice. Interestingly, genetic elimination of 4E-BP2 converted early-phase LTP to latephase LTP (L-LTP) in the Schaffer collateral pathway, likely as a result of increased eIF4F complex formation and translation initiation. A critical limit for activity-induced translation was revealed in the 4E-BP2 knock-out mice because L-LTP elicited by traditional stimulation paradigms was obstructed. Moreover, the 4E-BP2 knock-out mice also exhibited impaired spatial learning and memory and conditioned fear-associative memory deficits. These results suggest a crucial role for proper regulation of the eIF4F complex by 4E-BP2 during LTP and learning and memory in the mouse hippocampus. Copyright © 2005 Society for Neuroscience.

368. Identification of a new neuropeptide precursor reveals a novel source of extrinsic modulation in the feeding system of aplysia - Proekt A., Vilim F.S., Alexeeva V. et al. [Dr. K.R. Weiss, Department of Neuroscience, Mount Sinai School of Medicine, Box 1218, 1 Gustave Levy Place, New York, NY 10029, United States] - *J. NEUROSCI.* 2005 25/42 (9637-9648) - summ in ENGL

The Aplysia feeding system is advantageous for investigating the role of neuropeptides in behavioral plasticity. One family of Aplysia neuropeptides is the myomodulins (MMs), originally purified from one of the feeding muscles, the accessory radula closer (ARC). However, two MMs, MMc and MMe, are not encoded on the only known MM gene. Here, we identify MM gene 2 (MMG2), which encodes MMc and MMe and four new neuropeptides. We use matrix-assisted laser desorption/ionization time-of-flight mass spectrometry to verify that these novel MMG2-derived peptides (MMG2-DPs), as well as MMc and MMe, are synthesized from the precursor. Using antibodies against the MMG2-DPs, we demonstrate that neuronal processes that stain for MMG2-DPs are found in the buccal ganglion, which contains the feeding network, and in the buccal musculature including the ARC muscle. Surprisingly, however, no immunostaining is observed in buccal neurons including the ARC motoneurons. In situ hybridization reveals only few MMG2expressing neurons that are mostly located in the pedal ganglion. Using immunohistochemical and electrophysiological techniques. we demonstrate that some of these pedal neurons project to the buccal ganglion and are the likely source of the MMG2-DP innervation of the feeding network and musculature. We show that the MMG2-DPs are bioactive both centrally and peripherally: they bias egestive feeding programs toward ingestive ones, and they modulate ARC muscle contractions. The multiple actions of the MMG2-DPs suggest that these peptides play a broad role in behavioral plasticity and that the pedal-buccal projection neurons that express them are a novel source of extrinsic modulation of the feeding system of Aplysia. Copyright © 2005 Society for Neuroscience.

369. Proximal persistent Na+ channels drive spike afterdepolarizations and associated bursting in adult CA1 pyramidal cells - Yue C., Remy S., Su H. et al. [Dr. Y. Yaari, Department of Physiology, Hebrew University School of Medicine, P.O. Box 12272, Jerusalem 91121, Israel] - *J. NEUROSCI*. 2005 25/42 (9704-9720) - summ in ENGL

In many principal brain neurons, the fast, all-or-none Na+ spike initiated at the proximal axon is followed by a slow, graded afterdepolarization (ADP). The spike ADP is critically important in determining the firing mode of many neurons; large ADPs cause neurons to fire bursts of spikes rather than solitary spikes. Nonetheless, not much is known about how and where spike ADPs are initiated. We addressed these questions in adult CA1 pyramidal cells, which manifest conspicuous somatic spike ADPs and an associated propensity for bursting, using sharp and patch microelectrode recordings in acutely isolated hippocampal slices and single neurons. Voltage-clamp commands mimicking spike waveforms evoked transient Na+ spike currents that declined quickly after the spike but were followed by substantial sustained Na+ spike after currents. Drugs that blocked the persistent Na + current (I_{NaP}), markedly suppressed the sustained Na+ spike aftercurrents, as well as spike ADPs and associated bursting. $^{\circ}$ Ca²⁺ spike aftercurrents were much smaller, and reducing them had no noticeable effect on the spike ADPs. Truncating the apical dendrites affected neither spike ADPs nor the firing modes of these neurons. Application of I_{NaP} blockers to truncated neurons, or their focal application to the somatic region of intact neurons, suppressed spike ADPs

and associated bursting, whereas their focal application to distal dendrites did not. We conclude that the somatic spike ADPs are generated predominantly by persistent Na $^{+}$ channels located at or near the soma. Through this action, proximal $I_{\rm NaP}$ critically determines the firing mode and spike output of adult CA1 pyramidal cells. Copyright © 2005 Society for Neuroscience.

370. Modulation of presynaptic plasticity and learning by the H-ras/extracellular signal-regulated kinase/synapsin I signaling pathway - Kushner S.A., Elgersma Y., Murphy G.G. et al. [A.J. Silva, Department of Neurobiology, Brain Research Institute, University of California, Los Angeles, CA 90095-1761, United States] - *J. NEUROSCI.* 2005 25/42 (9721-9734) - summ in ENGL

Molecular and cellular studies of the mechanisms underlying mammalian learning and memory have focused almost exclusively on postsynaptic function. We now reveal an experience-dependent presynaptic mechanism that modulates learning and synaptic plasticity in mice. Consistent with a presynaptic function for endogenous H-ras/extracellular signal-regulated kinase (ERK) signaling, we observed that, under normal physiologic conditions in wild-type mice, hippocampus-dependent learning stimulated the ERK-dependent phosphorylation of synapsin 1, and MEK (MAP kinase kinase)/ERK inhibition selectively decreased the frequency of miniature EPSCs. By generating transgenic mice expressing a constitutively active form of H-ras (H-rasG12V), which is abundantly localized in axon terminals, we were able to increase the ERK-dependent phosphorylation of synapsin I. This resulted in several presynaptic changes, including a higher density of docked neurotransmitter vesicles in glutamatergic terminals, an increased frequency of miniature EPSCs, and increased paired-pulse fa-In addition, we observed facilitated neurotransmitter release selectively during high-frequency activity with consequent increases in long-term potentiation. Moreover, these mice showed dramatic enhancements in hippocampus-dependent learning. Importantly, deletion of synapsin I, an exclusively presynaptic protein, blocked the enhancements of learning, presynaptic plasticity, and long-term potentiation. Together with previous invertebrate studies, these results demonstrate that presynaptic plasticity represents an important evolutionarily conserved mechanism for modulating learning and memory. Copyright © 2005 Society for Neuroscience.

371. Emerging neurophysiological specialization for letter strings - Maurer U., Brem S., Bucher K. and Brandeis D. [D. Brandeis, Department of Child and Adolescent Psychiatry, University of Zürich, Neumünsterallee 9, CH-8032 Zürich, Switzerland] - *J. COGN. NEUROSCI.* 2005 17/10 (1532-1552) - summ in ENGL

In adult readers, printed words and other letter strings activate specialized visual functions within 200 msec, as evident from neurophysiological recordings of brain activity. These fast, specialized responses to letter strings are thought to develop through plastic changes in the visual system. However, it is unknown whether this specialization emerges only with the onset of word reading, or represents a precursor of literacy. We compared 6-year-old kindergarten children who could not yet read words to adult readers. Both age groups detected immediate repetitions of visually presented words, pseudowords, symbol strings, and pictures during event-related potential (ERP) mapping. Maps from seven corresponding ERP segments in children and adults were analyzed regarding fast (<250 msec) and slow (>300 msec) specialization for letter strings. Adults reliably differentiated words through increased fast (<150 msec) occipito-temporal N1 activity from symbols. Children showed a later, more mid-occipital N1 with marginal word-symbol differences, which were absent in those children with low letter knowledge. Children with high letter knowledge showed some fast sensitivity to letter strings, which was confined to right occipitotemporal sites, unlike the stronger adult N1 specialization. This suggests that a critical degree of early literacy induces some immature, but fast, specialization for letter strings before word reading becomes possible. Children also differentiated words from symbols in later segments through increased right occipito-temporal negativity for words. This slow specialization for letter strings was not modulated by letter knowledge and was absent in adults, possibly reflecting a visual precursor of literacy due to visual familiarity with letter strings. © 2005 Massachusetts Institute of Technology.

372. Specificity of the effect of a nicotinic receptor polymorphism on individual differences in visuospatial attention - Greenwood P.M., Fossella J.A. and Parasuraman R. [P.M. Greenwood, Department of Psychology, MSN 3F5, George Mason University, Fairfax, VA 22030-4444, United States] - *J. COGN. NEUROSCI.* 2005 17/10 (1611-1620) - summ in ENGL

Cortical neurotransmitter availability is known to exert domainspecific effects on cognitive performance. Hence, normal variation in genes with a role in neurotransmission may also have specific effects on cognition. We tested this hypothesis by examining associations between polymorphisms in genes affecting cholinergic and noradrenergic neurotransmission and individual differences in visuospatial attention. Healthy individuals were administered a cued visual search task which varied the size of precues to the location of a target letter embedded in a 15-letter array. Cues encompassed 1, 3, 9, or 15 letters. Search speed increased linearly with precue size, indicative of a spatial attentional scaling mechanism. The strength of attentional scaling increased progressively with the number of C alleles (0, 1, or 2) of the alpha-4 nicotinic receptor gene C1545T polymorphism (n = 104). No association was found for the dopamine beta hydroxylase gene G444A polymorphism (n = 135). These findings point to the specificity of genetic neuromodulation. Whereas variation in a gene linked to cholinergic transmission systematically modulated the ability to scale the focus of visuospatial attention, variation in a gene governing dopamine availability did not. The results show that normal variation in a gene controlling a nicotinic receptor makes a selective contribution to individual differences in visuospatial attention. © 2005 Massachusetts Institute of Technology

373. Effect of carbohydrate ingestion on brain exchange of amino acids during sustained exercise in human subjects - Blomstrand E., Møller K., Secher N.H. and Nybo L. [E. Blomstrand, Åstrand Laboratory, University College of Physical Education and Sports, Box 5626, S-114 86 Stockholm, Sweden] - *ACTA PHYSIOL. SCAND.* 2005 185/3 (203-209) - summ in ENGL

Aim: This study investigated the effect of prolonged exercise with and without carbohydrate intake on the brain exchange of amino acids, especially focussing on tryptophan and branched-chain amino acids (BCAA). Methods: Five male subjects exercised for 3 h on a cycle ergometer at 200 \pm 7 W on two occasions: either supplemented with a 6% carbohydrate solution or with flavoured water (placebo). Catheters were inserted into the right internal jugular vein and the radial artery of the non-dominant arm. The brain exchange of amino acids during exercise was calculated from the arterial-jugular venous concentration difference multiplied by plasma flow. Results: About 106 μ mol (22 mg) of tryptophan was taken up by the brain during exercise in the placebo trial, whereas no significant uptake was observed in the carbohydrate trial. In accordance, the arterial concentration of free tryptophan increased from 12 \pm 1 to 20 \pm 2 μ mol L⁻¹ during the placebo trial and was significantly higher compared with the glucose trial (14 \pm 1 μ mol L-1 at the end of exercise). Also, the arterial concentration of total tryptophan (free and albumin-bound) increased during the first 30 min of exercise in both trials, but returned to the basal level at 180 min of exercise. In both trials, BCAA were taken up by the brain while glutamine was released. Conclusion: The present data show that both tryptophan and BCAA are taken up by the brain during prolonged exercise, and we suggest that the cerebral uptake of tryptophan may relate to increased synthesis of serotonin (5-HT) in the brain. © 2005 Scandinavian Physiological Society.

374. Vasopressin release from the rat hypothalamo-neuro-hypophsial system: Effects of tachykinin NK-1 and NK-2 receptors agonists and antagonists - Juszczak M. [Dr. M. Juszczak, Department of Pathophysiology, Medical University of Lodz, Narutowicza 60, 90-136 Lodz, Poland] - NEUROENDOCRINOL. LETT. 2005 26/4 (367-372) - summ in ENGL

Objectives: Present experiments were undertaken to study the influence of peptide NK-1 and NK-2 receptor agonists and antagonists as well as substance P and neurokinin A (the natural ligands for these tachykinin receptors) on vasopressin (AVP) secretion from the rat hypothalamo-neurohypophysial (HN) system in vitro. Results: The results showed that both substance P and highly selective tachykinin NK-1 receptor agonist, i.e., [Sar⁹,Met(O₂)¹¹]-Substance

P, enhanced significantly AVP secretion, while the NK-1 receptor antagonist (Tyr6,D-Phe7,D-His9) -Substance P (6-11) - sendide was found to antagonize the substance P-induced hormone release from isolated rat HN system (all peptides at the concentration of 10-7 M/L). The NK-2 receptor selective agonist (β -Ala8)-Neurokinin A (4-10) was essentially inactive in modifying AVP release from the rat HN system in vitro, while neurokinin A (the natural ligand for this tachykinin receptor) was found to stimulate the AVP release; this effect of neurokinin A has been diminished by the NK-2 receptor antagonist (Tyr5,D-Trp6,8,9,Lys-Ntg $^{-10}$)-Neurokinin A (4-10). Conclusion: The present data indicate a role for tachykinin NK-1 (and possibly for NK-2) receptors in tachykinin-mediated stimulation of AVP secretion from the rat HN system in vitro. © Neuroendocrinology Letters.

375. In vivo human brain biochemistry after aerobic exercise: Preliminary report on functional magnetic resonance spectroscopy - Çağlar E., Sabuncuoğlu H., Keskin T. et al. [Dr. S. Keskil, F. Sokak No. 4/6, Gazi Osman Pafla, Ankara 06700, Turkey] - SURG. NEUROL. 2005 64/SUPPL. 2 (S2:53-S2:56) - summ in ENGL

Background: Our aim was to disclose whether the positive psychological changes observed after a single bout of aerobic exercise have a biochemical correlate that can be visualized by proton magnetic resonance spectroscopy (MRS) of the human brain. Methods: Right-handed male volunteers underwent psychological testing and MRS of the frontal lobe of the left hemisphere, both before and after 20 minutes of jogging at about 70% of their maximal aerobic capacity. Results: Although there was a significant decrease on the postexercise anxiety test scores (z = -2.201, P < .05), there was no significant difference between the preexercise and postexercise scores of positive and negative affect. Considering both "amplitude" and "area under the curve" values calculated for the peaks of metabolites N-acetylaspartate (NAA), creatine, and choline, none were found to be significantly changed (P > .05) after the exercise. Conclusion: This is, to our knowledge, the first study to report on a functional application of MRS to mood states. Because it offers the ability to directly measure metabolic changes in the brain during neuronal activation, "functional MRS" may be a potential new tool that may be used as an adjunct to functional magnetic resonance imaging. © 2005 Elsevier Inc. All rights reserved.

376. Distinct amygdala-autonomic arousal profiles in response to fear signals in healthy males and females - Williams L.M., Barton M.J., Kemp A.H. et al. [L.M. Williams, Brain Dynamics Centre, Westmead Millenium Institute, Westmead Hospital, Westmead, NSW 2145, Australia] - NEUROIMAGE 2005 28/3 (618-626) - summ in ENGL

The amygdala has a key role in regulating arousal and vigilance, and responds to both visual and vocal signals of fear, including facial expressions of fear. In this study, we used functional MRI to examine sex differences in the magnitude, extent, lateralization and time course of amygdala responses to facial signals of fear, in a relatively large sample of males and females. Skin conductance was recorded simultaneously with functional imaging to examine concomitant changes in emotional arousal, and to provide an independent index of response attenuation. Scanning and skin conductance recording was undertaken during perception of facial fear stimuli. Sex differences were apparent in the laterality and time course of fear perception. In males, the right amygdala and autonomic arousal attenuated over the late half of the experiment. By contrast, females showed persistent bilateral amygdala responses, with a tendency towards greater left amygdala engagement during the late phase. Females also showed a greater general extent of amygdala response. We suggest that distinct evolutionary pressures might contribute to a lower threshold for vigilance to signals of danger in females, reflected in a profile of sustained amygdala-arousal interaction. © 2005 Elsevier Inc. All rights reserved.

377. Selective influences of cross-modal spatial-cues on preattentive auditory processing: A whole-head magnetoencephalography study - Mathiak K., Hertrich I., Zvyagintsev M. et al. [K. Mathiak, Department of Psychiatry and Psychotherapy, RWTH Aachen, Pauwelsstr. 30, D-52074 Aachen, Germany] - NEUROIMAGE 2005 28/3 (627-634) - summ in ENGL

The processing streams of the various sensory modalities are known to interact within the central nervous system. These interactions differ depending on the level of stimulus representation and attention. The current study focused on cross-sensory influences on stimulus change detection during unattended auditory processing. We employed an oddball paradigm to assess cortical processing using whole-head magnetoencephalography (MEG) in 20 volunteers. While subjects performed distraction tasks of varying difficulties, auditory duration deviants were applied randomly to the left or the right ear preceded (200-400 ms) by oculomotor, static visual, or flow field co-stimulation at either side. Mismatch fields were recorded over both hemispheres. Changes in gaze direction and static visual stimuli elicited the most reliable enhancement of deviance detection at the same side (most prominent at the right auditory cortex). Under both conditions, the lateralized unattended and unpredictive pre-cues acted analogously to shifts in selective attention, but were not reduced by attentional load. Thus, the early cognitive representation of sounds seems to reflect automatic cross-modal interference. Preattentive multisensory integration may provide the neuronal basis for orienting reactions to objects in space and thus for voluntary control of selective attention. © 2005 Elsevier Inc. All rights reserved.

378. Classifying spatial patterns of brain activity with machine learning methods: Application to lie detection - Davatzikos C., Ruparel K., Fan Y. et al. [C. Davatzikos, Department of Radiology, University of Pennsylvania, 3600 Market Street, Philadelphia, PA 19104, United States] - *NEUROIMAGE* 2005 28/3 (663-668) - summ in ENGL

Patterns of brain activity during deception have recently been characterized with fMRI on the multi-subject average group level. The clinical value of fMRI in lie detection will be determined by the ability to detect deception in individual subjects, rather than group averages. High-dimensional non-linear pattern classification methods applied to functional magnetic resonance (fMRI) images were used to discriminate between the spatial patterns of brain activity associated with lie and truth. In 22 participants performing a forced-choice deception task, 99% of the true and false responses were discriminated correctly. Predictive accuracy, assessed by cross-validation in participants not included in training, was 88%. The results demonstrate the potential of non-linear machine learning techniques in lie detection and other possible clinical applications of fMRI in individual subjects, and indicate that accurate clinical tests could be based on measurements of brain function with fMRI. © 2005 Elsevier Inc. All rights reserved.

379. Cortical activity in multiple motor areas during sequential finger movements: An application of independent component analysis - Kansaku K., Muraki S., Umeyama S. et al. [K. Kansaku, Division of Cerebral Integration, National Institute for Physiological Sciences, National Institutes of Natural Sciences, 38 Nishigonaka, Myodaiji, Okazaki 444-8585, Japan] - NEUROIM-AGE 2005 28/3 (669-681) - summ in ENGL

Multiple cortical regions such as the supplementary motor area (SMA), premotor cortex (PM), and primary motor cortex (M1) are involved in the sequential execution of hand movements, but it is unclear how these areas collaborate in the preparation and execution of ipsilateral and contralateral hand movements. In this study, we used right-handed subjects to examine the spatial distribution and temporal profiles of motor-related activity during visually cued sequential finger movements by applying independent component analysis (ICA) to event-related functional magnetic resonance imaging (fMRI) signals. The particular merit of the ICA method is that it allows brain activity in individual subjects to be elucidated without making a priori assumptions about the anatomical areas that are activated or the temporal profile of activity. By applying ICA, we found that (1) the SMA contributed to both the preparation and execution of movements of the right and left hand; (2) the left M1 and dorsal premotor cortex (PMd) contributed to both the preparation and execution of movements of the right and left hand, whereas the right M1 and PMd contributed mainly to the execution of movements of the left hand; (3) pre-SMA areas were activated in some subjects in concert with the posterior parietal and prefrontal cortex; and (4) fMRI signals over superficial cortical draining veins could be distinguished from cortical activation. We suggest that

ICA is useful for categorizing distributed task-related activities in individual subjects into several spatially independent activities that represent functional units in motor control. © 2005 Elsevier Inc. All rights reserved.

380. Adrenergic receptors mediate stress-induced elevations in extracellular Hsp72 - Johnson J.D., Campisi J., Sharkey C.M. et al. [J.D. Johnson, Center for Neuroscience, Dept. of Integrative Physiology, Univ. of Colorado at Boulder, Boulder, CO 80309-0354, United States] - *J. APPL. PHYSIOL*. 2005 99/5 (1789-1795) - summ in ENGL

Heat-shock protein concentrations in the blood increase after exposure to a variety of stressors, including trauma and psychological stress. Although the physiological function of extracellular heat shock protein remains controversial, there is evidence that extracellular heat shock protein 72 (Hsp72) can facilitate immunologic responses. The signal(s) that mediate(s) the in vivo elevation of extracellular Hsp72 in the blood after stressor exposure remain(s)unknown. Here we report that Hsp72 increases in the circulation via an α_1 -adrenergic receptor-mediated signaling pathway. Activation of α_1 -adrenoceptors results in a rapid increase in circulating Hsp72, and blockade of α_1 -adrenoceptors prevents the stress-induced rise in circulating Hsp72. Furthermore, our studies exclude a role for β -adrenoceptors, glucocorticoids, and ACTH in mediating stress-induced elevations in circulating extracellular Hsp72. Understanding the signals involved in elevating extracellular Hsp72 could facilitate the use of extracellular Hsp72 to bolster immunity and perhaps prevent exacerbation of inflammatory diseases during stress. Copyright © 2005 the American Physiological Society.

381. Olfaction: Diverse species, conserved principles - Ache B.W. and Young J.M. [B.W. Ache, Departments of Zoology and Neuroscience, McKnight Brain Institute, University of Florida, Gainesville, FL 32610, United States] - *NEURON* 2005 48/3 (417-430) - summ in ENGL

Olfaction is a vitally important sense for all animals. There are striking similarities between species in the organization of the olfactory pathway, from the nature of the odorant receptor proteins, to perireceptor processes, to the organization of the olfactory CNS, through odor-guided behavior and memory. These common features span a phylogenetically broad array of animals, implying that there is an optimal solution to the problem of detecting and discriminating odors. Copyright ©2005 by Elsevier Inc.

382. A comparison of experience-dependent plasticity in the visual and somatosensory systems - Fox K. and Wong R.O.L. [K. Fox, Cardiff School of Biosciences, Cardiff University, Museum Avenue, Cardiff CF10 3US, United Kingdom] - *NEURON* 2005 48/3 (465-477) - summ in ENGL

In the visual and somatosensory systems, maturation of neuronal circuits continues for days to weeks after sensory stimulation occurs. Deprivation of sensory input at various stages of development can induce physiological, and often structural, changes that modify the circuitry of these sensory systems. Recent studies also reveal a surprising degree of plasticity in the mature visual and somatosensory pathways. Here, we compare and contrast the effects of sensory experience on the connectivity and function of these pathways and discuss what is known to date concerning the structural, physiological, and molecular mechanisms underlying their plasticity. Copyright ©2005 by Elsevier Inc.

383. Reliability and representational bandwidth in the auditory cortex - DeWeese M.R., Hromádka T. and Zador A.M. [A.M. Zador, Cold Spring Harbor Laboratory, Watson School of Biological Sciences, Cold Spring Harbor, NY 11724, United States] - NEURON 2005 48/3 (479-488) - summ in ENGL

It is unclear why there are so many more neurons in sensory cortex than in the sensory periphery. One possibility is that these "extra" neurons are used to overcome cortical noise and faithfully represent the acoustic stimulus. Another possibility is that even after overcoming cortical noise, there is "excess representational bandwidth" available and that this bandwidth is used to represent conjunctions of auditory and nonauditory information for computation. Here, we discuss recent data about neuronal reliability in auditory cortex showing that cortical noise may not be as high as

was previously believed. Although at present, the data suggest that auditory cortex neurons can be more reliable than those in the visual cortex, we speculate that the principles governing cortical computation are universal and that visual and other cortical areas can also exploit strategies based on similarly high-fidelity activity. Copyright ©2005 by Elsevier Inc.

384. Comparison of growth and exploratory behavior in mice fed an exclusively milk formula diet and mice fed a food-pellet diet post weaning - Ishii T., Itou T. and Nishimura M. [T. shii, Department of Pathobiological Science, Obihiro University of Agriculture and Veterinary Medicine, Obihiro, Hokkaido 080-8555, Japan] - LIFE SCI. 2005 78/2 (174-179) - summ in ENGL

An exclusively milk formula diet stunted the growth of mice immediately following weaning. Milk-fed mice displayed a low-frequency profile of exploratory behavior, while pellet-fed mice showed high-frequency exploration. In contrast to exploratory behavior, feeding behavior did not differ significantly between milk-and pellet-fed mice. Despite showing low-frequency exploratory behavior, mice on an exclusively milk formula diet showed no difference in behavioral activities analyzed by an automatic hole-board apparatus compared to pellet-fed mice. These results suggest that the growth stunt caused by an exclusively milk formula diet retards the acquisition of active exploratory behavior without affecting the emotional state of mice. © 2005 Elsevier Inc. All rights reserved.

See also: 462, 477, 483, 505, 507, 553, 564, 573, 581, 585, 588, 606, 608.

4.1. Sensory physiology

385. Whole-head MEG analysis of cortical spatial organization from unilateral stimulation of median nerve in both hands: No complete hemispheric homology - Theuvenet P.J., Van Dijk B.W., Peters M.J. et al. [P.J. Theuvenet, Department of Anesthesiology, Alkmaar Medical Center, Oranjelaan 61, 1815 JR Alkmaar, Netherlands] - NEUROIMAGE 2005 28/2 (314-325) - summ in ENGL

We examined the contralateral hemispheric cortical activity in MEG (151 ch) after unilateral median nerve stimulation of the right and left hand in twenty healthy right-handed subjects. The goal was to establish parameters to describe cortical activity of the hemispheric responses and to study the potential ability to assess differences in volunteers and patients. We focused on the withinsubject similarity and differences between evoked fields in both hands. Cortical activity was characterized by the overlay display of waveforms (CWP), number of peak stages, loci of focal maxima and minima in each stage, 3D topographic maps and exemplified equivalent current dipole characteristics. The paired-wise test was used to analyze the hemispheric differences. The waveform morphology was unique across the subjects, similar CWPs were noted in both hemispheres of the individual. The contralateral hemispheric responses showed a well defined temporal-spatial activation of six to seven stages in the 500 ms window. Consistently (in over 80% of subjects), the six stages across the subjects were 20M, 30M, 50M, 70M, 90M, and 150M. A 240M was present in the left hemisphere (LH) in 15/20 subjects and in the right hemisphere (RH) in 10/20. Statistics of the latencies and amplitudes of these seven stages were calculated. Our results indicated that the latency was highly consistent and exhibited no statistical mean difference for all stages. Furthermore, no mean amplitude differences between both hemispheres at each stage were found. The patterns of magnetic fields in both hemispheres were consistent in 70% of the subjects. A laterality index (L.I.) was used for defining the magnetic field amplitude differences between two hemispheres for each individual. Overall, the absolute amplitude of the brain responses was larger in the left than in the right hemisphere in the majority of subjects (16/20), yet a significant portion (4/20) exhibited right dominance of the N20m activity. Each individual exhibited a unique CWP, there was reliable consistency of peak latencies and mean amplitudes in median nerve MEG. Nevertheless, this study indicates the limitations of using the intact hemisphere responses to compare with those from the affected (brain) side and suggests caution in assuming full homology in the cortical organization of both hemispheres. This study provides some results to address clinical issues like which

parameter describes individual differences best. Whether a genuine difference is found or whether any difference may simply represent the variability encountered in a normal population. © 2005 Elsevier Inc. All rights reserved.

386. Multisensory and secondary somatosensory cortex in the rat - Menzel R.R. and Barth D.S. [Dr. D.S. Barth, Department of Psychology, University of Colorado, Campus Box 345, Boulder, CO 80309-0345, United States] - CEREB. CORTEX 2005 15/11 (1690-1696) - summ in ENGL

The function of secondary somatosensory (SII) cortex is poorly understood, but there is evidence to suggest that one of its roles may be in multisensory integration. This study used high-resolution field potential mapping coupled with laminar field potential and multiunit recording to examine the association between SII and multisensory (auditory-somatosensory) cortex in the rat. We demonstrate that while there is spatial overlap between unisensory areas of SII and multisensory regions, particularly for representations of the trunk and hind limbs, they form distinct somatotopic maps. We propose that multisensory cortex be considered functionally distinct from SII, and that SII may be more concerned with unisensory processing tasks. © The Author 2005. Published by Oxford University Press. All rights reserved.

387. Disruption of layer 4 development alters laminar processing in ferret somatosensory cortex - McLaughlin D.F. and Juliano S.L. [D.F. McLaughlin, Department of Anatomy and Cell Biology, USUHS, 4301 Jones Bridge Road, Bethesda, MD 20814, United States] - *CEREB. CORTEX* 2005 15/11 (1791-1803) - summ in ENGL

Treatment with the anti-mitotic agent methylazoxymethanol (MAM) on embryonic day 33 (E33) in ferrets changes features of somatosensory cortex. These include dramatic reduction of cells in layer 4, and altered distributions of thalamocortical afferent terminations and GABAA receptors. To determine the effect of the relative absence of layer 4 on processing of sensory stimuli we used current source-density profiles to assess laminar activity patterns. Nearly synchronous activation occurs across all layers in treated animals, which contrasts with the normal cortical activation pattern of initial sinks in layer 4. This change after MAM treatment is consistent with the absence of layer 4 cells and widespread termination of thalamocortical afferents. Using periodic stimulation at 'flutter' frequency, layer 4 neurons in normal somatosensory cortex fire reproducibly to the stimulus rate; the capacity for entrainment is best for layer 4 and weaker in the extragranular layers. The capacity to encode periodic sensory stimuli is disrupted in MAM-treated somatosensory cortex; after an initial response to the onset of periodic stimuli, neurons in all cortical layers show weak entrainment. Neural responses to sensory drive in E33 MAM-treated cortex are also embedded in levels of neural activity substantially above those in normal somatosensory cortex. Sustained stimulation additionally reveals different capacities in each layer for improved signal-to-noise ratios, with layer 4 neurons in normal animals exhibiting the most improved signaling over time. We conclude that normal thalamic terminations, an intact layer 4 and subsequent intracortical processing are integral to proper encoding of stimulus features. © The Author 2005. Published by Oxford University Press. All rights reserved.

388. The vibrissal system as a model of thalamic operations - Deschênes M., Timofeeva E., Lavallée P. and Dufresne C. [M. Deschênes, CRULRG, Université Laval, Quebec, Que. G1J 2G3, Canada] - *PROG. BRAIN RES.* 2005 149/- (31-40) - summ in ENGL

The highly segregated organization of the vibrissal system of rodents offers a unique opportunity to address key issues about thalamic operations in primary sensory and second order thalamic nuclei. In this short review, evidence showing that reticular thalamic neurons and relay cells with receptive fields on the same vibrissa form topographically closed loop connections has been summarized. Within whisker-related thalamic modules, termed barreloids, reticular axons synapse onto the cell bodies and dendrites of residing neurons as well as onto the distal dendrites of neurons that are located in adjacent barreloids. This arrangement provides a substrate for a mechanism of lateral inhibition whereby the spread of dendritic trees among surrounding barreloids determines whisker-specific patterns of lateral inhibition. The relay of

sensory inputs in the posterior group, a second order nucleus associated with the vibrissal system is also examined. It is shown that in lightly anesthetized rats posterior group cells are tonically inhibited by GABAergic neurons of the ventral division of zona incerta. These observations suggest that a mechanism of disinhibition controls transmission of sensory signals in the posterior group nucleus. We further propose that disinhibition operates in a top-down manner, via motor instructions sent by cortex to brainstem and spinal cord. In this way posterior group nucleus would forward to the cerebral cortex sensory information that is contingent upon its action. Copyright © 2005 Elsevier BV. All rights reserved.

389. GABA_A receptor subunit expression in the guinea pig vestibular nucleus complex during the development of vestibular compensation - Gliddon C.M., Darlington C.L. and Smith P.F. P. Smith, Department of Pharmacology and Toxicology, School of Medical Sciences, University of Otago, Dunedin, New Zealand] - EXP. BRAIN RES. 2005 166/1 (71-77) - summ in ENGL

The aim of this experiment was to investigate whether vestibular compensation following unilateral vestibular deafferentation (UVD) is associated with changes in the expression of GABA_A receptor subunits in the guinea pig vestibular nuclear complex (VNC) at 2, 10, and 30 h post-surgery. Using Western blotting, the α_1 and γ_2 subunits (but not the β_2 subunit) were detected in the VNC of labyrinthine-intact animals. However, there were no significant differences in the protein expression of the α_1 and γ_2 subunits within the ipsilateral or contralateral VNC at any time post-UVD compared to sham and anesthetic controls. Furthermore, UVD did not induce the expression of the β_2 protein. These results suggest that vestibular compensation in guinea pig, as in the rat, is not associated with changes in the protein levels of the GABA_A receptor subunits α_1 , β_2 , and γ_2 in the VNC. However, a limitation of this study is that the Western blotting technique can detect only changes that are larger than 30% and therefore small changes cannot be excluded. © Springer-Verlag 2005.

390. SVD-based optimal filtering for noise reduction in dual microphone hearing aids: A real time implementation and perceptual evaluation - Maj J.-B., Royackers L., Moonen M. and Wouters J. [J.-B. Maj, Lab. Exp. ORL, Katholieke Univesiteit Leuven, 3000 Leuven, Belgium] - *IEEE TRANS. BIOMED. ENG.* 2005 52/9 (1563-1573) - summ in ENGL

In this paper, the first real-time implementation and perceptual evaluation of a singular value decomposition (SVD)-based optimal filtering technique for noise reduction in a dual microphone behind-the-ear (BTE) hearing aid is presented. This evaluation was carried out for a speech weighted noise and multitalker babble, for single and multiple jammer sound source scenarios. Two basic microphone configurations in the hearing aid were used. The SVDbased optimal filtering technique was compared against an adaptive beamformer, which is known to give significant improvements in speech intelligibility in noisy environment. The optimal filtering technique works without assumptions about a speaker position, unlike the two-stage adaptive beamformer. However this strategy needs a robust voice activity detector (VAD). A method to improve the performance of the VAD was presented and evaluated physically. By connecting the VAD to the output of the noise reduction algorithms, a good discrimination between the speech-and-noise periods and the noise-only periods of the signals was obtained. The perceptual experiments demonstrated that the SVD-based optimal filtering technique could perform as well as the adaptive beamformer in a single noise source scenario, i.e., the ideal scenario for the latter technique, and could outperform the adaptive beamformer in multiple noise source scenarios. © 2005 IEEE.

391. Recording human evoked potentials that follow the pitch contour of a natural vowel - Dajani H.R., Purcell D., Wong W. et al. [H.R. Dajani, Institute of Biomaterials and Biomedical Engineering, University of Toronto, Toronto, Ont. M5S 3G9, Canada] - *IEEE TRANS. BIOMED. ENG.* 2005 52/9 (1614-1618) - summ in ENG.

We investigated whether pitch-synchronous neural activity could be recorded in humans, with a natural vowel and a vowel in which the fundamental frequency was suppressed. Small variations of speech periodicity were detected in the evoked responses using

a fine structure spectrograph (FSS). A significant response ($P \ll 0.001$) was measured in all seven normal subjects even when the fundamental frequency was suppressed, and it very accurately tracked the acoustic pitch contour (normalized mean absolute error < 0.57%). Small variations in speech periodicity, which humans can detect, are therefore available to the perceptual system as pitch-synchronous neural firing. These findings suggest that the measurement of pitch-evoked responses may be a viable tool for objective speech audiometry. © 2005 IEEE.

392. Right hemispheric predominance in the segregation of mistuned partials - Hiraumi H., Nagamine T., Morita T. et al. [Dr. H. Hiraumi, Department of Otolaryngology - Head and Neck Surgery, Graduate School of Medicine, Kyoto University, 54, Kawaharacho, Shogoin, Sakyo-ku, Kyoto, 606-8507, Japan] - *EUR. J. NEUROSCI*. 2005 22/7 (1821-1824) - summ in ENGL

To elucidate the central mechanisms of sound segregation, we compared responses to a harmonic sound and a mistuned sound using a whole-head magnetoencephalography system. The harmonic sound was composed of a 200-Hz tone and its 2nd to 12th harmonics. The mistuned sound had, instead of the 600-Hz harmonic, a 696-Hz tone. In the right hemisphere, the amplitude of N100m responses evoked by the mistuned sound was significantly larger and the peak latency significantly longer than that evoked by the harmonic sound, suggesting that the right hemisphere plays a more important role than the left in detecting mistuned partials. © Federation of European Neuroscience Societies.

393. On the use of superadditivity as a metric for characterizing multisensory integration in functional neuroimaging studies

- Laurienti P.J., Perrault T.J., Stanford T.R. et al. [P.J. Laurienti, Department of Radiology, Wake Forest University, School of Medicine, Medical Center Boulevard, Winston-Salem, NC 27157, United States] - EXP. BRAIN RES. 2005 166/3-4 (289-297) - summ in ENGL.

A growing number of brain imaging studies are being undertaken in order to better understand the contributions of multisensory processes to human behavior and perception. Many of these studies are designed on the basis of the physiological findings from single neurons in animal models, which have shown that multisensory neurons have the capacity for integrating their different sensory inputs and give rise to a product that differs significantly from either of the unisensory responses. At certain points these multisensory interactions can be superadditive, resulting in a neural response that exceeds the sum of the unisensory responses. Because of the difficulties inherent in interpreting the results of imaging large neuronal populations, superadditivity has been put forth as a stringent criterion for identifying potential sites of multisensory integration. In the present manuscript we discuss issues related to using the superadditive model in human brain imaging studies, focusing on population responses to multisensory stimuli and the relationship between single neuron measures and functional brain imaging measures. We suggest that the results of brain imaging studies be interpreted with caution in regards to multisensory integration. Future directions for imaging multisensory integration are discussed in light of the ideas presented. © Springer-Verlag 2005.

394. How single-trial electrical neuroimaging contributes to multisensory research - Gonzalez Andino S.L., Murray M.M., Foxe J.J. and Menendez R.G.D.P. [R.G.D.P. Menendez, Electrical Neuroimaging Group, Functional Brain Mapping Laboratory, University Hospital of Geneva, 24 Rue Micheli du Crest, 1211 Geneva, Switzerland] - *EXP. BRAIN RES.* 2005 166/3-4 (298-304) - summ in ENGL

This study details a method to statistically determine, on a millisecond scale and for individual subjects, those brain areas whose activity differs between experimental conditions, using single-trial scalp-recorded EEG data. To do this, we non-invasively estimated local field potentials (LFPs) using the ELECTRA distributed inverse solution and applied non-parametric statistical tests at each brain voxel and for each time point. This yields a spatio-temporal activation pattern of differential brain responses. The method is illustrated here in the analysis of auditory-somatosensory (AS) multisensory interactions in four subjects. Differential multisensory responses were temporally and spatially consistent across individuals, with

onset at ${\sim}50$ ms and superposition within areas of the posterior superior temporal cortex that have traditionally been considered auditory in their function. The close agreement of these results with previous investigations of AS multisensory interactions suggests that the present approach constitutes a reliable method for studying multisensory processing with the temporal and spatial resolution required to elucidate several existing questions in this field. In particular, the present analyses permit a more direct comparison between human and animal studies of multisensory interactions and can be extended to examine correlation between electrophysiological phenomena and behavior. © Springer-Verlag 2005.

395. The development of a dialogue between cortex and midbrain to integrate multisensory information - Stein B.E. [B.E. Stein, Department of Neurobiology and Anatomy, School of Medicine, Wake Forest University, Winston-Salem, NC 27157-1010, United States] - *EXP. BRAIN RES.* 2005 166/3-4 (305-315) - summ in ENGL

The anterior ectosylvian (AES) and rostral lateral suprasylvian (rLS) sulci send critical signals to multisensory superior colliculus (SC) neurons that enable them to integrate information from different senses. When either of these areas is temporarily deactivated in adult animals, the ability of SC neurons to integrate multisensory information and, thereby, enhance their responses to cross-modal stimuli is temporarily compromised. As a consequence, the ability to use cross-modal stimuli to enhance SC-mediated behavioral performance is also compromised. In contrast, removal of either one of these areas during early life has little effect on the development of multisensory processes in the SC or on SC-mediated multisensory behaviors and these animals seem very similar to normal controls. These observations suggest that there is considerable plasticity in these cortico-collicular systems during early life, with each area able to compensate for the early loss of the other. However, when both AES and rLS are removed early in life, there appears to be no compensation. The SC neurons now deal with sensory stimuli, even those embedded in multisensory complexes, as if they were there alone, precluding any SC-mediated behavioral benefit to cross-modal stimuli. © Springer-Verlag 2005.

396. Intrinsic connectivity of human superior colliculus - Tardif E., Delacuisine B., Probst A. and Clarke S. [E. Tardif, Institut de Physiologie, Université de Lausanne, rue du Bugnon 7, 1005 Lausanne, Switzerland] - *EXP. BRAIN RES.* 2005 166/3-4 (316-324) - summ in ENGL.

The superior colliculus (SC) is believed to play an important role in sensorimotor integration and orienting behavior. It is classically divided into superficial layers predominantly containing visual neurons and deep layers containing multisensory and premotor neurons. Investigations of intrinsic connectivity within the SC in non-human species initially led to controversy regarding the existence of interlaminar connections between superficial and deep layers. It now seems more likely that such connections exist in a number of species, including non-human primates. In the latter, anatomical data concerning intrinsic SC connectivity are restricted to a limited number of intracellularly labeled neurons. No studies have been conducted to investigate the existence of intrinsic connections of human SC. In the present study, DiI (1,1'-dioctadecyl-3,3,3',3'tetramethylindocarbocyanine perchlorate) and BDA (biotinylated dextran amine) were two tracers used in post-mortem human brains to examine intrinsic SC connections. Injections into the superficial layers revealed tangential connections within superficial layers and radial superficial-layer to deep-layer connections. Within superficial layers, horizontal connections were found over the entire rostro-caudal axis and were mostly directed laterally, i.e. toward the brachium of the inferior colliculus. Superficial-layer to deeplayer connections were more prominent in sections containing the injection site or located close to it. In these sections, an axon bundle having roughly the same diameter as the injection site crossed all deep layers, and individual axons displayed en passant or terminal boutons. The present results suggest that intrinsic connections within superficial layers and radial superficial-layers to deep-layers exist in human SC. The putative roles of these connections are discussed with regard to visual receptive field organization, as well as visuomotor and multisensory integration. © Springer-Verlag 2005.

397. Is the auditory sensory memory sensitive to visual information? - Besle J., Fort A. and Giard M.-H. [J. Besle, INSERM U280, Mental Processes and Brain Activation, 69675 Bron Cedex, France] - EXP. BRAIN RES. 2005 166/3-4 (337-344) - summ in ENGL

The mismatch negativity (MMN) component of auditory eventrelated brain potentials can be used as a probe to study the representation of sounds in auditory sensory memory (ASM). Yet it has been shown that an auditory MMN can also be elicited by an illusory auditory deviance induced by visual changes. This suggests that some visual information may be encoded in ASM and is accessible to the auditory MMN process. It is not known, however, whether visual information affects ASM representation for any audiovisual event or whether this phenomenon is limited to specific domains in which strong audiovisual illusions occur. To highlight this issue, we have compared the topographies of MMNs elicited by non-speech audiovisual stimuli deviating from audiovisual standards on the visual, the auditory, or both dimensions. Contrary to what occurs with audiovisual illusions, each unimodal deviant elicited sensory-specific MMNs, and the MMN to audiovisual deviants included both sensory components. The visual MMN was, however, different from a genuine visual MMN obtained in a visualonly control oddball paradigm, suggesting that auditory and visual information interacts before the MMN process occurs. Furthermore, the MMN to audiovisual deviants was significantly different from the sum of the two sensory-specific MMNs, showing that the processes of visual and auditory change detection are not completely independent. © Springer-Verlag 2005.

398. Simultaneity constancy: detecting events with touch and vision - Harrar V. and Harris L.R. [L.R. Harris, Department Psychology, York University, Toronto, Ont. M3J 1P3, Canada] - *EXP. BRAIN RES.* 2005 166/3-4 (465-473) - summ in ENGL

What are the consequences of visual and tactile neural processing time differences when combining multisensory information about an event on the body's surface? Visual information about such events reaches the brain at a time that is independent of the location of the event. However, tactile information about such events takes different amounts of time to be processed depending on the distance between the stimulated surface and the brain. To investigate the consequences of these differences, we measured reaction times to touches and lights on different parts of the body and the perceived subjective simultaneity (PSS) for various combinations. The PSSs for pairs of stimuli were predicted by the differences in reaction times. When lights and touches were on different body parts (i.e. the hand and foot) a trend towards compensation for any processing time differences was found, such that simultaneity was veridically perceived. When stimuli were both on the foot, subjects perceived simultaneity when the light came on significantly earlier than the touch, despite similar processing times for these stimuli. When the stimuli were both on the hand, however, there was complete compensation for the significant processing time differences between the light and touch such that simultaneity was correctly perceived, a form of simultaneity constancy. To identify if there was a single simultaneity constancy mechanism or multiple parallel mechanisms, we altered the PSS of an auditory-visual stimulus pair and looked for effects on the PSS of a visual-touch pair. After repeated exposure to a light/sound pair with a fixed time lag between them, there was no effect on the PSS of a touch-light pair, suggesting multiple parallel simultaneity constancy mechanisms. © Springer-Verlag 2005.

399. Dynamic circuitry for updating spatial representations. I. Behavioral evidence for interhemispheric transfer in the splitbrain macaque - Berman R.A., Heiser L.M., Saunders R.C. and Colby C.L. [C.L. Colby, 115 Mellon Institute, 4400 5th Ave, Pittsburgh, PA 15213, United States] - *J. NEUROPHYSIOL*. 2005 94/5 (3228-3248) - summ in ENGL

Internal representations of the sensory world must be constantly adjusted to take movements into account. In the visual system, spatial updating provides a mechanism for maintaining a coherent map of salient locations as the eyes move. Little is known, however, about the pathways that produce updated spatial representations. In the present study, we asked whether direct cortico-cortical links are required for spatial updating. We addressed this question by investigating whether the forebrain commissures-the direct path between the two cortical hemispheres-are necessary for updating

visual representations from one hemifield to the other. We assessed spatial updating in two split-brain monkeys using the double-step task, which involves saccades to two sequentially appearing targets. Accurate performance requires that the representation of the second target be updated to take the first saccade into account. We made two central discoveries regarding the pathways that underlie spatial updating. First, we found that split-brain monkeys exhibited a selective initial impairment on double-step sequences that required updating across visual hemifields. Second, and most surprisingly, these impairments were neither universal nor permanent: the monkeys were ultimately able to perform the across-hemifield sequences and, in some cases, this ability emerged rapidly. These findings indicate that direct cortical links provide the main substrate for updating visual representations, but they are not the sole substrate. Rather, a unified and stable representation of visual space is supported by a redundant cortico-subcortical network with a striking capacity for reorganization.

400. Dynamic circuitry for updating spatial representations. II. Physiological evidence for interhemispheric transfer in area LIP of the split-brain macaque - Heiser L.M., Berman R.A., Saunders R.C. and Colby C.L. [C.L. Colby, 115 Mellon Institute, 4400 5th Ave, Pittsburgh, PA 15213, United States] - *J. NEUROPHYSIOL.* 2005 94/5 (3249-3258) - summ in ENGL

With each eye movement, a new image impinges on the retina, yet we do not notice any shift in visual perception. This perceptual stability indicates that the brain must be able to update visual representations to take our eye movements into account. Neurons in the lateral intraparietal area (LIP) update visual representations when the eyes move. The circuitry that supports these updated representations remains unknown, however. In this experiment, we asked whether the forebrain commissures are necessary for updating in area LIP when stimulus representations must be updated from one visual hemifield to the other. We addressed this question by recording from LIP neurons in split-brain monkeys during two conditions: stimulus traces were updated either across or within hemifields. Our expectation was that across-hemifield updating activity in LIP would be reduced or abolished after transection of the forebrain commissures. Our principal finding is that LIP neurons can update stimulus traces from one hemifield to the other even in the absence of the forebrain commissures. This finding provides the first evidence that representations in parietal cortex can be updated without the use of direct cortico-cortical links. The second main finding is that updating activity in LIP is modified in the split-brain monkey: across-hemifield signals are reduced in magnitude and delayed in onset compared with within-hemifield signals, which indicates that the pathways for across-hemifield updating are less effective in the absence of the forebrain commissures. Together these findings reveal a dynamic circuit that contributes to updating spatial representations. Copyright © 2005 The American Physiological Society.

401. Sparsening and temporal sharpening of olfactory representations in the honeybee mushroom bodies - Szyszka P., Ditzen M., Galkin A. et al. [P. Szyszka, Institut für Biologie-Neurobiologie, Freie Universität Berlin, Königin-Luise-Strasse 28/30, 14195 Berlin, Germany] - *J. NEUROPHYSIOL*. 2005 94/5 (3303-3313) - summ in ENGL

We explored the transformations accompanying the transmission of odor information from the first-order processing area, the antennal lobe, to the mushroom body, a higher-order integration center in the insect brain. Using Ca2+ imaging, we recorded activity in the dendrites of the projection neurons that connect the antennal lobe with the mushroom body. Next, we recorded the presynaptic terminals of these projection neurons. Finally, we characterized their postsynaptic partners, the intrinsic neurons of the mushroom body, the clawed Kenyon cells. We found fundamental differences in odor coding between the antennal lobe and the mushroom body. Odors evoked combinatorial activity patterns at all three processing stages, but the spatial patterns became progressively sparser along this path. Projection neuron dendrites and boutons showed similar response profiles, but the boutons were more narrowly tuned to odors. The transmission from projection neuron boutons to Kenyon cells was accompanied by a further sparsening of the population

code. Activated Kenyon cells were highly odor specific. Furthermore, the onset of Kenyon cell responses to projection neurons occurred within the first 200 ms and complex temporal patterns were transformed into brief phasic responses. Thus two types of transformations occurred within the MB: sparsening of a combinatorial code, mediated by pre- and postsynaptic processing within the mushroom body microcircuits, and temporal sharpening of post-synaptic Kenyon cell responses, probably involving a broader loop of inhibitory recurrent neurons. Copyright © 2005 The American Physiological Society.

402. Chronic suppression of activity in barrel field cortex downregulates sensory responses in contralateral barrel field cortex - Li L., Rema V. and Ebner F.F. [F.F. Ebner, Dept. of Psychology, Vanderbilt University, Nashville, TN 37203, United States] - *J. NEUROPHYSIOL.* 2005 94/5 (3342-3356) - summ in ENGL

Numerous lines of evidence indicate that neural information is exchanged between the cerebral hemispheres via the corpus callosum. Unilateral ablation lesions of barrel field cortex (BFC) in adult rats induce strong suppression of background and evoked activity in the contralateral barrel cortex and significantly delay the onset of experience-dependent plasticity. The present experiments were designed to clarify the basis for these interhemispheric effects. One possibility is that degenerative events, triggered by the lesion, degrade contralateral cortical function. Another hypothesis, alone or in combination with degeneration, is that the absence of interhemispheric activity after the lesion suppresses contralateral responsiveness. The latter hypothesis was tested by placing an Alzet minipump subcutaneously and connecting it via a delivery tube to a cannula implanted over BFC. The minipump released muscimol, a GABA_A receptor agonist at a rate of $1 \mu l l h$, onto one barrel field cortex for 7 days. Then with the pump still in place, single cells were recorded in the contralateral BFC under urethan anesthesia. The data show a -50% reduction in principal whisker responses (D2) compared with controls, with similar reductions in responses to the D1 and D3 surround whiskers. Despite these reductions, spontaneous firing is unaffected. Fast spiking units are more sensitive to muscimol application than regular spiking units in both the response magnitude and the center/surround ratio. Effects of muscimol are also layer specific. Layer II/III and layer IV neurons decrease their responses significantly, unlike layer V neurons that fail to show significant deficits. The results indicate that reduced activity in one hemisphere alters cortical excitability in the other hemisphere in a complex manner. Surprisingly, a prominent response decrement occurs in the short-latency (3-10 ms) component of principal whisker responses, suggesting that suppression may spread to neurons dominated by thalamocortical inputs after interhemispheric connections are inactivated. Bilateral neurological impairments have been described after unilateral stroke lesions in the clinical literature. Copyright © 2005 The American Physiological Society.

403. Prevalence of stereotypical responses to mistuned complex tones in the inferior colliculus - Sinex D.G., Li H. and Velenovsky D.S. [D.G. Sinex, Utah State University, Department of Psychology, 2810 Old Main Hill, Logan, UT 84322-2810, United States] - *J. NEUROPHYSIOL.* 2005 94/5 (3523-3537) - summ in ENGL

The human auditory system has an exceptional ability to separate competing sounds, but the neural mechanisms that underlie this ability are not understood. Responses of inferior colliculus (IC)neurons to "mistuned" complex tones were measured to investigate possible neural mechanisms for spectral segregation. A mistuned tone is a harmonic complex tone in which the frequency of one component has been changed; that component may be heard as a separate sound source, suggesting that the mistuned tone engages the same mechanisms that contribute to the segregation of natural sounds. In this study, the harmonic tone consisted of eight harmonics of 250 Hz; in the mistuned tone, the frequency of the fourth harmonic was increased by 12% (120 Hz). The mistuned tone elicited a stereotypical discharge pattern, consisting of peaks separated by about 8 ms and a response envelope modulated with a period of 100 ms, which bore little resemblance to the discharge pattern elicited by the harmonic tone or to the stimulus waveform. Similar discharge patterns were elicited from many neurons with a range of characteristic frequencies, especially from neurons that

exhibited short-latency sustained responses to pure tones. In contrast, transient and long-latency neurons usually did not exhibit the stereotypical discharge pattern. The discharge pattern was generally stable when the stimulus level or component phase was varied; the major effect of these manipulations was to shift the phase of the response envelope. Simulation of IC responses with a computational model suggested that off-frequency inhibition could produce discharge patterns with these characteristics. Copyright © 2005 The American Physiological Society.

404. Laminar organization of response properties in primary visual cortex of the gray squirrel (Sciurus carolinensis) - Heimel J.A., Van Hooser S.D. and Nelson S.B. [J.A. Heimel, Netherlands Ophthalmic Research Institute, Meibergdreef 47, 1105 BA Amsterdam, Netherlands] - *J. NEUROPHYSIOL.* 2005 94/5 (3538-3554) - summ in ENGL

The gray squirrel (Sciurus carolinensis) is a diurnal highly visual rodent with a cone-rich retina. To determine which features of visual cortex are common to highly visual mammals and which are restricted to non-rodent species, we studied the laminar organization of response properties in primary visual area V1 of isoflurane-anesthetized squirrels using extra-cellular single-unit recording and sinusoidal grating stimuli. Of the responsive cells, 75% were tuned for orientation. Only 10% were directionally selective, almost all in layer 6, a layer receiving direct input from the dorsal lateral geniculate nucleus (LGN). Cone opponency was widespread but almost absent from layer 6. Median optimal spatial frequency tuning was 0.21 cycles/°. Median optimal temporal frequency a high 5.3 Hz. Layer 4 had the highest percentage of simple cells and shortest latency (26 ms). Layers 2/3 had the lowest spontaneous activity and highest temporal frequency tuning. Layer 5 had the broadest spatial frequency tuning and most spontaneous activity. At the layer 4/5 border were sustained cells with high cone opponency. Simple cells, determined by modulation to drifting sinusoidal gratings, responded with shorter latencies, were more selective for orientation and direction, and were tuned to lower spatial frequencies. A comparison with other mammals shows that although the laminar organization of orientation selectivity is variable, the cortical input layers contain more linear cells in most mammals. Nocturnal mammals appear to have more orientation-selective neurons in V1 than diurnal mammals of similar size. Copyright © 2005 The American Physiological Society.

405. Environmental enrichment increases paired-pulse depression in rat auditory cortex - Percaccio C.R., Engineer N.D., Pruette A.L. et al. [M.P. Kilgard, Neuroscience Program, School of Behavioral and Brain Sciences, University of Texas at Dallas, Richardson, TX 75083-0688, United States] - *J. NEUROPHYSIOL*. 2005 94/5 (3590-3600) - summ in ENGL

Temporal features are important for the identification of natural sounds. Earlier studies have shown that cortical processing of temporal information can be altered by long-term experience with modulated sounds. In a previous study, we observed that environmental enrichment dramatically increased the response of cortical neurons to single tone and noise burst stimuli in both awake and anesthetized rats. Here, we evaluate how enrichment influences temporal information processing in the auditory cortex. We recorded responses to repeated tones and noise bursts in awake rats using epidural evoked potentials and in anesthetized rats using microelectrodes. Enrichment increased the response of cortical neurons to stimuli presented at slow rates and decreased the response to stimuli presented at fast rates relative to controls. Our observation that enrichment substantially increased response strength and forward masking is consistent with earlier reports that longterm potentiation of cortical synapses is associated with increased paired-pulse depression. Enrichment also increased response synchronization at slow rates and decreased synchronization at fast rates. Paired-pulse depression increased within days of environmental enrichment and was restored to normal levels after return to standard housing conditions. These results are relevant to several clinical disorders characterized by abnormal gating of sensory information, including autism, schizophrenia, and dyslexia. Copyright © 2005 The American Physiological Society.

406. Sympathoinhibition from ventrolateral periaqueductal gray mediated by the caudal midline medulla - Dean C. [Dr. C. Dean, Dept. Anesthesiology/151, Zablocki VA Medical Center, Milwaukee, WI 53295, United States] - *AM. J. PHYSIOL. REGUL. INTEGR. COMP. PHYSIOL.* 2005 289/5 58-5 (R1477-R1481) - summ in ENGL

Activation of neurons in the ventrolateral region of the periaqueductal gray (vlPAG) can elicit a decrease in renal sympathetic nerve activity and blood pressure. The present study investigated whether the vlPAG-evoked sympathoinhibitory response depends on neurons in the caudal midline medulla (CMM). In pentobarbital-anesthetized rats, activation of neurons in the vlPAG evoked a decrease in renal sympathetic nerve activity to 29.4 \pm 4.8% below baseline levels and arterial blood pressure fell 8.9 \pm 1.6 mmHg (n = 20). Microinjection of the GABA agonist muscimol into sympathoinhibitory regions of the CMM significantly attenuated the vlPAG-evoked Sympathoinhibition to 17.9 \pm 4.1% below baseline and the depressor response to 4.3 \pm 1.2 mmHg. At 65% (13/20)of the sites examined, the vIPAG-evoked sympathoinhibition was responsive to CMM muscimol microiniection and attenuated from 34.2% to 11.5%, with the depressor response reduced from 14.8 to 3 mmHg. Microinjection of muscimol at the remaining 35% of the CMM sympathoinhibitory sites was ineffective on the vlPAGevoked sympathoinhibition and depressor response. These data indicate that sympathoinhibitory and hypotensive responses elicited by activation of neurons in the vIPAG can be mediated by neurons in the sympathoinhibitory region of the CMM. The finding that the vlPAG-evoked response is not affected by muscimol at all CMM sympathoinhibitory sites also suggests that sympathoinhibitory sites in the CMM are not homogeneous and can mediate functionally different responses.

407. Visual selection and posterior parietal cortex: Effects of repetitive transcranial magnetic stimulation on partial report analyzed by Bundesen's theory of visual attention - Hung J., Driver J. and Walsh V. [Dr. J. Hung, Department of Neurology, Chang Gung Memorial Hospital, Taipei 10507, Taiwan] - *J. NEU-ROSCI.* 2005 25/42 (9602-9612) - summ in ENGL

Posterior parietal cortex (PPC) may contribute to visual selection by exerting top-down influences on visual processing. To seek direct evidence for this, we used 10 Hz repetitive transcranial magnetic stimulation (rTMS) over right or left PPC in nine healthy volunteers during a partial (selective) report task that allows quantitative assessment of top-down control and other parameters. Participants reported digits in a relevant color ("targets") but not those in an irrelevant color (" nontargets") from a brief masked display, in which a target could appear alone or together with an accompanying item (nontarget or target) in the same or opposite hemifield. Generally, a given target is identified better when presented with a nontarget than with another target, indicating top-down selection of task-relevant targets; this applied here with no rTMS or left PPC rTMS. However, rTMS over the right PPC changed the performance pattern. A left target no longer impeded report of a right target more strongly than did a left nontarget, whereas the greater impact of a right target than a right nontarget in disrupting report of a left target was increased. Formal analysis in terms of Bundesen's (1990) theory of visual attention indicated that right PPC rTMS diminished top-down control for the left hemifield while enhancing this for the right hemifield, particularly for bilateral two-item displays. These findings indicate a role for right PPC in top-down spatial selection, which applies even when the target is defined by a nonspatial property (here color). Copyright © 2005 Society for Neuroscience.

408. Differential maturation of GABA action and anion reversal potential in spinal lamina I neurons: Impact of chloride extrusion capacity - Cordero-Erausquin M., Coull J.A.M., Boudreau D. et al. [Dr. Y. De Koninck, Division de Neurobiologie Cellulaire, Centre de Recherche Université Laval Robert-Giffard, 2601, Chemin de la Canardière, Québec, Que. G1J 2G3, Canada] - J. NEUROSCI. 2005 25/42 (9613-9623) - summ in ENGL

A deficit in inhibition in the spinal dorsal horn has been proposed to be an underlying cause of the exaggerated cutaneous sensory reflexes observed in newborn rats. However, the developmental shift in transmembrane anion gradient, potentially affecting the outcome of GABA_A transmission, was shown to be completed within

1 week after birth in the spinal cord, an apparent disparity with the observation that reflex hypersensitivity persists throughout the first 2-3 postnatal weeks. To further investigate this issue, we used several approaches to assess the action of GABA throughout development in spinal lamina I (LI) neurons. GABA induced an entry of extracellular calcium in LI neurons from postnatal day 0 (P0) to P21 rats, which involved T- and N-type voltage-gated calcium channels. Gramicidin perforated-patch recordings revealed that the shift in anion gradient was completed by P7 in LI neurons. However, high chloride pipette recordings demonstrated that these neurons had not reached their adult chloride extrusion capacity by P10-P11. Simultaneous patch-clamp recordings and calcium imaging revealed that biphasic responses to GABA, consisting of a primary hyperpolarization followed by a rebound depolarization, produced a rise in [Ca2+]i. Thus, even if E anion predicts GABAA-induced hyperpolarization from rest, a low chloride extrusion capacity can cause a rebound depolarization and an ensuing rise in [Ca²⁺]_i. We demonstrate that GABA action in LI neurons matures throughout the first 3 postnatal weeks, therefore matching the time course of maturation of withdrawal reflexes. Immature spinal GABA signaling may thus contribute to the nociceptive hypersensitivity in infant rats. Copyright © 2005 Society for Neuroscience.

409. Organization of the human trichromatic cone mosaic - Hofer H., Carroll J., Neitz J. et al. [H. Hofer, College of Optometry, University of Houston, 505 J. Davis Armistead Building, Houston, TX 77204-2020, United States] - *J. NEUROSCI.* 2005 25/42 (9669-9679) - summ in ENGL

Using high-resolution adaptive-optics imaging combined with retinal densitometry, we characterized the arrangement of short-S), middle- (M), and long- (L) wavelength-sensitive cones in eight human foveal mosaics. As suggested by previous studies, we found males with normal color vision that varied in the ratio of L to M cones (from 1.1:1 to 16.5:1). We also found a protan carrier with an even more extreme L:M ratio (0.37:1). All subjects had nearly identical S-cone densities, indicating independence of the developmental mechanism that governs the relative numerosity of L/M and S cones. L:M cone ratio estimates were correlated highly with those obtained in the same eyes using the flicker photometric electroretinogram (ERG), although the comparison indicates that the signal from each M cone makes a larger contribution to the ERG than each L cone. Although all subjects had highly disordered arrangements of L and M cones, three subjects showed evidence for departures from a strictly random rule for assigning the L and M cone photopigments. In two retinas, these departures corresponded to local clumping of cones of like type. In a third retina, the L:M cone ratio differed significantly at two retinal locations on opposite sides of the fovea. These results suggest that the assignment of L and M pigment, although highly irregular, is not a completely random process. Surprisingly, in the protan carrier, in which X-chromosome inactivation would favor L- or M-cone clumping, there was no evidence of clumping, perhaps as a result of cone migration during foveal development. Copyright © 2005 Society for Neuroscience.

410. Hunting increases adaptive auditory map plasticity in adult barn owls - Bergan J.F., Ro P., Ro D. and Knudsen E.I. [E.I. Knudsen, Department of Neurobiology, Stanford University School of Medicine, Stanford, CA 94305-5125, United States] - *J. NEURO-SCI.* 2005 25/42 (9816-9820) - summ in ENGL

The optic tectum (OT) of barn owls contains topographic maps of auditory and visual space. Barn owls reared with horizontally displacing prismatic spectacles (prisms) acquire a novel auditory space map in the OT that restores alignment with the prismatically displaced visual map. Although juvenile owls readily acquire alternative maps of auditory space as a result of experience, this plasticity is reduced greatly in adults. We tested whether hunting live prey, a natural and critically important behavior for barn owls, increases auditory map plasticity in adult owls. Two groups of naive adult owls were fit with prisms. The first group was fed dead mice during 10 weeks of prism experience, while the second group was required to hunt live prey for an identical period of time. When the owls hunted live prey, auditory maps shifted substantially farther (five times farther, on average) and the consistency of tuning curve shifts within each map increased. Only a short period of time in

each day, during which the two groups experienced different conditions, accounts for this effect. In addition, increased map plasticity correlated with behavioral improvements in the owls' ability to strike and capture prey. These results indicate that the experience of hunting dramatically increases adult adaptive plasticity in this pathway. Copyright © 2005 Society for Neuroscience.

411. Comparing the effects of auditory deprivation and sign language within the auditory and visual cortex - Fine I., Finney E.M., Boynton G.M. and Dobkins K.R. [K.R. Dobkins, Department of Psychology, University of California, San Diego, San Diego, CA 92093, United States] - *J. COGN. NEUROSCI.* 2005 17/10 (1621-1637) - summ in ENGL

To investigate neural plasticity resulting from early auditory deprivation and use of American Sign Language, we measured responses to visual stimuli in deaf signers, hearing signers, and hearing nonsigners using functional magnetic resonance imaging. We examined "compensatory hypertrophy" (changes in the responsivity/size of visual cortical areas) and "cross-modal plasticity" (changes in auditory cortex responses to visual stimuli). We measured the volume of early visual areas (V1, V2, V3, V4, and MT+). We also measured the amplitude of responses within these areas, and within the auditory cortex, to a peripheral visual motion stimulus that was attended or ignored. We found no major differences between deaf and hearing subjects in the size or responsivity of early visual areas. In contrast, within the auditory cortex, motion stimuli evoked significant responses in deaf subjects, but not in hearing subjects, in a region of the right auditory cortex corresponding to Brodmann's areas 41, 42, and 22. This hemispheric selectivity may be due to a predisposition for the right auditory cortex to process motion; earlier studies report a right hemisphere bias for auditory motion in hearing subjects. Visual responses within the auditory cortex of deaf subjects were stronger for attended than ignored stimuli, suggesting top-down processes. Hearing signers did not show visual responses in the auditory cortex, indicating that crossmodal plasticity can be attributed to auditory deprivation rather than sign language experience. The largest effects of auditory deprivation occurred within the auditory cortex rather than the visual cortex, suggesting that the absence of normal input is necessary for large-scale cortical reorganization to occur. © 2005 Massachusetts Institute of Technology.

412. Effects of vestibular rotatory accelerations on covert attentional orienting in vision and touch - Figliozzi F., Guariglia P., Silvetti M. et al. [Prof. F. Doricchi, Centro Ricerche di Neuropsicologia, Fondazione Santa Lucia, IRCCS, Via Ardeatina 306, 00179 Rome, Italy] - *J. COGN. NEUROSCI.* 2005 17/10 (1638-1651) - summ in ENGL

Peripheral vestibular organs feed the central nervous system with inputs favoring the correct perception of space during head and body motion. Applying temporal order judgments (TOJs) to pairs of simultaneous or asynchronous stimuli presented in the left and right egocentric space, we evaluated the influence of leftward and rightward vestibular rotatory accelerations given around the vertical head-body axis on covert attentional orienting. In a first experiment, we presented visual stimuli in the left and right hemifield. In a second experiment, tactile stimuli were presented to hands lying on their anatomical side or in a crossed position across the sagittal body midline. In both experiments, stimuli were presented while normal subjects suppressed or did not suppress the vestibulo-ocular response (VOR) evoked by head-body rotation. Independently of VOR suppression, visual and tactile stimuli presented on the side of rotation were judged to precede simultaneous stimuli presented on the side opposite the rotation. When limbs were crossed, attentional facilitatory effects were only observed for stimuli presented to the right hand lying in the left hemispace during leftward rotatory trials with VOR suppression. This result points to spatiotopic rather than somatotopic influences of vestibular inputs, suggesting that cross-modal effects of these inputs on tactile ones operate on a representation of space that is updated following arm crossing. In a third control experiment, we demonstrated that temporal prioritization of stimuli presented on the side of rotation was not determined by response bias linked to spatial compatibility between the directions of rotation and the directional labels used in TOJs (i.e., "left" or "right" first). These findings suggest that during passive rotatory head-body accelerations, covert attention is shifted toward the direction of rotation and the direction of the fast phases of the VOR. © 2005 Massachusetts Institute of Technology.

413. Hemeoxygenase-2 as an O₂ sensor in K⁺ channel-dependent chemotransduction - Kemp P.J. [P.J. Kemp, School of Biosciences, Cardiff University, Museum Avenue, Cardiff CF10 3US, United Kingdom] - *BIOCHEM. BIOPHYS. RES. COMMUN.* 2005 338/1 (648-652) - summ in ENGL

The physiological response of the carotid body is critically dependent upon oxygen-sensing by potassium channels expressed in glomus cells. One such channel is the large conductance, voltage- and calcium-dependent potassium channel, BK_{Ca} . Although it is well known that a decrease in oxygen evokes glomus cell depolarization, voltage-gated calcium entry, and transmitter release, the molecular identity of the upstream oxygen sensor has been the subject of some controversy for decades. Recently, we have demonstrated that hemeoxygenase-2 associates tightly with recombinant BK_{Ca} and that activity of this enzyme confers oxygen sensitivity to the BK_{Ca} channel complex. Similar observations were also made in native channels recorded from carotid body glomus cells, suggesting that hemoxygenase-2 functions as an oxygen sensor of native and recombinant BK_{Ca} channels. © 2005 Elsevier Inc. All rights reserved.

414. Humans as an animal model for systems-level organization of olfaction - Zelano C. and Sobel N. [C. Zelano, Program in Biophysics, University of California, Berkeley, Berkeley, CA 94720, United States] - *NEURON* 2005 48/3 (431-454) - summ in ENGL

The past 15 years have seen significant advances in the study of olfaction, with particular emphasis on elucidating the molecular building blocks of the sensory process. However, much of the systems-level organization of olfaction remains unexplored. Here, we provide an overview at this level, highlighting results obtained from studying humans, whom we think provide an underutilized, yet critical, animal model for olfaction. Copyright ©2005 by Elsevier Inc.

415. Taste recognition: Food for thought - Scott K. [K. Scott, Department of Molecular and Cell Biology, Helen Wills Neuroscience Institute, University of California, Berkeley, Berkeley, CA 94720, United States] - *NEURON* 2005 48/3 (455-464) - summ in ENGL

The ability to identify food that is nutrient-rich and avoid toxic substances is essential for an animal's survival. Although olfaction and vision contribute to food detection, the gustatory system acts as a final checkpoint control for food acceptance or rejection behavior. Recent studies with model organisms such as mice and Drosophila have identified candidate taste receptors and examined the logic of taste coding in the periphery. Despite differences in terms of gustatory anatomy and taste-receptor families, these gustatory systems share a basic organization that is different from other sensory systems. This review will summarize our current understanding of taste recognition in mammals and Drosophila, highlighting similarities and raising several as yet unanswered questions. Copyright ©2005 by Elsevier Inc.

See also: 421, 430, 436, 441, 447, 565.

4.2. Motor physiology

416. On the impact of attention and motor planning on the lateral geniculate nucleus - Casagrande V.A., Sáry G., Royal D. and Ruiz O. [V.A. Casagrande, Department of Cell and Developmental Biology, Vanderbilt University, Nashville, TN, United States] - *PROG. BRAIN RES.* 2005 149/- (11-29) - summ in ENGL

Although the lateral geniculate nucleus (LGN) is one of the most thoroughly characterized thalamic nuclei, its functional role remains controversial. Traditionally, the LGN in primates has been viewed as the lowest level of a set of feedforward parallel visual pathways to cortex. These feedforward pathways are pictured as connected hierarchies of areas designed to construct the visual image gradually - adding more complex features as one marches through successive levels of the hierarchy. In terms of synapse number and circuitry,

the anatomy suggests that the LGN can be viewed also as the ultimate terminus in a series of feedback pathways that originate at the highest cortical levels. Since the visual system is dynamic, a more accurate picture of image construction might be one in which information flows bidirectionally, through both the feedforward and feedback pathways constantly and simultaneously. Based upon evidence from anatomy, physiology, and imaging, we argue that the LGN is more than a simple gate for retinal information. Here, we review evidence that suggests that one function of the LGN is to enhance relevant visual signals through circuits related to both motor planning and attention. Specifically, we argue that major extraretinal inputs to the LGN may provide: (1) eye movement information to enhance and bind visual signals related to new saccade targets and (2) top-down and bottom-up information about target relevance to selectively enhance visual signals through spatial attention. Copyright © 2005 Elsevier BV. All rights reserved.

417. The internal model and the leading joint hypothesis: Implications for control of multi-joint movements - Dounskaia N. [N. Dounskaia, Department of Kinesiology, Arizona State University, P.O. Box 870404, Tempe, AZ 85287-0404, United States] - *EXP. BRAIN RES.* 2005 166/1 (1-16) - summ in ENGL

This article presents a theoretical generalization of recent experimental findings accumulated in support of two concepts of inter-segmental dynamics regulation during multi-joint movements. The concepts are the internal model of inter-segmental dynamics and the leading joint hypothesis (LJH). The internal model of limb dynamics is a well-established interpretation of feed-forward control. Recent experiments have generated new information about the organization of the internal model and its role in regulation of inter-segmental dynamics. The LJH, which proposes a simplified principle of the regulation of inter-segmental dynamics, is at the beginning stage of development. This paper outlines major results obtained in these two research directions and demonstrates that the two groups of findings complement and augment each other, suggesting a simple and robust hierarchical strategy of multi-joint movement control that exploits specific mechanical properties of human limbs. © Springer-Verlag 2005.

418. Age-related changes in grasping force modulation - Voelcker-Rehage C. and Alberts J.L. [C. Voelcker-Rehage, Jacobs Centre for Lifelong Learning and Institutional Development, International University Bremen, Bremen, Germany] - *EXP. BRAIN RES.* 2005 166/1 (61-70) - summ in ENGL

The aim of this study was to determine the effect of age on the modulation of forces produced by the digits and to determine the effects of practice on the control of these forces in young and older adults. Young (n=14, 19-28 years) and old (n=12, 67-75 years)adults used a precision grip to perform a variable force-tracking task (sine wave, 5-25% of maximum voluntary force) with their dominant hand. Participants performed 100 practice trials over 2 consecutive days. Results indicated that both groups improved accuracy of force tracking as a result of practice. Younger adults performed the task at a higher level in pre- and post-test conditions compared with older adults. Younger adults showed improvements in force control in force generation and release phases. Older adults reached performance levels comparable with younger adults' pretest performance, but only after extended practice. In contrast to young adults, older adults' performance during the force release phases remained quite variable. These data suggest that older adults are impaired in the accurate release of grip force. Varied force release patterns that disrupt the precision of force modulation may contribute to older adults' diminished dexterous abilities. © Springer-Verlag 2005.

419. Spatio-spectral filters for improving the classification of single trial EEG - Lemm S., Blankertz B., Curio G. and Müller K.-R. [S. Lemm, Department of Intelligent Data Analysis, FIRST Fraunhofer Institute, 12489 Berlin, Germany] - *IEEE TRANS. BIO-MED. ENG.* 2005 52/9 (1541-1548) - summ in ENGL

Data recorded in electroencephalogram (EEG)-based brain-computer interface experiments is generally very noisy, non-stationary, and contaminated with artifacts that can deteriorate discrimination/classification methods. In this paper, we extend the common spatial pattern (CSP) algorithm with the aim to alleviate these adverse

effects. In particular, we suggest an extension of CSP to the state space, which utilizes the method of time delay embedding. As we will show, this allows for individually tuned frequency filters at each electrode position and, thus, yields an improved and more robust machine learning procedure. The advantages of the proposed method over the original CSP method are verified in terms of an improved information transfer rate (bits per trial) on a set of EEGrecordings from experiments of imagined limb movements. © 2005 IEEE.

420. Visual spatial attention control in an independent brain-computer interface - Kelly S.P., Lalor E.C., Finucane C. et al. [S.P. Kelly, Department of Electronic and Electrical Engineering, University College Dublin, Belfield, Dublin 4, Ireland] - *IEEE TRANS. BIOMED. ENG.* 2005 52/9 (1588-1596) - summ in ENGL

This paper presents a novel brain computer interface (BCI)design employing visual evoked potential (VEP) modulations in a paradigm involving no dependency on peripheral muscles or nerves. The system utilizes electrophysiological correlates of visual spatial attention mechanisms, the self-regulation of which is naturally developed through continuous application in everyday life. An interface involving real-time biofeedback is described, demonstrating reduced training time in comparison to existing BCIs based on selfregulation paradigms. Subjects were cued to covertly attend to a sequence of letters superimposed on a flicker stimulus in one visual field while ignoring a similar stimulus of a different flicker frequency in the opposite visual field. Classification of left/right spatial attention is achieved by extracting steady-state visual evoked potentials (SSVEPs) elicited by the stimuli. Six out of eleven physically and neurologically healthy subjects demonstrate reliable control in binary decision-making, achieving at least 75% correct selections in at least one of only five sessions, each of approximately 12min duration. The highest-performing subject achieved over 90% correct selections in each of four sessions. This independent BCI may provide a new method of real-time interaction for those with little or no peripheral control, with the added advantage of requiring only brief training. © 2005 IEEE.

421. Somato-motor inhibitory processing in humans: A study with MEG and ERP - Nakata H., Inui K., Wasaka T. et al. [Dr. H. Nakata, Department of Integrative Physiology, National Institute for Physiological Sciences, Myodaiji, Okazaki, 444-8585, Japan] - *EUR. J. NEUROSCI.* 2005 22/7 (1784-1792) - summ in ENGL

The go/nogo task is a useful paradigm for recording event-related potentials (ERPs) to investigate the neural mechanisms of response inhibition. In nogo trials, a negative deflection at around 140-300 ms (N2), which has been called the 'nogo potential', is elicited at the frontocentral electrodes, compared with ERPs recorded in go trials. In the present study, we investigated the generators of nogo potentials by recording ERPs and by using magnetoencephalography (MEG) simultaneously during somatosensory go/nogo tasks to elucidate the regions involved in generating nogo potentials. ERP data revealed that the amplitude of the nogo-N140 component, which peaked at about 155 ms from frontocentral electrodes, was significantly more negative than that of go-N140. MEG data revealed that a long-latency response peaking at approximately 160 ms, termed nogo-M140 and corresponding to nogo-N140, was recorded in only nogo trials. The equivalent current dipole of nogo-M140 was estimated to lie around the posterior part of the inferior frontal sulci in the prefrontal cortex. These results revealed that both nogo-N140 and nogo-M140 evoked by somatosensory go/nogo tasks were related to the neural activity generated from the prefrontal cortex. Our findings combining MEG and ERPs clarified the spatial and temporal processing related to somato-motor inhibition caused in the posterior part of the inferior frontal sulci in the prefrontal cortex in humans. © Federation of European Neuroscience Societies.

422. Temperature compensation of neuromuscular modulation in Aplysia - Zhurov Y. and Brezina V. [V. Brezina, Department of Neuroscience, Box 1218, Mt. Sinai School of Medicine, 1 Gustave L. Levy Place, New York, NY 10029, United States] - *J. NEUROPHYSIOL.* 2005 94/5 (3259-3277) - summ in ENGL

Physiological systems that must operate over a range of temperatures often incorporate temperature-compensatory mechanisms to maintain their output within a relatively narrow, functional range of

values. We analyze here an example in the accessory radula closer (ARC) neuromuscular system, a representative part of the feeding neuromusculature of the sea slug Aplysia. The ARC muscle's two motor neurons, B15 and B16, release, in addition to ACh that contracts the muscle, modulatory peptide cotransmitters that, through a complex network of effects in the muscle, shape the ACh-induced contractions. It is believed that this modulation is critical in optimizing the performance of the muscle for successful, efficient feeding behavior. However, previous work has shown that the release of the modulatory peptides from the motor neurons decreases dramatically with increasing tem-perature. From 15 to 25°C, for example, release decreases 20-fold. Yet Aplysia live and feed successfully not only at 15°C, but at 25°C and probably at higher temperatures. Here, working with reduced B15/B16-ARC preparations in vitro as well as a mathematical model of the system, we have found a resolution of this apparent paradox. Although modulator release decreases 20-fold when the temperature is raised from 15 to 25°C, the observed modulation of contraction shape does not decrease at all. Two mechanisms are responsible. First, further downstream within the modulatory network, the modulatory effects themselvesexperimentally dissected by exogenous modulator application-have temperature dependencies opposite to that of modulator release, increasing with temperature. Second, the saturating curvature of the dose-response relations within the network diminishes the downstream impact of the decrease of modulator release. Thus two quite distinct mechanisms, one depending on the characteristics of the individual components of the network and the other emerging from the network's structure, combine to compensate for temperature changes to maintain the output of this physiological system. Copyright © 2005 The American Physiological Society.

423. A role for hip position in initiating the swing-to-stance transition in walking cats - McVea D.A., Donelan J.M., Tachibana A. and Pearson K.G. [D.A. McVea, Dept. of Physiology, University of Alberta, Edmonton, Alta. T6G 2H7, Canada] - *J. NEUROPHYSIOL.* 2005 94/5 (3497-3508) - summ in ENGL

In this investigation, we obtained data that support the hypothesis that afferent signals associated with hip flexion play a role in initiating the swing-to-stance transition of the hind legs in walking cats. Direct evidence came from observations in walking decerebrate cats. Assisting the flexion of the hip joint during swing advanced the onset of activity in ankle extensor muscles, and this advance was strongly correlated with a reduction in the duration of hip flexor muscle activity. The hip angle at the time of onset of the flexion to extension transition was similar during assisted and unassisted steps. Additional evidence for the hypothesis that sensory signals related to hip flexion are important in regulating the swing-to-stance transition came from four normal animals trained to walk in a variety of situations designed to alter the coordination of movements at the hip, knee, and ankle joints during the swing phase. Although there were exceptions in some tasks and preparations, the angle of the hip joint at the time of onset of extensor activity was generally less variable than that of the knee and ankle joints. We also found no clear relationships between the angle of the limb and body axes, or the length of the limb axis, and the time of onset of extensor activity. Finally, there were no indications that the stretching of ankle extensor muscles during swing was a factor in regulating the transition from swing-to-stance. Copyright © 2005 The American Physiological Society.

424. Slow oscillatory firing: A major firing pattern of dopamine neurons in the ventral tegmental area - Shi W.-X. [W.-X. Shi, Neuropsychopharmacological Research Unit, Yale University School of Medicine, 300 George St., New Haven, CT 06511, United States] - *J. NEUROPHYSIOL.* 2005 94/5 (3516-3522) - summ in FNGL

Using spectral analysis and in vivo single-unit recording in rats, the present study revealed a pronounced slow oscillation (SO) in the firing activity of about half the dopamine (DA) neurons recorded in the ventral tegmental area. DA neurons in this group tended to fire repetitive spike clusters, making them appear to be rhythmic bursting cells. However, only some of these burst-like events met the traditional "80/160 ms" burst criteria entirely. The observation that the SO could be found in nonbursting DA cells, occurred at frequencies different from those of bursts, and persisted after

bursts were digitally removed from spike trains further supports the suggestion that the SO is different from the traditionally defined bursting. Interspike intervals (ISIs) had been thought to be bimodally distributed in bursting DA neurons. This study found that some nonbursting DA cells also had a bimodal ISI distribution and a significant number of bursting cells did not. In the majority of cells where less than half the spikes occurred in bursts, a bimodal ISI distribution was highly predictive of the presence of the SO. Results further showed that the generation of the SO required forebrain inputs to DA neurons but not the adrenergic $\alpha1$ -receptor activation responsible for psychostimulant-induced increases in the SO. Taken together, these results suggest that the SO is distinter from the traditionally defined bursting and represents a major firing pattern of DA neurons in the ventral tegmental area. Copyright © 2005 The American Physiological Society.

425. Activity-independent coregulation of I_A and I_h in rhythmically active neurons - MacLean J.N., Zhang Y., Goeritz M.L. et al. [J.N. MacLean, Columbia University, Department of Biological Sciences, 1002 Fairchild Center, 1212 Amsterdam Avenue, New York, NY 10027, United States] - J. NEUROPHYSIOL. 2005 94/5 (3601-3617) - summ in ENGL

The fast transient potassium or A current (I_A) plays an important role in determining the activity of central pattern generator neurons. We have previously shown that the shal K+ channel gene encodes I_A in neurons of the pyloric network in the spiny lobster. To further study how I_A shapes pyloric neuron and network activity, we microinjected RNA for a shal-GFP fusion protein into four identified pyloric neuron types. Neurons expressing shal-GFP had a constant increase in I_A amplitude, regardless of cell type. This increase in I_A was paralleled by a concomitant increase in the hyperpolarization-activated cation current I_h in all pyloric neurons. Despite significant increases in these currents, only modest changes in cell firing properties were observed. We used models to test two hypotheses to explain this failure to change firing properties. First, this may reflect the mislocalization of the expressed shal protein solely to the somata and initial neurites of injected neurons, rendering it electrically remote from the integrating region in the neuropil. To test this hypothesis, we generated a multicompartment model where increases in I_A could be localized to the soma, initial neurite, or neuropil/axon compartments. Although spike activity was somewhat more sensitive to increases in neuropil/axon versus somatic/primary neurite IA, increases in IA limited to the soma and primary neurite still evoked much more dramatic changes than were seen in the shal-GFP-injected neurons. Second, the effect of the increased I_A could be compensated by the endogenous increase in I_h. To test this, we modeled the compensatory increases of I_A and Ih with a cycling two-cell model. We found that the increase in Ih was sufficient to compensate the effects of increased IA, provided that they increase in a constant ratio, as we observed experimentally in both shal-injected and noninjected neurons. Thus an activity independent homeostatic mechanism maintains constant neuronal activity in the face of dramatic increases in IA. Copyright © 2005 The American Physiological Society.

426. Melanocortin-4 receptor mRNA is expressed in sympathetic nervous system outflow neurons to white adipose tissue Song C.K., Jackson R.M., Harris R.B.S. et al. [Dr. T.J. Bartness, Dept. of Biology, Georgia State Univ., 24 Peachtree Center Ave NE, Atlanta, GA 30302-4010, United States] - *AM. J. PHYSIOL. REGUL. INTEGR. COMP. PHYSIOL.* 2005 289/5 58-5 (R1467-R1476) - summ in ENGL

Energy balance results from the coordination of multiple pathways affecting energy expenditure and food intake. Candidate neuropeptides involved in energy balance are the melanocortins. Several species, including Siberian hamsters studied here, decrease and increase food intake in response to stimulation and blockade of the melanocortin 4-receptor (MC4-R). In addition, central application of the MC3/4-R agonist melanotan-II decreases body fat (increases lipolysis) beyond that accounted for by its ability to decrease food intake. Because an increase in the sympathetic nervous system drive to white adipose tissue (WAT) is the principal initiator of lipolysis, we tested whether the sympathetic outflow circuitry from brain to WAT contained MC4-R mRNA expressing cells. This was accomplished by labeling the sympathetic outflow to inguinal

WAT using the pseudorabies virus (PRV), a transneuronal retrograde viral tract tracer, and then processing the brain for colocalization of PRV immunoreactivity with MC4-R mRNA, the latter assessed by in situ hybridization. MC4-R mRNA was impressively colocalized in PRV-labeled cells (approximately greater than 60%) in many brain areas across the neuroaxis, including those typically implicated in lipid mobilization (e.g., hypothalamic paraventricular, suprachiasmatic, arcuate and dorsomedial nuclei, lateral hypothalamic area), as well as those not traditionally identified with lipolysis (e.g., preoptic area, subzona incerta of the lateral hypothalamus, periaqueductal gray, solitary nucleus). These data provide compelling neuroanatomical evidence that could underlie a direct central modulation of the sympathetic outflow to WAT by the melanocortins through the MC4-Rs resulting in changes in lipid mobilization and adiposity. Copyright © 2005 the American Physiological Society.

427. The role of sensory network dynamics in generating a motor program - Levi R., Varona P., Arshavsky Y.I. et al. [R. Levi, Institute for Nonlinear Science, University of California, San Diego, 9500 Gilman Drive, San Diego, CA 92093, United States] - *J. NEUROSCI.* 2005 25/42 (9807-9815) - summ in ENGL

Sensory input plays a major role in controlling motor responses during most behavioral tasks. The vestibular organs in the marine mollusk Clione, the statocysts, react to the external environment and continuously adjust the tail and wing motor neurons to keep the animal oriented vertically. However, we suggested previously that during hunting behavior, the intrinsic dynamics of the statocyst network produce a spatiotemporal pattern that may control the motor system independently of environmental cues. Once the response is triggered externally, the collective activation of the statocyst neurons produces a complex sequential signal. In the behavioral context of hunting, such network dynamics may be the main determinant of an intricate spatial behavior. Here, we show that (1) during fictive hunting, the population activity of the statocyst receptors is correlated positively with wing and tail motor output suggesting causality, (2) that fictive hunting can be evoked by electrical stimulation of the statocyst network, and (3) that removal of even a few individual statocyst receptors critically changes the fictive hunting motor pattern. These results indicate that the intrinsic dynamics of a sensory network, even without its normal cues, can organize a motor program vital for the survival of the animal. Copyright © 2005 Society for Neuroscience.

See also: 461, 554.

4.3. Psychophysiology

428. Neonatal handling increases fear and aggression in lactating rats - Giovenardi M., De Azevedo M.S., Da Silva S.P. et al. [A.B. Lucion, Departamento de Fisiologia, Instituto de Ciencias Basicas Da Saude, UFRGS, Sarmento Leite 500, Porto Alegre, RS 90050-170, Brazil] - *PHYSIOL. BEHAV.* 2005 86/1-2 (209-217) - summ in ENGL

Neonatal handling reduces fear in male and cycling female rats, but increases maternal aggressive behavior against intruders to the nest area. Present study aimed to analyze the effects of neonatal handling on the maternal aggressive behavior and the activity in the open field with a predator of lactating rats on the 8th and the 18th postpartum days (periods of high and low aggressiveness). As pups, animals were divided into two groups: nonhandled (no neonatal manipulation) and handled (handling for 1 min during the first 10 days after delivery). As adults, females of both groups were impregnated and tested against a male intruder for aggressive behavior and in the open field with a cat inside a wire-meshed cage. Results showed that on the 8th day frequency of aggressive behaviors of handled females was higher than that of the nonhandled ones, but on the 18th day, no significant difference was detected. Surprisingly, in the open field test, handled females showed decreased locomotion and increased freezing on the 8th day compared to the nonhandled ones. The opposite relationship between increased aggressiveness with reduced fear is observed in the nonhandled control females in early and late lactation periods. However, neonatal handling abolishes this relationship. Apparently, the increased aggressiveness in neonatal handled lactating females does not depend on a decrease

in fear. Our findings support the hypothesis that long lasting effects of early life stimulation is a dynamic function depending on the behavioral system and the period of life analyzed. Moreover, they caution the relationship between aggressive behavior and fear. $\ @$ 2005 Elsevier Inc. All rights reserved.

429. Effects of long-term continuous exposure to light on memory and anxiety in mice - Castro J.P.M.V., Frussa-Filho R., Fukushiro D.F. et al. [V.C. Abfilo, Departamento de Farmacologia, Universidade Federal de São Paulo, Edifício Leal Prado, Rua Botucatu, 862, CEP 04023-062, São Paulo, SP, Brazil] - *PHYSIOL. BEHAV.* 2005 86/1-2 (218-223) - summ in ENGL

The studies on the relationship between the light/dark cycle and memory function mostly used protocols of acute disruption of the circadian rhythm. The aim of the present study is to verify the effects of long-term continuous exposure to light on memory, anxiety and motor parameters of mice tested in the plus-maze discriminative avoidance task. Mice were conditioned to choose between the two enclosed arms (one aversive and one non-aversive) while avoiding the open arms of a modified elevated plus-maze apparatus. Memory was evaluated by the time spent in the aversive enclosed arm, anxiety was evaluated by the time spent in the open arms and locomotor behavior was evaluated by number of entries in the arms of the maze. The results showed that long-term (35-42 days) continuous light exposure did not modify memory or anxiety parameters but increased locomotor activity. While the increase in locomotor behavior is in line with previous studies, the unexpected absence of alterations in memory and anxiety (reported to be influenced by the circadian rhythm) is discussed. © 2005 Elsevier Inc. All rights reserved.

430. Closer in time when farther in space - Spatial factors in audiovisual temporal integration - Noesselt T., Fendrich R., Bonath B. et al. [T. Noesselt, Department of Neurology II, Center for Advanced Imaging, Haus 1, Leipziger Str.44, 39120 Magdeburg, Germany] - *COGN. BRAIN RES.* 2005 25/2 (443-458) - summ in ENGL

We investigated the effect of visual eccentricity and spatial alignment on judgments of audiovisual synchrony. Sequences of flashes at 4, 6, and 8 Hz were presented centrally, or at horizontal eccentricities of 6° or 18°. Concurrent sequences of clicks were presented at the same rate as the flashes, or at higher or lower rates. Subjects judged whether the flash rate was the same as (synchronous with), faster than, or slower than the click rate. With the 4- and 6-Hz flash rates, subjects' judgments of audiovisual synchrony increased with increasing eccentricity, but only when the click rate was more rapid than the flash rate. This effect remained even when the size of the peripheral visual stimuli was adjusted to compensate for cortical magnification, and was not significantly influenced by the spatial proximity of the auditory and visual signals. However, it was absent when the auditory and visual stimuli were presented serially rather than concurrently. With the 8-Hz flash rate, synchrony judgments were prevalent irrespective of eccentricity. When two serially presented flash rates were compared, visual-visual matching judgments increased with eccentricity at flash rates of 6 Hz and higher, but decreased at flash rates below 6 Hz. Finally, when two concurrent flash rates were compared, visual-visual synchrony judgments increased with eccentricity at all flash-rate combinations. Together, these results suggest that while perceptual uncertainty can play a role in synchrony judgments at rates of 6 Hz and higher, below 6 Hz eccentricity produces a widening of the window of apparent audiovisual temporal synchrony which perceptual uncertainty cannot explain.

431. Cortical activation during Pavlovian fear conditioning depends on heart rate response patterns: An MEG study - Moratti S. and Keil A. [S. Moratti, Department of Psychology, University of Konstanz, P.O. Box D25, D-78457 Konstanz, Germany] - *COGN. BRAIN RES.* 2005 25/2 (459-471) - summ in ENGL

In the present study, we examined stimulus-driven neuromagnetic activity in a delayed Pavlovian aversive conditioning paradigm using steady state visual evoked fields (SSVEF). Subjects showing an accelerative heart rate (HR) component to the CS+ during learning trials exhibited an increased activation in sensory and parietal cortex due to CS+ depiction in the extinction block. This was accompanied

by a selective orientation response (OR) to the CS+ during extinction as indexed by HR deceleration. However, they did not show any differential cortical activation patterns during acquisition. In contrast, subjects not showing an accelerative HR component but rather unspecific HR changes during learning were characterized by greater activity in left orbito-frontal brain regions in the acquisition block but did not show differential SSVEF patterns during extinction. The results suggest that participants expressing different HR responses also differ in their stimulus-driven neuromagnetic response pattern to an aversively conditioned stimulus. © 2005 Elsevier B.V. All rights reserved.

432. Extended cocaine self-administration and deprivation produces region-specific and time-dependent changes in connexin36 expression in rat brain - McCracken C.B., Hamby S.M., Patel K.M. et al. [D.C.S. Roberts, Department of Physiology and Pharmacology, Wake Forest University School of Medicine, Winston-Salem, NC 27157, United States] - *SYNAPSE* 2005 58/3 (141-150) - summ in ENGL

Cocaine addiction is a disease that develops over time, and it is thought that drug-induced neuroadaptations underlie the changes in behavior seen across the addictive process. While a number of alterations in synaptic transmission have been identified, little is currently known regarding cocaine's effects on gap junctional communication between neurons. Here we examine the effects of a cocaine self-administration regimen, previously shown to increase the reinforcing efficacy of cocaine, on the expression of the neuron-specific gap junction-forming protein connexin36 (Cx36). Using real-time RT-PCR and immunoblotting, we show that binge cocaine self-administration produces region-specific and time-dependent changes in Cx36 mRNA and protein expression in the nucleus accumbens, prefrontal cortex, and hippocampus. A number of changes in Cx36 were present 1 day and 7 days following self-administration, and Cx36 mRNA and protein appeared to be differentially regulated in a region-specific manner. Cx36 protein was significantly decreased in the prefrontal cortex 7 days following self-administration, a time point when behavioral sensitization to the reinforcing effects of cocaine is observed. These results suggest that changes in neuronal gap junction expression may be one mechanism by which cocaine self-administration produces enduring changes in behavior. © 2005 Wiley-Liss, Inc.

433. High and low responders to novelty show differential effects in striatal glutamate - Shakil S.S., Holmer H.K., Moore C. et al. [Dr. C.K. Meshul, Neurocytology Lab. (RD-29), V.A. Medical Center, 3710 S.W. Veterans Hospital Road, Portland, OR 97239, United States] - *SYNAPSE* 2005 58/3 (200-207) - summ in ENGL

The goal of this study was to determine whether there was a difference in glutamate within the dorsolateral striatum in mice exhibiting either a high (HR) or low (LR) locomotor response to a novel environment. The number of line crossings over a 30-min-period when the mice were placed in a novel environment was determined, and those mice for which the values were above the mean were in the HR group and those with the values below the mean were in the LR group. In vivo microdialysis was carried out to determine the basal extracellular level of striatal glutamate, and the contralateral striatum was taken to measure the density of glutamate immunolabeling within nerve terminals making an asymmetrical (excitatory) synaptic contact using quantitative immuno-gold electron microscopy. There was a statistically significant difference (35%) in the basal extracellular level of striatal glutamate between the HR and LR groups, with the HR group having a lower level, compared with that of the LR group. There was a 25% difference in the density of nerve terminal glutamate immuno-gold labeling associated with the synaptic vesicle pool in the HR, compared with that in the LR group, but this difference was not statistically significant. There was no change in the basal extracellular level of striatal dopamine between the two groups, but there was a statistically significant difference (73%) in the basal turnover ratio of striatal dopamine and its metabolites in the HR, compared with that in the LR group. The data suggests that the difference in extracellular striatal glutamate between the HR and LR groups is not due to an alteration in basal extracellular dopamine but could be due to an increase in dopamine turnover. © 2005 Wiley-Liss, Inc.

434. Motor preparation in a memorised delay task - Jordan K., Hyland B.I., Wickens J.R. and Anson J.G. [J.G. Anson, Departments of Physiology, Anatomy and Structural Biology, School of Physical Education, University of Otago, 56, Dunedin, New Zealand] - *EXP. BRAIN RES.* 2005 166/1 (102-108) - summ in ENGL

The effect on reaction time (RT) and movement time (MT) of remembering which one of several targets to move to was investigated in 18 participants who completed 416 trials in each task. On each trial, participants moved their index finger from a central, illuminated switch (the stimulus) to one of eight targets located on the circumference of a 6 cm radius circle. A visual cue (illumination of the target) informed the participant of the appropriate target. In the memorised delay task, the cued target was lit for 300 ms followed by a variable (450-750 ms) foreperiod during which the participant was required to remember the location of the target until the stimulus light was extinguished. In the non-memorised delay task, the target remained lit during the entire foreperiod (750-1050 ms) until the response was completed. At the "go" signal (stimulus light extinguished) participants moved as quickly and accurately as possible to the cued target. Both RT and MT were significantly (p<0.05) longer in the memorised delay task. The increase in RT shows that remembering which target imposed a greater load on motor preparation even though all the information needed for preparing the response was presented in the cue at the beginning of each trial. The increase in MT raises the possibility that movement execution was also programmed during motor preparation. © Springer-Verlag

435. Striatal dopamine release in the rat during a cued leverpress task for food reward and the development of changes over time measured using high-speed voltammetry - Nakazato T. [T. Nakazato, Department of Physiology, Juntendo University, School of Medicine, 2-1-1 Hongo, Bunkyo-ku, Tokyo 113-8421, Japan] - EXP. BRAIN RES. 2005 166/1 (137-146) - summ in ENGL

Substantia nigra dopamine neuronal activity in the primate is thought to be related to the error in predicting reward delivery. Dopamine release in rat nucleus accumbens has been shown to increase in relation to drug/food-seeking behaviour. It is not known how the release of dopamine in the striatum corresponds to the many distinct steps of a rewarded, cued task (e.g. recognizing the cue, executing the behaviour, anticipating the reward, receiving the reward) and how dopamine release then changes over time as task performance improves. To investigate dopamine release during a rewarded, cued task and the development of changes in dopamine release over time, changes in extracellular striatal dopamine concentration during a rewarded, cued lever-press task were measured a few days every week for 5 months using high-speed in vivo voltammetry. Rats were trained to press a lever after a tone to obtain a food reward. The reaction time for the lever press decreased gradually as training continued. Changes in dopamine concentration were measured in the anterior striatum (ventral portion) during the task performance after an initial 6-day familiarization period, in which the animals learned that a lever press yielded food, and a 5-week period for surgery, recovery, and electrode preparation. During the task performance, dopamine concentration started to increase just after the cue, peaked near the time of the lever press, and returned to basal levels 1-2 s after the lever press. This pattern of changes in dopamine concentration was observed over the 5 months of testing, the peak dopamine concentration increasing steadily until peaking at week 7, at which time the task performance had not yet improved significantly from week 2. By week 13, task performance had significantly improved and peak dopamine concentration had begun to subside. Thus, the increase in dopamine concentration after the cue was highest while the task was not yet perfected and subsided toward the end of the learning process. It was concluded that striatal dopamine release during a cued lever-press task is relevant to the novelty of the conditions. © Springer-Verlag 2005.

436. Critical role of amygdala in flavor but not taste preference learning in rats - Touzani K. and Sclafani A. [Dr. A. Sclafani, Department of Psychology, Brooklyn College, City University of New York, Brooklyn, NY 11210, United States] - *EUR. J. NEUROSCI.* 2005 22/7 (1767-1774) - summ in ENGL

The role of the amygdala (AMY) in learning to associate complex flavor (taste + odor cues) with the oral and post-oral properties

of nutrients was examined. Rats with excitotoxic lesions of the basolateral AMY learned to prefer flavors paired with intragastric (IG) infusions of maltodextrin or corn oil (Experiment 1), although the preference was slightly attenuated. However, rats with large AMY lesions failed to develop a preference for flavors paired with IG infusions of the same nutrients (Experiments 2 and 4) but were able to learn a preference for a taste mixture paired with IG maltodextrin infusions (Experiment 3). The rats with large AMY lesions also did not acquire a preference for a flavor cue paired with the sweet taste of fructose (Experiment 5). Collectively, these data provide evidence that AMY is essential for flavor- but not taste-nutrient preference learning. © Federation of European Neuroscience Societies.

437. Fear learning induces persistent facilitation of amygdala synaptic transmission - Schroeder B.W. and Shinnick-Gallagher P. [Prof. P. Shinnick-Gallagher, Department of Pharmacology and Toxicology, Neuroscience Graduate Program, University of Texas Medical Branch, 301 University Blvd, Galveston, TX 77555-1031, United States] - *EUR. J. NEUROSCI.* 2005 22/7 (1775-1783) - summ in ENGL.

In the maintenance phase of fear memory, synaptic transmission is potentiated and the stimulus requirements and signalling mechanisms are altered for long-term potentiation (LTP) in the cortico-lateral amygdala (LA) pathway. These findings link amygdala synaptic plasticity to the coding of fear memories. Behavioural experiments suggest that the amygdala serves to store long-term fear memories. Here we provide electrophysiological evidence showing that synaptic alterations in rats induced by fear conditioning are evident in vitro 10 days after fear conditioning. We show that synaptic transmission was facilitated and that high-frequency stimulation dependent LTP (HFS-LTP) of the cortico-lateral amygdala pathway remained attenuated 10 days following fear conditioning. Additionally, we found that the low-frequency stimulation dependent LTP (LFS-LTP) measured 24 h after fear conditioning was absent 10 days post-training. The persistent facilitation of synaptic transmission and occlusion of HFS-LTP suggests that, unlike hippocampal coding of contextual fear memory, the cortico-lateral amygdala synapse is involved in the storage of long-term fear memories. However, the absence of LFS-LTP 10 days following fear conditioning suggests that amygdala physiology 1 day following fear learning may reflect a dynamic state during memory stabilization that is inactive during the long-term storage of fear memory. Results from these experiments have significant implications regarding the locus of storage for maladaptive fear memories and the synaptic alterations induced by these memories. © Federation of European Neuroscience Societies.

438. Exploring the functional architecture of person recognition system with event-related potentials in a within- and cross-domain self-priming of faces - Jemel B., Pisani M., Rousselle L. et al. [B. Jemel, Service de Recherche, Hôpital Rivière des Prairies 7070 Blv Perras, Montréal, Que. H1E 1A4, Canada] - NEUROPSY-CHOLOGIA 2005 43/14 (2024-2040) - summ in ENGL

In this paper, we explored the functional properties of person recognition system by investigating the onset, magnitude, and scalp distribution of within- and cross-domain self-priming effects on event-related potentials (ERPs). Recognition of degraded pictures of famous people was enhanced by a prior exposure to the same person's face (within-domain self-priming) or name (cross-domain self-priming) as compared to those preceded by neutral or unrelated primes. The ERP results showed first that the amplitude of the N170 component to famous face targets was modulated by within- and cross-domain self-priming, suggesting not only that the N170 component can be affected by top-down influences but also that this top-down effect crosses domains. Second, similar to our behavioral data, later ERPs to famous faces showed larger ERP self-priming effects in the within-domain than in the cross-domain condition. In addition, the present data dissociated between two topographically and temporally overlapping priming-sensitive ERP components: the first one, with a strongly posterior distribution arising at an early onset, was modulated more by within-domain priming irrespective whether the repeated face was familiar or not. The second component, with a relatively uniform scalp distribution, was modulated by within- and cross-domain priming of familiar

faces. Moreover, there was no evidence for ERP-induced modulations for unfamiliar face targets in the cross-domain condition. Together, our findings suggest that multiple neurocognitive events that are possibly mediated by distinct brain loci contribute to face priming effects. © 2005 Elsevier Ltd. All rights reserved.

439. A functional MRI study of preparatory signals for spatial location and objects - Corbetta M., Tansy A.P., Stanley C.M. et al. [M. Corbetta, Department of Neurology, Washington University School of Medicine, Box 8225, 4525 Scott Ave., St. Louis, MO 63110, United States] - *NEUROPSYCHOLOGIA* 2005 43/14 (2041-2056) - summ in ENGL

We investigated preparatory signals for spatial location and objects in normal observers using functional magnetic resonance imaging (fMRI). Activity for attention-directing cues was separated from activity for subsequent test arrays containing the target stimulus. Subjects were more accurate in discriminating a target face among distracters when they knew in advance its location (spatial directional cue), as compared to when the target could randomly appear at one of two locations (spatial neutral cue), indicating that the spatial cue was used. Spatially specific activations occurred in a region at the intersection of the ventral intraparietal sulcus and transverse occipital sulcus (vIPS-TOS), which showed significantly stronger activation for rightward- than leftward-directing cues, while other fronto-parietal areas were activated by the cue but did not show spatial specificity. In visual cortex, activity was weak or absent in retinotopic occipital regions following attentiondirecting cues and this activity was not spatially specific. In a separate task, subject discriminated a target outdoor scene among distracters after the presentation of spatial neutral cues. There was no significant difference in dorsal frontoparietal activity during the face versus scene discrimination task. Also, there was only weak evidence for selective preparatory activity in ventral object-selective regions, although the activation of these regions to the subsequent test array did depend upon which discrimination (face or place) was performed. We conclude first that under certain circumstances, spatial cues that produce strong behavioral effects may modulate parietal-occipital regions in a spatially specific manner without producing similar modulations in retinotopic occipital regions. Second, attentional modulations of object-selective regions in temporal-occipital cortex can occur even though preparatory object-selective modulations of those regions are absent or weak. © 2005 Elsevier Ltd. All rights reserved.

440. Neural dynamics of cross-modal and cross-temporal associations - Deco G., Ledberg A., Almeida R. and Fuster J. [G. Deco, Department of Technology, Universitat Pompeu Fabra, Passeig de Circumval.lació, 8, 08003 Barcelona, Spain] - *EXP. BRAIN RES.* 2005 166/3-4 (325-336) - summ in ENGL

We have studied a neurodynamic model of cross-modal and cross-temporal associations. We show that a network of integrate-and-fire neurons can generate spiking activity with realistic dynamics during the delay period of a paired associates task. In particular, the activity of the model resembles reported data from single-cell recordings in the prefrontal cortex. © Springer-Verlag 2005.

441. Brain stem response to speech: A biological marker of auditory processing - Johnson K.L., Nicol T.G. and Kraus N. [K.L. Johnson, Auditory Neuroscience Laboratory, Frances Searle Building, Northwestern University, 2240 Campus Drive, Evanston, IL 60208, United States] - *EAR HEAR*. 2005 26/5 (424-434) - summ in ENGL

The auditory brain stem response to speech mimics the acoustic characteristics of the speech signal with remarkable fidelity. This makes it possible to derive from it considerable theoretical and clinically applicable information relevant to auditory processing of complex stimuli. Years of research have led to the current characterization of these neural events with respect to the underlying acoustic information they reflect. The majority of data reviewed here originates from studies using a /da/ syllable to elicit the brain stem response, which consists of transient and periodic (frequency following) neural activity. We describe how the human auditory brain stem response separately encodes source and filter characteristics of the acoustic signal, which reflects paralinguistic and linguistic information simultaneously conveyed in speech. In normal-hearing

individuals, these two classes of response components (source and filter) are highly correlated within a class but not between classes. This response dissociation becomes pronounced when stimuli are presented in background noise or with faster stimulus rates. In addition, some learning-impaired children show a selective deficiency in the neural encoding of acoustic features associated with the filter characteristics of speech. These children show no deficits in the encoding of source components, further supporting the notion of separate neural mechanisms. Overall, the amditory brain stem response to speech provides a way to access stibcortical auditory processing mechanisms and may be tised as a biological marker of deficient sound encoding associated with learning and auditory processing disorders. Copyright © 2005 by Lippincott Williams & Wilkins

442. Lesions of the basal amygdala block expression of conditioned fear but not extinction - Anglada-Figueroa D. and Quirk G.J. [Dr. G.J. Quirk, Department of Physiology, Ponce School of Medicine, P.O. Box 7004, Ponce 00732, Puerto Rico] - *J. NEURO-SCI.* 2005 25/42 (9680-9685) - summ in ENGL

Although the role of the amygdala in acquisition of conditioned fear is well established, there is debate concerning the intra-amygdala circuits involved. The lateral nucleus of the amygdala (LA) is thought to be an essential site of plasticity in fear conditioning. The LA has both direct and indirect [via the basal nuclei: basal amyodala (BA)] projections to the central nucleus (Ce) of the amygdala, an essential output for fear behaviors. Lesions of the LA or Ce prevent acquisition of conditioned freezing to a conditioned stimulus, but BA lesions do not, suggesting that the BA is not normally involved in fear conditioning. If true, posttraining BA lesions should also have no effect. Replicating previous studies, we found that rats given electrolytic BA lesions before training acquired conditioned fear normally. They also showed normal long-term retention and extinction of conditioned fear. Unexpectedly, BA lesions made after training completely blocked expression of conditioned fear. Despite this deficit, lesioned rats were able to learn a new tone-shock association. Thus, although the LA-Ce system is sufficient for fear acquisition in the absence of the BA, it is not sufficient when the BA is present, suggesting that the BA is an important site of plasticity in fear conditioning. The pattern of lesion deficits we observed (after but not before training) might be explained by homeostatic mechanisms that balance plasticity over multiple inputs, regulating the influence of the BA and LA onto Ce output neurons. Copyright © 2005 Society for Neuroscience.

443. Analysis of single-unit responses to emotional scenes in human ventromedial prefrontal cortex - Kawasaki H., Adolphs R., Oya H. et al. [R. Adolphs, HSS 228-77, Caltech, Pasadena, CA 91125, United States] - *J. COGN. NEUROSCI.* 2005 17/10 (1509-1518) - summ in ENGL

Lesion and functional imaging studies in humans have shown that the ventral and medial prefrontal cortex is critically involved in the processing of emotional stimuli, but both of these methods have limited spatiotemporal resolution. Conversely, neurophysiological studies of emotion in nonhuman primates typically rely on stimuli that do not require elaborate cognitive processing. To begin bridging this gap, we recorded from a total of 267 neurons in the left and right orbital and anterior cingulate cortices of four patients who had chronically implanted depth electrodes for monitoring epilepsy. Peristimulus activity was recorded to standardized, complex visual scenes depicting neutral, pleasant, or aversive content. Recording locations were verified with postoperative magnetic resonance imaging. Using a conservative, multistep statistical evaluation, we found significant responses in 56 neurons; 16 of these were selective for only one emotion class, most often aversive. The findings suggest sparse and widely distributed processing of emotional value in the prefrontal cortex, with a predominance of responses to aversive stimuli. © 2005 Massachusetts Institute of Technology.

444. Left auditory cortex and amygdala, but right insula dominance for human laughing and crying - Sander K. and Scheich H. [K. Sander, Leibniz Institute for Neurobiology, Brenneckestrasse 6, 39118 Magdeburg, Germany] - *J. COGN. NEUROSCI.* 2005 17/10 (1519-1531) - summ in ENGL

Evidence suggests that in animals their own species-specific communication sounds are processed predominantly in the left hemisphere. In contrast, processing linguistic aspects of human speech involves the left hemisphere, whereas processing some prosodic aspects of speech as well as other not yet well-defined attributes of human voices predominantly involves the right hemisphere. This leaves open the question of hemispheric processing of universal (species-specific) human vocalizations that are more directly comparable to animal vocalizations. The present functional magnetic resonance imaging study addresses this question. Twenty subjects listened to human laughing and ciying presented either in an original or time-reversed version while performing a pitchshift detection task to control attention. Time-reversed presentation of these sounds is a suitable auditory control because it does not change the overall spectral content. The auditory cortex, amygdala, and insula in the left hemisphere were more strongly activated by original than by time-reversed laughing and crying. Thus, similar to speech, these nonspeech vocalizations involve predominantly lefthemisphere auditory processing. Functional data suggest that this lateralization effect is more likely based on acoustical similarities between speech and laughing or crying than on similarities with respect to communicative functions. Both the original and time-reversed laughing and crying activated more strongly the right insula, which may be compatible with its assumed function in emotional self-awareness. © 2005 Massachusetts Institute of Technology.

445. fMRI reveals a common neural substrate of illusory and real contours in V1 after perceptual learning - Maertens M. and Pollmann S. [M. Maertens, Institute of Psychology II, Department of Experimental Psychology, Otto-von-Guericke University, Universitätsplatz 2, D-39106 Magdeburg, Germany] - *J. COGN. NEUROSCI.* 2005 17/10 (1553-1564) - summ in ENGL

Perceptual learning involves the specific and relatively permanent modification of perception following a sensory experience. In psychophysical experiments, the specificity of the learning effects to the trained stimulus attributes (e.g., visual field position or stimulus orientation) is often attributed to assumed neural modifications at an early cortical site within the visual processing hierarchy. We directly investigated a neural correlate of perceptual learning in the primary visual cortex using fMRI. Twenty volunteers practiced a curvature discrimination on Kanizsa-type illusory contours in the MR scanner. Practice-induced changes in the BOLD response to illusory contours were compared between the pretraining and the posttraining block in those areas of the primary visual cortex (V1) that, in the same session, had been identified to represent real contours at corresponding visual field locations. A retinotopically specific BOLD signal increase to illusory contours was observed as a consequence of the training, possibly signaling the formation of a contour representation, which is necessary for performing the curvature discrimination. The effects of perceptual training were maintained over a period of about 10 months, and they were specific to the trained visual field position. The behavioral specificity of the learning effects supports an involvement of V1 in perceptual learning, and not in unspecific attentional effects. © 2005 Massachusetts Institute of Technology.

446. Interaction between syntax processing in language and in music: An ERP study - Koelsch S., Gunter T.C., Wittfoth M. and Sammler D. [S. Koelsch, Max-Planck-Institute of Cognitive Neuroscience, Stephanstr. 1a, 04103 Leipzig, Germany] - *J. COGN. NEUROSCI.* 2005 17/10 (1565-1577) - summ in ENGL

The present study investigated simultaneous processing of language and music using visually presented sentences and auditorily presented chord sequences. Music-syntactically regular and irregular chord functions were presented synchronously with syntactically correct or incorrect words, or with words that had either a high or a low semantic cloze probability. Music-syntactically irregular chords elicited an early right anterior negativity (ERAN). Syntactically incorrect words elicited a left anterior negativity (LAN). The LAN was clearly reduced when words were presented simultaneously with music-syntactically irregular chord functions. Processing of high and low cloze-probability words as indexed by the N400 was not affected by the presentation of irregular chord functions. In a control experiment, the LAN was not affected by physically deviant tones that elicited a mismatch negativity (MMN).

Results demonstrate that processing of musical syntax (as reflected in the ERAN) interacts with the processing of linguistic syntax (as reflected in the LAN), and that this interaction is not due to a general effect of deviance-related negativities that precede an IAN. Findings thus indicate a strong overlap of neural resources involved in the processing of syntax in language and music. © 2005 Massachusetts Institute of Technology.

447. Automatic encoding of polyphonic melodies in musicians and nonmusicians - Fujioka T., Trainor L.J., Ross B. et al. [Dr. T. Fujioka, Rotman Research Institute, 3560 Bathurst Street, Toronto, Ont. M6A 2E1, Canada] - *J. COGN. NEUROSCI.* 2005 17/10 (1578-1592) - summ in ENGL

In music, multiple musical objects often overlap in time. Western polyphonic music contains multiple simultaneous melodic lines (referred to as "voices") of equal importance. Previous electrophysiological studies have shown that pitch changes in a single melody are automatically encoded in memory traces, as indexed by mismatch negativity (MMN) and its magnetic counterpart (MMNm), and that this encoding process is enhanced by musical experience. In the present study, we examined whether two simultaneous melodies in polyphonic music are represented as separate entities in the auditory memory trace. Musicians and untrained controls were tested in both magnetoencephalogram and behavioral sessions. Polyphonic stimuli were created by combining two melodies (A and B), each consisting of the same five notes but in a different order. Melody A was in the high voice and Melody B in the low voice in one condition, and this was reversed in the other condition. On 50% of trials, a deviant final (5th) note was played either in the high or in the low voice, and it either went outside the key of the melody or remained within the key. These four deviations occurred with equal probability of 12.5% each. Clear MMNm was obtained for most changes in both groups, despite the 50% deviance level, with a larger amplitude in musicians than in controls. The response pattern was consistent across groups, with larger MMNm for deviants in the high voice than in the low voice, and larger MMNm for in-key than out-of-key changes, despite better behavioral performance for out-of-key changes. The results suggest that melodic information in each voice in polyphonic music is encoded in the sensory memory trace, that the higher voice is more salient than the lower, and that tonality may be processed primarily at cognitive stages subsequent to MMN generation. © 2005 Massachusetts Institute of Technology.

448. Who's in control? Proficiency and L1 influence on L2 processing - Elston-Güttler K.E., Paulmann S. and Kotz S.A. [K.E. Elston-Güttler, Max Planck Institute for Human Cognitive and Brain Sciences, Neurocognition of Language, 355 Stephanstraße 1a, D-04103 Leipzig, Germany] - *J. COGN. NEUROSCI.* 2005 17/10 (1593-1610) - summ in ENGL

We report three reaction time (RT)/event-related brain potential (ERP) semantic priming lexical decision experiments that explore the following in relation to L1 activation during L2 processing: (1) the role of L2 proficiency, (2) the role of sentence context, and (3) the locus of Ll activations (orthographic vs. semantic). All experiments used German (L1) homonyms translated into English (L2) to form prime-target pairs (pine-jaw for Kiefer) to test whether the L1 caused interference in an all-L2 experiment. Both RTs and ERPs were measured on targets. Experiment 1 revealed reversed priming in the N200 component and RTs for low-proficiency learners, but only RT interference for high-proficiency participants. Experiment 2 showed that once the words were processed in sentence context, the low-proficiency participants still showed reversed N200 and RT priming, whereas the high-proficiency group showed no effects. Experiment 3 tested native English speakers with the words in sentence context and showed a null result comparable to the high-proficiency group. Based on these results, we argue that cognitive control relating to translational activation is modulated by (1) L2 proficiency, as the early interference in the N200 was observed only for low-proficiency learners, and (2) sentence context, as it helps high-proficiency learners control L1 activation. As reversed priming was observed in the N200 and not the N400 component, we argue that (3) the locus of the L1 activations was orthographic. Implications in terms of bilingual word recognition and the functional role of the N200 ERP component are discussed. © 2005 Massachusetts Institute of Technology.

449. Neural correlates of syntactic processing in two-year-olds - Oberecker R., Friedrich M. and Friederici A.D. [A.D. Friederici, Max Planck Institute for Human Cognitive and Brain Sciences, PO Box 500 355, 04303 Leipzig, Germany] - *J. COGN. NEUROSCI.* 2005 17/10 (1667-1678) - summ in ENGL

Event-related brain potential (ERP) studies of sentence processing in adults have shown that phrase-structure violations are associated with two ERP components; an early left anterior negativity (ELAN) and a late, centro-parietal positivity (P600). Although the ELAN reflects highly automatic first-pass sentence parsing, the P600 has been interpreted to reflect later, more controlled processes. The present ERP study investigates the processing of phrase-structure violations in children below three years of age. Both children (mean age of 2.8 years) and adults passively listened to short active sentences that were either correct or syntactically incorrect. Adults displayed an ELAN that was followed by a P600 to the syntactic violation. Children also demonstrated a biphasic ERP pattern consisting of an early left hemispheric negativity and a late positivity. Both components, however, started later and persisted longer than those observed in adults. The left lateralization of the children's negativity suggests that this component can be interpreted as a child-specific precursor to the ELAN observed in adults. The appearance of the early negativity indicates that the neural mechanisms of syntactic parsing are present, in principle, during early language development. © 2005 Massachusetts Institute of Technology.

450. Anxiety, reactivity, and social stress-induced cortisol elevation in humans - Takahashi T., Ikeda K., Ishikawa M. et al. [T. Takahashi, Department of Behavioral Science, Faculty of Letters, Hokkaido University, N.10 W.7, Kita-ku, Sapporo 060-0810, Japan] - NEUROENDOCRINOL. LETT. 2005 26/4 (351-354) - summ in ENGL

Objectives: Traditionally, it has been hypothesized that highly anxious/emotionally reactive subjects may have exaggerated social stress response. We examined the relationship between self-reported anxiety, emotional reactivity, and social stress response. Methods: We investigated the relationship between personality scales of trait-state anxiety, subjective autonomic reactivity, and salivary cortisol levels before and after social stress exposure (Trier Social Stress Test) in 20 men. Results: Significant positive correlations between anxiety, subjective autonomic reactivity, and basal cortisol levels were observed, while neither anxiety nor subjective autonomic reactivity was correlated with social stress-induced cortisol elevation. Conclusions: The present results indicate (i)subjects with higher degrees of trait anxiety/subjective autonomic reactivity have higher basal cortisol levels, and (ii) in contrast to the traditional view, anxious personality is not strongly associated with exaggerated cortisol response to social stress. © Neuroendocrinology Letters.

451. Association of stress, hostility and plasma testosterone levels - King J.A., Rosal M.C., Ma Y. and Reed G.W. [Dr. J. King, University of Massachusetts Medical School, Center for Comparative NeuroImaging, Department of Psychiatry, 55 Lake Avenue, North Worcester, MA 01655, United States] - *NEUROENDOCRINOL. LETT.* 2005 26/4 (355-360) - summ in ENGL

Objectives: Many studies assessing the role of sex hormones. like testosterone, on stress and hostility factors have been primarily conducted in selected atypical populations such as violent criminals as well as androgen users and abusers. Therefore, the main aim of the current study was to investigate the association between testosterone levels and two psychosocial variables: stress and hostility in a cohort of healthy individuals who were members of a health maintenance organization (HMO). Methods: At five quarterly visits, psychosocial scales and blood draws were collected. Psychological stress was measured by using several scales that assessed different types of stress, including daily hassles, major life events and perceived stress. Similarly, different aspects of hostility were measured, among them cynicism, hostile affect and aggressive responding. Plasma collected from each visit was used for testosterone level determinations. Results: Testosterone levels were significantly associated with stress in both males and females. However, whereas this association exhibited a "threshold effect" in males, it demonstrated a direct and continuous linear relationship

between these variables in females. Hostility was not correlated with testosterone levels in neither males nor females. Conclusions: These results suggest that testosterone levels in normal males and females may be more reflective of an intricate balance between physiological responding and emotional coping to stressors than the hostility profile of the individual. © Neuroendocrinology Letters.

452. Neuropsychological test performance among Caribbeanborn and U.S.-born African American elderly: The role of age, education and reading level - Byrd D.A., Sanchez D. and Manly J.J. [Dr. J.J. Manly, G.H. Sergievsky Center, Pand S Box 16, 630 West 168th Street, New York, NY 10032, United States] - J. CLIN. EXP. NEUROPSYCHOL. 2005 27/8 (1056-1069) - summ in ENGL

Within-group variation is an important yet under-studied component of cross-cultural neuropsychology. The current study explored this potential source of variation in a neurologically healthy African American elderly sample by comparing the neuropsychological test performance of nondemented groups of Caribbean-born and U.S.-born African American elders who live in New York City. Caribbean-born elders resided in the U.S. for a mean of 41.5 years (SD = 17.0). Results indicate that in general, Caribbean-born elders in this cohort did not demonstrate a unique cognitive testing profile from U.S.-born African American elders. However, the Caribbean-born group demonstrated a higher quality of education than their U.S.-born counterparts. The influence of demographic factors (i.e., age and education) on neuropsychological test performance was markedly attenuated in Caribbean-born elders though reading level was the strongest predictor of test performance for all elders, regardless of birthplace. Copyright © Taylor & Francis Ltd.

453. Memory as the "whole brain work": A large-scale model based on "oscillations in super-synergy" - Başar E. [E. Başar, Dokuz Eylül University, Brain Dynamics Multidisciplinary Research Center, Department of Biophysics, 35340, Balçova, Izmir, Turkey] - *INT. J. PSYCHOPHYSIOL.* 2005 58/2-3 SPEC. ISS. (199-226) - summ in ENGL

According to recent trends, memory depends on several brain structures working in concert across many levels of neural organization; memory is a constant work-in progress." The proposition of a brain theory based on super-synergy in neural populations is most pertinent for the understanding of this constant work in progress. This report introduces a new model on memory basing on the processes of EEG oscillations and Brain Dynamics. This model is shaped by the following conceptual and experimental steps: 1. The machineries of super-synergy in the whole brain are responsible for formation of sensory-cognitive percepts. 2. The expression "dynamic memory" is used for memory processes that evoke relevant changes in alpha, gamma, theta and delta activities. The concerted action of distributed multiple oscillatory processes provides a major key for understanding of distributed memory. It comprehends also the phyletic memory and reflexes. 3. The evolving memory, which incorporates reciprocal actions or reverberations in the APLR alliance and during working memory processes, is especially emphasized. 4. A new model related to "hierarchy of memories as a continuum" is introduced. 5. The notions of "longer activated memory" and "persistent memory" are proposed instead of longterm memory. 6. The new analysis to recognize faces emphasizes the importance of EEG oscillations in neurophysiology and Gestalt analysis. 7. The proposed basic framework called "Memory in the Whole Brain Work" emphasizes that memory and all brain functions are inseparable and are acting as a "whole" in the whole brain. 8. The role of genetic factors is fundamental in living system settings and oscillations and accordingly in memory, according to recent publications. 9. A link from the "whole brain" to "whole body," and incorporation of vegetative and neurological system, is proposed, EEG oscillations and ultraslow oscillations being a control parameter.

454. Facial expressions of emotion reveal neuroendocrine and cardiovascular stress responses - Lerner J.S., Gonzalez R.M., Dahl R.E. et al. [Dr. J.S. Lerner, Carnegie Mellon University, Porter Hall 208, Pittsburgh, PA 15213, United States] - *BIOL. PSY-CHIATRY* 2005 58/9 (743-750) - summ in ENGL

Background: The classic conception of stress involves undifferentiated negative affect and corresponding biological reactivity. The present study hypothesized a new conception that disaggregates stress into emotion-specific, contrasting patterns of biological Methods: Ninety-two healthy adults engaged in stress-challenge tasks, during which cardiovascular responses, hypothalamic-pituitary-adrenocortical (HPA) axis responses (i.e., cortisol), emotional expressions (i.e., facial muscle movements), and subjective emotional experience (self-reported) were assessed. Results: Pronounced individual differences emerged in specific emotional responses to the stressors. Analyses of facial expressions revealed that the more fear individuals displayed in response to the stressors, the higher their cardiovascular and cortisol responses to stress. By contrast, the more anger and disgust (indignation) individuals displayed in response to the same stressors, the lower their cortisol levels and cardiovascular responses. Individual differences in optimistic appraisals appeared to mediate these correlated patterns. Conclusions: Facial expressions of emotion signal biological responses to stress. Fear expressions signal elevated cortisol and cardiovascular reactivity; anger and disgust signal attenuated cortisol and cardiovascular reactivity, patterns that implicate individual differences in stress appraisals. Rather than conceptualizing stress as generalized negative affect, studies can be informed by this emotion-specific approach to stress responses. © 2005 Society of Biological Psychiatry.

See also: 490, 580.

5. MUSCLE PHYSIOLOGY

455. Establishment of a protocol to test fatigue of the trunk muscles - Corin G., Strutton P.H. and McGregor A.H. [Dr. A.H. McGregor, East Wing, Charing Cross Hospital, Fulham Palace Road, Hammersmith, London W6 8RF, United Kingdom] - *BR. J. SPORTS MED.* 2005 39/10 (731-735) - summ in ENGL

Background: Muscle fatigue has high relevance in human performance yet little research has evaluated how it should be assessed. Objective: To perform a pilot study to identify suitable methods of generating and assessing fatigue of the trunk flexor and extensor muscles. Methods: Sixteen university rugby players (mean (SEM)age 21.9 (0.2) years) were recruited and subjected to four protocols (A, B, C, D), separated by a week to allow recovery, with peak torque being recorded during each test: A, isokinetic measurements before and after fatigue, with a 10 repetition isokinetic fatigue period; B, isokinetic measurements before and after fatigue with a 45 second isometric fatigue period; C, isometric measurements before and after fatigue with a 10 repetition isokinetic fatigue period; D, isometric measurements before and after fatigue with a 45 second isometric fatigue period. All were conducted during flexion and extension of the trunk on the Cybex Norm Isokinetic Dynamometer trunk flexion-extension unit. Results: All subjects completed all four protocols. Fatigue induction appeared more effective in flexion than extension. Significant differences in mean peak torque before and after fatigue were seen in protocols A, B, and D in flexion and only in protocol D for extension. In flexion, protocol D produced the greatest fatigue, peak torque being 16.2% less after than before fatigue, suggesting greatest sensitivity. Conclusions: Protocol D, which incorporates isometric testing and fatigue protocols, appears to be able to produce fatigue most effectively, and therefore may provide the most valid assessment of fatigue in the trunk flexor and extensor muscles.

456. Advanced procedures for separation and analysis of low molecular weight inhibitor (NCX_{IF}) of the cardiac sodium-calcium exchanger - Boyman L., Hiller R., Shpak B. et al. [D. Khananshvili, Department of Physiology and Pharmacology, Sackler School of Medicine, Tel-Aviv University, Ramat-Aviv 69978, Israel] - *BIOCHEM. BIOPHYS. RES. COMMUN.* 2005 337/3 (936-943) - summ in ENGL

A low molecular weight inhibitor (NCX_{IF}) of the cardiac Na/Ca exchanger, isolated from the calf ventricle tissue, is capable of regulating the muscle strip's contractility and relaxation without involving the β -activation pathway. The structural analysis of NCX_{IF} requires highly purified preparations that fulfill the demanding requirements for mass spectra and NMR analyses. No such preparation is yet available. To this end, new HPLC procedures

were developed by a combination of the reverse phase, normal phase, and HILIC (hydrophilic liquid chromatography) techniques. The specific activity of NCX_{IF} is 10⁵ times higher in the purified preparations (as compared to the crude extract) showing a 2-5% yield of total inhibitory activity and 20-100 μ g content of final material. The purification yield reveals that 1 kg ventricle muscle contains 0.1-0.2 mg NCX_{IF}, meaning that the tissue concentrations of NCX_{IF} may reach 10^{-7} - 10^{-6} M. The diode-array scanning of purified preparations of NCX_{IF} shows a homogeneous 3D peak with a maximal absorption at 202 nm. These spectral properties may represent a five-membered ring (e.g., proline, histidine) and/or simple chemical groups (like amine, carbonyl, ester, etc.), but not an aromatic ring or complex conjugates (alkyne, alkene, aldehyde, etc.). NCX_{IF} does not respond to phenol/sulfur reagent, suggesting that it lacks reducing (aldo) sugar. NCX_{IF} shows a faint response to fluorescamine, meaning that it may contain an amino group (or its derivative). It is believed that a combination of presently developed procedures with LC/MS and LC/MS/MS may provide a useful tool for structural analysis of NCX_{IF}. © 2005 Elsevier Inc. All rights reserved

457. Changes in the centrifugal gating effect on somatosensory evoked potentials depending on the level of contractile force—Wasaka T., Nakata H., Kida T. and Kakigi R. [T. Wasaka, Japan Space Forum, Tokyo, Japan] - EXP. BRAIN RES. 2005 166/1 (118-125) - summ in FNGL

In this study, we investigated the somatosensory evoked potentials (SEPs) during the preparatory period of self-initiated plantar flexion at different force levels of muscle contraction and elucidated the mechanism behind the centrifugal gating effect on somatosensory information processing. We recorded SEPs following stimulation of the tibial nerve at the popliteal fossa during the preparatory period of a 20% maximal voluntary contraction (MVC) and 50% MVC. The preparatory period was divided into two sub-periods based on the components of movement-related cortical potentials, the negative slope (NS sub-period) and the Bereitschaftspotential (BP sub-period). The subjects were instructed to concentrate on the movement and not to pay attention to the continuous electrical stimulation. Pre-movement SEPs were averaged separately during the two subperiods under each MVC condition. The mean amplitudes of BP and NS were larger during the 50% MVC than the 20% MVC. As for the components of SEPs, during the NS sub-period the amplitude of P30 under the 50% MVC and N40 under both conditions were significantly smaller than that in the stationary sequence, and N40 amplitude was significantly smaller during the 50% MVC than the 20% MVC. During the BP sub-period, the amplitude of P30 and N40 during the 50% MVC was significantly smaller than during the stationary sequence, while it was not significantly different between the 20% and 50% MVCs. In conclusion, the extent of the centrifugal gating effect on SEPs was dependent on the activities of motor-related areas, which generated the NS and BP. © Springer-Verlag

458. Contributions of Purkinje-myocardial coupling to suppression and facilitation of early afterdepolarization-induced triggered activity - Schafferhofer-Steltzer I., Hofer E., Huelsing D.J. et al. [Dr. A.E. Pollard, Department of Biomedical Engineering, Cardiac Rhythm Management Laboratory, University of Alabama at Birmingham, 1670 University Blvd., Birmingham, AL 35294, United States] - *IEEE TRANS. BIOMED. ENG.* 2005 52/9 (1522-1531) - summ in ENGL

Electrical loading by ventricular myocardium modulates conduction system repolarization near Purkinje-ventricular junctions (PVJs). We investigated how that loading suppresses and facilitates early afterdepolarizations (EADs) under conditions where there is a high degree of functional coupling between tissue types, which is consistent with the anatomic arrangement at the peripheral conduction system-myocardial interface. Experiments were completed in eight rabbit right ventricular (RV) free wall preparations. Free-running Purkinje strands were locally superfused, and action potentials were recorded from strands. RV free walls were bathed in normal solution. Surface electrograms were recorded near strand insertions into downstream free wall myocardium. Detailed histology was performed to assemble a computer model with interspersed Purkinje and ventricular myocytes weakly coupled throughout the

region. Delays from Purkinje upstrokes to downstream peripheral conduction system and myocardial activation were comparable between experiments and simulations, supporting model node-to-node electrical coupling, i.e., the functional coupling. Purkinje action potential duration (APD) prolongation with localized isoproterenol in experiments and calcium current enhancement in simulations failed to establish EADs. With myocardial APD prolongation by delayed rectifier potassium current inhibition or L-type calcium current enhancement accompanying Purkinje APD prolongation in simulations, however, EAD-induced triggered activity developed. Collectively, our findings suggest competing contributions of the myocardial sink when there is a high degree of functional coupling between tissue types, with the transition from suppression to facilitation of EAD-induced triggered activity depending critically upon myocardial APD prolongation. © 2005 IEEE.

459. The essential light chain N-terminal extension alters force and fiber kinetics in mouse cardiac muscle - Miller M.S., Palmer B.M., Ruch S. et al. [M.S. Miller, Dept. of Molecular Physiology and Biophysics, University of Vermont, 127 HSRF Bldg., 149 Beaumont Ave., Burlington, VT 05405, United States] - *J. BIOL. CHEM.* 2005 280/41 (34427-34434) - summ in ENGL

The functional significance of the actin-binding region at the N terminus of the cardiac myosin essential light chain (ELC) remains elusive. In a previous experiment, the endogenous ventricular ELC was replaced with a protein containing a 10-amino acid deletion at positions 5-14 (ELC1v Δ 5-14, referred to as 1v Δ 5-14), a region that interacts with actin (Sanbe, A., Gulick, J., Fewell, J., and Robbins, J. (2001) J. Biol. Chem. 276, 32682-32686). $1v\Delta5$ -14 mice showed no discernable mutant phenotype in skinned ventricular strips. However, because the myofilament lattice swells upon skinning, the mutant phenotype may have been concealed by the inability of the ELC to reach the actin-binding site. Using the same mouse model, we repeated earlier measurements and performed additional experiments on skinned strips osmotically compressed to the intact lattice spacing as determined by x-ray diffraction. $1v\Delta 5$ -14 mice exhibited decreased maximum isometric tension without a change in calcium sensitivity. The decreased force was most evident in 5-6-month-old mice compared with 13-15-month-old mice and may account for the greater ventricular wall thickness in young $1v\Delta 5$ -14 mice compared with age-matched controls. No differences were observed in unloaded shortening velocity at maximum calcium activation. However, 1vΔ5-14 mice exhibited a significant difference in the frequency at which minimum complex modulus amplitude occurred, indicating a change in cross-bridge kinetics. We hypothesize that the ELC N-terminal extension interaction with actin inhibits the reversal of the power stroke, thereby increasing isometric force. Our results strongly suggest that an interaction between residues 5-14 of the ELC N terminus and the C-terminal residues of actin enhances cardiac performance. © 2005 by The American Society for Biochemistry and Molecular Biology, Inc.

460. Magnetic resonance imaging of human extraocular muscles during static ocular counter-rolling - Demer J.L. and Clark R.A. [J.L. Demer, Jules Stein Eye Inst., UCLA, 100 Stein Plaza, Los Angeles, CA 90095-7002, United States] - *J. NEUROPHYSIOL.* 2005 94/5 (3292-3302) - summ in ENGL

The rectus extraocular muscle (EOM) pulleys constrain EOM paths. During visual fixation with head immobile, actively controlled pulleys are known to maintain positions causing EOM pulling directions to change by one-half the change in eye position. This pulley behavior is consistent with Listing's law (LL) of ocular torsion as observed during fixation, saccades, and pursuit. However, pulley behavior during the vestibulo-ocular reflex (VOR) has been unstudied. This experiment studied ocular counter-rolling (OCR), a static torsional VOR that violates LL but can be evoked during MRI. Tri-planar MRI was performed in 10 adult humans during central target fixation while positioned in right and left side down positions known to evoke static OCR. EOM cross-sections and paths were determined from area centroids. Paths were used to locate pulleys in three dimensions. Significant (P < 0.025) counter-rotational repositioning of the rectus pulley arrays of both orbits was observed in the coronal plane averaging 4.1° (maximum, $8.7^{\circ})$ from right to left side down positions for the inferior, medial, and superior rectus pulleys. There was a trend for the lateral rectus averaging

1.4°. Torsional shift of the rectus pulley array was associated with significant contractile cross-section changes in the superior and inferior oblique muscles. Torsional rectus pulley shift during OCR, which changes pulling directions of the rectus EOMs, correlates with known insertions of the oblique EOM orbital layers on rectus pulleys. The amount of pulley reconfiguration is roughly one-half of published values of ocular torsion during static OCR, an arrangement that would cause rectus pulling directions to change by less than one-half the amount of ocular torsion. Copyright © 2005 The American Physiological Society.

461. A spectrum from pure post-spike effects to synchrony effects in spike-triggered averages of electromyographic activity during skilled finger movements - Schieber M.H. and Rivlis G. [M.H. Schieber, University of Rochester Medical Center, Dept. of Neurology, Box 673, 601 Elmwood Ave., Rochester, NY 14642, United States] - *J. NEUROPHYSIOL.* 2005 94/5 (3325-3341) - summ in ENGL

During individuated finger movements, a high proportion of synchrony effects was found in spike-triggered averages (Spike-TAs) of rectified electromyographic activity aligned on the spikes discharged by primary motor cortex (MI) neurons. Because synchrony effects can be produced even if the trigger neuron itself provides no direct synaptic connections to motoneurons, such nonoscillatory synchrony effects often are discounted when considering control of motoneuron pools. We therefore examined the distinctions between pure postspike effects and synchrony effects. The criteria usually applied to distinguish pure and synchrony effectsonset latency and peak width-failed to separate the present SpikeTA effects objectively into distinct subpopulations. Synchrony effects generally were larger than pure effects. Many M1 neurons produced pure effects in some muscles while producing synchrony effects in others. M1 neurons producing no effects, only pure effects, only synchrony effects, or both pure and synchrony effects did not fall into different groups based on discharge characteristics during finger movements. Nor were neurons producing different types of SpikeTA effects segregated spatially in M1. These observations suggest that neurons producing pure and synchrony SpikeTA effects come from similar M1 populations. We discuss potential mechanisms that might have produced a continuous spectrum of variation from pure to synchrony effects in the present monkeys. Although synchrony effects cannot be taken as evidence of mono- or disynaptic connections from the recorded neuron to the motoneuron pool, the functional linkages indicated by synchrony effects represent a substantial fraction of M1 input to motoneuron pools during skilled, individuated finger movements. Copyright © 2005 The American Physiological Society.

462. Evoked H-reflex and V-wave responses during maximal isometric, concentric, and eccentric muscle contraction - Duclay J. and Martin A. [J. Duclay, INSERM/ERM 207 Motricité-Plasticité, Faculté des Sciences du Sport, BP 27, 877-21 078 Dijon Cedex, France] - *J. NEUROPHYSIOL.* 2005 94/5 (3555-3562) - summ in ENGL

This study was designed to investigate the modulations of Hreflex and V-wave responses during passive and maximal active dynamic actions. Experiments were performed on 16 healthy males [age: 24 ± 4 (SD) yr]. Maximal H-reflexes (H_{max}) and M-waves (M_{maxR}) were evoked at the same muscle length during passive isometric, shortening and lengthening actions and during maximal voluntary isometric, concentric, and eccentric plantar-flexion. In all contraction types, supra-maximal stimulus intensity was used to evoke the superimposed maximal M wave (MmaxA) and V wave (V) of the soleus muscle. At rest, the H_{max}/M_{maxR} ratio was significantly reduced during lengthening with respect to isometric and shortening actions (P < 0.05). For each action type, the ratio between H reflex superimposed to the contraction (H_{sup}) and M_{maxA} was not different from H_{max}/M_{maxR} ratio. When plantar flexors were maximally voluntary activated, the H_{sup}/M_{maxA} ratio was still lower during eccentric contraction as compared with isometric and concentric efforts (0.33 \pm 0.03 vs. 0.47 \pm 0.02 and 0.50 \pm 0.03, P concentric eriors (0.35 \pm 0.05 vs. 0.47 \pm 0.02 and 0.35 \pm 0.05, \star < 0.001), whereas V/M_{maxA} ratios were similar for all contraction types (isometric 0.26 \pm 0.02; concentric 0.23 \pm 0.03, and eccentric 0.24 \pm 0.02; P > 0.05). The V/M_{maxA} ratio was significantly lower than H_{sup}/M_{maxA} during isometric and concentric MVC (P

<0.001). No difference was observed between V/M_{maxA} and H_{sup}/M_{maxA} ratios during eccentric efforts. The H-reflex modulations, present during lengthening actions, were mainly attributed to presynaptic inhibition of Ia afferents and to homosynaptic postactivation depression. Results on V wave and H reflex suggest that during eccentric MVC, the spinal loop is specifically modulated by the supra-spinal centers and/or neural mechanisms at spinal level. Copyright © 2005 The American Physiological Society.

463. Deficiency of α -sarcoglycan differently affects fast- and slow-twitch skeletal muscles - Danieli-Betto D., Esposito A., Germinario E. et al. [R. Betto, Muscle Biology and Physiopathology Unit, Consiglio Nazionale Delle Ricerca Neuroscience Institute, Viale G. Colombo 3, 35121 Padova, Italy] - AM. J. PHYSIOL. REGUL. INTEGR. COMP. PHYSIOL. 2005 289/5 58-5 (R1328-R1337) - summ in ENGL

 α -Sarcoglycan (Sgca) is a transmembrane glycoprotein of the dystrophin complex located at skeletal and cardiac muscle sarcolemma. Defects in the α -sarcoglycan gene (Sgca) cause the severe human-type 2D limb girdle muscular dystrophy. Because Sgca-null mice develop progressive muscular dystrophy similar to human disorder they are a valuable animal model for investigating the physiopathology of the disorder. In this study, biochemical and functional properties of fast-twitch extensor digitorum longus (EDL) and slow-twitch soleus muscles of the Sgca-null mice were analyzed. EDL muscle of Sgca-null mice showed twitch and tetanic kinetics comparable with those of wild-type controls. In contrast, soleus muscle showed reduction of twitch half-relaxation time, prolongation of tetanic half-relaxation time, and increase of maximal rate of rise of tetanus. EDL muscle of Sgca-null mice demonstrated a marked reduction of specific twitch and tetanic tensions and a higher resistance to fatigue compared with controls, changes that were not evident in dystrophic soleus. Contrary to EDL fibers, soleus muscle fibers of Sgca-null mice distinctively showed right shift of the pCatension (pCa is the negative log of Ca²⁺ concentration) relationships and reduced sensitivity to caffeine of sarcoplasmic reticulum. Both EDL and soleus muscles showed striking changes in myosin heavychain (MHC) isoform composition, whereas EDL showed a larger number of hybrid fibers than soleus. In contrast to the EDL, soleus muscle of Sgca-null mice contained a higher number of regenerating fibers and thus higher levels of em-bryonic MHC. In conclusion, this study revealed profound distinctive biochemical and physiological modifications in fast- and slow-twitch muscles resulting from α -sarcoglycan deficiency. Copyright © 2005 the American Physiological Society.

464. Mitochondrial efficiency in rat skeletal muscle: Influence of respiration rate, substrate and muscle type - Mogensen M. and Sahlin K. [K. Sahlin, Stockholm University College of Physical Education and Sports, Box 5626, SE 11486 Stockholm, Sweden] - ACTA PHYSIOL. SCAND. 2005 185/3 (229-236) - summ in ENGL

Aim: To investigate the hypothesis that mitochondrial efficiency (i.e. P/O ratio) is higher in type I than in type II fibres during submaximal rates of respiration. Methods: Mitochondria were isolated from rat soleus and extensor digitorum longus (EDL) muscles, representing type I and type II fibres, respectively. Mitochondrial efficiency (P/O ratio) was determined with pyruvate (Pyr) or palmitoyl-L-carnitine (PC) during submaximal (constant rate of adenosine diphosphate infusion) and maximal (V_{max}, state 3) rates of respiration and fitted to monoexponential functions. Results: There was no difference in V_{max} between PC and Pyr in soleus but in EDL V max with PC was only 58% of that with Pyr. The activity of 3-hydroxyacyl-CoA dehydrogenase was threefold higher in soleus than in EDL. P/O ratio at V_{max} was 8-9% lower with PC [2.33 \pm 0.02 (soleus) and 2.30 \pm 0.02 (EDL)] than with Pyr [2.52 \pm 0.03 (soleus) and 2.54 ± 0.03 (EDL)] but not different between the two muscles (P > 0.05). P/O ratio was low at low rates of respiration and increased exponentially when the rate of respiration increased. The asymptotes of the curves were similar to P/O ratio at V_{max}. P/O ratio at submaximal respirations was not different between soleus and EDL neither with Pyr nor with PC. Conclusion: Mitochondrial efficiency, as determined in vitro, was not significantly different in the two fibre types neither at V_{max} nor at submaximal rates of respiration. The low V_{max} for PC oxidation in EDL may relate to

low activity of $\beta\text{-}\mathrm{oxidation.}$ © 2005 Scandinavian Physiological Society.

465. Signaling pathways in activity-dependent fiber type plasticity in adult skeletal muscle - Liu Y., Shen T., Randall W.R. and Schneider M.F. [M.F. Schneider, Department of Biochemistry and Molecular Biology, University of Maryland, School of Medicine, Baltimore, MD, United States] - *J. MUSCLE RES. CELL MOTIL.* 2005 26/1 (13-21) - summ in ENGL

Adult fast- and slow-twitch skeletal muscle fibers exhibit characteristic differences in functional properties due to differences in the isoforms and quantities of expression of most muscle proteins. However, these differences may be reversed by chronic electrical stimulation of denervated muscle with the pattern typical of the other fiber type. Here, we review three possible signaling pathways that may contribute to fast to slow fiber type transformation. The first pathway involves cytosolic activation of the Ca 2+ sensitive posphatase calcineurin (CaN) due to elevated cytosolic [Ca²⁺], resulting in dephosphorylation of cytoplasmic NFATc, translocation of dephosphorylated NFATc from cytoplasm into the nucleus and activation of slow fiber gene expression by NFATc in the nucleus. The second pathway involves elevated intranuclear [Ca²⁺] causing the activation of nuclear calmodulin dependent protein kinase, which phosphorylates HDAC within the nucleus and thereby permits nuclear efflux of HDAC, thus decreasing the HDAC suppression of MEF2 activation of slow fiber gene expression. The third possible pathway involves nuclear entry of CaN, dephosphorylation of intranuclear MEF2 and consequent increased activation of slow fiber type gene expression by dephosphorylated MEF2. Evidence for the first two pathways from our studies on adult fast twitch skeletal muscle fibers is briefly reviewed. © Springer 2005.

466. Age-related changes in ATP-producing pathways in human skeletal muscle in vivo - Lanza I.R., Befroy D.E. and Kent-Braun J.A. [J.A. Kent-Braun, Dept. of Exercise Science, Totman 108, Univ. of Massachusetts, Amherst, MA 01003, United States] - *J. APPL. PHYSIOL.* 2005 99/5 (1736-1744) - summ in ENGL

Energy for muscle contractions is supplied by ATP generated from 1) the net hydrolysis of phosphocreatine (PCr) through the creatine kinase reaction, 2) oxidative phosphorylation, and 3) anaerobic glycolysis. The effect of old age on these pathways is unclear. The purpose of this study was to examine whether age may affect ATP synthesis rates from these pathways during maximal voluntary isometric contractions (MVIC). Phosphorus magnetic resonance spectroscopy was used to assess high-energy phosphate metabolite concentrations in skeletal muscle of eight young (20-35 yr) and eight older (65-80 yr) men. Oxidative capacity was assessed from PCr recovery after a 16-s MVIC. We determined the contribution of each pathway to total ATP synthesis during a 60-s MVIC. Oxidative capacity was similar across age groups. Similar rates of ATP synthesis from PCr hydrolysis and oxidative phosphorylation were observed in young and older men during the 60-s MVIC. Glycolytic flux was higher in young than older men during the 60-s contraction (P < 0.001). When expressed relative to the overall ATP synthesis rate, older men relied on oxidative phosphorylation more than young men (P = 0.014) and derived a smaller proportion of ATP from anaerobic glycolysis (P < 0.001). These data demonstrate that although oxidative capacity was unaltered with age, peak glycolytic flux and overall ATP production from anaerobic glycolysis were lower in older men during a high-intensity contraction. Whether this represents an age-related limitation in glycolytic metabolism or a preferential reliance on oxidative ATP production remains to be determined. Copyright © 2005 the American Physiological Society.

467. Relationship between force and stiffness in muscle fibers after stretch - Rassier D.E. and Herzog W. [D.E. Rassier, Human Performance Laboratory, Faculty of Kinesiology, Univ. of Calgary, 2500 Univ. Dr., Calgary, Alta. T2N 1N4, Canada] - *J. APPL. PHYSIOL.* 2005 99/5 (1769-1775) - summ in ENGL

The purpose of this study was to evaluate the relationship between force and stiffness after stretch of activated fibers, while simultaneously changing contractility by interfering with the crossbridge kinetics and muscle activation. Single fibers dissected from lumbrical muscles of frogs were placed at a length 20% longer than the plateau of the force-length relationship, activated, and stretched

by 5 and 10% of fiber length (speed: 40% fiber length/s). Experiments were conducted with maximal and submaximal stimulation in Ringer solution and with the addition of 2 and 5 mM of the myosin inhibitor 2,3-butanedione monoxime (BDM) to the solution. The steady-state force after stretch of an activated fiber was higher than the isometric force produced at the corresponding length in all conditions investigated. Lowering the frequency of stimulation decreased the force and stiffness during isometric contractions, but it did not change force enhancement and stiffness enhancement after stretch. Administration of BDM decreased the force and stiffness during isometric contractions, but it increased the force enhancement and stiffness enhancement after stretch. The relationship between force enhancement and stiffness suggests that the increase in force after stretch may be caused by an increase in the proportion of cross bridges attached to actin. Because BDM places cross bridges in a weakly bound, pre-power-stroke state, our results further suggest that force enhancement is partially associated with a recruitment of weakly bound cross bridges into a strongly bound state. Copyright © 2005 the American Physiological Society.

468. Comparison between the effect of static contraction and tendon stretch on the discharge of group III and IV muscle afferents - Hayes S.G., Kindig A.E. and Kaufman M.P. [S.G. Hayes, Div. of Cardiovascular Medicine, Univ. of California, One Shields Dr., Davis, CA 95616, United States] - *J. APPL. PHYSIOL.* 2005 99/5 (1891-1896) - summ in ENGL

The exercise pressor reflex is evoked by both mechanical and metabolic stimuli. Tendon stretch does not increase muscle metabolism and therefore is used to investigate the mechanical component of the exercise pressor reflex. An important assumption underlying the use of tendon stretch to study the mechanical component of the exercise pressor reflex is that stretch stimulates the same group III mechanosensitive muscle afferents as does static contraction. We have tested the veracity of this assumption in decerebrated cats by comparing the responses of group III and IV muscle afferents to tendon stretch with those to static contraction. The tension-time indexes as well as the peak tension development for both maneuvers did not significantly differ. We found that static contraction of the triceps surae muscles stimulated 18 of 30 group III afferents and 8 of 11 group IV afferents. Similarly, tendon stretch stimulated 14 of 30 group III afferents and 3 of 11 group IV afferents. However, of the 18 group III afferents that responded to static contraction and the 14 group III afferents that responded to tendon stretch, only 7 responded to both stimuli. On average, the conduction velocities of the 18 group III afferents that responded to static contraction (11.6 \pm 1.6 m/s) were significantly slower (P = 0.03) than those of the 14 group III afferents that responded to tendon stretch (16.7 \pm 1.5 m/s). We have concluded that tendon stretch stimulated a different population of group III mechanosensitive muscle afferents than did static contraction. Although there is some overlap between the two populations of group III mechanosensitive afferents, it is not large, comprising less than half of the group III afferents responding to static contraction. Copyright © 2005 the American Physiological

469. Subcellular responses of p53 and Id2 in fast and slow skeletal muscle in response to stretch-induced overload - Siu P.M. and Alway S.E. [S.E. Alway, Div. of Exercise Physiology, School of Medicine, West Virginia Univ., Morgantown, WV 26506-9227, United States] - *J. APPL. PHYSIOL*. 2005 99/5 (1897-1904) - summ in ENGL

Tumor suppressor p53 and inhibitor of DNA-binding/differentiation Id2 were examined after 7 or 21 days of wing weighting in fast patagialis (PAT) and slow anterior latissimus dorsi (ALD) wing muscles of young adult and old Japanese quails. The contralateral wing served as the intra-animal control. Seven days of loading increased PAT and ALD muscle weight by 28 and 96%, respectively, in young birds. PAT and ALD muscle weight was 49 and 179% greater, respectively, than control muscles after 21 days of loading in young birds. In aged birds, no PAT or ALD hypertrophy was found after 7 days of loading; however, PAT and ALD muscle weight increased by 29 and 102%, respectively, after 21 days of loading. Id2 protein in the nuclear muscle fraction increased in both PAT and ALD muscles from young adult and old birds that were loaded for 7 days and in ALD muscles after 21 days of loading

relative to contralateral control muscles. Nuclear p53 protein was greater in 7- or 21-day loaded PAT and ALD muscles relative to control muscles in both age groups. Cytosolic Id2 and p53 protein contents were not changed in loaded PAT or ALD muscles relative to control muscles at any time point. These data suggest that nuclear, but not cytosolic, Id2 and p53 are responsive to stretch-induced muscle overload. Moreover, the attenuated ability of the aged skeletal muscle to achieve hypertrophy does not appear to be explained by the subcellular changes in Id2 and p53 content with overload. Copyright © 2005 the American Physiological Society.

470. An in vivo microanalytical technique for measuring the local biochemical milieu of human skeletal muscle - Shah J.P., Phillips T.M., Danoff J.V. and Gerber L.H. [J.P. Shah, Rehabilitation Medicine, NIH, Bethesda, MD 20814, United States] - *J. APPL. PHYSIOL.* 2005 99/5 (1977-1984) - summ in ENGL

Myofascial pain associated with myofascial trigger points (MTrPs) is a common cause of nonarticular musculoskeletal pain. Although the presence of MTrPs can be determined by soft tissue palpation, little is known about the mechanisms and biochemical milieu associated with persistent muscle pain. A microanalytical system was developed to measure the in vivo biochemical milieu of muscle in near real time at the subnanogram level of concentration. The system includes a microdialysis needle capable of continuously collecting extremely small samples ($\sim 0.5 \,\mu$ l) of physiological saline after exposure to the internal tissue milieu across a 105- μ m-thick semi-permeable membrane. This membrane is positioned 200 μ m from the tip of the needle and permits solutes of < 75 kDa to diffuse across it. Three subjects were selected from each of three groups (total 9 subjects): normal (no neck pain, no MTrP); latent (no neck pain, MTrP present); active (neck pain, MTrP present). The microdialysis needle was inserted in a standardized location in the upper trapezius muscle. Due to the extremely small sample size collected by the microdialysis system, an established microanalytical laboratory, employing immunoaffinity capillary electrophoresis and capillary electrochromatography, performed analysis of selected analytes. Concentrations of protons, bradykinin, calcitonin gene-related peptide, substance P, tumor necrosis factor- α , interleukin- 1β , serotonin, and norepinephrine were found to be significantly higher in the active group than either of the other two groups (P < 0.01). pH was significantly lower in the active group than the other two groups (P < 0.03). In conclusion, the described microanalytical technique enables continuous sampling of extremely small quantities of substances directly from soft tissue, with minimal system perturbation and without harmful effects on subjects. The measured levels of analytes can be used to distinguish clinically distinct groups.

471. Microvascular flow routes in muscle controlled by vasoconstrictors - Zhang L., Newman J.M.B., Richards S.M. et al. [J.M.B. Newman, Biochemistry, Medical School, University of Tasmania, Private Bag 58, Hobart, Tasmania 7001, Australia] - *MICROVASC. RES.* 2005 70/1-2 (7-16) - summ in ENGL

Vasoconstrictors can either increase or decrease metabolism of the constant flow pump-perfused rat hindlimb. In addition, there is indirect evidence from vascular casts, surface fluorometry, dye entrapment studies, and fluorescent microsphere mapping of flow that this may be due to redistribution of flow between putatively nutritive and non-nutritive routes within muscle. In the present study, we used two methods in an attempt to identify perfused nutritive and non-nutritive vessels in muscle sections: (i) a combination of perfusion fixation with glutaraldehyde and post-perfusion Griffonia simplicifolia lectin and (ii) perfusion with rhodamine-dextran70 (lysine fixable) and post-fixation with formaldehyde. Perfusions involved vehicle only (control, a mix of nutritive and non-nutritive flow), 15 nM angiotensin II (AII) to increase, or 1 μ M serotonin (5-HT) to decrease nutritive flow. Microscopic examination of muscle sections following AII showed an increase in perfused capillaries with fewer areas of under-perfusion, relative to control. In contrast, 5-HT caused a marked decrease in perfused capillaries relative to control and evidence that flow was carried by connective tissue vessels that on average were of greater diameter and were more sparsely distributed than capillaries. It is concluded that vasoconstrictors that alter hindlimb metabolism do so by intra-muscle redistribution between capillaries (nutritive) and non-nutritive (connective tissue) vessels within each muscle. $\ \, \odot \,$ 2005 Elsevier Inc. All rights reserved.

472. Skin blood flowmotion response to insulin iontophoresis in normal subjects - Rossi M., Maurizio S. and Carpi A. [M. Rossi, Dipartimento di Medicina Interna, Università degli Studi di Pisa, Via Roma 67, 56100 Pisa, Italy] - *MICROVASC. RES.* 2005 70/1-2 (17-22) - summ in ENGL

In order to explore the mechanisms directly involved in the insulin vasodilatory activity, we studied skin blood flowmotion by means of spectral analysis of the skin forearm laser Doppler (LD) signal registered before and after iontophoresis of insulin in saline (I.S.)-(0.1 ml Humulin R 100 IU/ml diluted 1/10 in 0.9% saline) or pure saline (P.S.) (0.1 ml of 0.9% saline) in twenty normal subjects. Skin LD blood perfusion was also measured in conventional perfusion unit (PU; 1 PU = 10 mV). Using a Fast Fourier transform algorithm, power density (PD) of the total flowmotion spectrum, from 0.009 to 1.6 Hz, was measured in PU/Hz. Power density of five skin flowmotion frequency intervals (F.I.) within 0.009-0.02 Hz, 0.02-0.06 Hz, 0.06-0.2 Hz, 0.2-0.6 Hz and 0.6-1.6 Hz (referred to endothelial, sympathetic, myogenic, respiratory and heart activity, respectively) was also measured in PU/Hz. The mean skin LD perfusion increment (expressed as percent change from baseline) was significantly higher after I.S. than after P.S. (P < 0.001, ANOVA for repeated measures). Skin flowmotion total spectrum mean PD value significantly increased following iontophoresis of both P.S. (from 1.06 \pm 0.62 to 1.86 \pm 0.94 PU/Hz, \dot{P} < 0.005) and I.S. (from 1.07 \pm 0.92 to 2.39 \pm 1.73 PU/Hz P < 0.00005), however, the mean PD increment was significantly higher after I.S. than after P.S. $(1.27 \pm 0.98 \text{ PU/Hz versus } 0.69 \pm 0.67 \text{ PU/Hz}, P < 0.05)$. Only the flowmotion component referred to myogenic activity showed a percent PD increase from baseline significantly higher in response to I.S. than to P.S. iontophoresis (114.5 \pm 21.8% versus 58.8 \pm 17.9%, respectively, P < 0.05). These findings show that insulin has a vasodilatory activity on skin microvascular district. The higher increase of total blood flowmotion PD and particularly of the component related to the myogenic activity in response to insulin iontophoresis suggests that the cutaneous vasodilatory activity of insulin is, in part, related to an important action of this hormone on skin microvascular smooth muscle. © 2005 Elsevier Inc. All rights reserved.

473. Resistance training effects on muscular strength of elderly are related to intensity and gender - Beneka A., Malliou P., Fatouros I. et al. [A. Beneka, Department of Physical Education and Sport Science, Democritus University of Thrace, Komotini, Greece] - *J. SCI. MED. SPORT* 2005 8/3 (274-283) - summ in ENGL

The purpose of this study was to determine whether a high intensity (HI) versus a moderate (MI) or low-intensity (LI) training program would be more effective in improving the isokinetic knee extension muscular performance in healthy inactive men and women. Sixty-four participants, men and women, were randomly assigned to one of four groups: control group (C), LI (50% of IRM), the MI group (70% of IRM) and the HI (90% of IRM). Participants exercised on three resistance exercise machines: leg extension, leg curls and leg press. The isokinetic testing method (concentric mode) applied prior to and at the end of the training period (16 weeks, three 3 times per week) to assess the knee muscular performance. MANOVA repeated measures revealed that the HI group demonstrated the most strength gains following a speed specificity pattern (most considerable improvement occurred at or near slow speeds from 7.3% to 11.2% for male and from 2.3% to 15.2% for female). In addition, males demonstrated a greater improvement of knee extension power output than females. In conclusion, HI strength training is proposed for elderly men and women as the most effective protocol. Furthermore only at low-velocity testing, women of the HI showed a greater change than men (p<0.05). Regarding strength increase in relation to various testing velocities, a greater increase was found in HI at low velocities. with the other training groups exhibiting almost similar strength increase at all tested speeds.

See also: 482, 483, 495, 496, 497, 515, 525, 528, 529, 531, 554,

561, 564, 569, 579, 580, 600, 613, 619, 620, 621, 624, 626, 627, 628, 629, 631, 635, 638.

6. CIRCULATION

474. Spatiotemporal characteristics of SR Ca²⁺ uptake and release in detubulated rat ventricular myocytes - Brette F., Despa S., Bers D.M. and Orchard C.H. [C.H. Orchard, Department of Physiology, University of Bristol, Medical Sciences Building, Bristol BS8 1TD, United Kingdom] - *J. MOL. CELL. CARDIOL.* 2005 39/5 (804-812) - summ in ENGL

In cardiac ventricular myocytes, sarcoplasmic reticulum (SR) Ca ²⁺ load is a key determinant of SR Ca²⁺ release. This release normally occurs predominantly from SR junctions at sarcolemmal invaginations (t-tubules), ensuring synchronous SR Ca2+ release throughout the cell. However under conditions of Ca²⁺ overload, spontaneous SR Ca²⁺ release and propagating Ca²⁺ waves can occur, which are pro-arrhythmic. We used detubulated rat ventricular myocytes to determine the dependence of Ca²⁺ wave propagation on SR Ca ²⁺ load, and the role of t-tubules in SR Ca²⁺ uptake and spontaneous release. After SR Ca²⁺ depletion, recovery of Ca ²⁺ transient amplitude (and SR Ca²⁺ load) was slower in detubulated than control myocytes (half-maximal recovery: 9.9 ± 1.4 vs. $5.5 \pm$ 0.7:beats). In detubulated myocytes the extent and velocity of Ca²⁺ propagation from the cell periphery increased with each beat and depended steeply on SR Ca²⁺ load. Isoproterenol (ISO) accelerated recovery, increased maximal propagation velocity and reduced the threshold SR Ca²⁺ load for propagation. Ca²⁺ spark frequency was uniform across control cell width and was similar at the periphery of detubulated cells. However, internal Ca²⁺ spark frequency in detubulated cells was 75% lower (despite comparable local SR Ca²⁺ load); this transverse spark frequency profile was similar to that in atrial myocytes. We conclude that: (1) t-tubule Ca²⁺ fluxes normally control SR Ca²⁺ refilling; (2) Ca²⁺ wave propagation depends steeply on SR Ca²⁺ content (3) SR-t-tubule junctions are important in initiating SR Ca²⁺ release and (4) ISO enhances propagation of SR Ca release, but not the initiation of SR Ca release events (for given SR Ca ²⁺ loads). © 2005 Elsevier Ltd. All rights reserved.

475. Enhanced activity of the myocardial Na+/H+ exchanger NHE-1 contributes to cardiac remodeling in atrial natriuretic peptide receptor-deficient mice - Kilic A., Velic A., De Windt L.J. et al. [Dr. M. Kuhn, Physiologisches Institut, Universität Würzburg, Köntgenring 9, D - 97070 Würzburg, Germany] - CIRCULATION 2005 112/15 (2307-2317) - summ in ENGL

Background - Atrial natriuretic peptide (ANP), through its guanylyl cyclase-A (GC-A) receptor, not only is critically involved in the endocrine regulation of arterial blood pressure but also locally moderates cardiomyocyte growth. The mechanisms underlying the antihypertrophic effects of ANP remain largely uncharacterized. We examined the contribution of the Na +/H+ exchanger NHE-1 to cardiac remodeling in GC-A-deficient (GC-A-/-) mice. Methods and Results - Fluorometric measurements in isolated adult cardiomyocytes demonstrated that cardiac hypertrophy in GC-A-/mice was associated with enhanced NHE-1 activity, alkalinization of intracellular pH, and increased Ca2+ levels. Chronic treatment of GC-A-/- mice with the NHE-1 inhibitor cariporide normalized cardiomyocyte pH and Ca2+ levels and regressed cardiac hypertrophy and fibrosis, despite persistent arterial hypertension. To characterize the molecular pathways driving cardiac hypertrophy in GC-A -/- mice, we evaluated the activity of 4 prohypertrophic signaling pathways: the mitogen-activated protein kinases (MAPK), the serine-threonine kinase Akt, calcineurin, and Ca²⁺/calmodulindependent kinase II (CaMKII). The results demonstrate that all 4 pathways were activated in GC-A^{-/-} mice, but only CaMKII and Akt activity regressed during reversal of the hypertrophic phenotype by cariporide treatment. In contrast, the MAPK and calcineurin/NFAT signaling pathways remained activated during regression of hypertrophy. Conclusions - On the basis of these results, we conclude that the ANP/GC-A system moderates the cardiac growth response to pressure overload by preventing excessive activation of NHE-1 and subsequent increases in cardiomyocyte intracellular pH, Ca²⁺. and CaMKII as well as Akt activity. © 2005 American Heart Association, Inc.

476. Blood pressure and arterial stiffness: A comparison of two devices for measuring Augmentationindex and Pulse Wave Velocity (Germ) - ARTERIELLER BLUTDRUCK UND DIE ELASTIZITÄT DER ARTERIENWAND AUGMENTATIONSINDEX (AIX) UND PULSWELLENGESCHWINDIGKEIT (PWV): EIN VERGLEICH VON ZWEI MESSGERÄTEN - Magometschnigg D. [Dr. D. Magometschnigg, Institut für Hypertoniker, Kinderspitalgasse 10/15, 1090 Wien, Austria] - WIEN. MED. WOCHENSCHR. 2005 155/17-18 (404-410) - summ in ENGL. GERM

Augmentationindex (AIx) and Pulse Wave Velocity (PWV) give much more information on the function of the arterial tree than that obtained by blood pressure recordings. The rediscovered value of arterial stiffness measured by means of AIx or PWV is now proven as an independent cardiovascular risk factor and helps to differentiate patients at risk and their cardiovascular treatment offer. In the last decade, the methods to measure and to calculate AIx and PWV have become increasingly simple. But as the different methods use different strategies for measuring and calculating these parameters, the results concerning the same term vary, depending on the device used We undertook nearly simultaneous recordings of AIx in 400 and of PWV in 100 treated hypertensive patients with the very new TensioClinic® device developed by M. Illyés, and compared those data with measurements obtained by the SphygmoCor® device. The absolute values of m (mean) and SD (standard deviation) of AIx were when TensioClinic® was used m: -6.2% ± SD:37.9% and by SphygmoCor® m: 26,2% ± SD: 11,8%. The differences were caused by the different methods. As both devices measure the same quality of vascular function, the results correlate closely with a correlation coefficient r = 0.77. In PWV the results of Aortic PWV measured by TensioClinic® were m: 9.1 ± SD: 1.8m/sec and of brachial PWV measured by SphygmoCor®: 8.4 ± SD: 1.5 m/sec. As in AIx, these results were also different, but in contrast to AIx they did not correlate (r = -0.04) because PWV depend on the artery and its physical characteristics, and we measured once the aorta (TensioClinic®) and once predominantly the arteria brachialis (SphygmoCor®). © Springer-Verlag 2005.

477. Heart rate and systolic blood pressure variability: The impact of thinness and aging in human male subjects - Vaz M., Sucharita S. and Bharathi A.V. [M. Vaz, Division of Nutrition, Department of Physiology, St. John's Medical College, Bangalore 560034, India] - *J. NUTR. HEALTH AGING* 2005 9/5 (341-345) - summ in ENGL

Background: Life spans are steadily increasing in developing countries where 'thinness' is widely prevalent. However, the interaction of aging and thinness has been poorly studied in terms of its physiological consequences. Objective: To determine the impact of aging and 'thinness' (body mass index (BMI) < 18.5 kg/m2) on resting heart rate and systolic blood pressure (SBP) variability indices in the frequency domain. Subjects: Ninety seven healthy male subjects were divided into two age categories; young; 18-30 yrs and old > 60 yrs. The subjects were further divided on the basis of BMI into young, thin (n=32), young, normal BMI (BMI 18.5-25, n=27), old, thin (n=15) and old, normal BMI (n=23) groups. Methods: Cardiac autonomie nerve function was determined using heart rate variability indices in the frequency domain (low frequency, cardiac sympathetic 0.04-0.15Hz; high frequency, cardiac parasympathetic 0.15-0.4Hz). Vasomotor sympathetic activity was determined from the low frequency component of SBP variability. Baroreflex sensitivity was determined from the spectral power of both RR variability and SBP variability between 0.07 to 0.14 Hz. Results: Thinness was associated with a reduction in the absolute total, low and high frequency heart rate power spectrum as compared to individuals of normal BMI, but this difference was only apparent in young adults (P < 0.05) and not in older subjects. The age related decline in heart rate variability (absolute units) was apparent for subjects of both low and normal BMI (P < 0.05). There were no differences in SBP variability either with age or BMI. Conclusions: The data suggest that aging has a pronounced effect on heart rate variability, which may mask differences in heart rate variability related to thinness. The Journal of Nutrition, Health & Aging©.

478. Endogenous vascular hydrogen peroxide regulates arteriolar tension in vivo - Suvorava T., Lauer N., Kumpf S. et al. [Dr.

G. Kojda, Institut für Pharmakologie und Klinische Pharmakologie, Heinrich-Heine-Universität, Moorenstr. 5, 40225 Düsseldorf, Germany] - CIRCULATION 2005 112/16 (2487-2495) - summ in FNGI.

Background - Although many studies suggested direct vasomotor effects of hydrogen peroxide (H2O2) in vitro, little is known about the vasomotor effects of H₂O₂ in vivo. Methods and Results - We have generated mice overexpressing human catalase driven by the Tie-2 promoter to specifically target this transgene to the vascular tissue. Vessels of these mice (cat++) expressed significantly higher levels of catalase mRNA, protein, and activity. The overexpression was selective for vascular tissue, as evidenced by immunohistochemistry in specimens of aorta, heart, lung, and kidney. Quantification of reactive oxygen species by fluorescence signals in cat++ versus catalase-negative (cat n) mice showed a strong decrease in aortic endothelium and left ventricular myocardium but not in leukocytes. Awake male cat++ at 3 to 4 months of age had a significantly lower systolic blood pressure (sBP, 102.7±2.2 mm Hg, n=10) compared with their transgene-negative littermates (catⁿ, 115.6 ± 2.5 mm Hg, P=0.0211) and C57BL/6 mice (118.4±3.06 mm Hg, n=6). Treatment with the catalase inhibitor aminotriazole increased sBP of cat⁺⁺ to 117.3±4.3 mm Hg (P=0.0345), while having no effect in catⁿ (118.4 \pm 2.4 mm Hg, n=4, P>0.05). In contrast, treatment with the NO-synthase inhibitor nitro-L-arginine methyl ester (100 mg kg BW-1 d-1) increased sBP in cat⁺⁺ and C57B1/6 to a similar extent. Likewise, phosphorylation of vasodilator-stimulated phosphoprotein in skeletal muscle, left ventricular myocardium, and lung was identical in cat ++ and catⁿ. Endothelium- and NO-dependent aortic vasodilations were unchanged in cat⁺⁺. Aortic KCl contractions were significantly lower in cat⁺⁺ and exogenous H_2O_2 (10 μ mol/L)-induced vaso-constriction. Conclusions - These data suggest that endogenous H₂O₂ may act as a vasoconstrictor in resistance vessels and contribute to the regulation of blood pressure. © 2005 American Heart Association, Inc.

479. Role of nitric oxide in mediating in vivo vascular responses to calcitonin gene-related peptide in essential and peripheral circulations in the fetus - Thakor A.S. and Giussani D.A. [Dr. D.A. Giussani, Department of Physiology, University of Cambridge, Cabridge, CB2 3EG, United Kingdom] - *CIRCULATION* 2005 112/16 (2510-2516) - summ in ENGL

Background - The role of calcitonin gene-related peptide (C-GRP) in cardiovascular regulation is gaining clinical and scientific interest. In the adult, in vivo studies have shown that CGRPstimulated vasodilation in several vascular beds depends, at least in part, on nitric oxide (NO). However, whether CGRP acts as a vasodilator in the fetus in vivo and whether this effect is mediated via NO have been addressed only minimally. This study tested the hypothesis that CGRP has potent NO-dependent vasodilator actions in essential and peripheral vascular beds in the fetus in late gestation. Methods and Results - Under anesthesia, 5 fetal sheep at 0.8 gestation were instrumented with vascular catheters and Transonic flow probes around an umbilical artery and a femoral artery. Five days later, fetuses received 2- and 5- μ g doses of exogenous CGRP intra-arterially in randomized order. Doses were repeated during NO blockade with the NO clamp. This technique permits blockade of de novo synthesis of NO while compensating for tonic production of the gas, thereby maintaining basal cardiovascular function. CGRP resulted in potent and long-lasting NO-dependent dilation in the umbilical and femoral circulations, hypotension, and a positive cardiac chronotropic effect. During NO blockade, the femoral vasodilator response to CGRP was diminished. In contrast, in the umbilical vascular bed, the dilator response was not only prevented but reversed to vasoconstriction. Conclusions - CGRP has potent NO-dependent vasodilator actions in fetal essential and peripheral vascular beds. CGRP-induced NO-dependent effects in the umbilical vascular bed may provide an important mechanism in the control and maintenance of umbilical blood flow during pregnancy. © 2005 American Heart Association, Inc.

480. Correlation between mRNA levels and functional role of α_1 - adrenoceptor subtypes in arteries: Evidence of α_{1L} as a functional isoform of the α_{1A} -adrenoceptor - Martí D., Miquel R., Ziani K. et al. [P. D'Ocon, Departamento de Farmacología,

Facultat de Farmàcia, Universitat de València, Avda, Vicent Andres Estelles s/n, Burjassot, 46100 València, Spain] - AM. J. PHYSIOL. HEART CIRC. PHYSIOL. 2005 289/5 58-5 (H1923-H1932) - summ in FNGL.

The mRNA levels for the three α_1 -adrenoceptor subtypes, α_{1A} , α_{1B} , and α_{1D} , were quantified by real-time RT-PCR in arteries from Wistar rats. The α_{1D} -adrenoceptor was prominent in both aorta (79.0%) and mesenteric artery (68.7%), α_{1A} predominated in tail (61.7%) and small mesenteric artery (73.3%), and both α_{1A} and α_{1D} -subtypes were expressed at similar levels in iliac artery. The mRNA levels of the α_{1B} -subtype were a minority in all vessels (1.7-11.1%). Concentration-response curves of contraction in response to phenylephrine or relaxation in response to α_1 -adrenoceptor antagonists on maximal sustained contraction induced by phenylephrine were constructed from control vessels and vessels pretreated with 100 μ mol/l chloroethylclonidine (CEC) for 30 min. The significant decrease in the phenylephrine potency observed after CEC treatment together with the inhibitory potency displayed by 8-{2-[4-(2-methoxyphenyl)-1-piperazinyl]-8-azaspiro (4,5) decane-7-dionedihydrochloride} (BMY-7378, an α_{1D} -adrenoceptor antagonist) confirm the relevant role of α_{1D} -adrenoceptors in aorta and iliac and proximal mesenteric arteries. The potency of 5methylurapidil (an α_{1A} -adrenoceptor antagonist) and the changes in the potency of both BMY-7378 and 5-methylurapidil after CEC treatment provided evidence of a mixed population of α_{1A} - and α_{1D} -adrenoceptors in iliac and distal mesenteric arteries. The low potency of prazosin (pIC $_{50}$ < 9) as well as the high 5-methylurapidil potency in tail and small mesenteric arteries suggest the main role of $\alpha_{\rm IA}/\alpha_{\rm IL}$ -adrenoceptors with minor participation of the $\alpha_{\rm ID}$ -subtype. The mRNA levels and CEC treatment corroborated this pattern and confirmed that the α_{1L} - adrenoceptor could be a functional isoform of the α_{1A} -subtype. Copyright © 2005 the American Physiological Society.

481. Novel determinant of PKC-ε anchoring at cardiac Z-lines - Robia S.L., Kang M. and Walker J.W. [J.W. Walker, Dept. of Physiology, 1300 Univ. Ave., Madison, WI 53706, United States] - AM. J. PHYSIOL. HEART CIRC. PHYSIOL. 2005 289/5 58-5 (H1941-H1950) - summ in ENGL

The Z-line represents a critical link between the transverse tubule network and cytoskeleton of cardiac cells with a role in anchoring structural proteins, ion channels, and signaling molecules. Protein kinase C- ϵ (PKC- ϵ) regulates cardiac excitability, cardioprotection, and growth, possibly as a consequence of translocation to the Z-line/T tubule region. To investigate the mechanism of PKC- ϵ translocation, fragments of its NH2-terminal 144-amino acid variable domain, $\epsilon V1$, were fused with green fluorescent protein and evaluated by quantitative Fourier image analysis of decorated myocytes. Deletion of 23 amino acids from the NH₂-terminus of ϵ V1. including an EAVSLKPT motif important for binding to a receptor for activated C kinase (RACK2), reduced but did not abolish Z-line binding. Further deletions of up to 84 amino acids from the NH2terminus of $\epsilon V1$ also did not prevent Z-line decoration. However, deletions of residues 85-144 from the COOH-terminus strongly reduced Z-line binding. COOH-terminal deletions caused 2.5-fold greater loss of binding energy ($\Delta\Delta G$) than did NH₂-terminal deletions. Synthetic peptides derived from these regions modulated $\epsilon V1$ binding and cardiac myocyte function, but also revealed considerable heterogeneity within populations of adult cardiac myocytes. The COOH-terminal subdomain important for Z-line anchoring maps to a surface in the $\epsilon V1$ crystal structure that complements the eight-amino acid RACK2 binding site and two previously identified membrane docking motifs. PKC- ϵ anchoring at the cardiac Zline/T tubule appears to rely on multiple points of contact probably involving protein-lipid and protein-protein interactions. Copyright © 2005 the American Physiological Society.

482. Splanchnic hyperemia and hypervolemia during Valsalva maneuver in postural tachycardia syndrome - Stewart J.M., Medow M.S., Montgomery L.D. et al. [J.M. Stewart, Research Division and Hypotension Laboratory, New York Medical College, 19 Bradhurst Ave., Hawthorne, NY 10532, United States] - *AM. J. PHYSIOL. HEART CIRC. PHYSIOL.* 2005 289/5 58-5 (H1951-H1959) - summ in ENGL

Prior work demonstrated dependence of the change in blood pressure during the Valsalva maneuver (VM) on the extent of thoracic hypovolemia and splanchnic hypervolemia. Thoracic hypovolemia and splanchnic hypervolemia characterize certain patients with postural tachycardia syndrome (POTS) during orthostatic stress. These patients also experience abnormal phase II hypotension and phase IV hypertension during VM. We hypothesize that reduced splanchnic arterial resistance explains aberrant VM results in these patients. We studied 17 POTS patients aged 15-23 yr with normal resting peripheral blood flow by strain gauge plethysmography and 10 comparably aged healthy volunteers. All had normal blood volumes by dye dilution. We assessed changes in estimated thoracic, splanchnic, pelvic-thigh, and lower leg blood volume and blood flow by impedance plethysmography throughout VM performed in the supine position. Baseline splanchnic blood flow was increased and calculated arterial resistance was decreased in POTS compared with control subjects. Splanchnic resistance decreased and flow increased in POTS subjects, whereas splanchnic resistance increased and flow decreased in control subjects during stage II of VM. This was associated with increased splanchnic blood volume, decreased thoracic blood volume, increased heart rate, and decreased blood pressure in POTS. Pelvic and leg resistances were increased above control and remained so during stage IV of VM, accounting for the increased blood pressure overshoot in POTS. Thus splanchnic hyperemia and hypervolemia are related to excessive phase II blood pressure reduction in POTS despite intense peripheral vasoconstriction. Factors other than autonomic dysfunction may play a role in POTS

483. Frequency-dependent baroreflex modulation of blood pressure and heart rate variability in conscious mice - Fazan Jr. R., De Oliveira M., Dias Da Silva V.J. et al. [R. Fazan Jr., Dept. of Physiology, School of Medicine of Ribeirão Preto-USP, 14049-900 Ribeirão Preto, SP, Brazil] - *AM. J. PHYSIOL. HEART CIRC. PHYSIOL.* 2005 289/5 58-5 (H1968-H1975) - summ in ENGL

The goal of this study was to determine the baroreflex influence on systolic arterial pressure (SAP) and pulse interval (PI) variability in conscious mice. SAP and PI were measured in C57B1/6J mice subjected to sinoaortic deafferentation (SAD, n = 21) or sham surgery (n = 20). Average SAP and PI did not differ in SAD or control mice. In contrast, SAP variance was enhanced (21 ± 4 vs. $9.5 \pm 1 \text{ mmHg}^2$) and PI variance reduced ($8.8 \pm 2 \text{ vs. } 26 \pm 6 \text{ ms}^2$ ms2) in SAD vs. control mice. High-frequency (HF: 1-5 Hz) SAP variability quantified by spectral analysis was greater in SAD (8.5 \pm 2.0 mmHg²) compared with control (2.5 \pm 0.2 mmHg²) mice, whereas low-frequency (LF: 0.1-1 Hz) SAP variability did not differ between the groups. Conversely, LF PI variability was markedly reduced in SAD mice (0.5 \pm 0.1 vs. 10.8 \pm 3.4 ms²). LF oscillations in SAP and PI were coherent in control mice (coherence = 0.68 ± 0.00 0.05), with changes in SAP leading changes in PI (phase = -1.41 ± 0.06 radians), but were not coherent in SAD mice (coherence = 0.08 ± 0.03). Blockade of parasympathetic drive with atropine decreased average PI, PI variance, and LF and HF PI variability in control (n = 10) but had no effect in SAD (n = 6) mice. In control mice, blockade of sympathetic cardiac receptors with propranolol increased average PI and decreased PI variance and LF PI variability (n = 6). In SAD mice, propranolol increased average PI (n = 6). In conclusion, baroreflex modulation of PI contributes to LF, but not HF PI variability, and is mediated by both sympathetic and parasympathetic drives in conscious mice.

484. GRO family chemokines are specialized for monocyte arrest from flow - Smith D.F., Galkina E., Ley K. and Huo Y. [Y. Huo, Univ. of Minnesota, Cardiovascular Division, Vascular Biology Center, 420 Delaware St. SE, Minneapolis, MN 55455, United States] - *AM. J. PHYSIOL. HEART CIRC. PHYSIOL.* 2005 289/5 58-5 (H1976-H1984) - summ in ENGL

Chemokines participate in various processes of monocyte recruitment including monocyte arrest and migration. Our group and others have demonstrated that growth-related oncogene (GRO)- α (CXCL1) can support monocyte arrest in models of inflammation. Here we employed a parallel plate-flow chamber and Transwell reconstitution assay to test whether GRO family chemokines were sufficient for Mono Mac 6 (a human monocytic cell line) and isolated human monocyte recruitment. Our study shows that 1) GRO- α ,

 $-\beta$ (CXCL2), and -7 (CXCL3) all act as arrest chemokines for monocyte adhesion on vascular cell adhesion molecule (VCAM)-1 under flow in the presence of P-selectin; 2) CXCR2 is the functional receptor for GRO-family chemokines in monocyte arrest; however, CXCR2 is not an arrest chemokine receptor in general, since epithelial neutrophil-activating peptide ENA-78 failed to arrest monocytes; 3) GRO- α , - β , and - γ all fail to increase intracellular free Ca2+ or mediate monocyte chemotaxis; and 4) signaling through $G\alpha_i$ protein, phosphoinositide 3-kinase, and actin polymerization but not Ca 2+ mobilization or the mitogen-activated kinases p38 and MAPK/extracellular signal-related kinase are necessary for GRO- α -mediated Mono Mac 6 cell arrest under flow. We conclude that the GRO-family chemokines are specialized monocyte-arrest chemokines. Their role in monocyte recruitment in inflammation can be inhibited by blocking CXCR2 function or downstream signaling events. Copyright © 2005 the American Physiological Society.

485. Impaired cardiac and sympathetic autonomic control in rats differing in acetylcholine receptor sensitivity - Padley J.R., Overstreet D.H., Pilowsky P.M. and Goodchild A.K. [A.K. Goodchild, Hypertension and Stroke Research Laboratories, Dept. of Neurosurgery, Royal North Shore Hospital, St. Leonards, NSW, Australia] - *AM. J. PHYSIOL. HEART CIRC. PHYSIOL.* 2005 289/5 58-5 (H1985-H1992) - summ in ENGL

Acetylcholine receptors (AChR) are important in premotor and efferent control of autonomic function; however, the extent to which cardiovascular function is affected by genetic variations in AChR sensitivity is unknown. We assessed heart rate variability (HRV) and baroreflex sensitivity (BRS) in rats bred for resistance (FRL) or sensitivity (FSL) to cholinergic agents compared with Sprague-Dawley rats (SD), confirmed by using hypothermic responses evoked by the muscarinic agonist oxotremorine (0.2 mg/kg ip) ($n \ge 9$ rats/group)-Arterial pressure, ECG, and splanchnic sympathetic (SNA) and phrenic (PNA) nerve activities were acquired under anesthesia (urethane 1.3 g/kg ip). HRV was assessed in time and frequency domains from short-term R-R interval data, and spontaneous heart rate BRS was obtained by using a sequence method at rest and after administration of atropine methylnitrate (mATR, 2 mg/kg iv). Heart rate and SNA baroreflex gains were assessed by using conventional pharmacological methods. FRL and FSL were normotensive but displayed elevated heart rates, reduced HRV and HF power, and spontaneous BRS compared with SD. mATR had no effect on these parameters in FRL or FSL, indicating reduced cardiovagal tone. FSL exhibited reduced PNA frequency, longer baroreflex latency, and reduced baroreflex gain of heart rate and SNA compared with FRL and SD, indicating in FSL dual impairment of cardiac and circulatory baroreflexes. These findings show that AChR resistance results in reduced cardiac muscarinic receptor function leading to cardiovagal insufficiency. In contrast, AChR sensitivity results in autonomic and respiratory abnormalities arising from alterations in central muscarinic and or other neurotransmitter receptors. Copyright © 2005 the American Physiological Society.

486. Atrial natriuretic peptide induces shedding of endothelial glycocalyx in coronary vascular bed of guinea pig hearts - Bruegger D., Jacob M., Rehm M. et al. [M. Rehm, Clinic for Anesthesiology, Ludwig-Maximilians-Univ., Marchioninistr. 15, D-81377 Munich, Germany] - AM. J. PHYSIOL. HEART CIRC. PHYSIOL. 2005 289/5 58-5 (H1993-H1999) - summ in ENGL

Atrial natriuretic peptide (ANP) is reported to enhance vascular permeability in vivo. Our aim was to evaluate the impact of ANP on coronary extravasation of fluids and macromolecules and on the integrity of the endothelial glycocalyx. Isolated guinea pig hearts (n = 6/group) were perfused with Krebs-Henseleit buffer in a Langendorff mode. A 6% hydroxyethyl starch (HES) solution was infused into the coronary system for 20 min without (Control group) and simultaneously with (ANP group) ANP at 10-9 M. In two further series, the glycocalyx was enzymatically degraded by means of heparinase (Hep) application (10 IU over 15 min), followed again by the infusion of HES in the absence (Hep group) and presence (ANP+Hep group) of ANP. Net fluid filtration, extravasation of HES, electron microscopic visualization of the glycocalyx, and quantification of shedding of syndecan-1, a component of the glycocalyx, were determined. An increase in fluid leak was observed

in ANP, ANP+Hep, and Hep hearts [+29%, +31%, +14%, respectively; a decrease was observed in Control hearts (-13%)]. Similarly, an accelerated extravasation of colloid was observed in these three groups. Coronary release of syndecan-1 increased 9- to 18-fold during infusion of ANP. Electron microscopy revealed a dramatic degradation of the glycocalyx after ANP. These results indicate that the endothelial glycocalyx serves as a barrier to transmural exchange of fluid and colloid in the coronary vascular system. ANP causes rapid shedding of individual components of the glycocalyx and histologically detectable degradation. Thus the permeability-increasing effect of ANP may be at least partially related to changes in the integrity of the endothelial glycocalyx. Copyright ⊚ 2005 the American Physiological Society.

487. Regulation of angiotensin-converting enzyme production by nicotine in human endothelial cells - Saijonmaa O., Nyman T. and Fyhrquist F. [O. Saijonmaa, Minerva Institute for Medical Research, Biomedicum Helsinki, Haartmaninkatu 8, FIN-00290, Helsinki, Finland] - *AM. J. PHYSIOL. HEART CIRC. PHYSIOL.* 2005 289/5 58-5 (H2000-H2004) - summ in ENGL

Nicotine, a component of cigarette smoke, has been implicated in the pathogenesis of cardiovascular disease. We examined whether nicotine regulates angiotensin-converting enzyme (ACE)-, an enzyme that plays an important role in the pathophysiology of atherosclerosis and hypertension. Human umbilical cord vein endothelial cells were treated with nicotine (0.1-1 µM) alone or in combination with vascular endothelial growth factor (VEGF; 0.5 nM) or GF-109203X (GFX; $2.5 \mu\text{M}$). The amount of ACE in intact endothelial cells was measured by an inhibitor-binding assay method, and ACE mRNA levels were quantified using LightCycler technology. Phosphorylated PKC levels were measured by Western immunoblotting. Nicotine did not modulate basal ACE production but significantly potentiated VEGF-induced ACE upregulation. Treatment of endothelial cells with the PKC inhibitor GFX totally blocked VEGF- and nicotine-induced ACE upregulation. VEGF induced PKC phosphorylation, which was potentiated by cotreatment with nicotine. We conclude that nicotine significantly potentiated VEGF-induced ACE upregulation. This effect was probably mediated by PKC phosphorylation. The interaction of nicotine with VEGF in ACE induction may contribute to the pathogenesis of smoking-related cardiovascular disease. Copyright © 2005 the American Physiological Society.

488. Activation of PKC modulates blood-brain barrier endothelial cell permeability changes induced by hypoxia and posthypoxic reoxygenation - Fleegal M.A., Hom S., Borg L. K. and Davis T.P. [T.P. Davis, Dept. of Medical Pharmacology, College of Medicine, Univ. of Arizona, 1501 N. Campbell Ave., Tucson, AZ 85724, United States] - *AM. J. PHYSIOL. HEART CIRC. PHYSIOL.* 2005 289/5 58-5 (H2012-H2019) - summ in ENGL

The blood-brain barrier (BBB) is a metabolic and physiological barrier important for maintaining brain homeostasis. The aim of this study was to determine the role of PKC activation in BBB paracellular permeability changes induced by hypoxia and posthypoxic reoxygenation using in vitro and in vivo BBB models. In rat brain microvessel endothelial cells (RMECs) exposed to hypoxia (1% O₂-99% N₂; 24 h), a significant increase in total PKC activity was observed, and this was reduced by posthypoxic reoxygenation $(95\% \text{ room air-} 5\% \text{ CO}_2)$ for 2 h. The expression of PKC- β 11, PKC- γ , PKC- η , PKC- μ , and PKC- λ also increased following hypoxia (1% O2-99% N2; 24 h), and these protein levels remained elevated following posthypoxic reoxygenation (95% room air-5% CO ₂; 2 h). Increases in the expression of PKC- ϵ and PKC- ζ were also observed following posthypoxic reoxygenation (95% room air-5% CO₂; 2 h). Moreover, inhibition of PKC with chelerythrine chloride (10 μ M) attenuated the hypoxia-induced increases in [14C]sucrose permeability. Similar to what was observed in RMECs, total PKC activity was also stimulated in cerebral microvessels isolated from rats exposed to hypoxia (6% O_2 -94% N_2 ; 1 h) and posthypoxic reoxygenation (room air; 10 min). In contrast, hypoxia (6% O₂-94% N₂; 1 h) and posthypoxic reoxygenation (room air; 10 min) significantly increased the expression levels of only PKC- γ and PKC- θ in the in vivo hypoxia model. These data demonstrate that hypoxia-induced BBB paracellular permeability changes occur via a PKC-dependent mechanism, possibly by differentially regulating the protein expression of the 11 PKC isozymes. Copyright $\@$ 2005 the American Physiological Society.

489. The influence of body size on measurements of overall cardiac function - Chantler P.D., Clements R.E., Sharp L. et al. [D.F. Goldspink, Henry Cotton Campus, 15-21 Webster St., Liverpool L3 2ET, United Kingdom] - *AM. J. PHYSIOL. HEART CIRC. PHYSIOL.* 2005 289/5 58-5 (H2059-H2065) - summ in ENGL

The purpose of this study was to determine the best scaling method to account for the effects of body size on measurements of overall cardiac function and subsequently the interpretation of data based on cardiac power output (CPO). CPO was measured at rest (CPO_{rest}) and at maximal exercise (CPO_{max}) on 88 and 103 healthy but untrained men and women, respectively, over the age range of 20-70 yr. Cardiac reserve (CR) was calculated as CPOmax - CPO_{rest}, CPO_{max}, and CR were all significantly related to body mass (BM), body surface area (BSA), and lean body mass (LBM). The linear regression model failed to completely normalize these measurements. In contrast, the allometric model produced size-independent values of CPO. Furthermore, all the assumptions associated with the allometric model were achieved. For CPO_{rest}, mean body size exponents were BM^{0.33}, BSA^{0.60}, and LBM ^{0.47}. For CPO_{max}, the exponents were BM^{0.41}, BSA^{0.81}, and LBM^{0.71}. For CR, mean body size exponents were BM^{0.44}, BSA^{0.87}, and LBM^{0.79}. LBM was identified (from the root-mean-squares errors of the separate regression models) as the best physiological variable (based on its high metabolic activity) to be scaled in the allometric model. Scaling of CPO to LBMb (where b is the scaling exponent)dramatically reduced the between-gender differences with only a 7% difference in CPO_{rest} and CPO_{max} values. In addition, the gender difference in CR was completely removed. To avoid erroneous interpretations and conclusions being made when comparing data between men and women of different ages, the allometric scaling of CPO to LBMb would seem crucial. Copyright © 2005 the American Physiological Society.

490. Naloxone does not influence cardiovascular responses to mild mental stress in postmenopausal women - Litschauer B., Schaller G. and Wolzt M. [M. Wolzt, Medical Univ. Vienna, Dept. of Clinical Pharmacology, AKH-Wien, Währinger Gürtel 18-20, A-1090 Vienna, Austria] - *AM. J. PHYSIOL. HEART CIRC. PHYSIOL.* 2005 289/5 58-5 (H2120-H2125) - summ in ENGL

The interaction between central opioid activity, sex hormones, and the cardiovascular reactivity to stress is unknown. Twentyeight healthy postmenopausal women, 16 without, and 12 with hormone replacement therapy (HRT) participated in this randomized, double-blind, cross-over study. The opioid receptor antagonist naloxone or placebo was administered intravenously on 2 different days and mild mental stress was induced by the Stroop Color-Word Test. Cardiovascular responses were assessed noninvasively by impedance cardiography. Stress significantly increased stroke volume, cardiac output, blood pressure, and heart rate, which was not influenced by opioid receptor blockade. Whereas naloxone increased cortisol plasma concentrations irrespective of HRT status, luteinizing hormone concentrations, which were higher in non-HRT compared with HRT women, were increased by naloxone in women with HRT only. These data suggest that the opioidergic tone of the hypothalamus-pituitary-adrenal axis persists in postmenopausal women, irrespective of HRT use, while the opioidergic tone on the hypothalamus-pituitary-gonadal axis seems to depend on an estrogenic milieu. Naloxone does not alter cardiovascular mental stress reactions in postmenopausal women independent of their hormone substitution status. Copyright © 2005 the American Physiological Society.

491. Regulation of capillary hydraulic conductivity in response to an acute change in shear - Kim M.-H., Harris N.R. and Tarbell J.M. [N.R. Harris, Louisiana State Univ. Health Sciences Center, Dept. of Molecular and Cellular Physiology, 1501 Kings Highway, Shreveport, LA 71130, United States] - *AM. J. PHYSIOL. HEART CIRC. PHYSIOL.* 2005 289/5 58-5 (H2126-H2135) - summ in ENGL

The effects of mechanical perturbations (shear stress, pressure) on microvascular permeability primarily have been examined in micropipette- cannulated vessels or in endothelial monolayers in vitro.

The objective of this study is to determine whether acute changes in blood flow shear stress might influence measurements of hydraulic conductivity (Lp) in autoperfused microvessels in vivo. Rat mesenteric microvessels were observed via intravital microscopy. Occlusion of a third-order arteriole with a micropipette was used to divert and increase flow through a nonoccluded capillary or fourth-order arteriolar branch. Transvascular fluid filtration rate in the branching vessel was measured with a Landis technique. Flow (shear)-induced increases in L $_{\rm p}$ disappeared within 20-30 s of the removal of the shear and could be eliminated with nitric oxide synthase inhibition. The shear-induced increase in Lp was greater in capillaries compared with terminal arterioles. An acute change in shear may regulate Lp by a nitric oxide-dependent mechanism that displays heterogeneity within a microvascular network. Copyright © 2005 The American Physiological Society.

492. Paradoxical hypotension following increased hematocrit and blood viscosity - Martini J., Carpentier B., Negrete A.C. et al. [J. Martini, Dept. of Bioengineering, Univ. of California, San Diego, 9500 Gilman Dr., San Diego, CA 92093-0412, United States] - *AM. J. PHYSIOL. HEART CIRC. PHYSIOL.* 2005 289/5 58-5 (H2136-H2143) - summ in ENGL

Hematocrit (Hct) of awake hamsters and CD-1 mice was acutely increased by isovolemic exchange transfusion of packed red blood cells (RBCs) to assess the relation between Hct and blood pressure. Increasing Hct 7-13% of baseline decreased mean arterial blood pressure (MAP) by 13 mmHg. Increasing Hct above 19% reversed this trend and caused MAP to rise above baseline. This relationship is described by a parabolic function ($R^2 = 0.57$ and P < 0.05). Hamsters pretreated with the nitric oxide (NO) synthase (NOS) inhibitor N ω -nitro-L-arginine methyl ester (L-NAME) and endothelial NOS-deficient mice showed no change in MAP when Hct was increased by < 19%. Nitrate/nitrite plasma levels of Hctaugmented hamsters increased relative to control and L-NAME treated animals. The blood pressure effect was stable 2 h after exchange transfusion. These findings suggest that increasing Hct increases blood viscosity, shear stress, and NO production, leading to vasodilation and mild hypotension. This was corroborated by measuring A1 arteriolar diameters (55.0 \pm 21.5 μ m) and blood flow in the hamster window chamber preparation, which showed statistically significant increased vessel diameter (1.04 \pm 0.1 relative to baseline) and microcirculatory blood flow (1.39 \pm 0.68 relative to baseline) after exchange transfusion with packed RBCs. Larger increases of Hct (> 19% of baseline) led blood viscosity to increase > 50%, overwhelming the NO effect through a significant viscosity-dependent increase in vascular resistance, causing MAP to rise above baseline values. Copyright © 2005 The American Physiological Society.

493. Increased expression of iNOS is associated with endothelial dysfunction and impaired pressor responsiveness in streptozotocin-induced diabetes - Nagareddy P.R., Xia Z., McNeill J.H. and MacLeod K.M. [K.M. MacLeod, Div. of Pharmacology and Toxicology, Faculty of Pharmaceutical Sciences, Univ. of British Columbia, Vancouver, BC V6T 1Z3, Canada] - *AM. J. PHYSIOL. HEART CIRC. PHYSIOL.* 2005 289/5 58-5 (H2144-H2152) - summing ENCL

Studies in streptozotocin (STZ)-induced diabetic rats have demonstrated cardiovascular abnormalities such as depressed mean arterial blood pressure (MABP) and heart rate (HR), endothelial dysfunction, and attenuated pressor responses to vasoactive agents. We investigated whether these abnormalities are due to diabetesassociated activation of inducible nitric oxide synthase (iNOS). In addition, the effect of the duration of diabetes on these abnormalities was also evaluated. Diabetes was induced by administration of 60 mg/kg STZ via the tail vein. One, 3, 9, or 12 wk after STZ injection, MABP, HR, and endothelial function were measured in conscious unrestrained rats. Pressor response curves to bolus doses of methoxamine (MTX) and angiotensin II (ANG II) were constructed in the presence of N-[3(aminomethyl)benzyl]-acetamidine, dihydrochloride (1400W), a specific inhibitor of iNOS. Depressed MABP and HR and impairment of endothelial function were observed as early as 3 wk after induction of diabetes. Acute inhibition of iNOS with 1400W (3 mg/kg iv) restored the attenuated pressor responses to both MTX and ANG II without affecting the basal MABP

and HR. Immunohistochemical and Western analysis blot studies in cardiovascular tissues revealed decreased expression of endothelial nitric oxide synthase (eNOS) concomitant with increased expression of iNOS and nitrotyrosine with the progression of diabetes. Our findings suggest that induction of iNOS in cardiovascular tissues is dependent on the duration of diabetes and contributes significantly to the depressed pressor responses to vasoactive agents and potentially to endothelial dysfunction. Copyright © 2005 the American Physiological Society.

494. Fas-independent mitochondrial damage triggers cardiomyocyte death after ischemia-reperfusion - Gomez L., Chavanis N., Argaud L. et al. [M. Ovize, INSERM E0226, Laboratoire de Physiologie Lyon-Nord, 8 Ave. Rockefeller, 69373 Lyon, France] - AM. J. PHYSIOL. HEART CIRC. PHYSIOL. 2005 289/5 58-5 (H2153-H2158) - summ in ENGL

The Fas/Fas ligand and mitochondria pathways have been involved in cell death in several cell types. We combined the genetic inactivation of the Fas receptor (lpr mice), on the one hand, to the pharmacological inhibition of the mitochondrial permeability transition pore (mPTP), on the other hand, to investigate which of these pathways is predominantly activated during prolonged ischemia-reperfusion. Anesthetized C57BL/6JICO (control) and C57BL/6-lpr mice were pretreated with either saline or cyclosporin A (CsA; 40 mg/kg, 3 times a day), an inhibitor of the mPTP, and underwent 25 min of ischemia and 24 h of reperfusion. After 24 h of reperfusion, hearts were harvested: infarct size was assessed by 2,3,5-triphenyltetrazolium chloride staining, myocardial apoptosis by caspase 3 activity, and mitochondrial permeability transition by Ca 2+-induced mPTP opening using a potentiometric approach. Infarct size was comparable in untreated control and lpr mice, ranging from 77 \pm 5% to 83 \pm 3% of the area at risk. CsA significantly reduced infarct size in control and lpr hearts. Control and lpr hearts exhibited comparable increase in caspase 3 activity that averaged 57 ± 18 and 49 ± 5 pmol min⁻¹ mg⁻¹, respectively. CsA treatment significantly reduced caspase 3 activity in control and lpr hearts. The Ca 2+ overload required to open the mPTP was decreased to a similar extent in lpr and controls. CsA significantly attenuated Ca2+-induced mPTP opening in both groups. Our results suggest that the Fas pathway likely plays a minor role, whereas mitochondria are preferentially involved in mice cardiomyocyte death after a lethal ischemia-reperfusion injury. Copyright © 2005 the American Physiological Society.

495. Regulation of energy liberation during steady sarcomere shortening - Tchaicheeyan O. and Landesberg A. [A. Landesberg. Dept. of Biomedical Engineering, TECHNION-IIT, Haifa 32000, Israel] - *AM. J. PHYSIOL. HEART CIRC. PHYSIOL.* 2005 289/5 58-5 (H2176-H2182) - summ in ENGL

Energy liberation rate (E) during steady muscle shortening is a monotonic increasing or biphasic function of the shortening velocity (V). The study examines three plausible hypotheses for explaining the biphasic E-V relationship (EVR): 1) the cross-bridge (XB)turnover rate from non-force-generating (weak) to force-generating (strong) conformation decreases as V increases; 2) XB kinetics is determined by the number of strong XBs (XB-XB cooperativity); and 3) the affinity of troponin for calcium is modulated by the number of strong XBs (XB-Ca cooperativity). The relative role of the various energy-regulating mechanisms is not well defined. The hypotheses were tested by coupling calcium kinetics with XB cycling. All three hypotheses yield identical steady-state characteristics: 1) hyperbolic force-velocity relationship; 2) quasi-linear stiffness-force relationship; and 3) biphasic EVR, where E declines at high V due to decrease in the number of cycling XBs or in the weak-to-strong transition rate. The hypotheses differ in the ability to describe the existence of both monotonic and biphasic EVRs and in the effect of intracellular free calcium concentration ([Ca²⁺]_i) on the EVR peak. Monotonic and biphasic EVRs with a shift in EVR peak to higher velocity at higher [Ca2+]i are obtained only by XB-Ca cooperativity. XB-XB cooperativity provides only biphasic EVRs. A direct effect of V on XB kinetics predicts that EVR peak is obtained at the same velocity independently of [Ca²⁺]i. The study predicts that measuring the dependence of the EVR on $[Ca^{2+}]_i$ allows us to test the hypotheses and to identify the dominant energy-regulating mechanism. The established XB-XB and XB-Ca

mechanisms provide alternative explanations to the various reported EVRs. Copyright © 2005 the American Physiological Society.

496. Specific enhancement of sarcomeric response to Ca²⁺ protects murine myocardium against ischemia-reperfusion dysfunction - Arteaga G.M., Warren C.M., Milutinovic S. et al. [G.M. Arteaga, Dept. of Pediatrics, MC 901, College of Medicine, 835 S. Wolcott Ave., Chicago, IL 60612-7342, United States] - *AM. J. PHYSIOL. HEART CIRC. PHYSIOL.* 2005 289/5 58-5 (H2183-H2192) - summ in ENGL

Alteration in myofilament response to Ca2+ is a major mechanism for depressed cardiac function after ischemia-reperfusion (I/R) dysfunction. We tested the hypothesis that hearts with increased myofilament response to Ca ²⁺ are less susceptible to I/R. In one approach, we studied transgenic (TG) mice with a constitutive increase in myofilament Ca²⁺ sensitivity in which the adult form of cardiac troponin I (cTnI) is stoichiometrically replaced with the embryonic/neonatal isoform, slow skeletal TnI (ssTnI). We also studied mouse hearts with EMD-57033, which acts specifically to enhance myofilament response to Ca²⁺. We subjected isolated, perfused hearts to an I/R protocol consisting of 25 min of no-flow ischemia followed by 30 min of reperfusion. After I/R, developed pressure and rates of pressure change were significantly depressed and end-diastolic pressure was significantly elevated in nontransgenic (NTG) control hearts. These changes were significantly blunted in TG hearts and in NTG hearts perfused with EMD-57033 during reperfusion, with function returning to nearly baseline levels. Ca²⁺- and cross bridge-dependent activation, protein breakdown, and phosphorylation in detergent-extracted fiber bundles were also investigated. After I/R NTG fiber bundles exhibited a significant depression of cross bridge-dependent activation and Ca²⁺-activated tension and length dependence of activation that were not evident in TG preparations. Only NTG hearts demonstrated a significant increase in cTnI phosphorylation. Our results support the hypothesis that specific increases in myofilament Ca²⁺ sensitivity are able to diminish the effect of I/R on cardiac function. Copyright © 2005 the American Physiological Society.

497. Clusterin: A protective mediator for ischemic cardiomyocytes? - Krijnen P.A.J., Cillessen S.A.G.M., Manoe R. et al. [P.A.J. Krijnen, VU Univ. Medical Center, Dept. of Pathology, De Boelelaan 1117, 1007 MB Amsterdam, Netherlands] - AM. J. PHYSIOL. HEART CIRC. PHYSIOL. 2005 289/5 58-5 (H2193-H2202) - summ in ENGL.

We examined the relationship between clusterin and activated complement in human heart infarction and evaluated the effect of this protein on ischemic rat neonatal cardiomyoblasts (H9c2) and isolated adult ventricular rat cardiomyocytes as in vitro models of acute myocardial infarction. Clusterin protects cells by inhibiting complement and colocalizes with complement on jeopardized human cardiomyocytes after infarction. The distribution of clusterin and complement factor C3d was evaluated in the infarcted human heart. We also analyzed the protein expression of clusterin in ischemic H9c2 cells. The binding of endogenous and purified human clusterin on H9c2 cells was analyzed by flow cytometry. Furthermore, the effect of clusterin on the viability of ischemically challenged H9c2 cells and isolated adult ventricular rat cardiomyocytes was analyzed. In human myocardial infarcts, clusterin was found on scattered, morphologically viable cardiomyocytes within the infarcted area that were negative for complement. In H9c2 cells, clusterin was rapidly expressed after ischemia. Its expression was reduced after reperfusion. Clusterin bound to single annexin V-positive or annexin V and propidium iodide-positive H9c2 cells. Clusterin inhibited ischemia-induced death in H9c2 cells as well as in isolated adult ventricular rat cardiomyocytes in the absence of complement. We conclude that ischemia induces the upregulation of clusterin in ischemically challenged, but viable, cardiomyocytes. Our data suggest that clusterin protects cardiomyocytes against ischemic cell death via a complement-independent pathway. Copyright © 2005 the American Physiological Society.

498. Reversal of delayed vasospasm by an inhibitor of the synthesis of **20-HETE** - Takeuchi K., Renic M., Bohman Q.C. et al. [R.J. Roman, Dept. of Physiology, Medical College of Wisconsin, 8701 Watertown Plank Rd., Milwaukee, WI 53226, United States]

- *AM. J. PHYSIOL. HEART CIRC. PHYSIOL.* 2005 289/5 58-5 (H2203-H2211) - summ in ENGL

This study characterized the time course of changes in cerebral blood flow (CBF) and vascular diameter in a dualhemorrhage model of subarachnoid hemorrhage (SAH) in rats and examined whether acute blockade of the synthesis of 20-hydroxyeicosatetraenoic acid (20-HETE) with N-(3-chloro-4morpholin-4-yl) phenyl-N'-hydroxyimido formamide (TS-011) can reverse delayed vasospasm in this model. Rats received an intracisternal injection of blood (0.4 ml) on day 0 and a second injection 2 days later. CBF was sequentially measured using laser-Doppler flowmetry, and the diameters of the cerebral arteries were determined after filling the cerebral vasculature with a casting compound. CBF fell to 67% of control after the first intracisternal injection of blood but returned to a value near control 24 h later. CBF again fell to 63% of control after a second intracisternal injection of blood and remained 30% below control for 5 days. The fall in CBF after the second intracisternal injection of blood was associated with a sustained 30% reduction in the diameters of the middle cerebral. posterior communicating, and basilar arteries. Acute blockade of the synthesis of 20-HETE with TS-011 (0.1 mg/kg iv), 5 days after the second SAH, increased the diameters of the cerebral arteries, and CBF returned to control. These results indicate that the rats develop delayed vasospasm after induction of the dual-hemorrhage model of SAH and that blockade of the synthesis of 20-HETE fully reverses cerebral vasospasm in this model. They also implicate 20-HETE in the development and maintenance of delayed cerebral vasospasm. Copyright © 2005 the American Physiological Society.

499. Maturation enhances fluid shear-induced activation of eNOS in perfused ovine carotid arteries - White C.R., Hamade M.W., Siami K. et al. [W.J. Pearce, Center for Perinatal Biology, Loma Linda Univ., Loma Linda, CA 92350, United States] - AM. J. PHYSIOL. HEART CIRC. PHYSIOL. 2005 289/5 58-5 (H2220-H2227) - summ in ENGL

The present study tests the hypothesis that age-dependent increases in endothelial vasodilator capacity are due to maturational increases in endothelial nitric oxide (NO) synthesis and release. Intact 4-cm carotid artery segments taken from term fetal lambs and nonpregnant adult sheep were perfused by using a closed system that enabled independent control of flow and inflow pressure and facilitated complete recovery of all NO released. Fluid shear stress induced a graded release of NO (in nmol NO min cm⁻² of luminal surface area) that was significantly greater in adult (890 \pm 140) than in fetal (300 \pm 40) carotid arteries at corresponding values of shear stress (5.9 \pm 0.3 dyn/cm²) but was independent of inflow pressure in both age groups. These age-related differences in NO release were not attributable to corresponding differences in endothelial NO synthase (eNOS) abundance, as eNOS protein levels (in ng of eNOS/cm² of luminal surface area) were similar in adult (14 ± 2) and fetal (12 + 1) arteries. Adult (80 + 15) and fetal (89 + 32) levels of eNOS mRNA (in 10⁶ copies/cm² of luminal surface area) were also similar. However, when NO release was normalized relative to the associated mass of eNOS protein to estimate eNOSspecific activity in situ, this value (in nmol NO g of eNOS-1 \min^{-1}) was significantly greater in adult (177 ± 44) than in fetal (97 \pm 36) arteries when the endothelium was maximally activated by A-23187. Similarly, the slope of the relation between fluid shear stress and estimated eNOS-specific activity (in nmol NO μ g of eNOS⁻¹ min⁻¹ per dyn/cm²) was also significantly greater in adult (6.8 ± 0.1) than in fetal (2.9 ± 0.1) arteries, which suggests that eNOS may be more sensitive to or more efficiently coupled to activating stimuli in adult compared with fetal arteries. We conclude that maturational increases in endothelial vasodilator capacity are attributable to age-dependent increases in NO release secondary to elevated eNOS-specific activity and involve more efficient coupling between endothelial activation and enhancement of eNOS activity in adult compared with fetal arteries. Copyright © 2005 the American Physiological Society.

500. Collagen and elastin cross-linking: A mechanism of constrictive remodeling after arterial injury - Brasselet C., Durand E., Addad F. et al. [A. Lafont, Hôpital Européen Georges Pompidou, Service de Cardiologie, 20, rue Leblanc, 75340 Paris Cedex

07, France] - AM. J. PHYSIOL. HEART CIRC. PHYSIOL. 2005 289/5 58-5 (H2228-H2233) - summ in ENGL

Constrictive remodeling after arterial injury is related to collagen accumulation. Cross-linking has been shown to induce a scar process in cutaneous wound healing and is increased after arterial injury. We therefore evaluated the effect of cross-linking inhibition on qualitative and quantitative changes in collagen, elastin, and arterial remodeling after balloon injury in the atherosclerotic rabbit model. Atherosclerotic-like lesions were induced in femoral arteries of 28 New Zealand White rabbits by a combination of air desiccation and a high-cholesterol diet. After 1 mo, balloon angioplasty was performed in both femoral arteries. Fourteen rabbits were fed β -aminopropionitrile (β -APN, 100 mg/kg) and compared with 14 untreated animals. The remodeling index, i.e., the ratio of external elastic lamina at the lesion site to external elastic lamina at the reference site, was determined 4 wk after angioplasty for both groups. Pyridinoline was significantly decreased in arteries from β -APN-treated animals compared with controls, confirming inhibition of collagen cross-linking: 0.30 (SD 0.03) and 0.52 (SD 0.02) mmol/mol hydroxyproline, respectively (P=0.002). Scanning and transmission electron microscopy showed a profound disorganization of collagen fibers in arteries from β -APN-treated animals. The remodeling index was significantly higher in β -APN-treated than in control animals [1.1 (SD 0.3) vs. 0.8 (SD 0.3), P = 0.03], indicating favorable remodeling. Restenosis decreased by 33% in β -APN-treated animals: 32% (SD 16) vs. 48% (SD 24) (P = 0.02). Neointimal collagen density was significantly lower in β -APN-treated animals than in controls: 23.0% (SD 3.8) vs. 29.4% (SD 4.0) (P = 0.004). These findings suggest that collagen and elastin cross-linking plays a role in the healing process via constrictive remodeling and restenosis after balloon injury in the atherosclerotic rabbit model. Copyright © 2005 the American Physiological

501. Functional changes in adenylyl cyclases and associated decreases in relaxation responses in mesenteric arteries from diabetic rats - Matsumoto T., Wakabayashi K., Kobayashi T. and Kamata K. [K. Kamata, Dept. of Physiology and Morphology, Institute of Medicinal Chemistry, Hoshi Univ., Shinagawa-ku, Tokyo 142-8501, Japan] - AM. J. PHYSIOL. HEART CIRC. PHYSIOL. 2005 289/5 58-5 (H2234-H2243) - summ in ENGL

To assess the functional change in adenylyl cyclases (AC)associated with the diabetic state, we investigated AC-mediated relaxations and cAMP production in mesenteric arteries from rats with streptozotocin (STZ)-induced diabetes. The relaxations induced by the water-soluble forskolin (FSK) analog NKH477, which is a putative ACS activator, but not by the β -adrenoceptor agonist isoproterenol (Iso) and the AC activator FSK, were reduced in intact diabetic mesenteric artery. In diabetic rats, however, Iso-, FSK-, and NKH477-induced relaxations were attenuated in the presence of inhibitors of nitric oxide synthase and cyclooxygenase. To exclude the influence of phosphodiesterase (PDE), we also examined the relaxations induced by several AC activators in the presence of 3isobutyl-1-methylxanthine (IBMX; a PDE inhibitor). Under these conditions, the relaxation induced by Iso was greatly impaired in STZ-diabetic rats. This Iso-induced relaxation was significantly attenuated by pretreatment with SQ-22536, an AC inhibitor, in mesenteric rings from age-matched controls but not in those from STZ-diabetic rats. Under the same conditions, the relaxations induced by FSK or NKH477 were impaired in STZ-diabetic rats. Neither FSK- nor A-23187 (a Ca²⁺ ionophore)-induced cAMP production was significantly different between diabetics and controls. However, cAMP production induced by Iso or NKH477 was significantly impaired in diabetic mesenteric arteries. Expression of mRNAs and proteins for AC5/6 was lower in diabetic mesenteric arteries than in controls. These results suggest that AC-mediated relaxation is impaired in the STZ-diabetic rat mesenteric artery, perhaps reflecting a reduction in AC5/6 activity. Copyright © 2005 the American Physiological Society.

502. Peroxynitrite hyperpolarizes smooth muscle and relaxes internal carotid artery in rabbit via ATP-sensitive K+ channels - Ohashi M., Faraci F. and Heistad D. [D. Heistad, Dept. of Internal Medicine, Univ. of Iowa, 200 Hawkins Dr., Iowa City, IA 52242-

1801, United States] - AM. J. PHYSIOL. HEART CIRC. PHYSIOL. 2005 289/5 58-5 (H2244-H2250) - summ in ENGL

The goal of this study was to determine the effects of peroxynitrite (ONOO-) on smooth muscle membrane potential and vasomotor function in rabbit carotid arteries. ONOO- is known to affect vascular tone by several mechanisms, including effects on K+ channels. Xanthine (X, 0.1 mM), xanthine oxidase (XO, 0.01 U/ml), and a low concentration of sodium nitroprusside (SNP, 10 nM) were used to generate ONOO. In the common carotid artery, X and XO (X/XO) in the presence of SNP tended to increase tension. In contrast, in the internal carotid artery, X/XO in the presence of SNP transiently hyperpolarized the membrane (-8.5 \pm 1.8 mV, mean \pm SE) and decreased tension (by 85 \pm 5.6%). In internal carotid arteries, in the absence of SNP, X/XO did not hyperpolarize the membrane and produced much less relaxation (by 23 \pm 5.6%) than X/XO and SNP. Ebselen (50 μ M) inhibited both hyperpolarization and relaxation to X/XO and SNP, and uric acid (100 μ M) inhibited relaxation. Glibenclamide (1 μ M) abolished hyperpolarization and inhibited relaxation during X/XO and SNP. Charybdotoxin (100 nM) or tetraethylammonium (1 mM) did not affect hyperpolarization or relaxation, respectively. These results suggest that ONOOhyperpolarizes and relaxes smooth muscle in rabbit internal carotid artery but not in common carotid artery through activation of KATP channels.

503. Late preconditioning induced by NO donors, adenosine A_1 receptor agonists, and δ_1 -opioid receptor agonists is mediated by iNOS - Guo Y., Stein A.B., Wu W.-J. et al. [R. Bolli, Division of Cardiology, Univ. of Louisville, Louisville, KY 40292, United States] - AM.J.PHYSIOL.HEART CIRC.PHYSIOL. 2005 289/5 58-5 (H2251-H2257) - summ in ENGL

Although ischemia-induced late preconditioning (PC) is known to be mediated by inducible nitric oxide (NO) synthase (iNOS), the role of this enzyme in pharmacologically induced late PC remains unclear. We tested whether targeted disruption of the iNOS gene abrogates late PC elicited by three structurally different NO donors [diethylenetriamine/NO (DETA/NO), nitroglycerin (NTG), and Snitroso-N-acetyl-penicillamine (SNAP)], an adenosine A₁ receptor agonist [2-chloro-N6-cyclopentyladenosine (CCPA)], and a δ_1 -opioid receptor agonist (TAN-670). The mice were subjected to a 30-min coronary occlusion followed by 24 h of reperfusion. In iNOS knockout (iNOS-/-) mice, infarct size was similar to wildtype (WT) controls, indicating that iNOS does not modulate infarct size in the absence of PC. Pretreatment of WT mice with DETA/NO, NTG, SNAP, TAN-670, or CCPA 24 h before coronary occlusion markedly reduced infarct size. In iNOS-/- mice, however, the late PC effect elicited by DETA/NO, NTG, SNAP, TAN-670, and CCPA was completely abrogated. Furthermore, in WT mice pretreated with TAN-670 or CCPA, the selective iNOS inhibitor 1400W also abolished the delayed PC properties of these drugs; 1400W had no effect in WT mice. These data demonstrate that iNOS plays an obligatory role in NO donor-induced, adenosine A₁ receptor agonist-induced, and δ_1 -opioid receptor agonist-induced late PC, underscoring the critical role of this enzyme as a common mediator of cardiac adaptations to stress. Copyright © 2005 the American Physiological Society.

504. Thyroid hormone interacts with PPAR α and PGC-1 during mitochondrial maturation in sheep heart - McClure T.D., Young M.E., Taegtmeyer H. et al. [M.A. Portman, Children's Hospital and Regional Medical Center W4841, 4800 Sand Point Way NE, Seattle, WA 98105, United States] - AM.J. PHYSIOL. HEART CIRC. PHYSIOL. 2005 289/5 58-5 (H2258-H2264) - summ in ENGL

Thyroid hormone (TH) promotes cardiac mitochondrial maturation and substrate metabolism after birth. This regulation involves ligand-dependent binding of nuclear TH receptors to target gene elements. TH also putatively controls genes indirectly by modulating transcription and/or translation of other nuclear steroid receptors and coactivators, such as peroxisome proliferator-activated receptor- α (PPAR α) and peroxisome proliferator-activated receptor- γ coactivator-1 (PGC-1). We tested the hypothesis that TH influences PPAR α and PGC-1 regulation of metabolic genes during postnatal maturation in sheep heart in vivo. We measured their mRNAs and/or protein levels and downstream targets in left ventricle from lambs: fetal (F), 30-day-old after postnatal thyroidectomy (THY),

and 30-day-old euthyroid (Con). Both PPAR $\!\alpha$ and PGC-1 mRNA expression decreased from F to Con, while PGC-1 protein increased substantially and PPAR α did not change. THY limited this mRNA response and attenuated the paradoxical postnatal PGC-1 protein elevation but did not alter mRNA levels for PPAR α , nuclear respiratory factor-1 and hypoxia-inducible factor-1 α . THY promotion in PPAR α mRNA did not change PPAR α protein or mRNA for PPAR α target genes, pyruvate-dehydrogenase kinase 4 (PDK4)and muscle type carnitine palmitoyltransferase I (mCPTI). THY reduction in PGC-1 protein occurred, while reducing cytochrome c oxidase and cytochrome c content and decreasing cardiac maximal inherent respiratory capacity. These data imply that TH modulates mitochondrial maturation partly through posttranscriptional control of PGC-1, while any important regulation of PDK4 and mCPTI by change in PPAR α protein expression remains doubtful. Also, the paradoxical expression pattern between mRNA and protein, particularly for PGC-1, suggests a feedback control mechanism. Copyright © 2005 the American Physiological Society.

505. Phase dynamics in cerebral autoregulation - Latka M., Turalska M., Glaubic-Latka M. et al. [M. Latka, Institute of Physics, Wroclaw Univ. of Technology, Wybrzeze Wyspianskiego 27, 50-370 Wroclaw, Poland] - *AM. J. PHYSIOL. HEART CIRC. PHYSIOL.* 2005 289/5 58-5 (H2272-H2279) - summ in ENGL

Complex continuous wavelet transforms are used to study the dynamics of instantaneous phase difference $\Delta \phi$ between the fluctuations of arterial blood pressure (ABP) and cerebral blood flow velocity (CBFV) in a middle cerebral artery. For healthy individuals, this phase difference changes slowly over time and has an almost uniform distribution for the very low-frequency (0.02-0.07 Hz) part of the spectrum. We quantify phase dynamics with the help of the synchronization index $\hat{\gamma} = (\sin ADelta; \hat{\phi})^2 + (\cos A\Delta \phi)^2$ that may vary between 0 (uniform distribution of phase differences, so the time series are statistically independent of one another) and 1 (phase locking of ABP and CBFV, so the former drives the latter). For healthy individuals, the group-averaged index γ has two distinct peaks, one at 0.11 Hz [γ = 0.59 \pm 0.09] and another at 0.33 Hz (γ = 0.55 ± 0.17). In the very low-frequency range (0.02-0.07 Hz), phase difference variability is an inherent property of an intact autoregulation system. Consequently, the average value of the synchronization parameter in this part of the spectrum is equal to 0.13 \pm 0.03. The phase difference variability sheds new light on the nature of cerebral hemodynamics, which so far has been predominantly characterized with the help of the high-pass filter model. In this intrinsically stationary approach, based on the transfer function formalism, the efficient autoregulation is associated with the positive phase shift between oscillations of CBFV and ABP. However, the method is applicable only in the part of the spectrum (0.1-0.3 Hz) where the coherence of these signals is high. We point out that synchrony analysis through the use of wavelet transforms is more general and allows us to study nonstationary aspects of cerebral hemodynamics in the very low-frequency range where the physiological significance of autoregulation is most strongly pronounced.

506. Vasoconstriction during venous congestion: Effects of venoarteriolar response, myogenic reflexes, and hemodyoamics of changing perfusion pressure - Okazaki K., Fu Q., Martini E.R. et al. [Q. Fu, Institute for Exercise and Environmental Medicine, 7232 Greenville Ave, Dallas, TX 75231, United States] - *AM. J. PHYSIOL. REGUL. INTEGR. COMP. PHYSIOL.* 2005 289/5 58-5 (R1354-R1359) - summ in ENGL

We dissected the relative contribution of arteriovenous hemodynamics, the venoarteriolar response (VAR), and the myogenic reflex toward a decrease in local blood flow induced by venous congestion. Skin blood flow (SkBF) was measured in 12 supine subjects via laser-Doppler flowmetry 1) over areas of forearm and calf skin, in which the VAR was blocked by using eutectic mixture of local anesthetics (EMLA sites) and 2) over the contralateral forearm or calf skin (control sites), using two different techniques: limb dependency of 23-37 cm below the heart and cuff inflation to 40 mmHg. During limb dependency, SkBF decreased at the control sites, whereas it remained unchanged at the EMLA sites. In contrast, during cuff inflation, SkBF decreased at the control sites and also decreased at the EMLA sites. The percent change in SkBF

from baseline was greater during cuff inflation than limb dependency at both the control sites and the EMLA sites. Estimated skin vascular resistance remained unchanged at the EMLA sites during cuff inflation, as well as limb dependency. Thus the decrease in SkBF during venous congestion with cuff inflation is not solely due to the cutaneous VAR but also to a reduction in local perfusion pressure. The VAR is therefore most specifically quantified by venous congestion induced by limb dependency, rather than cuff inflation. Finally, from both techniques, we calculated that during venous congestion induced by limb dependency (calf), $\sim\!45\%$ of the nonbaroreflex vasoconstriction is induced by the VAR and $\sim\!55\%$ by the myogenic reflex. Copyright © 2005 the American Physiological Society.

507. Role of pressor mechanisms from the NTS and CVLM in control of arterial pressure - Moreira T.S., Sato M.A., Takakura A.C.T. et al. [E. Colombari, Dept. of Physiology, Universidade Federal de São Paulo/EPM, Rua Botucatu, São Paulo, SP, Brazil] - *AM. J. PHYSIOL. REGUL. INTEGR. COMP. PHYSIOL.* 2005 289/5 58-5 (R1416-R1425) - summ in ENGL

In the present study, we investigated the effects of inhibition of the caudal ventrolateral medulla (CVLM) with the GABA_A agonist muscimol combined with the blockade of glutamatergic mechanism in the nucleus of the solitary tract (NTS) with kynurenic acid (kyn) on mean arterial pressure (MAP), heart rate (HR), and regional vascular resistances. In male Holtzman rats anesthetized intravenously with urethane/chloralose, bilateral injections of muscimol (120 pmol) into the CVLM or bilateral injections of kyn (2.7 nmol) into the NTS alone increased MAP to 186 ± 11 and to 142 \pm 6 mmHg, respectively, vs. control: 105 \pm 4 mmHg; HR to 407 \pm 15 and to 412 \pm 18 beats per minute (bpm), respectively, vs. control: 352 ± 12 bpm; and renal, mesenteric and hindquarter vascular resistances. However, in rats with the CVLM bilaterally blocked by muscimol, additional injections of kyn into the NTS reduced MAP to 88 ± 5 mmHg and mesenteric and hindquarter vascular resistances below control baseline levels. Moreover, in rats with the glutamatergic mechanisms of the NTS blocked by bilateral injections of kyn, additional injections of muscimol into the CVLM also reduced MAP to 92 ± 2 mmHg and mesenteric and hindquarter vascular resistances below control baseline levels. Simultaneous blockade of NTS and CVLM did not modify the increase in HR but also abolished the increase in renal vascular resistance produced by each treatment alone. The results suggest that important pressor mechanisms arise from the NTS and CVLM to control vascular resistance and arterial pressure under the conditions of the present study. Copyright © 2005 the American Physiological Society.

508. Arnold Heller and the lymph pump - Aukland K. [K. Aukland, Department of Biomedicine, Section of Physiology, Jonas Lies vei 91, 5009 Bergen, Norway] - *ACTA PHYSIOL. SCAND.* 2005 185/3 (171-180) - summ in ENGL

This article reviews studies on lymph propulsion in the lymph vessels by active contraction of the vessels, first described by Arnold Heller in 1869 in German language, and here translated into English. His observations were first confirmed by Beatrice Carrier (1926) and Howard Flory et al. (1927), and several groups were active up to World war II. Few publications appeared in the period 1940-1960, followed by increasing activity and development of new experimental techniques for use both in various experimental animals and in humans. Recently it has been shown that passive lymph flow may add to active propulsion. Both mechanisms depend on lymph formation, i.e. the uptake of interstitial fluid by the initial lymph vessels which is still not well understood. © 2005 Scandinavian Physiological Society.

509. Left ventricular pressure-volume relationships during normal growth and development in the adult rat - Studies in 8- and 50-week-old male Wistar rats - Bal M.P., De Vries W.B., Van Der Leij F.R. et al. [Dr. P. Steendijk, Leiden University Medical Center, PO Box 9600, 2300 RC Leiden, Netherlands] - ACTA PHYSIOL. SCAND. 2005 185/3 (181-191) - summ in ENGL

Aims: Left ventricular (LV) pressure-volume relations provide relatively load-independent indexes of systolic and diastolic LV function, but few data are available on pressure-volume relations

during growth and development in the normal adult heart. Furthermore, to quantify intrinsic ventricular function the indexes should be normalized for heart weight. However, in many studies the indexes are reported in absolute terms, or body weight-correction is used as a surrogate for heart weight-correction. Methods: We determined pressure-volume relations in young (8-week-old, n = 13) and middle-aged (50-week-old, n = 19) male Wistar rats in relation to their heart and body weights. The animals were anaesthetized and a 2F pressure-conductance catheter was introduced into the LV to measure pressure-volume relations. Results: Heart and body weights were significantly higher in the 50-week-old rats, whereas the heart-to-body weight ratio was significantly lower (2.74 \pm 0.32 vs. 4.41 ± 0.37 mg g⁻¹, P < 0.001). Intrinsic systolic function, quantified by the slopes of the end-systolic pressure-volume relation (EES), the dP/dt_{MAX} vs. end-diastolic volume relation (S-dP), and the preload recruitable stroke work relation (PRSW), normalized for heart weight, was slightly decreased in the 50-week-old rats (S-dP: -6%, P < 0.004; PRSW: -3%, P < 0.06). Heart weight-corrected diastolic indexes were not significant different. The absolute indexes qualitatively showed the same results, but body-weight corrected pressure-volume indexes showed improved systolic function and significantly depressed diastolic function. Conclusions: Intrinsic systolic function slightly decreases from the juvenile to the middleaged period in normal male Wistar rats. Furthermore, correction of pressure-volume indexes for body weight is not an adequate surrogate for heart weight-correction in these animals. © 2005 Scandinavian Physiological Society.

510. Force-frequency relation in frog-ventricle is dependent on the direction of sodium/calcium exchange in diastole - Subramani S., Balakrishnan S., Jyoti T. et al. [Prof. S. Subramani, Department of Physiology, Christian Medical College, Vellore 632 002, India] - *ACTA PHYSIOL. SCAND.* 2005 185/3 (193-202) - summ in ENGL

Aim: Force of contraction increases with stimulus-frequency in mammalian and amphibian hearts under control conditions. Here, we have analysed the mechanism of the force-frequency relation (FFR) in frog-ventricle. Methods: Circular strips of frog-ventricle were subjected to field-stimulation with frequencies in the range 0.03-0.2 Hz and force recorded on a chart-recorder. In another protocol, varying rest-periods were imposed while the preparation beat steadily at 0.2 Hz and the effect of rest on post-rest beat amplitude was noted. Results: Under control conditions, a positive FFR and a rest-induced decay of contraction amplitude (RID) were seen in the frequency range 0.03-0.2 Hz. With cadmium, nifedipine, nickel (40 μ mol L⁻¹), ryanodine and adrenaline (all drugs at 10 μ mol L⁻¹ concentration, except nickel), the positive FFR and RID seen under control conditions persisted. When the bathing solution contained ouabain (10 μmol L-1) or low external sodium (40 mmol L-1), or high external calcium (5 mmol L-1), the FFR turned negative in the frequency range stated above and there were rest-induced potentiations (RIP). Conclusion: When the conditions favour a net leak of calcium in diastole from intracellular stores via the calcium-extrusive mode of sodium-calcium exchanger (NCX), FFR is positive. An increase in frequency lessens the diastolic interval and therefore the diastolic calcium leak, thereby augmenting force. On the other hand, interventions which favour the calcium-acquisitive mode of NCX during diastole, changed the pattern of RID to RIP and converted FFR from positive to negative. With net diastolic calcium uptake, there is better store-filling and therefore higher force at lower frequencies. © 2005 Scandinavian Physiological

511. Arterial vascularization of primary motor cortex (precentral gyrus) - Ugur H.C., Kahilogullari G., Coscarella E. et al. [Dr. H.C. Ugur, Department of Neurosurgery, School of Medicine, Ankara University, Samanpazari, Ankara, Turkey] - *SURG. NEUROL.* 2005 64/SUPPL. 2 (S2:48-S2:52) - summ in ENGL

Background: The precentral gyrus (PG) is the primary motor area and is one of the most eloquent brain regions of neurosurgical interest. Although the arterial supply to the PG is generally known, contributions from different arterial branches such as the anterior cerebral artery (ACA), posterior cerebral artery (PCA), and middle cerebral artery (MCA) have not been comprehensively studied. The aim of the present study was to provide detailed information about

the arteries of the PG. Methods: Twenty adult human brains (40 hemispheres) were obtained, and ACA, MCA, and PCA were separately cannulated and injected with latex. The PG was identified. Results: The ACA supplied the medial one third and the MCA supplied the lateral two thirds of the PG. The PCA did not reach the PG in any of the hemispheres. In 16 hemispheres (40%), the callosomarginal artery and, in 13 hemispheres (32.5%), the pericallosal artery were dominant for the medial one third of the PG. In 11 hemispheres (27.5%), equal dominance was observed. MCA branches at the lateral tip of the PG were classified into precentral, central, and postcentral groups. In 29 hemispheres (72.5%), the central group, and in 4 hemispheres (10%), the precentral group were dominant for the lateral two thirds of the PG. In 7 hemispheres (17.5%), the precentral and central groups were equally dominant. No dominance was identified for the postcentral group. Conclusion: In each hemisphere, the PG was supplied by different vascularization patterns of ACA and MCA. The present study is the first to describe and discuss these details. Therefore, awareness of this pattern will provide a great contribution to surgical interventions. © 2005 Elsevier Inc. All rights reserved.

512. Hemodynamic and autonomic changes induced by Ironman: Prediction of competition time by blood pressure variability - Gratze G., Rudnicki R., Urban W. et al. [F. Skrabal, Krankenhaus der Barmherzigen Brüder, Teaching Hospital of Medical Univ. Graz, Marschallgasse 12, 8010 Graz, Austria] - J. APPL. PHYSIOL. 2005 99/5 (1728-1735) - summ in ENGL

We hypothesized that the extreme endurance exercise of an Ironman competition would lead to long-standing hemodynamic and autonomic changes. We investigated also the possibility of predicting competition performance from baseline hemodynamic and autonomic parameters. We have investigated 27 male athletes before competition, 1 h after, and then for the following week after the competition. The Task Force monitor was used to measure beatto-beat hemodynamic and autonomic parameters during supine rest and active standing. Heart rate (P < 0.001) was increased, and stroke index (P = 0.011), systolic blood pressure (P = 0.004), diastolic blood pressure (P < 0.001), total peripheral resistance index (P < 0.001), and baroreceptor reflex sensitivity (P < 0.001) were decreased after the competition. The 0.05- to 0.17-Hz band of heart rate and blood pressure variability was increased (P < 0.001 and P < 0.001, respectively), the 0.17- to 0.40-Hz band of heart rate interval variability was decreased after the competition (P < 0.001). All parameters returned to baseline values 3 days after the competition. After the competition, the autonomic response to orthostasis was significantly impaired. The 0.05- to 0.17-Hz band of diastolic blood pressure variability before competition and weekly net exercise training, but not the other hemodynamic and autonomic parameters, were related to competition time in multivariate regression analysis (multiple r = 0.70, P < 0.001). The marked hemodynamic and autonomic changes after an ultraendurance race, which are compatible with myocardial depression in the face of sympathetic activation and reduction of afterload, return to baseline after only 1-3 days. Because the 0.05- to 0.17-Hz band of diastolic blood pressure variability contributes to the prediction of competition time, the analysis of blood pressure variability in the frequency domain deserves further study for the prediction of endurance capacity. Copyright © 2005 the American Physiological Society.

513. Errors of measurement for blood volume parameters: A meta-analysis - Gore C.J., Hopkins W.G. and Burge C.M. [C.J. Gore, Australian Institute of Sport, P.O. Box 176, Belconnen, ACT 2616, Australia] - *J. APPL. PHYSIOL.* 2005 99/5 (1745-1758) - summ in ENGL

The volume of red blood cells (VRBC) is used routinely in the diagnostic workup of polycythemia, in assessing the efficacy of erythropoietin administration, and to study factors affecting oxygen transport. However, errors of various methods of measurement of VRBC and related parameters are not well characterized. We meta-analyzed 346 estimates of error of measurement of VRBC for techniques based on Evans blue (VRBC,EVans), 51 chromium-labeled red blood cells (VRBC,51Cr), and carbon monoxide (CO) rebreathing (VRBC,CO), as well as hemoglobin mass with the carbon-monoxide method (MHb,CO), in athletes and active and inac-tive subjects

undergoing various experimental and control treatments lasting minutes to months. Subject characteristics and experimental treatments had little effect on error of measurement, but measures with the smallest error showed some increase in error with increasing time between trials. Adjusted to 1 day between trials and expressed as coefficients of variation, mean errors for $M_{Hb,CO}$ (2.2%; 90% confidence interval 1.4-3.5%) and V $_{RBC,51Cr}$ (2.8%; 2.4-3.2%)-were much less than those for V $_{RBC,Evans}$ (6.7%; 4.9-9.4%) and V $_{RBC,CO}$ (6.7%; 3,4-14%). Most of the error of V $_{RBC,Evans}$ was due to error in measurement of volume of plasma via Evans blue dye (6.0%; 4.5-7.8%), which is the basis of V $_{RBC,Evans}$. Most of the error in V $_{RBC,co}$ was due to estimates from laboratories with a relatively large error in $M_{Hb,co}$, the basis of V $_{RBC,co}$ V $_{RBC,51Cr}$ and $M_{Hb,CO}$ are the best measures for research on blood-related changes in oxygen transport, With care, V $_{RBC,Evans}$ is suitable for clinical applications of blood-volume measurement. Copyright © 2005 the American Physiological Society.

See also: 514, 534, 536, 540, 541, 546, 555, 557, 570, 591, 592, 607, 609, 610, 611, 613, 619, 621, 622, 623, 626, 630.

7. RESPIRATION

514. Hypoxic pulmonary vasoconstriction in reptiles: A comparative study of four species with different lung structures and pulmonary blood pressures - Skovgaard N., Abe A.S., Andrade D.V. and Wang T. [N. Skovgaard, Dept. of Zoophysiology, University of Aarhus, Bldg. 131, DK-8000 Aarhus C, Denmark] - AM. J. PHYSIOL. REGUL. INTEGR. COMP. PHYSIOL. 2005 289/5 58-5 (R1280-R1288) - summ in ENGL

Low O2 levels in the lungs of birds and mammals cause constriction of the pulmonary vasculature that elevates resistance to pulmonary blood flow and increases pulmonary blood pressure. This hypoxic pulmonary vasoconstriction (HPV) diverts pulmonary blood flow from poorly ventilated and hypoxic areas of the lung to more well-ventilated parts and is considered important for the local matching of ventilation to blood perfusion. In the present study, the effects of acute hypoxia on pulmonary and systemic blood flows and pressures were measured in four species of anesthetized reptiles with diverse lung structures and heart morphologies: varanid lizards (Varanus exanthematicus), caimans (Caiman latirostris)-, rattlesnakes (Crotalus durissus), and tegu lizards (Tupinambis merianae). As previously shown in turtles, hypoxia causes a reversible constriction of the pulmonary vasculature in varanids and caimans, decreasing pulmonary vascular conductance by 37 and 31%, respectively. These three species possess complex multicameral lungs, and it is likely that HPV would aid to secure ventilation-perfusion homogeneity. There was no HPV in rattlesnakes, which have structurally simple lungs where local ventilation-perfusion inhomogeneities are less likely to occur. However, tegu lizards, which also have simple unicameral lungs, did exhibit HPV, decreasing pulmonary vascular conductance by 32%, albeit at a lower threshold than varanids and caimans (6.2 kPa oxygen in inspired air vs. 8.2 and 13.9 kPa, respectively). Although these observations suggest that HPV is more pronounced in species with complex lungs and functionally divided hearts, it is also clear that other components are involved. Copyright © 2005 the American Physiological Society.

515. Respiratory muscle responses elicited by dorsal periaqueductal gray stimulation in rats - Zhang W., Hayward L.F. and Davenport P.W. [P.W. Davenport, Dept. of Physiological Sciences, HSC, Univ. of Florida, Gainesville, FL 32610, United States] - *AM. J. PHYSIOL. REGUL. INTEGR. COMP. PHYSIOL.* 2005 289/5 58-5 (R1338-R1347) - summ in ENGL

The periaqueductal gray matter is an essential neural substrate for central integration of defense behavior and accompanied autonomic responses. The dorsal half of the periaqueductal gray matter (dPAG) is also involved in mediating emotional responses of anxiety and fear, psychological states that often are associated with changes in ventilation. However, information regarding respiratory modulation elicited from this structure is limited. The present study was undertaken to investigate the relationship between stimulus frequency and magnitude on ventilatory pattern and

respiratory muscle activity in urethane-anesthetized, spontaneously breathing rats. Electrical stimulation in the dPAG-recruited abdominal muscle activity increased ventilation and increased respiratory frequency by significantly shortening both inspiratory time and ex-Ventilation increased within the first breath after piratory time. the onset of stimulation, and the respiratory response increased with increasing stimulus frequency and magnitude. dPAG stimulation also increased baseline EMG activity in the diaphragm and recruited baseline external abdominal oblique EMG activity, normally quiescent during eupneic breathing. Significant changes in cardiorespiratory function were only evoked by stimulus intensities $> 10 \,\mu\text{A}$ and when stimulus frequencies were $> 10 \,\text{Hz}$. Respiratory activity of both the diaphragm and abdominal muscles remained elevated for a minimum of 60 s after cessation of stimulation. These results demonstrate that there is a short-latency respiratory response elicited from the dPAG stimulation, which includes both inspiratory and expiratory muscles. The changes in respiratory timing suggest rapid onset and sustained poststimulus dPAG modulation of the brain stem respiratory network that includes expiratory muscle recruitment. Copyright © 2005 the American Physiological Society.

516. Dipalmitoylphosphatidylcholine is not the major surfactant phospholipid species in all mammals - Lang C.J., Postle A.D., Orgeig, S. et al. [S. Orgeig, Environmental Biology, School of Earth and Environmental Sciences, Univ. of Adelaide, Adelaide, SA 5005, Australia] - *AM. J. PHYSIOL. REGUL. INTEGR. COMP. PHYSIOL.* 2005 289/5 58-5 (R1426-R1439) - summ in ENGL

Pulmonary surfactant, a complex mixture of lipids and proteins, lowers the surface tension in terminal air spaces and is crucial for lung function. Within an animal species, surfactant composition can be influenced by development, disease, respiratory rate, and/or body temperature. Here, we analyzed the composition of surfactant in three heterothermic mammals (dunnart, bat, squirrel), displaying different torpor patterns, to determine: 1) whether increases in surfactant cholesterol (Chol) and phospholipid (PL)saturation occur during long-term torpor in squirrels, as in bats and dunnarts; 2) whether surfactant proteins change during torpor; and 3) whether PL molecular species (molsp) composition is altered. In addition, we analyzed the molsp composition of a further nine mammals (including placental/marsupial and hetero-/homeothermic contrasts) to determine whether phylogeny or thermal behavior determines molsp composition in mammals. We discovered that like bats and dunnarts, surfactant Chol increases during torpor in squirrels. However, changes in PL saturation during torpor may not be universal. Torpor was accompanied by a decrease in surfactant protein A in dunnarts and squirrels, but not in bats, whereas surfactant protein B did not change in any species. Phosphatidylcholine (PC)16:0/16:0 is highly variable between mammals and is not the major PL in the wombat, dunnart, shrew, or Tasmanian devil. An inverse relationship exists between PC16:0/16:0 and two of the major fluidizing components, PC16:0/16:1 and PC16:0/14:0. The PL molsp profile of an animal species is not determined by phylogeny or thermal behavior. We conclude that there is no single PL molsp composition that functions optimally in all mammals; rather, surfactant from each animal is unique and tailored to the biology of that animal. Copyright © 2005 the American Physiological Society.

517. Gene expression profiling of the long-term adaptive response to hypoxia in the gills of adult zebrafish - Van Der Meer D.L.M., Van Den Thillart G.E.E.J.M., Witte F. et al. [C.P. Bagowski, nstitute of Biology, Univ. of Leiden, Wassenaarseweg 64, 2333 AL Leiden, Netherlands] - AM. J. PHYSIOL. REGUL. INTEGR. COMP. PHYSIOL. 2005 289/5 58-5 (R1512-R1519) - summ in ENGL

Low oxygen levels (hypoxia) play a role in clinical conditions such as stroke, chronic ischemia, and cancer. To better understand these diseases, it is crucial to study the responses of vertebrates to hypoxia. Among vertebrates, some teleosts have developed the ability to adapt to extremely low oxygen levels. We have studied long-term adaptive responses to hypoxia in adult zebrafish. We used zebrafish that survived severe hypoxic conditions for 3 wk and showed adaptive behavioral and phenotypic changes. We used cDNA microarrays to investigate hypoxia-induced changes in expression of 15,532 genes in the respiratory organs (the gills). We have identified 367 differentially expressed genes of which 117 showed hypoxia-induced and 250 hypoxia-reduced expressions.

Metabolic depression was indicated by repression of genes in the TCA cycle in the electron transport chain and of genes involved in protein biosynthesis. We observed enhanced expression of the monocarboxylate transporter and of the oxygen transporter myoglobin. The hypoxia-induced group further included the genes for Niemann-Pick C disease and for Wolman disease [lysosomal acid lipase (LAL)]. Both diseases lead to a similar intra- and extracellular accumulation of cholesterol and glycolipids. The Niemann-Pick C protein binds to cholesterol from internal lysosomal membranes and is involved in cholesterol trafficking. LAL is responsible for lysosomal cholesterol degradation. Our data suggest a novel adaptive mechanism to hypoxia, the induction of genes for lysosomal lipid trafficking and degradation. Studying physiological responses to hypoxia in species tolerant for extremely low oxygen levels can help identify novel regulatory genes, which may have important clinical implications. Copyright © 2005 the American Physiological Society.

518. NHE3 in an ancestral vertebrate: Primary sequence, distribution, localization, and function in gills - Choe K.P., Kato A., Hirose S. et al. [K.P. Choe, Anesthesiology Research Div., Vanderbilt Univ. Medical Center, T-4202 Medical Center North, 1161 21st Ave. South, Nashville, TN 37232-2520, United States] - *AM. J. PHYSIOL. REGUL. INTEGR. COMP. PHYSIOL.* 2005 289/5 58-5 (R1520-R1534) - summ in ENGL

In mammals, the Na^+/H^+ exchanger 3 (NHE3) is expressed with Na+/K+-ATPase in renal proximal tubules, where it secretes H+ and absorbs Na+ to maintain blood pH and volume. In elasmobranchs (sharks, skates, and stingrays), the gills are the dominant site of pH and osmoregulation. This study was conducted to determine whether epithelial NHE homologs exist in elasmobranchs and, if so, to localize their expression in gills and determine whether their expression is altered by environmental salinity or hypercapnia. Degenerate primers and RT-PCR were used to deduce partial sequences of mammalian NHE2 and NHE3 homologs from the gills of the euryhaline Atlantic stingray (Dasyatis sabina). Real-time PCR was then used to demonstrate that mRNA expression of the NHE3 homolog increased when stingrays were transferred to low salinities but not during hypercapnia. Expression of the NHE2 homolog did not change with either treatment. Rapid amplification of cDNA was then used to deduce the complete sequence of a putative NHE3. The 2,744-base pair cDNA includes a coding region for a 2,511amino acid protein that is 70% identical to human NHE3 (SLC9A3). Antisera generated against the carboxyl tail of the putative stingray NHE3 labeled the apical membranes of Na+/K+-ATPase-rich epithelial cells, and acclimation to freshwater caused a redistribution of labeling in the gills. This study provides the first NHE3 cloned from an elasmobranch and is the first to demonstrate an increase in gill NHE3 expression during acclimation to low salinities, suggesting that NHE3 can absorb Na+ from ion-poor environments. Copyright © 2005 the American Physiological Society.

519. Physiologic evaluation of different levels of assistance during noninvasive ventilation delivered through a helmet - Costa R., Navalesi P., Antonelli M. et al. [Dr. G. Conti, Policlinico A. Gemelli, Largo A. Gemelli 8, 00168 Rome, Italy] - *CHEST* 2005 128/4 (2984-2990) - summ in ENGL

Objective: To evaluate the effects of various levels of pressure support (PS) during noninvasive ventilation delivered through a helmet on breathing pattern, inspiratory effort, CO2 rebreathing, and comfort. Design: Physiologic study. Setting: University-affiliated hospital. Patients and participants: Eight healthy volunteers. Interventions: Volunteers received ventilation through a helmet with four different PS/positive end-expiratory pressure combinations (5/5 cm H₂O, 10/5 cm H₂O, 15/5 cm H₂O, and 10/10 cm H₂O) applied in random order. Measurements and results: The ventilatory respiratory rate, esophageal respiratory rate (RRpes), airway pressure, esophageal pressure tracings, esophageal swing, and pressure-time product (PTP) [PTP per breath, PTP per minute, and PTP per liter] were evaluated. We also measured the partial pressure of inspired CO₂ (PiCO₂) at the airway opening, mean partial pressure of expired CO₂ (PeCO₂), CO₂ production (VCO₂), minute ventilation (VE) delivered to the helmet (VEh), and the true inspired VE. By subtracting VE from VEh, we obtained the VE washing the helmet (VEwh). A visual analog scale (from 0 to 10)was used to evaluate comfort. Compared to spontaneous breathing, different levels of PS progressively increased tidal volume (VT) and decreased RRpes, reducing inspiratory effort. The increased levels of assistance did not produce significant changes in PiCO₂, end-tidal CO₂, and VCO₂. PeCO₂ had a slight decrease when increasing the level of PS from 5 to 10 cm H_2O (p < 0.05). Despite the presence of constant values of $\dot{V}E$, the increase of PS produced an increase in VEwh, without significant differences comparing 10 cm H 2O and 15 cm H₂O of PS. The subjects had a slight but not significant increase in discomfort by augmenting the level of assistance. At the highest level of PS (15 cm H₂O), the discomfort was significantly higher (p < 0.001) than at the other levels of assistance. Conclusion: In volunteers, the helmet is efficient in ventilation, allowing a VT increase and RRpes reduction. A significant discomfort was present only at the highest level of assistance; however, it did not affect patient/ventilator interaction.

520. Static versus prospective gated non-breath hold volumetric MDCT imaging of the lungs - Saba O.I., Chon D., Beck K. et al. [Dr. E.A. Hoffman, Department of Biomedical Engineering, University of Iowa, 200 Hawkins Drive, Iowa City, IA 52242, United States] - *ACAD. RADIOL.* 2005 12/11 (1371-1384) - summ in ENGL

Rationale and Objectives. The study's aim is to establish lungimaging methods that provide for the ability to image the lung under dynamic non-breath hold conditions while providing "virtual breath hold" quantifiable volumetric image data sets. Static breath hold images are used as the gold standard for evaluating these virtual breath hold images in both a phantom and sheep. Materials and Methods. Axial methods for gating image acquisition to multiple points in the respiratory cycle interleaved with incremental table stepping during multidetector-row computed tomographic (MDCT) scanning were developed. Data sets are generated over multiple breaths, providing volume images representative of multiple points within a respiratory cycle. To determine the reproducibility and accuracy of the methods, six anesthetized sheep were studied by means of MDCT in nongated and airway-pressure (P awy)-gated modes in which P_{awy} was 0, 7, and 15 cm H ₂O. Results. No significant differences were found between coefficients of variation in air volume measured from repeated static scans (1.74% \pm 1.78%), gated scans: inspiratory (1.2% \pm 0.44%) or expiratory gated (1.39% \pm 0.98%), or between static (1.74% \pm 1.78%) and gated (1.39% \pm 0.98%) scanning at similar P_{awy} (P > .1). Measured air volumes were larger from static versus gated scans by $5.85\% \pm 3.77\%$ at 7 cm H₂O and $4.45\% \pm 3.6\%$ at 15 cm H₂O of P_{awy} (P < .05), consistent with hysteresis. Differences between air volumes at 7 and 15 cm H₂O measured from either static or gated scans or that delivered by a super syringe were insignificant (P < .05). Visual accuracy of three-dimensional anatomic geometry was achieved, and landmark certainty was within 1 mm across respiratory cycles. Conclusions. A method has been shown that provides for accurate gating to respiratory signals during axial scanning. High-resolution volumetric image data sets are achievable while the scanned subject is breathing. Images are quantitatively similar to breath hold images, with differences likely explained by known pressure-volume hysteresis effects. © AUR, 2005.

521. Detection of age-dependent changes in healthy adult lungs with diffusion-weighted ³He MRI - Fain S.B., Altes T.A., Panth S.R. et al. [Dr. S.B. Fain, Medical Physics, University of Wisconsin, Madison, WI 53792, United States] - *ACAD. RADIOL.* 2005 12/11 (1385-1393) - summ in ENGL

Rationale and Objectives. To investigate changes in lung microstructure in healthy adult subjects with no smoking history using diffusion-weighted $^3\mathrm{He}$ MRI. Materials and Methods. Diffusion magnetic resonance imaging using hyperpolarized helium 3 ($^3\mathrm{He}$)-was applied to healthy volunteers to explore the dependence of lung microstructural changes with age, reflected by changes in the apparent diffusion coefficient (ADC) of $^3\mathrm{He}$ in lung air spaces. Data from three sites (University of Virginia (UVa), N = 25; University of Wisconsin (UW), N = 8; University of Nottingham (UN), N = 11) were combined in pooled analysis, including a total of N = 44 subjects (age range, 18-69 years; average age, 41.7 \pm 16.7 years).

Results. ADC was found to depend on age at all three sites (UW, R = +0.95, P = .0003; UVa, R = +0.74, P < .0001; UN, R = +0.96, P < .0001). Increases in mean ADCs with age appeared similar across sites (UW, +0.0017 cm²s-¹y-¹; UVa, +0.0015 cm²s-¹y-¹; pooled, +0.0015 cm²s-¹y-¹; P = .71). In a regional analysis performed on UW data, the increase in ADC affected all regions of the lung, but the apical and middle regions showed a greater increase compared with the base of the lung. Conclusion. Results suggest the observed age dependence of the ADC may be caused by changes in lung microstructure that increase alveolar volume during the aging process. © AUR. 2005.

522. Regional ventilation and lung mechanics using X-ray CT - Simon B.A. [Dr. B.A. Simon, Department of Anesthesiology, Tower 711, Johns Hopkins Hospital, Baltimore, MD 21287-8711, United States] - *ACAD. RADIOL.* 2005 12/11 (1414-1422) - summ in ENGL

Advances in computed tomographic (CT) imaging of the lung in the past decade, particularly with increased speed, resolution, gating capability, and rapidly expanding volumetric image acquisition, along with advances in image processing, have expanded the repertoire of imaging methods beyond anatomic visualization into the noninvasive study of regional lung physiological function. Recognizing that significant local disease or dysfunction can exist before global measures begin to deteriorate, the motivation for the development and application of these regional techniques is to further our understanding of the basic pathophysiological characteristics of evolving lung disease and, ultimately, develop sensitive measures for its early detection. This review emphasizes the key elements of ventilation and lung mechanics relevant for regional approaches and CT measurement principles available for their study. Examples of established and evolving methods for imaging regional ventilation and mechanics, including the xenon CT ventilation method; the relationship between changing regional CT density and air volume change; and registration-based methods for examining regional lung expansion and strain, are presented. © AUR, 2005.

523. Respiratory muscle performance with stretch-shortening cycle manoeuvres: Maximal inspiratory pressure-flow curves - Tzelepis G.E., Zakynthinos S., Mandros C. et al. [Dr. G.E. Tzelepis, Department of Pathophysiology, University of Athens Medical School, 75 M. Asias Street, 11527 Athens, Greece] - *ACTA PHYSIOL. SCAND.* 2005 185/3 (251-256) - summ in ENGL

Aim: To test the hypothesis that the maximal inspiratory muscle (IM) performance, as assessed by the maximal IM pressure-flow relationship, is enhanced with the stretch-shortening cycle (SSC). Methods: Maximal inspiratory flow-pressure curves were measured in 12 healthy volunteers (35 ± 6) years) during maximal single efforts through a range of graded resistors (4-, 6-, and 8-mm diameter orifices), against an occluded airway, and with a minimal load (wide-open resistor). Maximal inspiratory efforts were initiated at a volume near residual lung volume (RV). The subjects exhaled to RV using slow (S) or fast (F) manoeuvres. With the S manoeuvre, they exhaled slowly to RV and held the breath at RV for about 4 s prior to maximal inspiration. With the F manoeuvre, they exhaled rapidly to RV and immediately inhaled maximally without a post-expiratory hold; a strategy designed to enhance inspiratory pressure via the SSC. Results: The maximal inspiratory pressure-flow relationship was linear with the S and F manoeuvres ($r^2 = 0.88$ for S and $r^2 = 0.88$ for F manoeuvre, P < 0.0005 in all subjects). With the F manoeuvre, the pressure-flow relationship shifted to the right in a parallel fashion and the calculated maximal power increased by approximately 10% (P < 0.05) over that calculated with the S manoeuvre. Conclusion: The maximal inspiratory pressure-flow capacity can be enhanced with SSC manoeuvres in a manner analogous to increases in the force-velocity relationship with SSC reported for skeletal muscles. © 2005 Scandinavian Physiological Society.

524. Sonography of pleural space in healthy individuals - Kocijančič K., Kocijančič I. and Vidmar G. [Dr. K. Kocijančič, Institute of Radiology, Clinical Center, Zaloška 7, SI-1000 Ljubljana, Slovenia] - *J. CLIN. ULTRASOUND* 2005 33/8 (386-389) - summ in ENGL

Purpose. This research was performed to detect physiologic pleural fluid by chest ultrasonography, to assess the frequency of this

finding, and to check the status of pleural space, searching for possible individual variations of the amounts of pleural fluid. Materials and Methods. In the baseline study, chest ultrasonography of both pleural spaces was performed in a group of 106 healthy volunteers, searching for pleural fluid, first in the lateral decubitus position and then leaning on the elbow. An anechoic fluid layer at least 2-mm thick was taken as a positive result. The follow-up study was repeated on each subject after 2-4 months. Results. In the baseline study, a 2-mm-thick pleural fluid layer was found in 28 of 106 (26%) volunteers, both sided in 17 of 28 (61%), and unilaterally in 11 of 28 (39%). The follow-up study, showed a fluid layer in 24 of 106 (23%) volunteers, on both sides in 14 of 24 (58%), and unilaterally in 10 of 24 (42%). In the first study, the mean fluid layer thickness in the decubitus examination position was 2.9 mm (SD, 0.4 mm) and in elbow examination position 2.8 mm (SD, 0.4 mm). On follow-up study, the mean fluid layer thickness in both examination positions was the same, 3.1 mm (SD, 0.6 mm). Taking into consideration baseline and follow-up studies, the fluid was observed in 32 subjects, and 21 (66%) of them showed pleural fluid twice. Their mean fluid layer (3.1 mm) was significantly larger than the group of subjects with only one positive result (2.5 mm), with p values of <.01 for the baseline and <.05 for the follow-up study. Conclusion. In experimental conditions, small amounts of pleural fluid can be detected by chest sonography in healthy individuals. Our research suggests that there are individuals with sonographically permanently less ("dry pleural space") or more ("wet pleural space") physiologic pleural fluid. © 2005 Wiley Periodicals, Inc.

525. Tumor necrosis factor- α and malnutrition-induced inhibition of diaphragm fiber growth in young rats - Lewis M.I., Da X., Li H. and Fournier M. [M.I. Lewis, Cedars-Sinai Medical Center, 8700 Beverly Blvd., Los Angeles, CA 90048, United States] - *J. APPL. PHYSIOL.* 2005 99/5 (1649-1657) - summ in ENGL

Tumor necrosis factor (TNF)- α has been implicated in several muscle-wasting disorders, with increased levels of the cytokine reported in malnourished children. The role of TNF- α in mediating malnutrition-induced inhibition of diaphragm (DIA) muscle growth in young growing rats was evaluated. Three groups of rats were of normal food intake for 7 days); and 3) ND + rat specific anti-TNF- α antibody. DIA fiber cross-sectional areas were determined. Serum and muscle TNF- α levels were measured by real-time PCR, ELISA, and immunohistochemistry. Body weights decreased 20% in ND rats and increased 46% in CTL animals. Anti-TNF- α had no effect on body weight or on DIA mass in ND animals. significantly reduced cross-sectional areas of all fiber types (33-46%). Anti-TNF- α failed to attenuate ND-induced inhibition of DIA fiber growth. Serum TNF- α levels increased 2.6-fold in ND animals, with levels suppressed to below CTL values with anti-TNF- α . DIA TNF- α mRNA and protein levels increased two- to threefold in ND rats. Anti-TNF- α antibodies suppressed muscle levels of the cytokine in ND animals to near CTL values. TNF- α immunoreactivity in all DIA fibers revealed similar directions of change in both ND groups. Direction and magnitude of change in DIA phosphorylated p38 MAPK (a likely second messenger of TNF- α) tracked those of TNF- α . Muscle levels of IGF-I mRNA and phosphorylated Akt were markedly reduced in ND animals with no change following anti-TNF- α therapy. Thus rat anti-TNF- α at a dose known to neutralize the cytokine failed to attenuate or reverse ND-induced inhibition of DIA fiber growth in our model. Copyright © 2005 the American Physiological Society.

526. Cyclopiazonic acid activates a Ca²⁺-permeable, nonselective cation conductance in porcine and bovine tracheal smooth muscle - Helli P.B., Pertens E. and Janssen L.J. [L.J. Janssen, St. Joseph's Hospital, 50 Charlton Ave. East, Hamilton, Ont. L8N 4A6, Canada] - *J. APPL. PHYSIOL.* 2005 99/5 (1759-1768) - summ in ENGL

Capacitative Ca^{2+} entry has been examined in several tissues and, in some, appears to be mediated by nonselective cation channels collectively referred to as "store-operated" cation channels; however, relatively little is known about the electrophysiological properties of these channels in airway smooth muscle. Consequently we examined the electrophysiological characteristics and changes in intracellular Ca $^{2+}$ concentration associated with a cyclopiazonic

acid (CPA)-evoked current in porcine and bovine airway smooth muscle using patch-clamp and Ca 2+-fluorescence techniques. In bovine tracheal myocytes, CPA induced an elevation of intracellular Ca²⁺ that was dependent on extracellular Ca²⁺ and was insensitive to nifedipine (an L-type voltage-gated Ca2+ channel inhibitor). Using patch-clamp techniques and conditions that block both K+ and CP currents, we found that CPA rapidly activated a membrane conductance (I_{CPA}) in porcine and bovine tracheal myocytes that exhibits a linear current-voltage relationship with a reversal potential around 0 mV. Replacement of extracellular Na+ resulted in a marked reduction of I_{CPA} at physiological membrane potentials (i.e., -60 mV) that was accompanied by a shift in the reversal potential for I_{CPA} toward more negative membrane potentials. In addition, I_{CPA} was markedly inhibited by 10 μ M Gd³⁺ and La³⁺ but was largely insensitive to 1 μM nifedipine. We conclude that CPA induces capacitative Ca²⁺ entry in porcine and bovine tracheal smooth muscle via a Gd3+and La³⁺-sensitive, nonselective cation conductance. Copyright © 2005 the American Physiological Society.

527. Ovalbumin sensitization alters the ventilatory responses to chemical challenges in guinea pigs - Xu F., Zhuang J., Zhou T. and Lee L.-Y. [F. Xu, Pathophysiology Program, Lovelace Respiratory Research Institute, 2425 Ridgecrest Dr. SE, Albuquerque, NM 87108, United States] - *J. APPL. PHYSIOL*. 2005 99/5 (1782-1788) - summ in ENGL

Patients with chronic bronchial asthma show a depressed ventilatory response to hypoxia (DVH), but the underlying mechanism remains unclear. We tested whether DVH existed in ovalbumin (Ova)-treated guinea pigs, an established animal model of asthma. Twelve guinea pigs were exposed to Ova (1% in saline) or saline aerosol (control) for 5 min, 5 days/wk, for 2 wk. After completing aerosol exposure, the animals were anesthetized and exposed to systemic hypoxia. Ova treatment had no effects on animal body weight, baseline cardiorespiratory variables, or arterial blood O₂ and CO₂ tensions, but it attenuated the ventilatory response to hypoxia (10 breaths of pure N_2) by 65% (P < 0.05). When the animals were subjected to intracarotid injections of sodium cyanide (20 μ g) and doxapram (2 mg) to selectively stimulate carotid chemoreceptors, the ventilatory responses were reduced by 50% (P < 0.05) and 74% (P < 0.05), respectively. In contrast, Ova exposure failed to affect the ventilatory response to CO2 (7% CO2-21% unbalance N2 for 5 min; P > 0.05). Furthermore, the apneic response evoked by stimulating bronchopulmonary C fibers (PCFs) with right atrial injection of capsaicin (5 μ g) was markedly increased in the Ovasensitized group (5.02 \pm 1.56 s), compared with the control group $(1.82 \pm 0.45 \text{ s}; P < 0.05)$. These results suggest that Ova sensitization induces a DVH in guinea pigs, which probably results from an attenuation of the carotid chemoreceptor-mediated ventilatory excitation and an enhancement of the PCF-mediated ventilatory inhibition. Copyright © 2005 the American Physiological Society.

528. Effects of augmented respiratory muscle pressure production on locomotor limb venous return during calf contraction exercise - Miller J.D., Pegelow D.F., Jacques A.J. and Dempsey J.A. [J.D. Miller, University of Iowa, 3408 Eckstein Medical Research Building, Iowa City, IA 52242, United States] - *J. APPL. PHYSIOL.* 2005 99/5 (1802-1815) - summ in ENGL

We determined effects of augmented inspiratory and expiratory intrathoracic pressure or abdominal pressure (Pab) excursions on within-breath changes in steady-state femoral venous blood flow (\dot{Q}_{fv}) and net \dot{Q}_{fv} during tightly controlled (total breath time = 4 s, duty cycle = 0.5) accessory muscle/"rib cage" ($\Delta Pab < 2$ cmH $_2O$) or diaphragmatic ($\Delta Pab > 5$ cmH $_2O$) breathing. Selectively augmenting inspiratory intrathoracic pressure excursion during rib cage breathing augmented inspiratory facilitation of \dot{Q}_{fv} from the resting limb (69% and 89% of all flow occurred during nonloaded and loaded inspiration, respectively); however, net \dot{Q}_{fv} in the steady state was not altered because of slight reductions in femoral venous return during the ensuing expiratory phase of the breath. Selectively augmenting inspiratory esophageal pressure excursion during a predominantly diaphragmatic breath at rest did not alter within-breath changes in \dot{Q}_{fV} relative to nonloaded conditions (net retrograde flow = -9 \pm 12% and -4 \pm 9% during nonloaded and loaded inspiration, respectively), supporting the notion that the inferior vena cava is

completely collapsed by relatively small increases in gastric pressure. Addition of inspiratory + expiratory loading to diaphragmatic breathing at rest resulted in reversal of within-breath changes in $\dot{Q}_{\rm fv}$, such that >90% of all anterograde $\dot{Q}_{\rm fv}$ occurred during inspiration. Inspiratory + expiratory loading also reduced steady-state $\dot{Q}_{\rm fv}$ during mild- and moderate-intensity calf contractions compared with inspiratory loading alone. We conclude that 1) exaggerated inspiratory pressure excursions may augment within-breath changes in femoral venous return but do not increase net $\dot{Q}_{\rm fv}$ in the steady state and 2) active expiration during diaphragmatic breathing reduces the steady-state hyperemic response to dynamic exercise by mechanically impeding venous return from the locomotor limb, which may contribute to exercise limitation in health and disease. Copyright © 2005 the American Physiological Society.

529. Smooth muscle dynamics and maximal expiratory flow in asthma - Lambert R.K. and Wilson T.A. [T.A. Wilson, 107 Akerman Hall, 110 Union St. SE, Minneapolis, MN 55455, United States] - *J. APPL. PHYSIOL.* 2005 99/5 (1885-1890) - summ in ENGL

A computational model for maximal expiratory flow in constricted lungs is presented. The model was constructed by combining a previous computational model for maximal expiratory flow in normal lungs and a previous mathematical model for smooth muscle dynamics. Maximal expiratory flow-volume curves were computed for different levels of smooth muscle activation. The computed maximal expiratory flow-volume curves agree with data in the literature on flow in constricted nonasthmatic subjects. In the model, muscle force during expiration depends on the balance between the decrease in force that accompanies muscle shortening and the recovery of force that occurs during the time course of expiration, and the computed increase in residual volume (RV) depends on the magnitude of force recovery. The model was also used to calculate RV for a vital capacity maneuver with a slow rate of expiration, and RV was found to be further increased for this maneuver. We propose that the measurement of RV for a vital capacity maneuver with a slow rate of expiration would provide a more sensitive test of smooth muscle activation than the measurement of maximal expiratory flow. Copyright © 2005 the American Physiological Society.

530. Ventilation is unstable during drowsiness before sleep onset - Thomson S., Morrell M.J., Cordingley J.J. and Semple S.J. [S.J.

Thomson S., Morrell M.J., Cordingley J.J. and Semple S.J. [S.J. Semple, Dept. of Respiratory Medicine, Charing Cross Hospital, Fulham Palace Rd., London W6 8RF, United Kingdom] - J. APPL. PHYSIOL. 2005 99/5 (2036-2044) - summ in ENGL

Ventilation is unstable during drowsiness before sleep onset. We have studied the effects of transitory changes in cerebral state during drowsiness on breath duration and lung volume in eight healthy subjects in the absence of changes in airway resistance and fluctuations of ventilation and CO2 tension, characteristic of the onset of non-rapid eye movement sleep. A volume-cycled ventilator in the assist control mode was used to maintain CO 2 tension close to that when awake. Changes in cerebral state were determined by the EEG on a breath-by-breath basis and classified as alpha or theta breaths. Breath duration and the pause in gas flow between the end of expiratory airflow and the next breath were computed for two alpha breaths which preceded a theta breath and for the theta breath itself. The group mean (SD) results for this alpha-to-theta transition was associated with a prolongation in breath duration from 5.2 (SD 1.3) to 13.0 s (SD 2.1) and expiratory pause from 0.7 (SD 0.4) to 7.5 s (SD 2.2). Because the changes in arterial CCh tension (Paco2) are unknown during the theta breaths, we made in two subjects a continuous record of Pa_{CO2} in the radial artery. Pa_{CO2} remained constant from the alpha breaths through to the expiratory period of the theta breath by which time the duration of breath was already prolonged, representing an immediate and altered ventilatory response to the prevailing Pa_{CO2} . In the eight subjects, the CO_2 tension awake was 39.6 Torr (SD 2.3) and on assisted ventilation 38.0 Torr (1.4). We conclude that the ventilatory instability recorded in the present experiments is due to the apneic threshold for CO2 being at or just below that when awake. Copyright © 2005 the American Physiological Society.

See also: 533, 591, 595, 616, 634.

8. DIGESTION

531. Effect of progesterone on calcium activated potassium currents and intracellular calcium in guinea pig colon myocytes - Xu L., Chen J., Yu B. et al. [Dr. B. Yu, Department of Gastroenterology, Renmin Hospital, Wuhan University, Wuhan, China] - METHODS FIND. EXP. CLIN. PHARMACOL. 2005 27/7 (475-482) - summ in ENGL

Aims: To study the effects of progesterone on contractile activity of smooth muscle strips and on ion currents and intracellular Ca2+ ([Ca²⁺]i) intensity in single colonie myocytes in guinea pig proximal colons. Methods: Strips and single cells were dissected from female guinea pig proximal colon. Contraction of strips through an isotonic transducer was assessed and the responsible currents to progesterone were recorded with EPC-9 amplifier in nystatin perforated whole-cell configuration. Detection of [Ca 2+]i fluorescence loading fura-2 acetoxymethylester (fura-2/AM) was measured with confocal microscope. Results: Progesterone significantly inhibited contraction of guinea pig colon strips in a dose-dependent pattern. Inhibitory concentration 50 (IC₅₀) of progesterone in longitudinal strips and circular strips was, respectively, 9.7 μ M and 1.0 nM. Iberiotoxin (IbTX) partially blocked inhibition of progesterone in both oriented smooth muscle strips. Ca^{2+} activated K^+ (K_{ca}) channel currents recorded by depolarizing pulse protocol were enhanced by progesterone to 138% \pm 13% (n = 9, p < 0.01), and to 143% \pm 72% (n = 8, p < 0.01) when perfused with 10 μ M onapristone. Progesterone reduced L-Ca²⁺ currents to 67% \pm 6% (n = 7, p < 0.01) and had no effect with 5 μ M nicardipine in bath solution. $[Ca^{2+}]i$ fluorescence was reduced by progesterone to 75% \pm 72% (n = 8, p < 0.01). Conclusions: Progesterone decreases the contraction of colonic smooth muscles by enhancing K_{Ca} currents and reducing Ca + influx. © 2005 Prous Science. All rights reserved.

532. Porcine, mouse and human galactose 3-O-sulphotransferase-2 enzymes have different substrate specificities; the porcine enzyme requires basic compounds for its catalytic activity - Seko A., Sumiya J.-I. and Yamashita K. [K. Yamashita, Department of Biochemistry, Sasaki Institute, 2-2, Kanda-Surugadai, Chiyodaku, Tokyo 101-0062, Japan] - *BIOCHEM. J.* 2005 391/1 (77-85) - summ in ENGL.

Sulphation of galactose at the C-3 position is one of the major post-translational modifications of colorectal mucin. Thus we partially purified a Gal 3-O-sulphotransferase from porcine colonic mucosa (pGal3ST) and studied its enzymatic characteristics. The enzyme was purified 48500-fold by sequential chromatographies on hydroxyapatite, Con A (concanavalin A)-Sepharose, porcine colonic mucin-Sepharose, Cu²⁺-chelating Sepharose and AMP-agarose. Interestingly, the purified pGal3ST required submillimolar concentrations of spermine or basic lipids, such as D-sphingosine and N,N-dimethylsphingosine, for enzymatic activity. pGal3ST recognized $Gal\beta 1 \rightarrow 3GalNAc$ (core 1) as an optimal substrate, and had weaker activity for Gal β 1 \rightarrow 3GlcNAc (type 1) and Gal β 1 4GlcNAc (type 2). Substrate competition experiments proved that a single enzyme catalyses sulphation of all three oligosaccharides. Among the four human Gal3STs cloned to date, the substrate specificity of pGal3ST is most similar to that of human Gal3ST-2, which is also strongly expressed in colonic mucosa, although the kinetics of pGal3ST and human Gal3ST-2 were rather different. To determine whether pGal3ST is the orthologue of human Gal3ST-2, a cDNA encoding porcine Gal3ST-2 was isolated and the enzyme was expressed in COS-7 cells for analysis of substrate specificity. This revealed that porcine Gal3ST-2 has the same specificity as pGal3ST, indicating that pGal3ST is indeed the porcine equivalent of Gal3ST-2. The substrate specificity of mouse Gal3ST-2 was also different from those of human and porcine Gal3ST-2 enzymes. Mouse Gal3ST-2 preferred core 1 and type 2 glycans to type 1, and the K_m values were much higher than those of human Gal3ST-2. These results suggest that porcine Gal3ST-2 requires basic compounds for catalytic activity and that human, mouse and porcine Gal3ST-2 orthologues have diverse substrate specificities. © 2005 Biochemical Society.

533. Effect of nasal continuous or intermittent positive airway pressure on nonnutritive swallowing in the newborn lamb - Samson N., St. Hilaire M., Nsegbe E. et al. [J.-P. Fraud, Dept. of Pediatrics, Univ. of Sherbrooke, Sherbrooke, Que. J1H 5N4, Canada] - *J. APPL. PHYSIOL.* 2005 99/5 (1636-1642) - summ in FNGI.

The present study was aimed at investigating the effects of nasal continuous positive airway pressure (nCPAP; 6 cmH2O) or intermittent positive pressure ventilation (nIPPV; 10/4 cmH₂O) on nonnutritive swallowing (NNS) and on the coordination between NNS and phases of the respiratory cycle, while taking into account the potential effects of states of alertness. Twelve full-term lambs were chronically instrumented at 48 h after birth for polysomnographic recordings, including NNS, diaphragm electromyographic activity, respiratory movements, pulse oximetry, and states of alertness. Studies in control conditions, with nCPAP and nIPPV, were performed in random order in nonsedated lambs at 4, 5, and 6 days of life. Results demonstrate that nCPAP significantly decreased overall NNS frequency, more specifically isolated NNS during quiet sleep and bursts of NNS in active sleep. In comparison, the effects of nIPPV on NNS frequency were more variable, with an inhibition of NNS only in wakefulness and an increase in isolated NNS frequency in active sleep. In addition, neither nCPAP nor nIPPV disrupted the coordination between NNS and phases of the respiratory cycle. In conclusion, nCPAP inhibits NNS occurrence in newborn lambs. Clinical relevance of this novel finding is related to the importance of NNS for clearing the upper airways from secretions and gastric content frequently regurgitated in the neonatal period. Copyright © 2005 the American Physiological Society.

See also: 567, 568, 571.

9. EXCRETION

534. Testosterone supplementation in aging men and women: Possible impact on cardiovascular-renal disease - Reckelhoff J.F., Yanes L.L., Iliescu R. et al. [J.F. Reckelhoff, Dept. of Physiology and Biophysics, Univ. of Mississippi Medical Center, 2500 N. State St., Jackson, MS 39216-4505, United States] - *AM. J. PHYS-IOL. RENAL PHYSIOL.* 2005 289/5 58-5 (F941-F948) - summ in FNG1.

Treatment of aging men and women with testosterone supplements is increasing. The supplements are given to postmenopausal women mainly to improve their libido and to aging men to improve muscle mass and bone strength, to improve libido and quality of life, to prevent and treat osteoporosis, and, with the phosphodiesterase-5 inhibitors, such as sildenafil, to treat erectile dysfunction. The increased use of testosterone supplements in aging individuals has occurred despite the fact that there have been no rigorous clinical trials examining the effects of chronic testosterone on the cardiovascular-renal disease risk. Studies in humans and animals have suggested that androgens can increase blood pressure and compromise renal function. Androgens have been shown to increase tubular sodium and water reabsorption and activate various vasoconstrictor systems in the kidney, such as the renin-angiotensin system and endothelin. There is also evidence that androgens may increase oxidative stress. Furthermore, the kidney contains the enzymes necessary to produce androgens de novo. This review presents an overview of the data from human and animal studies in which the role of androgens in promoting renal and cardiovascular diseases has been investigated. Copyright © 2005 the American Physiological Society.

535. Expression and functions of annexins in the kidney - Markoff A. and Gerke V. [A. Markoff, Institute of Medical Biochemistry, Centre for Molecular Biology of Inflammation, University of Muenster, Von Esmarch str. 56, 48149 Muenster, Germany] - *AM. J. PHYSIOL. RENAL PHYSIOL.* 2005 289/5 58-5 (F949-F956) - summ in ENGL

This review article summarizes current knowledge about the locations and possible functions of annexin family members in the kidney. Beginning with an introduction on common structural and biochemical features as well as general functional characteristics of annexins, the paper focuses on individual members with

documented and/or proposed physiological relevance for renal development, structure, and functions. Three main aspects of annexin function in kidney epithelia emerge from the available experimental data. First, annexins are required for membrane organization and membrane transport events required for the establishment/maintenance of epithelial polarity. Second, there is accumulating evidence of an association of annexins with ion channels, as membraneguiding auxiliary proteins or modulators of channel activity. Last but not least, some annexins seem to work as extracellular autocrine modulators of receptor function under different physiological conditions. Copyright © 2005 the American Physiological Society.

536. Increased expression of ENaC subunits and increased apical targeting of AQP2 in the kidneys of spontaneously hypertensive rats - Kim S.W., Wang W., Kwon T.-H. et al. [S. Nielsen, Water and Salt Research Center, Bldg. 233/234, Univ. of Aarhus, DK-8000 Aarhus C, Denmark] - AM. J. PHYSIOL. RENAL PHYSIOL. 2005 289/5 58-5 (F957-F968) - summ in ENGL

In models of genetic hypertension, renal tubular dysfunction could be involved in the increased sodium and water reabsorption. However, the molecular basis for the increased renal sodium and water retention remains largely undefined in spontaneously hypertensive rats (SHR). We hypothesized that dysregulation of renal epithelial sodium channels (ENaC), sodium (co)transporters, or aquaporin-2 (AQP2) could be involved in the pathogenesis of hypertension in SHR. Six-week-old or twelve-week-old SHR and corresponding age-matched Wistar-Kyoto control rats (WKY) were studied. In both SHR groups, systolic blood pressure was markedly increased, whereas urine output, creatinine clearance, and urinary sodium excretion were decreased compared with corresponding WKY. Moreover, urine osmolality and urine-to-plasma osmolality ratio were increased compared with WKY. Semiquantitative immunoblotting demonstrated that the protein abundance of β - and γ -subunits of ENaC was increased in the cortex and outer stripe of the outer medulla and inner stripe of the outer medulla (ISOM) in SHR, whereas α -ENaC abundance was increased in ISOM. Immunoperoxidase microscopy confirmed the increased labeling of β -ENaC and γ -ENaC subunits in the late distal convoluted tubule, connecting tubule, and cortical and outer medullary collecting duct segments. In contrast, subcellular localization of α -ENaC, β -ENaC, and γ -ENaC was not changed. Expression of sodium/hydrogen exchanger type 3, bumetanide-sensitive Na-K-2Cl cotransporter, and thiazide-sensitive Na-Cl cotransporter was not altered in SHR. AQP2 levels were increased in the ISOM in SHR, and immunoperoxidase microscopy demonstrated an increased apical labeling of AQP2 in the inner medullary collecting duct in SHR. These results suggest that the increased protein abundance of ENaC subunits as well as the increased apical targeting of AQP2 may contribute to renal sodium and water retention observed during the development of hypertension in SHR.

537. PKA-dependent ENaC trafficking requires the SNARE-binding protein complexin - Butterworth M.B., Frizzell R.A., Johnson J.P. et al. [M.B. Butterworth, Dept. of Cell Biology and Physiology, S375 Biological Science Tower, Univ. of Pittsburgh, Pttsburgh, PA 15261, United States] - *AM. J. PHYSIOL. RENAL PHYSIOL.* 2005 289/5 58-5 (F969-F977) - summ in ENGL

Acute regulation of epithelial sodium channel (ENaC) function at the apical surface of polarized kidney cortical collecting duct (CCD) epithelial cells occurs in large part by changes in channel number, mediated by membrane vesicle trafficking. Several soluble N-ethyl-maleimide-sensitive factor attachment protein receptors (SNARE) have been implicated in this process. A novel SNAREbinding protein, complexin, has been identified in nervous tissue which specifically binds to and stabilizes SNARE complexes at synaptic membranes to promote vesicle fusion. To test whether this protein is present in mouse CCD (mCCD) cells and its possible involvement in acute ENaC regulation, we cloned complexin (isoform II) from a mouse kidney cDNA library. Complexin II mRNA coexpressed with α -, β -, and γ -ENaC subunits in Xenopus laevis oocytes reduced sodium currents to $16 \pm 3\%$ (n = 19) of control values. Short-circuit current (Isc) measurements on mCCD cell lines stably over- or underexpressing complexin produced similar results. Basal I $_{sc}$ was reduced from 12.0 \pm 1.0 (n = 15) to 2.0 \pm 0.4 (n = 15) and 1.8 ± 0.3 (n = 17) μ A/cm², respectively. Similarly

forskolin-stimulated I_{sc} was reduced from control values of 20.0 ± 2 to 2.7 ± 0.5 and $2.3 \pm 0.4 \,\mu$ A/cm² by either increasing or decreasing complexin expression. Surface biotinylation demonstrated that the complexin-induced reduction in basal Isc was due to a reduction in apical membrane-resident ENaC and the inhibition in forskolin stimulation was due to the lack of ENaC insertion into the apical membrane to increase surface channel number. Immunofluorescent localization of SNARE proteins in polarized mCCD epithelia detected the presence of syntaxins 1 and 3 and synaptosomal-associated protein of 23 kDa (SNAP-23) at the apical membrane, and vesicle-associated membrane protein (VAMP2) was localized to intracellular compartments. These findings identify SNAREs that may mediate ENaC-containing vesicle insertion in mCCD epithelia and suggest that stabilization of SNARE interactions by complexin is an essential aspect of the regulated trafficking events that increase apical membrane ENaC density either by constitutive or regulated trafficking pathways. Copyright © 2005 the American Physiological Society.

538. Mechanoregulation of intracellular Ca²⁺ concentration is attenuated in collecting duct of monocilium-impaired orpk mice - Liu W., Murcia N.S., Duan Y. et al. [L.M. Satlin, Mount Sinai School of Medicine, Box 1664, One Gustave L. Levy Place, New York, NY 10029, United States] - *AM. J. PHYSIOL. RENAL PHYSIOL.* 2005 289/5 58-5 (F978-F988) - summ in ENGL

Autosomal recessive polycystic kidney disease (ARPKD) is characterized by the progressive dilatation of collecting ducts, the nephron segments responsible for the final renal regulation of sodium, potassium, acid-base, and water balance. Murine models of ARPKD possess mutations in genes encoding cilia-associated proteins, including Tg737 in orpk mice. New findings implicate defects in structure/function of primary cilia as central to the development of polycystic kidney disease. Our group (Liu W, Xu S, Woda C, Kim P. Weinbaum S. and Satlin LM. Am J Physiol Renal Physiol 285: F998-F1012, 2003) recently reported that increases in luminal flow rate in rabbit collecting ducts increase intracellular Ca2+ concentration ([Ca²⁺]_i) in cells therein. We thus hypothesized that fluid shear acting on the apical membrane or hydrodynamic bending moments acting on the cilium increase renal epithelial [Ca²⁺]_i. To further explore this, we tested whether flow-induced [Ca²⁺]_i transients in collecting ducts from mutant orpk mice, which possess structurally abnormal cilia, differ from those in controls. Isolated segments from 1- and 2-wk-old mice were microperfused in vitro and loaded with fura 2; [Ca2+]i was measured by digital ratio fluorometry before and after the rate of luminal flow was increased. All collecting ducts responded to an increase in flow with an increase in [Ca²⁺]i, a response that appeared to be dependent on luminal Ca²⁺ entry. However, the magnitude of the increase in [Ca²⁺]_i in 2- but not 1-wk-old mutant orpk animals was blunted. We speculate that this defect in mechano-induced Ca 2+ signaling in orpk mice leads to aberrant structure and function of the collecting duct in ARPKD. Copyright © 2005 the American Physiological Society.

539. Prostaglandin E₂ EP2 and EP4 receptor activation mediates cAMP-dependent hyperpolarization and exocytosis of renin in juxtaglomerular cells - Friis U.G., Stubbe J., Uhrenholt T.R. et al. [B.L. Jensen, Dept. of Physiology and Pharmacology, Univ. of Southern Denmark, Winslowparken 21, DK-5000 Odense C, Denmark] - AM. J. PHYSIOL. RENAL PHYSIOL. 2005 289/5 58-5 (F989-F997) - summ in ENGL

PGE₂ and PGI₂ stimulate renin secretion and cAMP accumulation in juxtaglomerular granular (JG) cells. We addressed, at the single-cell level, the receptor subtypes and intracellular transduction mechanisms involved. Patch clamp was used to determine cell capacitance (C m), current, and membrane voltage in response to PGE₂, EP2 and EP4 receptor agonists, and an IP receptor agonist. PGE₂ (0.1 μ mol/l) increased C_m significantly, and the increase was abolished by intracellular application of the protein kinase A antagonist Rp-8-CPT-cAMPS. EP2-selective ligands butaprost (1 μ mol/l), AE1-259-01 (1 mmol/l), EP4-selective agonist AE1-329 (1 mmol/l), and IP agonist iloprost (1 μ mol/l) significantly increased C_m mediated by PKA. The EP4 antagonist AE3-208 (10 mmol/l)-blocked the effect of EP4 agonist but did not alter the response to PGE₂. Application of both EP4 antagonist and EP2-antagonist AH-6809 abolished the effects of PGE₂ on C_m and current. EP2 and

EP4 ligands stimulated cAMP formation in JG cells. PGE $_2$ rapidly stimulated renin secretion from superfused JG cells and diminished the membrane-adjacent granule pool as determined by confocal microscopy. The membrane potential hyperpolarized significantly after PGE $_2$, butaprost, AE1-329 and AE1-259 and outward current was augmented in a PKA-dependent fashion. PGE $_2$ -stimulated outward current, but not C_m change, was abolished by the BK $_{Ca}$ channel inhibitor iberiotoxin (300 nmol/l). EP2 and EP4 mRNA was detected in sampled JG cells, and the preglomerular and glomerular vasculature was immunopositive for EP4. Thus IP, EP2, and EP4 receptors are associated with JG cells, and their activation leads to rapid PKA-mediated exocytotic fusion and release of renin granules. Copyright © 2005 the American Physiological Society.

540. Angiotensin II, reactive oxygen species, and Ca²⁺ signaling in afferent arterioles - Fellner S.K. and Arendshorst W.J. [S.K. Fellner, Dept. of Cell and Molecular Physiology, Univ. of North Carolina at Chapel Hill, Chapel Hill, NC 27599-7545, United States] - *AM. J. PHYSIOL. RENAL PHYSIOL.* 2005 289/5 58-5 (F1012-F1019) - summ in ENGL

In afferent arteriolar vascular smooth muscle cells, ANG II induces a rise in cytosolic Ca^{2+} ($[Ca^{2+}]_i$) via inositol trisphosphate receptor (IP₃R) stimulation and by activation of the adenine diphosphate ribose (ADPR) cyclase to form cyclic ADPR, which sensitizes the ryanodine receptor (RyR) to Ca²⁺. We hypothesize that ANG II stimulation of NAD(P)H oxidases leads to the formation of superoxide anion (O2·), which, in turn, activates ADPR cyclase. Afferent arterioles were isolated from rat kidney with the magnetized microsphere and sieving technique and loaded with fura-2 to measure $[Ca^{2+}]_i$. ANG II rapidly increased $[Ca^{2+}]_i$ by 124 ± 12 nM. In the presence of apocynin, a specific inhibitor of NAD(P)H oxidase assembly, the $[Ca^{2+}]_i$ response was reduced to 35 \pm 5 nM (P < 0.01). Tempol, a superoxide dismutase mimetic, did not alter the [Ca²⁺] response to ANG II at a concentration of 10-4 M (99 ± 12 nM), but 10^{-3} M tempol reduced the response to 32 ± 3 nM (P < 0.01). The addition of nicotinamide, an inhibitor of ADPR cyclase, to apocynin or tempol (10⁻³ M) resulted in no further inhibition. Measurement of superoxide production with the fluorescent probe tempo 9-AC showed that ANG II caused an increase of 48 \pm 20 arbitrary units; apocynin or diphenyl iodonium (an inhibitor of flavoprotein oxidases) inhibited the response by 94%. Hydrogen peroxide (H₂O₂) was studied at physiological (10⁻⁷ M) and higher concentrations. In the presence of H₂O₂ (10 -7 M), neither baseline $[Ca^{2+}]_i$ nor the response to ANG II was altered (125 ± 15 nM), whereas H₂O₂ (10⁻⁶ and 10⁻⁵ M) inhibited the [Ca ²⁺]_i response to ANG II by 35 and 46%, respectively. We conclude that ANG II rapidly activates NAD(P)H oxidases of afferent arterioles, leading to the formation of O₂, which then stimulates ADPR cyclase to form cADPR. cADPR, by sensitizing the RyR to Ca²⁺, augments the Ca²⁺ response (calcium-induced calcium release) initiated by activation of the IP₃R. Copyright © 2005 the American Physiological Society.

541. Renocortical mRNA expression of vasoactive factors during spironolactone protective effect in chronic cyclosporine nephrotoxicity - Pérez-Rojas J.M., Derive S., Blanco J.A. et al. [N.A. Bobadilla, Unidad de Fisiología Molecular, Vasco de Quiroga No. 15, Tlalpan, 14000 México City, Mexico] - AM. J. PHYSIOL. RENAL PHYSIOL. 2005 289/5 58-5 (F1020-F1030) - summ in ENGL.

We showed that spironolactone reduced structural damage and prevented renal dysfunction in chronic cyclosporine (CsA) nephrotoxicity. These findings evidenced an aldosterone renal vascular effect under this condition. To investigate aldosterone's role in modulating renal vascular tone, renocortical vasoactive pathways mRNA levels in chronic CsA nephrotoxicity as well as spironolactone's effect on renal function in acute CsA nephrotoxicity were evaluated. Two experimental sets were designed. For chronic nephrotoxicity, rats fed with low-sodium diet were divided into groups receiving vehicle, spironolactone (Sp), CsA, and CsA+Sp, for 21 Creatinine clearance, survival percentage, and renocortical mRNA levels of pro-renin, angiotensinogen (Ang), angiotensin receptors (AT1A, AT1B, and AT 2), preproendothelin, endothelin receptors (ETA, ETB), cyclooxygenase-2 (COX-2), and adenosine receptors (Ad $_1$, Ad $_{2A}$, Ad $_{2B}$, and Ad $_3$) were analyzed. For acute nephrotoxicity, similar groups fed with a standard chow diet for 7 days were included. Serum potassium and sodium, glomerular filtration rate (GFR), and renal blood flow (RBF) were determined. In chronic model, CsA produced pro-renin and ET upregulation, altered adenosine receptors expression, and reduced Ang, AT_{1A}, AT_{1B}, ET_B, and COX-2 mRNA levels. Spironolactone protective effect in chronic nephrotoxicity was associated with prevention of pro-renin upregulation and increased AT 2, together with ET_B reduction. In acute nephrotoxicity, spironolactone completely prevented GFR and RBF reduction induced by CsA. Our results suggest that aldosterone contributes to renal vasoconstriction observed in CsA nephrotoxicity and that renoprotection conferred by spironolactone was related to modification of renocortical vasoactive pathways expression, in which pro-renin normalization was the most evident change in chronic nephropathy. Finally, our data point to spironolactone as a potential treatment to reduce CsA nephrotoxicity in transplant patients. Copyright © 2005 the American Physiological Society.

542. Stimulation of Na⁺ transport by AVP is independent of PKA phosphorylation of the Na-K-ATPase in collecting duct principal cells - Mordasini D., Bustamante M., Rousselot M. et al. [E. Féraille, Service de Néphrologie, Fondation pour Recherches Médicales, 64 Ave. de la Roseraie, CH-1211 Geneva 4, Switzerland] - *AM. J. PHYSIOL. RENAL PHYSIOL.* 2005 289/5 58-5 (F1031-F1039) - summ in ENGL

Arginine-vasopressin (AVP) stimulates Na+ transport and Na-K-ATPase activity via cAMP-dependent PKA activation in the renal cortical collecting duct (CCD). We investigated the role of the Na-K-ATPase in the AVP-induced stimulation of transepithelial Na⁺ transport using the mpkCCD_{c14} cell model of mammalian collecting duct principal cells. AVP (10-9 M) stimulated both the amiloridesensitive transport measured in intact cells and the maximal Na pump current measured by the ouabain-sensitive short-circuit current in apically permeabilized cells. These effects were associated with increased Na-K-ATPase cell surface expression, measured by Western blotting after streptavidin precipitation of biotinylated cell surface proteins. The effects of AVP on Na pump current and Na-K-ATPase cell surface expression were dependent on PKA activity but independent of increased apical Na+ entry. Time course experiments revealed that in response to AVP, the cell surface expression of both endogenous Na-K-ATPase and hybrid Na pumps containing a c-myc-tagged wild-type human α_1 -subunit increased transiently. Na-K-ATPase cell surface expression was maximal after 30 min and then declined toward baseline after 60 min. Immunoprecipitation experiments showed that PKA activation did not alter total phosphorylation levels of the endogenous Na-K-ATPase α -subunit. In addition, mutation of the PKA phosphorylation site (S943A or S943D) did not alter the time course of increased cell surface expression of c-myc-tagged Na-K-ATPase in response to AVP or to dibutyryl-cAMP. Therefore, stimulation of Na-K-ATPase cell surface expression by AVP is dependent on PKA but does not rely on α_1 -subunit phosphorylation on serine 943 in the collecting duct principal cells. Copyright © 2005 the American Physiological Society.

543. Activation of NAD(P)H oxidase by outward movements of H+ ions in renal medullary thick ascending limb of Henle - Li N., Zhang G., Yi F.-X. et al. [N. Li, Dept. of Pharmacology and Toxicology, Medical College of Virginia, Virginia Commonwealth Univ., P.O. Box 980613, Richmond, VA 23298, United States] - *AM. J. PHYSIOL. RENAL PHYSIOL.* 2005 289/5 58-5 (F1048-F1056) - summ in ENGL

The present study was designed to test the hypothesis that the production of superoxide $(O_{\overline{2}}\cdot)$ by NAD(P)H oxidase is coupled to tubular metabolic activity through ionic activation mediated by H+ movement across cell membrane. Using dual fluorescent microscopic imaging analysis, intracellular $O_{\overline{2}}\cdot$ levels and pH (pH $_{i}$) in renal medullary thick ascending limb of Henle (TALH) cells were simultaneously measured. It was found that intracellular $O_{2}\cdot$ levels in these cells were increased in parallel to the elevation of pH $_{i}$ by outflow of H+ induced via NH $_{4}$ Cl loading followed by rapid removal. This increase in intracellular $O_{2}\cdot$ levels was substantially blocked by an inhibitor of Na+/H+ exchanger, methylisobutyl-amiloride (MIA; 100 μ M), a chemical SOD mimetic, Tiron (1 mM) or an inhibitor of NAD(P)H oxidase, diphenylene iodonium (DPI; 100

 μM). In additional groups of TALHs, a proton ionophore, carbonyl-cyanide m-chlorophenylhydrazone (10 μM) was used to produce H+ conductance, leading to H+ flux across cell membrane depending on extracellular pH. The efflux of H+ increased both pH_i and intracellular O_2^- levels, but the influx of H+ did not increase intracellular O_2^- levels. The H+ efflux-induced increase in intracellular O_2^- levels was completely blocked by DPI and another NAD(P)H oxidase inhibitor, apocynin (100 μM). In in invo experiments, renal medullary infusion of MIA (100 μM) was found to significantly decrease the concentrations of H_2O_2 in the renal medullary interstitum. These results suggest that it is the outward movements of H + ions that activates NAD(P)H oxidase to produce O_2 - in TALH cells. This H+ outflow-associated activation of NAD(P)H oxidase importantly contributes to tissue levels of reactive oxygen species in the renal medulla. Copyright © 2005 the American Physiological Society.

544. Involvement of tyrosine kinase and PI3K in the regulation of OAT3-mediated estrone sulfate transport in isolated rabbit renal proximal tubules - Soodvilai S., Wright S.H., Dantzler W.H. and Chatsudthipong V. [V. Chatsudthipong, Dept. of Physiology, Faculty of Science, Mahidol Univ., Bangkok 10400, Thailand] - AM. J. PHYSIOL. RENAL PHYSIOL. 2005 289/5 58-5 (F1057-F1064) - summ in ENGL

It was shown previously that OAT3 activity was differentially regulated by protein kinases including MAPK, PKA, and PKC The present study investigated the short-term effect of tyrosine kinase and phosphatidylinositol 3-kinase (PBK) on OAT3-mediated organic anion transport in S2 segments of renal proximal tubules. Genistein, a tyrosine kinase inhibitor, and wortmannin, a PI3K inhibitor, inhibited transport of estrone sulfate, a prototypic substrate for OAT3, in a dose-dependent manner. Previously, we showed that epidermal growth factor (EGF) stimulated OAT3 activity via the MAPK pathway. In the present study, we investigated whether EGF-stimulated OAT3 activity was dependent on tyrosine kinase and PI3K. We showed that EGF stimulation of OAT3 was reduced by inhibition of tyrosine kinase or PI3K, suggesting that they play a role in the stimulatory process. Inhibitory effects also indicated that tyrosine kinase and PI3K are involved in the MAPK pathway for EGF stimulation of OAT3 in intact renal proximal tubules, with PI3K acting upstream and tyrosine kinase acting downstream of mitogen-activated/extracellular signal-regulated kinase kinase activation. Copyright © 2005 the American Physiological Society.

545. Mineralocorticoids decrease the activity of the apical small-conductance K channel in the cortical collecting duct - Wei Y., Babilonia E., Sterling H. et al. [W.-H. Wang, Dept. of Pharmacology, New York Medical College, Valhalla, NY 10595, United States] - AM. J. PHYSIOL. RENAL PHYSIOL. 2005 289/5 58-5 (F1065-F1071) - summ in ENGL

We used the patch-clamp technique to examine the effect of DOCA treatment (2 mg/kg) on the apical small-conductance K (SK) channels, epithelial Na channels (ENaC), and the basolateral 18-pS K channels in the cortical collecting duct (CCD). Treatment of rats with DOCA for 6 days significantly decreased the plasma K from 3.8 to 3.1 meq and reduced the activity of the SK channel, defined as NP₀, from 1.3 in the CCD of control rats to 0.6. In contrast, DOCA treatment significantly increased ENaC activity from 0.01 to 0.53 and the basolateral 18-pS K channel activity from 0.67 to 1.63. Moreover, Western blot analysis revealed that DOCA treatment significantly increased the expression of the nonreceptor type of protein tyrosine kinase (PTK), cSrc, and the tyrosine phosphorylation of ROMK in the renal cortex and outer medulla. The possibility that decreases in apical SK channel activity induced by DOCA treatment were the result of stimulation of PTK activity was further supported by experiments in which inhibition of PTK with herbimycin A significantly increased NPo from 0.6 to 2.1 in the CCD from rats receiving DOCA. Also, when rats were fed a high-K (10%) diet, DOCA treatment did not increase the expression of c-Src and decrease the activity of the SK channel in the CCD. We conclude that DOCA treatment decreased the apical SK channel activity in rats on a normal-K diet and that an increase in PTK expression may be responsible for decreased channel activity in the CCD from DOCA-treated rats. Copyright © 2005 the American Physiological Society.

546. Effect of COX inhibitors and NO on renal hemodynamics following ischemia-reperfusion injury in normotensive and hypertensive rats - Knight S. and Johns E.J. - *AM. J. PHYSIOL. RENAL PHYSIOL.* 2005 289/5 58-5 (F1072-F1077) - summ in ENGL

The processes involved in the renal damage resulting from ischemia-reperfusion injury are poorly understood. This study examined the contribution of prostaglandins and nitric oxide (NO) in the vascular responses to ischemia-reperfusion injury in the kidneys of normotensive and hypertensive rats. Groups of Wistar and stroke-prone spontaneously hypertensive rats (SHRSP) were dosed with polyethylene glycol vehicle, aspirin (53.5 mg kg⁻¹ day⁻¹), NOaspirin (100 mg kg⁻¹ day⁻¹), or celecoxib (10 mg kg⁻¹ day⁻¹) for 7 days. On day 7, rats were anesthetized with chloralose/urethane and the left kidney was exposed to a 30-min period of ischemia followed by 90-min reperfusion. Renal cortical and medullary perfusions were monitored throughout using laser-Doppler flowmetry. In the vehicle- and celecoxib-treated Wistar rats, cortical and medullary postischemic perfusion was reduced to 66 and 62% and 53 and 62%, respectively (all P < 0.05), of baseline. The ischemia-induced reductions in cortical and medullary flux were ameliorated in the aspirin and NO-aspirin groups where flux fell to 96 and 78% and 105 and 83%, respectively ($\dot{P} < 0.05$). There was a fall in cortical and medullary flux in the postischemic period in the vehicle-treated SHRSP to 82 and 77% (P < 0.05). These findings show that nonselective cyclooxygenase (COX) inhibition, and to an even greater extent NO donation, provided protection to the renal vasculature from ischemic injury in the Wistar rat but not in the SHRSP. This would suggest that prostaglandins are less important in the development of renal ischemia-reperfusion injury during hypertension and both COX isoforms must be inhibited to offset the decrease in renal hemodynamics. Copyright © 2005 the American Physiological Society.

547. Mesangial cell-reduced $\mathrm{Ca^{2+}}$ signaling in high glucose is due to inactivation of phospholipase $\mathrm{C-\beta_3}$ by protein kinase C - Frecker H., Munk S., Wang H. and Whiteside C. [C. Whiteside, Univ. of Toronto, 1 King's College Circle, Toronto, Ont. M5S 1A8, Canada] - $AM.\ J.\ PHYSIOL.\ RENAL\ PHYSIOL.\ 2005\ 289/5\ 58-5$ (F1078-F1087) - summ in ENGL

In high glucose, glomerular mesangial cells (MCs) demonstrate impaired Ča²⁺ signaling in response to seven-transmembrane receptor stimulation. To identify the mechanism, we first postulated decreased release from intracellular stores. Intracellular Ca2+ was measured in fluo-3-loaded primary cultured rat MCs using confocal fluorescence microscopy. In high glucose (HG) 30 mM for 48 h, the 25 nM ionomycin-stimulated intracellular Ca2+ response was reduced to 82% of that observed in normal glucose (NG). In NG 5.6 mM, Ca2+ responses to endothelin (ET)-1 and platelet-derived growth factor (PDGF) were unchanged in cells cultured in 50 nM Ca²⁺ vs. 1.8 mM Ca²⁺. Depletion of intracellular Ca²⁺ stores with thapsigargin eliminated ET-1-stimulated Ca²⁺ responses. Incubation in 30 mM glucose (HG) for 48 h or stimulation with phorbol myristate acetate (PMA) for 10 min eliminated the Ca2+ response to ET-1 but had no effect on the PDGF response. Down-regulation of protein kinase C (PKC) with 24-h PMA or inhibition with Gö6976 in HG normalized the Ca²⁺ response to ET-1. Because ET-1 and PDGF stimulate Ca²⁺ signaling through different phospholipase C pathways, we hypothesized that, in HG, PKC selectively phosphorylates and inhibits PLC- β_3 . Using confocal immunofluorescence imaging, in NG, a 1.6- to 1.7-fold increase in PLC- β_3 Ser¹¹⁰⁵ phosphorylation was observed following PMA or ET-1 stimulation for 10 min. In HG, immunofluorescent imaging and immunoblotting showed increased PLC- β_3 phosphorylation, without change in total PLC- β_3 , which was reversed with 24-h PMA or Gö6976. We conclude that reduced Ca2+ signaling in HG cannot be explained by reduced Ca²⁺ stores but is due to conventional PKC-dependent phosphorylation and inactivation of PLC- β_3 . Copyright © 2005 the American Physiological Society.

548. Hypoxia-inducible factor modulates tubular cell survival in cisplatin nephrotoxicity - Tanaka T., Kojima I., Ohse T. et al. [M. Nangaku, Division of Nephrology and Endocrinology, Univ. of Tokyo School of Medicine, 7-3-1, Hongo, Bunkyo-ku, Tokyo,

Japan] - AM. J. PHYSIOL. RENAL PHYSIOL. 2005 289/5 58-5 (F1123-F1133) - summ in ENGL

Hypoxia-inducible factor (HIF)-1 is a transcription factor mediating cellular response to hypoxia. Although it is expressed in tubular cells of the ischemic kidney, its functional role is not fully clarified in the pathological context. In this study, we investigated a role of HIF in tubular cell apoptosis induced by cisplatin. HIF-1 α was expressed in tubular cells in the outer medulla 3 days after cisplatin (6 mg/kg) administration. With the in vivo administration of cobalt to activate HIF, the number of apoptotic renal tubular cells became much smaller in the outer medulla, compared with the vehicle group. We also examined the functional role of HIF-1 in vitro using immortalized rat proximal tubular cells (IRPTC). In hypoxia, IRPTC that express dominant-negative (dn) HIF-1 α showed impaired survival in cisplatin injury at variable doses (25- $100 \mu M$, 24 h), which was not obvious in normoxia. The observed difference in cell viability in hypoxia was associated with the increased number of apoptotic cells in dnHIF-1 α clones (Hoechst 33258 staining). Studies on intracellular signaling revealed that the degree of cytochrome c release, dissipation of mitochondrial membrane potentials, and caspase-9 activity were all more prominent in dnHIF-1 α clones than in control IRPTC, pointing to the accelerated signaling of mitochondrial pathways. We propose that HIF-1 mediates cytoprotection against cisplatin injury in hypoxic renal tubular cells, by reducing the number of apoptotic cells through stabilization of mitochondrial membrane integrity and suppression of apoptosis signaling. A possibility was suggested that activation of HIF-1 could be a new promising therapeutic target for hypoxic renal diseases. Copyright © 2005 the American Physiological Society.

549. Association of CD2AP with dynamic actin on vesicles in podocytes - Welsch T., Endlich N., Gökce G. et al. [K. Endlich, Institut für Anatomie und Zellbiologie I, Universität Heidelberg, INF 307, D-69120 Heidelberg, Germany] - *AM. J. PHYSIOL. RENAL PHYSIOL.* 2005 289/5 58-5 (F1134-F1143) - summ in ENGL

The docking protein CD2AP (CD2-associated protein) serves a nonredundant function in podocytes as CD2AP knockout mice die of renal failure at the age of 6-7 wk. Furthermore, haploinsufficiency due to mutation of the CD2AP gene is associated with focal segmental glomerulosclerosis in humans. Although CD2AP has been shown to interact with proteins regulating actin polymerization, with proteins of the slit diaphragm, and with the endocytic machinery, its critical function in podocytes remains unclear. In conditionally immortalized mouse podocytes, we demonstrate that CD2AP colocalizes with cortactin and F-actin in spots of ≥ 0.5 - μ m diameter. Confocal time-lapse microscopy in living podocytes expressing GFP-CD2AP or GFP-actin revealed that spots are motile, possess a limited lifetime, and are frequently associated with vesicles. A significant portion of spot-associated vesicles belongs to a later endosomal-sorting compartment, characterized by delayed uptake of fluorescent dextran (10 kDa) and by colocalization with Rab4, but not Rab5 and AP-2. Rapid accumulation of microinjected G-actin in spots and abrogation of spot motility by jasplakinolide demonstrate that spot movements depend on actin polymerization. Furthermore, a high turnover (half-time < 10 s) of CD2AP in spots was demonstrated by FRAP (fluorescence recovery after photobleaching). Our results demonstrate that CD2AP is associated with dynamic actin in a specific late endosomal compartment in podocytes, suggesting that CD2AP might be crucially involved in endosomal sorting and/or trafficking via regulation of actin assembly on vesicles. Copyright © 2005 the American Physiological Society.

550. PPAR γ **agonists exert antifibrotic effects in renal tubular cells exposed to high glucose** - Panchapakesan U., Sumual S., Pollock C.A. and Chen X. [C.A. Pollock, Dept. of Medicine, Royal North Shore Hospital, Sydney, NSW 2065, Australia] - *AM. J. PHYSIOL. RENAL PHYSIOL.* 2005 289/5 58-5 (F1153-F1158) - summ in ENGL

Peroxisome proliferator-activated receptor- γ (PPAR- γ) are ligand-activated transcription factors that regulate cell growth, inflammation, lipid metabolism, and insulin sensitivity. We recently demonstrated that PPAR γ agonists limit high glucose-induced inflammation in a model of proximal tubular cells (PTC; Panchapakesan U, Pollock CA, and Chen XM. Am J Physiol Renal Physiol

287: F528-F534, 2004). However, the role of PPAR- γ in the excess extracellular matrix production is largely unknown. We evaluated the effect of 24- to $4\hat{8}$ -h 8 μ M L-805 $\hat{6}4\hat{5}$ or 10 μ M pioglitazone on 25 mM D-glucose-induced markers of fibrosis in HK-2 cells. High D-glucose induced nuclear binding of activator protein-1 (AP-1) to $140.8 \pm 10.9\%$ (P < 0.05), which was attenuated with L-805645 and pioglitazone to 82.3 ± 14.4 (P < 0.01 vs. high D-glucose) and $99.3 \pm 12.2\%$ (P < 0.05 vs. high D-glucose), respectively. High D-glucose increased total production of transforming growth factor (TGF)- β_1 139.6 \pm 6.5% (P < 0.05), which was reversed with L-805645 and pioglitazone to 68.73 \pm 5.7 (P < 0.01 vs. high D-glucose) and $112 \pm 13.6\%$ (P < 0.05 vs. high D-glucose). L-805645 and pioglitazone reduced high D-glucose-induced fibronectin from 156.0 ± 24.9 (P < 0.05) to 81.9 ± 16.0 and $57.4 \pm 12.7\%$, respectively (both P < 0.01 vs. high D-glucose). Collagen IV was not induced by high D-glucose. L-805645 and pioglitazone suppressed collagen IV to 68.0 ± 14.5 (P < 0.05) and $46.5 \pm 11.6\%$ (P < 0.01) vs. high D-glucose, respectively. High D-glucose increased the nuclear binding of NF- κB to 167 \pm 22.4% (P < 0.05), which was not modified with PPAR- γ agonists. In conclusion, PPAR- γ agonists exert antifibrotic effects in human PTC in high glucose by attenuating the increase in AP-1, TGF- β_1 , and the downstream production of the extracellular matrix protein fibronectin. Copyright © 2005 the American Physiological Society

551. New aristolochic acid, aristololactam and renal cytotoxic constituents from the stem and leaves of Aristolochia contorta - Zhang C.-Y., Wang X., Su T. et al. [C.-Y. Zhang, Department of Natural Medicines, School of Pharmaceutical Sciences, Peking University, Beijing, China] - *PHARMAZIE* 2005 60/10 (785-788) - summ in ENGL.

Two novel phenanthrene derivatives, aristololactam IVa (1) and 9-hydroxy aristolochic acid I (2) were isolated from the stem and leaves of Aristolochia contorta Bunge, together with 17 known compounds (3-19). The structures of these compounds were determined by spectroscopic analysis. The phenanthrenes obtained were tested for cytotoxicity against renal proximal tubular epithelial cell line (HK-2). Aristololactam IVa and 7-methoxy aristololactam IV were found to have strong cytotoxic activity against HK-2 cells with a potency similar to or even stronger than those of aristolochic acid I and aristololactam I.

552. Characterization of a rabbit kidney prostaglandin $F_{2\alpha}$ receptor exhibiting G_i -restricted signaling that inhibits water absorption in the collecting duct - Hébert R.L., Carmosino M., Saito O. et al. [M.D. Breyer, Div. of Nephrology, VAMC Vanderbilt University, Nashville, TN 37232, United States] - *J. BIOL. CHEM.* 2005 280/41 (35028-35037) - summ in ENGL

PGF₂₀ is the most abundant prostaglandin detected in urine; however, its renal effects are poorly characterized. The present study cloned a PGF-prostanoid receptor (FP) from the rabbit kidney and determined the functional consequences of its activation. Nuclease protection assay showed that FP mRNA expression predominates in rabbit ovary and kidney. In situ hybridization revealed that renal FP expression predominates in the cortical collecting duct (CGD)-Although FP receptor activation failed to increase intracellular Ca2+, it potently inhibited vasopressin-stimulated osmotic water permeability (L_p, 10⁻⁷ cm/(atm s)) in in vitro microperfused rabbit CCDs. Inhibition of L_p by the FP selective agonist latanoprost was additive to inhibition of vasopressin action by the EP selective agonist sulprostone. Inhibition of L_p by latanoprost was completely blocked by pertussis toxin, consistent with a uncoupled mechanism. Heterologous transfection of the rabbit FPr into HEK293 cells also showed that latanoprost inhibited cAMP generation via a pertussis toxin-sensitive mechanism but did not increase cell Ca²⁺. These studies demonstrate a functional FP receptor on the basolateral membrane of rabbit CCDs. In contrast to the Ca2+ signal transduced by other FP receptors, this renal FP receptor signals via a PT-sensitive mechanism that is not coupled to cell Ca²⁺. © 2005 by The American Society for Biochemistry and Molecular Biology,

553. Endogenous central κ -opioid systems augment renal sympathetic nerve activity to maximally retain urinary sodium during hypotonic saline volume expansion - Gottlieb H.B. and

Kapusta D.R. [D.R. Kapusta, Dept. of Pharmacology and Experimental Therapeutics, Louisiana State Univ. Health Sciences Center, 1901 Perdido St., New Orleans, LA 70112, United States] - AM. J. PHYSIOL. REGUL. INTEGR. COMP. PHYSIOL. 2005 289/5 58-5 (R1289-R1296) - summ in ENGL

Intracerebroventricular injection of κ -opioid agonists produces diuresis, antinatriuresis, and a concurrent increase in renal sympathetic nerve activity (RSNA). The present study examined whether endogenous central κ -opioid systems contribute to the renal excretory responses produced by the stress of an acute hypotonic saline volume expansion (HSVE). Cardiovascular, renal excretory, and RSNA responses were measured during control, acute HSVE (5% body weight, 0.45 M saline over 30 min), and recovery (70 min) in conscious rats pretreated intracerebroventricularly with vehicle or the $\kappa\text{-opioid}$ receptor antagonist nor-binaltorphimine (nor-BNI). In vehicle-pretreated rats. HSVE produced a marked increase in urine flow rate but only a low-magnitude and delayed natriuresis. RSNA was not significantly suppressed during the HSVE or recovery periods. In nor-BNI-treated rats, HSVE produced a pattern of diuresis similar to that observed in vehicle-treated rats. However, during the HSVE and recovery periods, RSNA was significantly decreased, and urinary sodium excretion increased in nor-BNI-treated animals. In other studies performed in chronic bilateral renal denervated rats, HSVE produced similar diuretic and blunted natriuretic responses in animals pretreated intracerebroventricularly with vehicle or nor-BNI. Thus removal of the renal nerves prevented nor-BNI from enhancing urinary sodium excretion during HSVE. These findings indicate that in conscious rats, endogenous central κ -opioid systems are activated during hypotonic saline volume expansion to maximize urinary sodium retention by a renal sympathoexcitatory pathway that requires intact renal nerves. Copyright © 2005 the American Physiological Society.

554. Sexually dimorphic micturition in rats: Relationship of perineal muscle activity to voiding pattern - Cruz Y. and Downie J.W. [J.W. Downie, Dept. of Pharmacology, Faculty of Medicine, Sir Charles Tupper Medical Bldg., 5850 College St., Halifax, NS B3H 1X5, Canada] - *AM. J. PHYSIOL. REGUL. INTEGR. COMP. PHYSIOL.* 2005 289/5 58-5 (R1307-R1318) - summ in ENGL

In the present study we examined the possibility that striated muscle activity may underlie sexually dimorphic micturition in rats. Micturition dynamics, the gross anatomy of the external urethral sphincter, and the participation of the striated perineal muscles in micturition were compared in urethane-anesthetized adult male and female rats. Bladder contraction characteristics, particularly the magnitude of bladder high-frequency pressure waves during voiding, differed between sexes. Dissections indicated that the sphincter was more extensive and thicker in males than in females. Electromyography showed that in both sexes the sphincter discharged in bursts that correlated with the rising phase of high-frequency bladder pressure oscillations. Regional differences in discharge pattern were seen in the sphincters of males, with the proximal part of the sphincter showing components activated during bladder filling. Bulbospongiosus, ischiocavernosus, and cremaster muscles also were activated during bladder contraction in males. In both sexes transection of the motor branch of the lumbosacral plexus eliminated the bladder high-frequency oscillations and reduced voided volume. Neurectomy did not affect bladder pressure but reduced voiding efficiency by 45% in males. In females the bladder pressure was dramatically decreased, but voiding efficiency only decreased by 24%. Our findings suggest that, in rats, striated perineal muscles contribute to the sexually dimorphic micturition. Activity of the dimorphic perineal muscles may regulate genital and urinary urethra expulsive functions, helping to expel seminal plug and fluids through the long urethra in the male. Copyright © 2005 the American Physiological Society.

555. Saline-induced natriuresis and renal blood flow in conscious dogs: Effects of sodium infusion rate and concentration - Sandgaard N.C.F., Andersen J.L., Holstein-Rathlou N.-H. and Bie P. [Dr. N.C.F. Sandgaard, Department of Physiology and Pharmacology, University of Southern Denmark, Odense University, 21 Winsloewparken, DK-5000 Odense, Denmark] - ACTA PHYSIOL. SCAND. 2005 185/3 (237-250) - summ in ENGL

Aim: This study focused on static and dynamic changes in total

renal blood flow (RBF) during volume expansion and tested whether a change in RBF characteristics is a necessary effector mechanism in saline-induced natriuresis. Methods: The aortic flow subtraction technique was used to measure RBF continuously. Identical amounts of NaCl (2.4 mmol kg-1) were given as slow isotonic (Iso, 120 min), slow hypertonic (Hyper, 120 min), and rapid isotonic loads (IsoRapid, 30 min). Results: During Iso and IsoRapid, arterial blood pressure increased slightly (6-7 mmHg), and during Hyper it remained unchanged. Iso and Hyper increased sodium excretion (4 \pm 1 to 57 \pm 27 and 10 \pm 4 to 79 \pm 28 μ mol min⁻¹, respectively) and decreased plasma renin activity (by 38% and 29%), angiotensin II (by 56% and 58%) and aldosterone (by 47% and 65%), while RBF remained unchanged. IsoRapid caused a similar increase in sodium excretion (to 72 \pm 19 μ mol min⁻¹), a similar decrease in renin system activity, but a 15% elevation of RBF (282 \pm 22 to 324 ± 35 mL min⁻¹). Selected frequency domain parameters of RBF autoregulation did not change in response to any load. Conclusions: In response to slow saline loading simulating daily sodium intake, the rate of sodium excretion may increase 10-20-fold without any change in mean arterial blood pressure or in RBF. Regulatory responses to changes in total body NaCl levels appears, therefore, to be mediated primarily by neurohumoral mechanisms and may occur independent of changes in arterial pressure or RBF. © 2005 Scandinavian Physiological Society.

556. Kidneys extract BNP and NT-proBNP in healthy young men - Schou M., Dalsgaard M.K., Clemmesen O. et al. [M. Schou, Dept. of Endocrinology and Cardiology, Frederiksberg Univ. Hospital, Ndr Fasanvej 57-59, DK-2000 Frederiksberg, Denmark] - *J. APPL PHYSIOL.* 2005 99/5 (1676-1680) - summ in ENGL

Renal metabolism of the cardiac marker NHa-terminal-pro-brain natriuretic peptide (NT-proBNP) has been suggested. Therefore, we determined the renal extraction ratios of NT-proBNP and its bioactive coproduct brain natriuretic peptide (BNP) at rest and during exercise. In addition, the cerebral ratios were evaluated. Ten young healthy men were investigated at baseline, during moderate cycle exercise (heart rate: 140, Borg scale: 14-15), and in the recovery with BNP and NT-proBNP measured from the brachial artery and the jugular and renal veins, and the renal and cerebral extraction ratios (Ext-Ren and Ext-Cer, respectively) were calculated. Cardiac output, stroke volume, heart rate, mean arterial pressures, and estimated glomerular filtration were determined. BNP and NTproBNP were extracted by the kidneys but not by the brain. We observed no effect of exercise. The mean values (± SE) of Ext-Ren of NT-proBNP were similar (0.19 \pm 0.05, 0.21 \pm 0.06, and 0.12 \pm 0.03, respectively) during the three sessions (P > 0.05). Also the Ext-Ren of BNP were similar (0.18 \pm 0.07, 0.15 \pm 0.11, and 0.14 ± 0.06 , respectively; P > 0.05). There were no significant differences between Ext-Ren of BNP and NT-proBNP during the three sessions (P > 0.05). The Ext-Cer of both peptides varied insignificantly between -0.21 \pm 0.15 and 0.11 \pm 0.08. The renal extraction ratio of both BNP and NT-proBNP is ~ 0.15 -0.20. There is no cerebral extraction, and short-term moderate exercise does not affect these values. Our findings suggest that the kidneys extract BNP and NT-proBNP to a similar extent in healthy young men. Copyright © 2005 the American Physiological Society.

See also: 557, 562, 563.

10. REPRODUCTION

557. Renal 20-HETE inhibition attenuates changes in renal hemodynamics induced by L-NAME treatment in pregnant rats - Huang H., Zhou Y., Raju V.T. et al. [M.-H. Wang, Dept. of Physiology, Medical College of Georgia, Augusta, GA 30912, United States] - *AM. J. PHYSIOL. RENAL PHYSIOL.* 2005 289/5 58-5 (F1116-F1122) - summ in ENGL

We previously reported that inhibition of nitric oxide (NO)-synthesis by N-nitro-L-arginine methyl ester (L-NAME) during late pregnancy leads to increased production of renal vascular 20-hydroxyeicosatetraenoic acid (20-HETE), a cytochrome P-450 (CYP) 4A-derived vasoconstrictor, in pregnant rats. However, the effect of upregulation of vascular 20-HETE production on renal

function after NO inhibition is not known. To test the hypothesis that increased gestational vascular 20-HETE synthesis after NO inhibition is involved in mediating blood pressure and renal functional changes, we first determined the IC50 value of the effect of nitroprusside (SNP), a NO donor, on renal 20-HETE production in cortical microsomes. We then divided pregnant rats and age-matched virgin rats into a vehicle control group, an L-NAME treatment group (0.25 mg/ml in drinking water), and a group treated with L-NAME plus N-methylsulfonyl-12,12-dibromododec-11-enamide (DDMS; CYP4A-selective inhibitor, 10 mg kg-1 day-1 iv). After 4 days of treatment, we measured blood pressure, renal blood flow (RBF), renal vascular resistance (RVR), and glomerular filtration rate (GFR) in each group. The addition of SNP (IC₅₀ = 22 μ M) decreased renal cortical 20-HETE production. In pregnant rats, L-NAME treatment led to significantly higher mean arterial pressure (MAP) and RVR, and lower RBF and GFR. Combined treatment with DDMS and L-NAME significantly attenuated the increases in MAP and RVR and the decrease in GFR, but not the reduction in RBF induced by L-NAME treatment. L-NAME and L-NAME plus DDMS had no significant impact on renal hemodynamics in virgin rats. In addition, chronic treatment with DDMS selectively inhibited cortical 20-HETE production without a significant effect on CYP4A expression in L-NAME-treated pregnant rats. In conclusion, NO effectively inhibits renal cortical microsomal 20-HETE production in female rats. In pregnant rats, the augmentation of renal 20-HETE production after NO inhibition is associated with increased MAP and RVR, whereas decreased GFR is negated by treatment of a selective and competitive CYP4A inhibitor. These results demonstrate that the interaction between renal 20-HETE and NO is important in the regulation of renal function and blood pressure in pregnant rats. Copyright © 2005 the American Physiological Society.

558. The microtubule plus-end-tracking protein CLIP-170 associates with the spermatid manchette and is essential for spermatogenesis - Akhmanova A., Mausset-Bonnefont A.-L., Van Cappellen W. et al. [N. Galjart, Department of Cell Biology and Genetics, Erasmus MC, 3000 DR Rotterdam, Netherlands] - GENES DEV. 2005 19/20 (2501-2515) - summ in ENGL

CLIP-170 is a microtubule "plus-end-tracking protein" implicated in the control of microtubule dynamics, dynactin localization, and the linking of endosomes to microtubules. To investigate the function of mouse CLIP-170, we generated CLIP-170 knockout and GFP-CLIP-170 knock-in alleles. Residual CLIP-170 is detected in lungs and embryos of homozygous CLIP-170 knockout mice, but not in other tissues and cell types, indicating that we have generated a hypomorphic mutant. Homozygous CLIP-170 knockout mice are viable and appear normal. However, male knockout mice are subfertile and produce sperm with abnormal heads. Using the knock-in mice, we followed GFP-CLIP-170 expression and behavior in dissected, live testis tubules. We detect plus-end-tracking GFP-CLIP-170 in spermatogonia. As spermatogenesis proceeds, GFP-CLIP-170 expression increases and the fusion protein strongly marks syncytia of differentiated spermatogonia and early prophase spermatocytes. Subsequently GFP-CLIP-170 levels drop, but during spermiogenesis (post-meiotic development), GFP-CLIP-170 accumulates again and is present on spermatid manchettes and centrosomes. Bleaching studies show that, as spermatogenesis progresses, GFP-CLIP-170 converts from a mobile plus-end-tracking protein to a relatively immobile protein. We propose that CLIP-170 has a structural function in the male germline, in particular in spermatid differentiation and sperm head shaping. © 2005 by Cold Spring Harbor Laboratory Press.

559. Molecular cloning and characterization of three novel lysozyme-like genes, predominantly expressed in the male reproductive system of humans, belonging to the C-type lysozyme/alpha-lactalbumin family - Zhang K., Gao R., Zhang H. et al. [L. Yu, State Key Laboratory of Genetic Engineering, School of Life Siences, Fudan University, Shanghai 200433, China] - *BIOL. REPROD.* 2005 73/5 (1064-1071) - summ in ENGL

Lysozymes, especially c-type lysozymes, are well-recognized bacteriolytic factors widely distributed in the animal kingdom and play a mainly protective role in host defense. The relatives of c-type lysozymes, alpha-lactalbumins, however, are only found in

mammalian milk and possess a distinct biological function. These two proteins, having similar amino acid sequences, gene structure, and dimensional conformation, belong to the c-type lysozyme/alpha-lactalbumin family. Using human lysozyme as an information probe, we cloned four human cDNAs encoding homologues of human lysozyme; these were named LYZL2, LYZL4, LYZL6, and SPACA3 by the HUGO Gene Nomenclature Committee. Of these four, SPACA3 has been reported to code an intra-acrosomal sperm protein SLLP1. To our knowledge, the other three are reported here for the first time. Using Northern blot hybridization, including 16 different human tissues, we found that these four lysozyme-like genes were all highly expressed in the testis/epididymis. Further analysis of one, LYZL4, by in situ hybridization revealed that its mRNA was only detected in the epithelium of human epididymis, most abundantly in the caput, suggesting that LYZL4 plays a physiological role in male reproduction. By sequence analysis, we found that two essential catalytic residues of the human lysozyme were conserved in LYZL2 and LYZL6, whereas one site in LYZL4 and two sites in SPACA3 were replaced. The LYZL2, LYZL4, LYZL6, and SPACA3 genes were mapped to human chromosome 10p11.23, 3p21.33, 17q11.2, and 17q12, respectively, and displayed a similar genomic structure. Our data suggest that these four lysozyme-like genes, which have arisen from a common progenitor gene, play a major role in human reproduction. © 2005 by the Society for the Study of Reproduction, Inc.

560. Does body volume constrain reproductive output in lizards? - Du W., Ji X. and Shine R. [R. Shine, School of Biological Sciences A08, University of Sydney, Sydney, NSW 2006, Australia] - *BIOL. LETT.* 2005 1/1 (98-100) - summ in ENGL

The numbers and sizes of eggs produced by adult females ultimately determine the viability of populations, as well as the evolutionary fitness of the females themselves. Despite an enormous amount of literature on the adaptive significance of fecundity variation within and among populations, simpler questions-such as the proximate mechanisms by which a female determines her clutch size-have attracted less attention. Our surgical manipulations show that the amount of space available to hold eggs within a female's abdomen influences her total reproductive allocation, enabling her to flexibly modify her reproductive output as she grows larger. © 2005 The Royal Society.

See also: 585, 587.

11. METABOLISM AND ENERGY BALANCE

561. Physiological role of carnosine in contracting muscle Begum G., Cunliffe A. and Leveritt M. [G. Begum, Dept. of Human and Health Sciences, University of Westminster, London W1W 6UW, United Kingdom] - *INT. J. SPORT NUTR. EXER. METABOL.* 2005 15/5 (493-514) - summ in ENGL

High-intensity exercise leads to reductions in muscle substrates (ATP, PCr, and glycogen) and a subsequent accumulation of metabolites (ADP, Pi, H +, and Mg²⁺) with a possible increase in free radical production. These factors independently and collectively have deleterious effects on muscle, with significant repercussions on high-intensity performance or training sessions. The effect of carnosine on overcoming muscle fatigue appears to be related to its ability to buffer the increased H+ concentration following highintensity work. Carnosine, however, has other roles such as an antioxidant, a metal chelator, a Ca2+ and enzyme regulator, an inhibitor of protein glycosylation and protein-protein cross-linking. To date, only 1 study has investigated the effects of carnosine supplementation (not in pure form) on exercise performance in human subjects and found no improvement in repetitive high-intensity work. Much data has come from in vitro work on animal skeletal muscle fibers or other components of muscle contractile mechanisms. Thus further research needs to be carried out on humans to provide additional understanding on the effects of carnosine in vivo. © 2005, Human Kinetics, Inc.

562. RANK ligand and TNF- α mediate acid-induced bone calcium efflux in vitro - Frick K.K., LaPlante K. and Bushinsky D.A. [K.K. Frick, Univ. of Rochester School of Medicine and Dentistry,

Nephrology Division, Box 675, 601 Elmwood Ave., Rochester, NY 14642, United States] - AM. J. PHYSIOL. RENAL PHYSIOL. 2005 289/5 58-5 (F1005-F1011) - summ in ENGL

Chronic metabolic acidosis stimulates net calcium efflux from bone due to increased osteoclastic bone resorption and decreased osteoblastic collagen synthesis. Previously, we determined that incubation of neonatal mouse calvariae in medium simulating physiological metabolic acidosis leads to a significant, cyclooxygenase-dependent, increase in RNA for bone cell receptor activator of NF-κB ligand (RANKL) compared with incubation in neutral pH medium. In this study, we tested the hypothesis that the acidmediated increase in RANKL expression is a primary mechanism for the stimulated osteoclastic resorption. Acid medium increased the medium concentration of sRANKL without altering the concentration of the decoy receptor osteoprotegerin (OPG). Inhibition of the RANKL pathway with concentrations of OPG up to 25 ng/ml, far greater than physiological, did not significantly decrease the robust acid-induced Ca efflux from bone nor did incubation of the calvariae with a different inhibitor, RANK/Fc (up to 50 ng/ml). Thus acid-induced net Ca efflux appears to involve mechanisms in addition to the RANK/RANKL pathway. Osteoblasts also produce TNF- α , another cytokine that stimulates the maturation and activity of osteoclasts. Incubation of calvariae in acid medium caused a significant increase in TNF- α levels. Incubation of calvariae with anti-TNF (up to 250 ng/ml) did not significantly decrease acidinduced net Ca efflux. However, the combination of RANK/Fc plus anti-TNF caused a significant but subtotal reduction in acid-induced Ca efflux, whereas the combination of RANK/Fc plus an isotypematched control for the anti-TNF had no effect on Ca release. Thus simultaneous inhibition of RANKL and TNF- α is necessary to reduce acid-induced, cell-mediated net Ca efflux from bone; however, additional osteoblast-produced factors must also be involved in acid-induced, cell-mediated bone resorption. Copyright © 2005 the American Physiological Society.

563. Vitamin D receptor-independent FGF23 actions in regulating phosphate and vitamin D metabolism - Shimada T., Yamazaki Y., Takahashi M. et al. [T. Yamashita, Pharmaceutical Research Laboratories, Kirin Brewery Co., Ltd., 3 Miyahara, Takasaki, Gunma 370-1295, Japan] - AM. J. PHYSIOL. RENAL PHYSIOL. 2005 289/5 58-5 (F1088-F1095) - summ in ENGL

FGF23 suppresses both serum phosphate and 1,25-dihydroxyvitamin D [1,25D] levels in vivo. Because 1,25D itself is a potent regulator of phosphate metabolism, it has remained unclear whether FGF23-induced changes in phosphate metabolism were caused by a 1,25D-independent mechanism. To address this issue, we intravenously administered recombinant FGF23 to vitamin D receptor (VDR) null (KO) mice as a rapid bolus injection and evaluated the early effects of FGF23. Administration of recombinant FGF23 further decreased the serum phosphate level in VDR KO mice, accompanied by a reduction in renal sodium-phosphate cotransporter type IIa (NaPi2a) protein abundance and a reduced renal 25-hydroxyvitamin D-1 α -hydroxylase (1 α OHase) mRNA level. Thus FGF23-induced changes in NaPi2a and 1α OHase expression are independent of the 1,25D/VDR system. However, 24-hydroxylase (24OHase) mRNA expression remained undetectable by the treatment with FGF23. We also analyzed the regulatory mechanism for FGF23 expression. The serum FGF23 level was almost undetectable in VDR KO mice, whereas dietary calcium supplementation significantly increased circulatory levels of FGF23 and its mRNA abundance in bone. This finding indicates that calcium is another determinant of FGF23 production that occurs independently of the VDR-mediated mechanism. In contrast, dietary phosphate supplementation failed to induce FGF23 expression in the absence of VDR, whereas marked elevation in circulatory FGF23 was observed in wild-type mice fed with a high-phosphate diet. Taken together, FGF23 works, at least in part, in a VDR-independent manner, and FGF23 production is also regulated by multiple mechanisms involving VDR-independent pathways. Copyright © 2005 the American Physiological Society.

564. Inhibition of hypothalamic fatty acid synthase triggers rapid activation of fatty acid oxidation in skeletal muscle - Cha S.H., Hu Z., Chohnan S. and Lane M.D. [M.D. Lane, Department of Biological Chemistry, Johns Hopkins University School of

Medicine, Baltimore, MD 21205, United States] - PROC. NATL. ACAD. SCI. U. S. A. 2005 102/41 (14557-14562) - summ in ENGL

Malonyl-CoA functions as a mediator in the hypothalamic sensing of energy balance and regulates the neural physiology that governs feeding behavior and energy expenditure. The central administration of C75, a potent inhibitor of the fatty acid synthase (FAS), increases malonyl-CoA concentration in the hypothalamus and suppresses food intake while activating fatty acid oxidation in skeletal muscle. Closely correlated with the increase in muscle fatty acid oxidation is the phosphorylation/inactivation of acetyl-CoA carboxylase, which leads to reduced malonyl-CoA concentration. Lowering muscle malonyl-CoA, a potent inhibitor of carnitine/palmitoyl-CoA transferase 1 (CPT1), releases CPT1 from inhibitory constraint, facilitating the entry of fatty acids into mitochondria for β oxidation. Also correlated with these events are C75-induced increases in the expression of skeletal muscle peroxisome proliferator-activated receptor α (PPAR α), a transcriptional activator of fatty acid oxidizing enzymes, and uncoupling protein 3 (UCP3), a thermogenic mitochondrial uncoupling protein. Phentolamine, an α -adrenergic blocking agent, prevents the C75-induced increases of skeletal muscle UCP3 and whole body fatty acid oxidation and C75-induced decrease of skeletal muscle malonyl-CoA. Thus, the sympathetic nervous system is implicated in the transmission of the "malonyl-CoA signal" from brain to skeletal muscle. Consistent with the up-regulation of UCP3 and PPAR α is the concomitant increase in the expression of PGC1 α , transcriptional coactivator of the UCP3 and PPAR α -activated genes. These findings clarify the mechanism by which the hypothalamic malonyl-CoA signal is communicated to metabolic systems in skeletal muscle that regulate fatty acid oxidation and energy expenditure. © 2005 by The National Academy of Sciences of the USA.

565. Decreased metabolic response to visual stimulation in the superior colliculus of mice lacking the glial glutamate transporter GLT-1 - Herard A.-S., Dubois A., Escartin C. et al. [Dr. G. Bonvento, CEA CNRS URA 2210, Service Hospitalier Frédéric Joliot, 4, place du General Leclerc, 91401 Orsay Cedex, France] - EUR. J. NEUROSCI. 2005 22/7 (1807-1811) - summ in ENGL

During a specific task, an increase in glucose utilization anatomically restricted to the functionally activated region(s) is a landmark of brain physiology. While this response represents the biological bases for functional brain imaging, the underlying signalling pathway(s) are still not fully characterized. Recent evidence suggests that glial glutamate (re)uptake plays a key role. We provide evidence that the metabolic response to synaptic activation (i.e. enhancement of glucose uptake) is decreased in the superior colliculus during visual stimulation in young adult mice deficient in the glial glutamate transporter GLT-1. A similar reduction was not observed in the glial glutamate transporter GLAST-knockout mice. Consistent with our previous observation obtained in the somatosensory cortex, our data suggest that a metabolic crosstalk takes place between neurons and astrocytes in the adult brain which would be regulated by synaptic activity and mediated by GLT-1. © Federation of European Neuroscience Societies.

566. Initial entry of IRAP into the insulin-responsive storage compartment occurs prior to basal or insulin-stimulated plasma membrane recycling - Liu G., Hou J.C., Watson R.T. and Pessin J.E. [J.E. Pessin, Dept. of Pharmacological Sciences, Stony Brook University, Stony Brook, NY 11794-8651, United States] - AM. J. PHYSIOL. ENDOCRINOL. METAB. 2005 289/5 52-5 (E746-E752) - summ in ENGL

To examine the acquisition of insulin sensitivity after the initial biosynthesis of the insulin-responsive aminopeptidase (IRAP), 3T3-L1 adipocytes were transfected with an enhanced green fluorescent protein-IRAP (EGFP-IRAP) fusion protein. In the absence of insulin, IRAP was rapidly localized (1-3 h) to secretory membranes and retained in these intracellular membrane compartments with little accumulation at the plasma membrane. However, insulin was unable to induce translocation to the plasma membrane until 6-9 h after biosynthesis. This was in marked contrast to another type II membrane protein (syntaxin 3) that rapidly defaulted to the plasma membrane 3 h after expression. In parallel with the time-dependent acquisition of insulin responsiveness, the newly synthesized IRAP protein converted from a brefeldin A-sensitive to a brefeldin

A-insensitive state. The initial trafficking of IRAP to the insulin-responsive compartment was independent of plasma membrane endocytosis, as expression of a dominant-interfering dynamin mutant (Dyn/K44A) inhibited transferrin receptor endocytosis but had no effect on the insulin-stimulated translocation of the newly synthesized IRAP protein. Copyright © 2005 the American Physiological Society.

567. Differential effects of pharmacological liver X receptor activation on hepatic and peripheral insulin sensitivity in lean and ob/ob mice - Grefhorst A., Van Dijk T.H., Hammer A. et al. [A. Grefhorst, Center for Liver, Digestive, and Metabolic Diseases, Laboratory of Pediatrics, Univ. Medical Center Groningen, P.O. Box 30.001, 9700 RB Groningen, Netherlands] - *AM. J. PHYSIOL. ENDOCRINOL. METAB.* 2005 289/5 52-5 (E829-E838) - summ in ENGL

Liver X receptor (LXR) agonists have been proposed to act as anti-diabetic drugs. However, pharmacological LXR activation leads to severe hepatic steatosis, a condition usually associated with insulin resistance and type 2 diabetes mellitus. To address this apparent contradiction, lean and ob/ob mice were treated with the LXR agonist GW-3965 for 10 days. Insulin sensitivity was assessed by hyperinsulinemic-euglycemic clamp studies. Hepatic glucose production (HGP) and metabolic clearance rate (MCR) of glucose were determined with stable isotope techniques. Blood glucose and hepatic and whole body insulin sensitivity remained unaffected upon treatment in lean mice, despite increased hepatic triglyceride contents (61.7 \pm 7.2 vs. 12.1 \pm 2.0 nmol/mg liver, P < 0.05). In ob/ob mice, LXR activation resulted in lower blood glucose levels and significantly improved whole body insulin sensitivity. GW-3965 treatment did not affect HGP under normo- and hyperinsulinemic conditions, despite increased hepatic triglyceride contents (221 \pm 13 vs. 176 \pm 19 nmol/mg liver, P < 0.05). Clamped MCR increased upon GW-3965 treatment (18.2 \pm 1.0 vs. 14.3 \pm 1.4 ml kg⁻¹ min⁻¹, P = 0.05). LXR activation increased white adipose tissue mRNA levels of Glut4, Acc1 and Fas in ob/ob mice only. In conclusion, LXR-induced blood glucose lowering in ob/ob mice was attributable to increased peripheral glucose uptake and metabolism, physiologically reflected in a slightly improved insulin sensitivity. Remarkably, steatosis associated with LXR activation did not affect hepatic insulin sensitivity. Copyright © 2005 the American Physiological Society.

568. Targeted intestinal overexpression of the immediate early gene tis7 in transgenic mice increases triglyceride absorption and adiposity - Wang Y., Iordanov H., Swietlicki E.A. et al. [D.C. Rubin, Division of Gastroenterology, Washington University School of Medicine, Box 8124, 660 South Euclid Ave., St. Louis, MO 63110, United States] - *J. BIOL. CHEM.* 2005 280/41 (34764-34775) - summ in ENGL

Following loss of functional small bowel surface area due to surgical resection, the remnant gut undergoes an adaptive response characterized by increased crypt cell proliferation and enhanced villus height and crypt depth, resulting in augmented intestinal nutrient absorptive capacity. Previous studies showed that expression of the immediate early gene tis7 is markedly up-regulated in intestinal enterocytes during the adaptive response. To study its role in the enterocyte, transgenic mice were generated that specifically overexpress TIS7 in the gut. Nucleotides -596 to +21 of the rat liver fatty acid-binding protein promoter were used to direct abundant overexpression of TIS7 into small intestinal upper crypt and villus enterocytes. TIS7 transgenic mice had increased total body adiposity and decreased lean muscle mass compared with normal littermates. Oxygen consumption levels, body weight, surface area, and small bowel weight were decreased. On a high fat diet, transgenic mice exhibited a more rapid and proportionately greater gain in body weight with persistently elevated total body adiposity and increased hepatic fat accumulation. Bolus fat feeding resulted in a greater increase in serum triglyceride levels and an accelerated appearance of enterocytic, lamina propria, and hepatic fat Changes in fat homeostasis were linked to increased expression of genes involved in enterocytic triglyceride metabolism and changes in growth with decreased insulin-like growth factor-1 expression. Thus, TIS7 overexpression in the intestine altered growth, metabolic rate, adiposity, and intestinal triglyceride absorption. These results suggest that TIS7 is a unique mediator of nutrient absorptive and metabolic adaptation following gut resection.

569. Sex differences in glycolysis during brief, intense isometric contractions - Russ D.W., Lanza I.R., Rothman D. and Kent-Braun J.A. [Dr. J.A. Kent-Braun, Department of Exercise Science, Totman 108, University of Massachusetts, Amherst, MA 01035, United States] - *MUSCLE NERVE* 2005 32/5 (647-655) - summ in ENGL

We have previously observed less muscle fatigue in women than men under conditions of intact circulation, but similar fatigue across the sexes during local ischemia. Thus, we hypothesized that women utilize their aerobic metabolic pathways to a greater extent than do men. To test this hypothesis, we examined the extent to which different pathways of intramuscular adenosine triphosphate (ATP) production were utilized by men and women during maximal voluntary isometric contractions. Force production during 15-s and 60-s contractions were recorded in parallel sessions. In one session, central activation was assessed with electrical stimulation. In the other, phosphorus magnetic resonance spectroscopy was used to quantify muscle oxidative capacity, and the contributions of glycolysis and oxidative phosphorylation to ATP synthesis during the 60-s contraction. Fatigue and central activation were similar in men and women during both the 15-s and 60-s contractions. The rate constants of phosphocreatine recovery following the 15-s contraction were similar in men and women, indicating similar oxidative capacities. Men exhibited greater acidosis and peak glycolytic rates compared with women during the 60-s contraction, with no differences observed in creatine kinase flux or the percent of oxidative capacity utilized. We conclude that men exhibit greater in vivo glycolysis during brief, intense isometric contractions. Although this metabolic difference did not contribute to any observable differences in fatigue in the present study, these results highlight a potentially important mechanism to explain sex-related differences in muscle function. © 2005 Wiley Periodicals, Inc.

570. Na⁺-K⁺ pump activation inhibits endothelium-dependent relaxation by activating the forward mode of Na⁺/Ca²⁺ exchanger in mouse aorta - Kim M.Y., Seol G.H., Liang G.H. et al. [S.H. Suh, Dept. of Physiology, College of Medicine, Ewha Women's Univ., 911-1 Mok-6-dong, Yang Chun-gu, Seoul, South Korea] - *AM. J. PHYSIOL. HEART CIRC. PHYSIOL.* 2005 289/5 58-5 (H2020-H2029) - summ in ENGL

The effect of Na+-K+ pump activation on endothelium-dependent relaxation (EDR) and on intracellular Ca2+ concentration ([Ca2+]i) was examined in mouse aorta and mouse aortic endothelial cells (MAECs). The Na+-K+ pump was activated by increasing extracellular K⁺ concentration ([K ⁺]_o) from 6 to 12 mM. In aortic rings, the Na+ ionophore monensin evoked EDR, and this EDR was inhibited by the Na +/Ca²⁺ exchanger (NCX; reverse mode) inhibitor KB-R7943. Monensin-induced Na+ loading or extracellular Na+ depletion (Na+ replaced by Li+) increased [Ca 2+]i in MAECs, and this increase was inhibited by KB-R7943. Na+-K+ pump activation inhibited EDR and [Ca2+]i increase (K+-induced inhibition of EDR and [Ca²+]; increase). The Na*-K* pump inhibitor ouabain inhibited K*-induced inhibition of EDR. Monensin (>0.1 μ M) and the NCX (forward and reverse mode) inhibitors 2'4'-dichlorobenzamil > 10 μ M) or Ni²⁺ (>100 μ M) inhibited K+-induced inhibition of EDR and [Ca 2+]i increase. KB-R7943 did not inhibit K +-induced inhibition at up to 10 μM but did at 30 μM . In current-clamped MAECs, an increase in [K+]o from 6 to 12 mM depolarized the membrane potential, which was inhibited by ouabain, Ni 2+, or KB-R7943. In a ortic rings, the concentration of cGMP was significantly increased by acetylcholine and decreased on increasing [K+]o from 6 to 12 mM. This decrease in cGMP was significantly inhibited by pretreating with ouabain (100 μ M), Ni²⁺ (300 μ M), or KB-R7943 $(30 \mu M)$. These results suggest that activation of the forward mode of NCX after Na+-K+ pump activation inhibits Ca²⁺ mobilization in endothelial cells, thereby modulating vasomotor tone. Copyright © 2005 the American Physiological Society.

571. Route-dependent effect of nutritional support on liver glucose uptake - Chen S.-S., Torres-Sanchez C.J., Hosein N. et al. [O.P. McGuinness, 702 Light Hall, Dept. Molecular Physiology and Biophysics, Vanderbilt Univ., Nashville, TN 37232-0615, United

States] - AM. J. PHYSIOL. REGUL. INTEGR. COMP. PHYSIOL. 2005 289/5 58-5 (R1319-R1327) - summ in ENGL

The liver is a major site of glucose disposal during chronic (5 day) total parenteral (TPN) and enteral (TEN) nutrition. Net hepatic glucose uptake (NHGU) is dependent on the route of delivery when only glucose is delivered acutely; however, the hepatic response to chronic TPN and TEN is very similar. We aimed to determine whether the route of nutrient delivery altered the acute (first 8 h) response of the liver and whether chronic enteral delivery of glucose alone could augment the adaptive response to TPN. Chronically catheterized conscious dogs received either TPN or TEN containing glucose, Intralipid, and Travasol for either 8 h or 5 days. Another group received TPN for 5 days, but ∼50% of the glucose in the nutrition was given via the enteral route (TPN+EG). Hepatic metabolism was assessed with tracer and arteriovenous difference techniques. In the presence of similar arterial plasma glucose levels (~6 mM), NHGU and net hepatic lactate release increased approximately twofold between 8 h and 5 days in TPN and TEN. NHGU $(26\pm1~vs.~23\pm3~\mu mol~kg^{-1}~min^{-1})$ and net hepatic lactate release $(44\pm1~vs.~34\pm6~\mu mol~kg^{-1}~min^{-1})$ in TPN+EG were similar to results for TPN, despite lower insulin levels $(96\pm6~vs.~58\pm$ 16 pM, TPN vs. TPN+EG). TEN does not acutely enhance NHGU or disposition above that seen with TPN. However, partial delivery of enteral glucose is effective in decreasing the insulin requirement during chronic TPN. Copyright © 2005 the American Physiological

572. Human sulfate kinetics - Hoffer L.J., Hamadeh M.J., Robitaille L. and Norwich K.H. [L.J. Hoffer, Lady Davis Institute for Medical Research, Jewish General Hospital, 3755 Cote-Ste-Catherine Road, Montreal, Que. H3T 1E2, Canada] - *AM. J. PHYSIOL. REGUL. INTEGR. COMP. PHYSIOL.* 2005 289/5 58-5 (R1372-R1380) - summ in ENGL

Electrospray tandem mass spectrometry was used to determine steady-state serum and urinary inorganic sulfate and sulfate ester kinetic profiles of nine normal men after intravenous injection of the stable isotope sodium [34S]sulfate. Sulfate ester appearance was traced by eliminating inorganic sulfate from samples, followed by hydrolysis of sulfate esters to inorganic sulfate for analysis. Whole body inorganic sulfate turnover in steady state was calculated using standard tracer techniques. Rate of appearance and disappearance of inorganic sulfate was $841 \pm 49 \mu \text{mol/h}$. Average urinary inorganic sulfate excretion was $609 \pm 41 \mu \text{mol/h}$, and the whole body sulfation rate (total rate of disappearance minus rate of urinary excretion) was 232 \pm 36 μ mol/h. Tracer-labeled sulfate esters appeared in serum and urine within 1 h of tracer injection. The kinetics of inorganic sulfate and sulfate esters were linked by means of a compartmental model. The appearance and excretion of sulfate esters accounted for $\sim 50\%$ of the total sulfation rate. These results indicate that human whole body sulfation accounts for $\sim 27\%$ of inorganic sulfate turnover and that extracellular inorganic sulfate is an important pool for intracellular sulfation. A substantial fraction of newly synthesized sulfate esters promptly enters the extracellular space for excretion in the urine. Copyright © 2005 the American Physiological Society.

573. Different signaling in pig anterior pituitary cells by GNRH and its complexes with copper and nickel - Kochman K., Blitek A., Kaczmarek M. et al. [Prof. K. Kochman, The Kielanowski Institute of Animal Physiology and Nutrition, Polish Academy of Sciences, 05-110 Jablonna, Poland] - NEUROENDOCRINOL. LETT. 2005 26/4 (377-382) - summ in ENGL

Gonadotropin releasing hormone (GnRH) is an essential factor in the regulation of synthesis and release of pituitary gonadotropins. After binding to specific receptors and coupling with G proteins, it triggers the intracellular signaling involving the synthesis of inositol phosphates and diacylglycerol. Previously we have showed that certain metal complexes with GnRH, i.e. copper (Cu-GnRH) and nickel (Ni-GnRH) are able to bind to the GnRH receptors. The intracellular signalling of these complexes, however, has not been yet elucidated. In this experiment, the ability of the Cu-GnRH and Ni-GnRH complexes to modulate cAMP synthesis and phosphoinositols formation in the pig anterior pituitary cells in vitro was studied. The native GnRH and its metal complexes stimulated the luteinizing hormone (LH) release. but, only the effect of Cu-GnRH was found

to be a dose-dependent. The metal complexes did not significantly influence inositol phosphates accumulation, while their effect on cAMP synthesis was significantly more potent than that of GnRH alone. We conclude that the Cu-GnRH and Ni-GnRH complexes increase LH release in the porcine pituitary cells although their intracellular signaling is different from that of the native GnRH. It seems that metal complexes with GnRH deserve more attention in further studies. © Neuroendocrinology Letters.

574. Labeled CO₂ production and oxidative vs nonoxidative disposal of labeled carbohydrate administered at rest - Folch N., Péronnet F., Péan M. et al. [F. Péronnet, Département de Kinésiologie, Université de Montréal, Montréal, Que. H3C 3J7, Canada] - *METAB. CLIN. EXP.* 2005 54/11 (1428-1434) - summ in ENGL

Carbon isotopes (*C) have been extensively used in man to describe oxidative vs nonoxidative disposal of an exogenous load of labeled carbohydrate (*C-CHO) at rest in various experimental situations. It is hypothesized that V*CO2 reflects *C-CHO oxidation. However, when glycogen is synthesized through the indirect pathway (which is responsible for ~50% of glycogen storage), *C could be lost, diluted, and exchanged in the pyruvate-lactate pool, in the pool of tricarboxylic acid cycle intermediates, as well as at the entrance of the tricarboxylic acid cycle, and along the pathway of gluconeogenesis. This could result in a lower *C/C in the glycogen stored than in the CHO administered, in an increased production of *CO2, and, respectively, in an overestimation and an underestimation of the oxidative and nonoxidative disposal of the CHO load. Results from the present experiment offer a support to this hypothesis. Over a 10-hour period after ingestion of a ¹³C-pasta meal (313 \pm 10 g dry mass or 258 \pm 8 g of glucose) in 12 healthy subjects (6 men and 6 women), exogenous CHO oxidation computed from V13CO₂ (recovery factor, 0.54) significantly exceeded total CHO oxidation computed by indirect respiratory calorimetry corrected for urea excretion: 154.2 ± 2.6 vs 133.5 ± 3.2 g. In an additional study conducted in rats, $^{13}\text{C}/^{12}\text{C}$ in glycogen stores was significantly \sim 50% lower than in the ¹³C-CHO ingested, over a wide range of enrichment. These results suggest that because of dilution, loss, and exchange of *C in the indirect pathway of glycogen synthesis, the oxidative vs nonoxidative disposal of exogenous *C-CHO cannot be accurately tracked from V*CO₂. © 2005 Elsevier Inc. All rights reserved.

575. A white blood cell count in the normal concentration range is independently related to cardiorespiratory fitness in apparently healthy Korean men - Kim D.-J., Noh J.-H., Lee B.-W. et al. [M.-K. Lee, Department of Medicine, Samsung Medical Center, Sungkyunkwan University School of Medicine, Seoul 135-710, South Korea] - *METAB. CLIN. EXP.* 2005 54/11 (1448-1452) - summ in ENGL

Despite the documented health benefits of physical activity, the mechanism whereby physical activity prevents cardiovascular disease is incompletely understood. In the present study, we investigated the relationship between white blood cell (WBC) count and cardiorespiratory fitness (Vo2max) after adjusting for several well-known cardiovascular risk factors. Subjects who visited our health promotion center for a medical checkup and treadmill test (n = 8241; age: median, 48 years; range, 16-79 years) were classified into 3 groups based on their WBC counts (group 1, 2200-5300 μ L, n = 2823; group 2, 5301-6500 μ L, n = 2709; group 3, 6501-10 000 μ L, n = 2709). After adjusting for age, body mass index, body fat percentage, smoking history, systolic blood pressure, diastolic blood pressure, serum lipid profile, and fasting plasma glucose, Vo2max still showed a significant association with WBC count (partial r = -0.11, P < .001). In logistic regression analyses, subjects in the highest WBC tertile showed lower Vo2max compared with those in the lowest WBC tertile after adjusting for age and cardiovascular risk factors (odds ratio, 0.42; 95% confidence interval, 0.36-0.49 for the highest Vo₂max tertile). These results suggest that a WBC count in the normal concentration range is independently related to cardiorespiratory fitness in Korean men. © 2005 Elsevier Inc. All rights reserved

576. First records of dive durations for a hibernating sea turtle - Hochscheid S., Bentivegna F. and Hays G.C. [S. Hochscheid,

Stazione Zoologica Anton Dohrn, Villa Comunale 1, 80121 Naples, Italy] - *BIOL. LETT.* 2005 1/1 (82-86) - summ in ENGL

The first published record, from the early 1970s, of hibernation in sea turtles is based on the reports of the indigenous Indians and fishermen from Mexico, who hunted dormant green turtles (Chelonia mydas) in the Gulf of California. However, there were no successful attempts to investigate the biology of this particular behaviour further. Hence, data such as the exact duration and energetic requirements of dormant winter submergences are lacking. We used new satellite relay data loggers to obtain the first records of up to 7 h long dives of a loggerhead turtle (Caretta caretta) overwintering in Greek waters. These represent the longest dives ever reported for a diving marine vertebrate. There is strong evidence that the dives were aerobic, because the turtle surfaced only for short intervals and before the calculated oxygen stores were depleted. This evidence suggests that the common belief that sea turtles hibernate underwater, as some freshwater turtles do, is incorrect. © 2005 The Royal Society.

577. Relative contribution of abundant and rare species to species-energy relationships - Evans K.L., Greenwood J.J.D. and Gaston K.J. [K.L. Evans, Biodiversity and Macroecology Group, Department of Animal and Plant Sciences, University of Sheffield, Sheffield S10 2TN, United Kingdom] - *BIOL. LETT.* 2005 1/1 (87-90) - summ in ENGL

A major goal of ecology is to understand spatial variation in species richness. The latter is markedly influenced by energy availability and appears to be influenced more by common species than rare ones; species-energy relationships should thus be stronger for common species. Species-energy relationships may arise because high-energy areas support more individuals, and these larger populations may buffer species from extinction. As extinction risk is a negative decelerating function of population size, this more-individuals hypothesis (MIH) predicts that rare species should respond more strongly to energy. We investigate these opposing predictions using British breeding bird data and find that, contrary to the MIH, common species contribute more to species-energy relationships than rare ones. © 2005 The Royal Society.

578. Faster development does not lead to correlated evolution of greater pre-adult competitive ability in Drosophila melanogaster - Shakarad M., Prasad N.G., Gokhale K. et al. [M. Shakarad, Behaviour, Ecology and Evolution Laboratory, Biology Department, Poornaprajna Institute of Scientific Research, P. O. Box 18, Devanahalli-562 110, Bangalore, India] - *BIOL. LETT.* 2005 1/1 (91-94) - summ in ENGL

In comparisons across Drosophila species, faster pre-adult development is phenotypically correlated with increased pre-adult competitive ability, suggesting that these two traits may also be evolutionary correlates of one another. However, correlations between traits within- and among-species can differ, and in most cases it is the within-species genetic correlations that are likely to act as constraints on adaptive evolution. Moreover, laboratory studies on Drosophila melanogaster have shown that the suite of traits that evolves in populations subjected to selection for faster development is the opposite of the traits that evolve in populations selected for increased pre-adult competitive ability. This observation led us to propose that, despite having a higher carrying capacity and a reduced minimum food requirement for completing development than controls, D. melanogaster populations subjected to selection for faster development should have lower competitive ability than controls owing to their reduced larval feeding rates and urea tolerance. Here, we describe results from pre-adult competition experiments that clearly show that the faster developing populations are substantially poorer competitors than controls when reared at high density in competition with a marked mutant strain. We briefly discuss these results in the context of different formulations of density-dependent selection theory. © 2005 The Royal Society.

579. Alterations in tissue aerobic capacity may play a role in premigratory fattening in shorebirds - Selman C. and Evans P.R. [C. Selman, Centre for Diabetes and Endocrinology, Rayne Institute, University College London, 5 University Street, London WC1E 6JF, United Kingdom] - *BIOL. LETT.* 2005 1/1 (101-104) - summ in ENGL.

Migratory shorebirds show regulated seasonal increases in body mass (BM) even in captivity, consisting primarily, but not exclusively, of fat. We examined whether captive red knot (Calidris canutus) exhibited seasonal alterations in mitochondrial volume (liver, pectoral muscle) and/or succinate dehydrogenase (SDH)activity (liver, pectoral muscle, heart, small intestine) during three distinct life-cycle stages: stable BM, spring peak in BM, and as BM rapidly declined after the spring peak. Mitochondrial volume in liver and pectoral muscle and SDH activity in liver and heart did not alter with life-cycle stage. However, red knot undergoing premigratory fattening exhibited significantly lower pectoral muscle SDH activity in concert with significantly elevated activity in the small intestine compared with the other two time-points, suggesting that tissue metabolic rate alters with life-cycle stage. The increased intestinal SDH activity may indicate an elevation in energy assimilation at a time when intestine hypertrophy occurs, thus maximizing BM increase prior to putative migration. The concomitant decrease in pectoral muscle activity may act to reduce overall metabolic rate, or at least help counter the elevation in intestinal mass-specific metabolic rate. Both tissues hypertrophy prior to migration in wild red knot, but hypertrophy of the intestine precedes that of pectoral muscle. Indeed, it appears that the intestinal mass undergoes atrophy by the time pectoral muscle hypertrophy occurs in wild red knot. Thus, physiological adjustments in tissue metabolism may be an important factor in the life-history strategies of migrating shorebirds. © 2005 The Royal Society.

See also: 597, 600, 601, 614, 615, 625, 632, 635.

12. THERMOREGULATION AND SWEATING

580. Attenuation of sensory and affective responses to heat pain: Evidence for contralateral mechanisms - Gallez A., Albanese M.-C., Rainville P. and Duncan G.H. [G.H. Duncan, Université de Montréal, Succ. Centre-Ville, Montréal, Que. H3C 1J7, Canada] - *J. NEUROPHYSIOL.* 2005 94/5 (3509-3515) - summ in ENGL

Attenuation of responses to repeated sensory events has been thoroughly studied in many modalities; however, attenuation of pain perception has not yet benefitted from such extensive investigation. Described here are two psychophysical studies that examined the effects of repeated exposure to thermal stimuli, assessing potential attenuation of the perception of pain and its possible spatial specificity. Twenty-two subjects were presented thermal stimuli to the volar surface of the right and left forearms. Twelve subjects in study 1 received the same stimuli and conditions on each of five daily experimental sessions, whereas 10 subjects in study 2 received thermal stimuli, which were restricted to one side for four daily sessions and then applied to the other side on the fifth session. Ratings of warmth intensity, pain intensity, and pain unpleasantness were recorded while the subjects performed a thermal sensory discrimination task. Results of study 1 demonstrate that repeated stimulation with noxious heat can lead to long-term attenuation of pain perception; results of study 2 extend these findings of attenuation to both pain intensity and unpleasantness and show that this effect is highly specific to the exposed body side for both aspects of the pain experience. We suggest that the functional plasticity underlying this attenuation effect lies in brain areas with a strong contralateral pattern of pain-related activation. Copyright © 2005 The American Physiological Society.

581. Heat shock-mediated thermoprotection of larval locomotion compromised by ubiquitous overexpression of Hsp70 in **Drosophila melanogaster** - Klose M.K., Chu D., Xiao C. et al. [R.M. Robertson, Department of Biology, Queen's University, 3118 Biosciences Complex, Kingston, Ont. K7L 3N6, Canada] - *J. NEU-ROPHYSIOL.* 2005 94/5 (3563-3572) - summ in ENGL

Maintaining the competence of locomotor circuitry under stressful conditions can benefit organisms by enabling locomotion to more tolerable microhabitats. We show that prior heat shock protects locomotion and the locomotor central pattern generator of larval Drosophila against subsequent hyperthermic stress. We combined molecular genetic, electrophysiological, and behavioral techniques to investigate heat shock-mediated thermoprotection. Prior heat shock increased the distance traveled by larvae during hyperthermia

before failure. The frequency of the rhythm of peristaltic locomotor contractions and the velocity of locomotion were both less thermosensitive after heat shock and were less susceptible to failure at high temperatures. Rhythmic coordinated motor patterns, recorded intracellularly as excitatory junction potentials in body wall muscles of dissected preparations, were centrally generated because patterns could still be generated in the absence of sensory feedback (sensory function disrupted with shibire). Prior heat shock protected central circuit operation during hyperthermic stress by increasing the temperature at which it failed. Overexpression of Hsp70 after a heat shock using transgenic flies (traII) did not enhance thermoprotection, as expected, but had deleterious effects on parameters of behavior. Copyright © 2005 The American Physiological Society.

582. Thermoregulatory responses to lipopolysaccharide in the mouse: Dependence on the dose and ambient temperature - Rudaya A.Y., Steiner A.A., Robbins J.R. et al. [A.A. Romanovsky, Trauma Research, St. Joseph's Hospital, 350 W. Thomas Rd., Phoenix, AZ 85013, United States] - AM. J. PHYSIOL. REGUL. INTEGR. COMP. PHYSIOL. 2005 289/5 58-5 (R1244-R1252) - summ in ENGL

Most published studies of thermoregulatory responses of mice to LPS involved a stressful injection of LPS, were run at a poorly controlled and often subneutral ambient temperature (T_a) , and paid little attention to the dependence of the response on the LPS dose. These pitfalls have been overcome in the present study. Male C57BL/6 mice implanted with jugular vein catheters were kept in an environmental chamber at a tightly controlled T a. The relationship between the Tas used and the thermoneutral zone of the mice was verified by measuring tail skin temperature, either by infrared thermography or thermocouple thermometry. Escherichia coli LPS in a wide dose range (10^{0} - 10^{4} μ g/kg) was administered through an extension of the jugular catheter from outside the chamber. The responses observed were dose dependent. At a neutral Ta, low (just suprathreshold) doses of LPS (10^0 - $10^1 \mu g/kg$) caused a monophasic fever. To a slightly higher dose ($10^{1.5} \mu g/kg$), the mice responded with a biphasic fever. To even higher doses ($10^{1.75}$ - $10^4 \mu g/kg$), they responded with a polyphasic fever, of which three distinct phases were identified. The dose dependence and dynamics of LPS fever in the mouse appeared to be remarkably similar to those seen in the rat. However, the thermoregulatory response of mice to LPS in a subthermoneutral environment is remarkably different from that of rats. Although very high doses of LPS ($10^4 \mu g/kg$) did cause a late (latency, ~ 3 h) hypothermic response in mice, the typical early (latency, 10-30 min) hypothermic response seen in rats did not occur. The present investigation identifies experimental conditions to study LPS-induced mono-, bi-, and polyphasic fevers and late hypothermia in mice and provides detailed characteristics of these responses. Copyright © 2005 the American Physiological Society.

583. Expanding the febrigenic role of cyclooxygenase-2 to the previously overlooked responses - Steiner A.A., Rudaya A.Y., Robbins J.M. et al. [A.A. Romanovsky, Trauma Research, St. Joseph's Hospital, 350 W. Thomas Rd., Phoenix, AZ 85013, United States] - *AM. J. PHYSIOL. REGUL. INTEGR. COMP. PHYSIOL.* 2005 289/5 58-5 (R1253-R1257) - summ in ENGL

Previous studies on the role of cyclooxygenase (COX)-1 and -2 in fever induced by intravenous LPS have failed to investigate the role of these isoenzymes in the earliest responses: monophasic fever (response to a low, near-threshold dose of LPS) and the first phase of polyphasic fever (response to higher doses). We studied these responses in 96 mice that were COX-1 or COX-2 deficient (-/-) or sufficient (+/+). Each mouse was implanted with a temperature telemetry probe into the peritoneal cavity and a jugular catheter. The study was conducted at a tightly controlled, neutral ambient temperature (31°C). To avoid stress hyperthermia (which masks the onset of fever), all injections were performed through a catheter extension. The +/+ mice responded to intravenous saline with no change in deep body temperature. To a low dose of LPS (1 μ g/kg iv), they responded with a monophasic fever. To a higher dose (56 μ g/kg), they responded with a polyphasic fever. Neither monophasic fever nor the first phase of polyphasic fever was attenuated in the COX-1 -/- mice, but both responses were absent in the COX-2 -/- mice. The second and third phases of polyphasic fever were also missing in the COX-2 -/- mice. The present study identifies a new,

critical role for COX-2 in the mediation of the earliest responses to intravenous LPS: monophasic fever and the first phase of polyphasic fever. It also suggests that no product of the COX-1 gene, including the splice variant COX-1b (COX-3), is essential for these responses. Copyright © 2005 the American Physiological Society.

584. Lipopolysaccharide-induced fever in Pekin ducks is mediated by prostaglandins and nitric oxide and modulated by adrenocortical hormones - Gray D.A., Maloney S.K. and Kamerman P.R. [D.A. Gray, School of Physiology, Univ. of the Witwatersrand, Medical School, 7 York Rd., Parktown 2193, Johannesburg, South Africa] - AM. J. PHYSIOL. REGUL. INTEGR. COMP. PHYSIOL. 2005 289/5 58-5 (R1258-R1264) - summ in ENGL.

Information on avian fever is limited, and, in particular, very little is known about the mediators and modulators of the febrile response in birds. Therefore, in this study, the possible mediatory roles of nitric oxide (NO) and prostaglandins (PGs), together with a potential modulatory role for adrenocortical hormones in the generation of fever was investigated in conscious Pekin ducks. Their body temperatures were continuously measured by abdominally implanted temperature-sensitive data loggers. The febrile response induced by intramuscular injection of LPS at a dose of 100 µg/kg was compared with and without inhibition of NO production by N-nitro-L-arginine methyl ester (L-NAME), inhibition of PG synthesis (by diclofenac), and elevation of circulating concentrations of dexamethasone and corticosterone (by exogenous administration). LPS administration induced a marked, monophasic fever with a rise in temperature of more than 1°C after 3-4 h. In the presence of L-NAME, diclofenac, and adrenocorticoids at doses that had no effect upon normal body temperature in afebrile ducks, there was a significant inhibition of the LPS-induced fever. In addition, during the febrile response, the blood concentration of corticosterone was significantly elevated (from a basal level of 73.6 \pm 9.8 ng/ml to a peak level of 132.6 ± 16.5 ng/ml). The results strongly suggest that the synthesis of both NO and PGs is a vital step in the generation of fever in birds and that the magnitude of the response is subject to modulation by adrenocorticoids. Copyright © 2005 the American Physiological

585. Fever suppression in near-term pregnant rats is dissociated from LPS-activated signaling pathways - Mouihate A., Ellis S., Harré E.-M. and Pittman Q.J. [A. Mouihate, Hotchkiss Brain Institute, Dept. of Physiology and Biophysics, Univ. of Calgary, 3330 Hospital Drive NW, Calgary, Alta. T2N 4N1, Canada] - *AM. J. PHYSIOL. REGUL. INTEGR. COMP. PHYSIOL.* 2005 289/5 58-5 (R1265-R1272) - summ in ENGL

Near-term pregnant rats show a suppressed fever response to LPS that is associated with reduced induction of cyclooxygenase (COX)-2 in the hypothalamus. The objective of this study is to explore whether the LPS-activated signaling pathways in the fevercontrolling region of the hypothalamus are specifically altered at near term. Three rat groups consisting of 15-day pregnant rats, near-term 21- to 22-day pregnant rats, and day 5 lactating rats were injected with a febrile dose of LPS (50 μ g/kg ip). The hypothalamic preoptic area and the organum vasculosum of the lamina terminalis (OVLT) were collected 2 h after LPS injection. activation of three transcription modulators, nuclear factor- κB (NFκB), extracellular signal-regulated kinase 1/2 (ERK1/2), and signal transducer and activator of transcription 5 (STAT5), was assessed using semiquantitative Western blot analysis. LPS activated the NF- κ B pathway in all rat groups, and this response was not altered at near term. ERK1/2 and STAT5 were constitutively activated during all reproductive stages, and their levels were not significantly affected by LPS injection. Plasma levels of the proinflammatory cytokines (IL-1 β , IL-6, TNF- α , and IFN- γ), anti-inflammatory cytokines (IL-4, IL-10, and IL-1 receptor antagonist), and corticosterone were unaffected during the three reproductive stages after LPS challenge. We observed a sharp decrease in the expression of a prostaglandin-producing enzyme called lipocalin-prostaglandin D₂ synthase in near-term pregnant and lactating rats. fever suppression at near term is not due to an alteration in either LPS-activated intracellular signaling pathways or LPS-induced proand anti-inflammatory cytokine production. Copyright © 2005 the American Physiological Society.

See also: 589, 622, 633.

13. BODY FLUIDS

586. Insulin secretion by rat lachrymal glands: Effects of systemic and local variables - Cunha D.A., Carneiro E.M., De Alves M.C. et al. [E.M. Rocha, Departamento de Oftalmologia, FMRP, USP, Av. Bandeirantes, 3900, Ribeirao Preto, Sao Paulo, 14049-900, Brazil] - *AM. J. PHYSIOL. ENDOCRINOL. METAB.* 2005 289/5 52-5 (E768-E775) - summ in ENGL

To understand the secretory mechanisms and physiological role of insulin in the tear film, the present study examined 1) the time course of insulin secretion in the tear film under glucose intravenous stimulation, 2) the glucose- and carbachol-induced insulin secretion from isolated lachrymal gland (LG), 3) the effect of insulin on glucose consumption by the cornea, and 4) the expression of insulin. pancreatic duodenal homeobox-1 (PDX-1), and glucose transport proteins (GLUTs) in LG tissue. The insulin level in the tear film of 8-wk-old male Wistar rats increased from 0.6 ± 0.45 to 3.7+ 1.3 ng/ml in the initial minutes after glucose stimulation. In vitro assays demonstrated that higher glucose concentrations from 2.8 to 16.7 mM, 200 μ M carbachol, or 40 mM KCl significantly increased insulin secretion from lacrimal glands compared with controls, but did not detect C-peptide as measured by RIA. Glucose consumption by corneal tissue, evaluated by radiolabeled D-[U- 14 C]glucose uptake, was 24.07 \pm 0.61 and was enhanced to 31.63 \pm 3.15 nmol cornea⁻¹ 2 h⁻¹ in the presence of 6 nM insulin (P = 0.033) and to 37.5 \pm 3.7 nmol cornea⁻¹ 2 h⁻¹ in the presence of 11.2 mM glucose (P = 0.015). Insulin and PDX-1 mRNA was detected in LG. Insulin was located in the apical areas of acinar cells by immunoperoxidase and the expression of GLUT-1, but not PDX-1, was confirmed by Western blot. These findings suggest that insulin secretion in the tear film is influenced by local stimuli such as nutrient and neural inputs and that this hormone plays a metabolic role in ocular surface tissues. These data also indicate that under normal conditions the insulin secreted by LG is stored, but it is not clear that is locally produced in the LG. Copyright © 2005 the American Physiological Society.

587. Interactions between the rabbit CSN1 gene and the nuclear matrix of stably transfected HC11 mammary epithelial cells vary with its level of expression - Poussin K., Hayes H., Pauloin A. et al. [E. Devinoy, Unité de Génomique et Physiologie de la Lactation, INRA, 78 352 Jouy en Josas Cedex, France] - *J. CELL. BIOCHEM.* 2005 96/3 (611-621) - summ in ENGL

The expression of casein genes is specific to the mammary gland and maximal during lactation. However, among the numerous mammary cell lines described so far, only a few express some casein genes. The regulatory regions of casein genes have been largely described but the mechanisms explaining the mammary specific expression of these genes, and their silencing in most mammary cell lines, have not yet been fully elucidated. To test the hypothesis that the nuclear location of the casein genes may affect their expression, we transfected HC11 mouse mammary cell line with a 100 kb DNA fragment surrounding the rabbit alpha S1 casein gene. We derived stable clones which express or not the transfected rabbit casein gene, in the same cellular context, independently of the number of transgene copies. Metaphase spreads were prepared from the different clones and the transfected genes were localized. Unexpectedly, we observed that in the original HC11 cell line the number of chromosomes per metaphase spread is close to 80, suggesting that HC11 cells have undergone a duplication event, since the mouse karyotype is 2n=40. In alpha S1 casein expressing cells, the expression level does not clearly correlate with a localization of the transfected DNA proximal to the centromeres or the telomeres. Analysis of the localization of the transfected DNA in nuclear halos allows us to conclude that when expressed, transfected DNA is more closely linked to the nuclear matrix. The next step will be to study the attachment of the endogenous casein gene in mammary nuclei during lactation. @ 2005 Wiley-Liss, Inc.

588. Inhibition of vasopressin secretion when dehydrated rats drink water - Stricker E.M. and Hoffmann M.L. [E.M. Stricker, Dept. of Neuroscience, 446 Crawford Hall, Univ. of Pittsburgh,

Pittsburgh, PA 15260, United States] - AM. J. PHYSIOL. REGUL. INTEGR. COMP. PHYSIOL. 2005 289/5 58-5 (R1238-R1243) - summ in ENGL

The present study determined whether vasopressin (VP) secretion is inhibited by an oropharyngeal signal associated with swallowing fluids when dehydrated rats drink water, as it is when dehydrated dogs are used as experimental subjects (Thrasher, TN, Keil LC, and Ramsay DJ. Am J Physiol Regul Integr Comp Physiol 253: R509-R515, 1987). VP levels in systemic plasma (pVP) fell rapidly when rats drank water after overnight water deprivation. Systemic plasma Na+ concentration (pNa) also fell, but that change likely contributed little to the early inhibition of VP secretion. In contrast, consumption of water by dehydrated rats with an open gastric fistula had no effect on pVP, nor did consumption of isotonic saline by dehydrated rats; in neither case was pNa affected by fluid consumption. These findings provide no evidence that the act of drinking inhibits VP secretion in dehydrated rats. Thus some postgastric effect of the ingested water seems to be responsible for the inhibitory signal. These results are consistent with previous suggestions that an early inhibitory stimulus for VP secretion in rats is provided by postgastric visceral osmo- or Na+ receptors that sense the composition of the ingested fluid. Copyright © 2005 the American Physiological

589. Thermal effects of dorsal head immersion in cold water on nonshivering humans - Giesbrecht G.G., Lockhart T.L., Bristow G.K. and Steinman A.M. [G.G. Giesbrecht, 211 Max Bell Centre, Univ. of Manitoba, Winnipeg, Man. R3T 2N2, Canada] - *J. APPL. PHYSIOL*. 2005 99/5 (1958-1964) - summ in ENGL

Personal floatation devices maintain either a semirecumbent flotation posture with the head and upper chest out of the water or a horizontal flotation posture with the dorsal head and whole body immersed. The contribution of dorsal head and upper chest immersion to core cooling in cold water was isolated when the confounding effect of shivering heat production was inhibited with meperidine (Demerol, 2.5 mg/kg). Six male volunteers were immersed four times for up to 60 min, or until esophageal temperature = 34°C. An insulated hoodless dry suit or two different personal floatation devices were used to create four conditions: 1) body insulated, head out; 2) body insulated, dorsal head immersed; 3) body exposed, head (and upper chest) out; and 4) body exposed, dorsal head (and upper chest) immersed. When the body was insulated, dorsal head immersion did not affect core cooling rate (1.1°C/h) compared with head-out conditions (0.7°C/h). When the body was exposed, however, the rate of core cooling increased by 40% from 3.6°C/h with the head out to 5.0°C/h with the dorsal head and upper chest immersed (P < 0.01). Heat loss from the dorsal head and upper chest was approximately proportional to the extra surface area that was immersed (-10%). The exaggerated core cooling during dorsal head immersion (40% increase) may result from the extra heat loss affecting a smaller thermal core due to intense thermal stimulation of the body and head and resultant peripheral vasoconstriction. Dorsal head and upper chest immersion in cold water increases the rate of core cooling and decreases potential survival time.

See also: 633.

14. ALTITUDE, AVIATION AND SPACE PHYSIOLOGY

590. The feasibility of laryngoscope-guided tracheal intubation in microgravity during parabolic flight: A comparison of two techniques - Groemer G.E., Brimacombe J., Haas T. et al. [J. Brimacombe, Department of Anesthesia and Intensive Care, Cairns Base Hospital, The Esplanade, Cairns, QLD 4870, Australia] - ANESTH. ANALG. 2005 101/5 (1533-1535) - summ in ENGL

We determined the feasibility of laryngoscope-guided tracheal intubation (LG-TI) in microgravity obtained during parabolic flight and tested the hypothesis that LG-TI is similarly successful in the free-floating condition, with the patient's head gripped between the anesthesiologist's knees, as in the restrained condition, with the torso strapped to the surface. Three personnel with no experience in airway management or microgravity participated in the study. LG-TI of a sophisticated full-size manikin was attempted on seven occasions in each condition by each investigator after ground-based

training. The parabolic flights, which took place in an Airbus 300 over the Atlantic Ocean, provided 23 s of microgravity. During this time, the investigator opened a box with airway equipment, performed LG-TI, and attached and held onto a self-inflating bag. The efficacy of ventilation was assessed during level flight by squeezing the bag and noting whether the manikin sensors indicated a tidal volume ≥300 mL. There were no differences in ventilation success (41% versus 33%) or time to successful insertion (both 18s) between the free-floating and the restrained conditions. More than 90% of failures were caused by the inability to insert the tracheal tube within 23 s. There were no differences in performance among investigators. We conclude that LG-TI is feasible in microgravity obtained during parabolic flight, but the success rate is infrequent because of severe time restrictions. There were no differences in success rate between the free-floating condition, with the head gripped between the knees, and the restrained condition, with the torso strapped to the surface. ©2005 by the International Anesthesia Research Society.

591. Nitric oxide and cardiopulmonary hemodynamics in Tibetan highlanders - Hoit B.D., Dalton N.D., Erzurum S.C. et al. [B.D. Hoit, 11100 Euclid Ave., Cleveland, OH 44106-5038, United States] - *J. APPL. PHYSIOL.* 2005 99/5 (1796-1801) - summ in FNGI.

When O2 availability is reduced unavoidably, as it is at high altitude, a potential mechanism to improve O2 delivery to tissues is an increase in blood flow. Nitric oxide (NO) regulates blood vessel diameter and can influence blood flow. This field study of intrapopulation variation at high altitude tested the hypothesis that the level of exhaled NO (a summary measure of pulmonary synthesis, consumption, and transfer from cells in the airway) is directly proportional to pulmonary, and thus systemic, blood flow. Twenty Tibetan male and 37 female healthy, nonsmoking, native residents at 4,200 m (13,900 ft), with an average O₂ saturation of hemoglobin of 85%, participated in the study. The geometric mean partial pressure of NO exhaled at a flow of 17 ml/s was 23.4 nmHg, significantly lower than that of a sea-level reference group. However, the rate of NO transfer out of the airway wall was seven times higher than at sea level, which implied the potential for vasodilation of the pulmonary blood vessels. Mean pulmonary blood flow (measured by cardiac index) was 2.7 ± 0.1 (SE) l/min, and mean pulmonary artery systolic pressure was 31.4 ± 0.9 (SE) mmHg. Higher exhaled NO was associated with higher pulmonary blood flow; yet there was no associated increase in pulmonary artery systolic pressure. The results suggest that NO in the lung may play a key beneficial role in allowing Tibetans at 4,200 m to compensate for ambient hypoxia with higher pulmonary blood flow and O 2 delivery without the consequences of higher pulmonary arterial pressure.

592. Portal vein cross-sectional area and flow and orthostatic tolerance: A **90-day bed rest study** - Arbeille P.P., Besnard S.S., Kerbeci P.P. and Monty D.M. [P.P. Arbeille, Unité Médecine et Physiologie Spatiale, Departement de Médecine Nucléaire et Ultrasons, Centres Hospitaliers Universitaires Trousseau, 37044 Tours, France] - *J. APPL. PHYSIOL.* 2005 99/5 (1853-1857) - summ in ENGL

The objective of this study was to evaluate the changes in the portal vein cross-sectional area (PV CSA) and flow during a stand test associated with orthostatic intolerance. Eighteen subjects underwent a 90-day head-down tilt (HDT) bed rest at 6°: 9 controls (Con) and 9 with flywheel exercise countermeasures (CM). At post-HDT, nine subjects (5 CM, 4 Con) were tolerant, and nine were intolerant. The PV CSA was measured by echography. We found that at HDT day 85, the PV CSA at rest had increased less in the CM subjects than in the Con (+12 vs. +27% from pre-HDT supine; P < 0.05), whereas it increased similarly in tolerant and intolerant subjects (23 and 16%, respectively). Two days after the HDT, there was a decrease in the PV CSA supine compared with the pre-HDT PV CSA supine that was similar for all groups (Con: -11%, CM: -21%; tolerant: -10%, intolerant: -16%; P < 0.05). The PV CSA decreased significantly less from supine to standing in the Con than in the CM group (-2 vs. -10% compared with the pre-HDT stand test; P < 0.05). The PV CSA also decreased significantly from supine to standing compared with the pre-HDT stand test in the tolerant group but not in the intolerant group (-20 vs. +2%; P < 0.05). From these findings, we conclude the following. 1) Because the portal vein is the only output from the splanchnic vascular area, we suggest that the lower reduction in the PV CSA and flow associated with orthostatic intolerance was related to a lower splanchnic arterial vasoconstriction. 2) The flywheel exercise CM helped to reduce the distention of the splanchnic network at rest and to maintain partially the splanchnic vasoconstriction, but it did not reduce the orthostatic intolerance. Copyright © 2005 the American Physiological Society.

15. WORK AND SPORT

593. Suicide in athletes: A review and commentary - Baum A.L. [Dr. A.L. Baum, 5522 Warwick Place, Chevy Chase, MD 20815, United States] - *CLIN. SPORTS MED.* 2005 24/4 SPEC. ISS. (853-869) - summ in ENGL

Not only are athletes at risk for psychiatric illness, but they are at risk of suicide. In an effort to learn more about suicide in athletes and those connected to the sports arena, a review of the medical literature from 1960 to 2000 was conducted through Medline, and a review of the periodical literature from 1980 to 2000 was conducted through Infotrac. These reviews revealed 71 cases of athletes who have either contemplated, attempted, or completed suicide. In this article, these cases are analyzed by sport, gender, and age. Through inference, an attempt to establish the etiologic basis for these behaviors is undertaken. Intervention and prevention strategies are discussed, based on the available data. © 2005 Elsevier Inc. All rights reserved.

594. Multiple sprint work: Physiological responses, mechanisms of fatigue and the influence of aerobic fitness - Glaister M. [Dr. M. Glaister, School of Human Sciences, St. Mary's College, College of the University of Surrey, Waldegrave Road, Strawberry Hill, Twickenham, TW1 4SX, United Kingdom] - *SPORTS MED*. 2005 35/9 (757-777) - summ in ENGL

The activity patterns of many sports (e.g. badminton, basketball, soccer and squash) are intermittent in nature, consisting of repeated bouts of brief (<6-second) maximal/near-maximal work interspersed with relatively short (\le 60-second) moderate/low-intensity recovery periods. Although this is a general description of the complex activity patterns experienced in such events, it currently provides the best means of directly assessing the physiological response to this type of exercise. During a single short (5- to 6-second) sprint, adenosine triphosphate (ATP) is resynthesised predominantly from anaerobic sources (phosphocreatine [PCr] degradation and glycolysis), with a small (< 10%) contribution from aerobic metabolism. During recovery, oxygen uptake (VO2) remains elevated to restore homeostasis via processes such as the replenishment of tissue oxygen stores, the resynthesis of PCr, the metabolism of lactate, and the removal of accumulated intracellular inorganic phosphate (Pi). If recovery periods are relatively short, VO2 remains elevated prior to subsequent sprints and the aerobic contribution to ATP resynthesis increases. However, if the duration of the recovery periods is insufficient to restore the metabolic environment to resting conditions, performance during successive work bouts may be compromised. Although the precise mechanisms of fatigue during multiple sprint work are difficult to elucidate, evidence points to a lack of available PCr and an accumulation of intracellular Pi as the most likely causes. Moreover, the fact that both PCr resynthesis and the removal of accumulated intracellular Pi are oxygen-dependent processes has led several authors to propose a link between aerobic fitness and fatigue during multiple sprint work. However, whilst the theoretical basis for such a relationship is compelling, corroborative research is far from substantive. Despite years of investigation, limitations in analytical techniques combined with methodological differences between studies have left many issues regarding the physiological response to multiple sprint work unresolved. As such, multiple sprint work provides a rich area for future applied sports science research. © 2005 Adis Data Information BV. All rights reserved.

595. Maximum oxygen uptake and objectively measured physical activity in Danish children 6-7 years of age: The Copenhagen school child intervention study - Eiberg S., Hasselstrom H., Grønfeldt V. et al. [Prof. L.B. Andersen, Department of Health, Norwegian University of Sport and Physical Education, Oslo 0806,

Norway] - BR. J. SPORTS MED. 2005 39/10 (725-730) - summ in ENGL

Objectives: To provide normative data on maximum oxygen uptake (VO₂MAX) and physical activity in children 6-7 years of age and analyse the association between these variables. Methods: VO₂MAX was measured in 366 boys (mean (SD) 6.8 (0.4) years of age) and 332 girls (6.7 (0.4) years of age) from preschool classes in two suburban communities in Copenhagen, during a progressive treadmill exercise. Habitual physical activity was measured with accelerometers. Results: Boys had higher VO 2MAX both in absolute values (1.19 (0.18) v 1.06 (0.16) litres/min (+11%), p<0.001) and relative to body weight (48.5 (6.0) v 44.8 (5.6) ml/kg/min (+8%); p<0.001) than girls. The difference in VO 2MAX between boys and girls decreased to +2% when expressed relative to lean body mass (LBM). Absolute VO₂MAX was related to LBM, body mass, and stature (all p<0.001). Boys were more physically active than girls (mean counts +9.4%, p<0.001), and even when boys and girls with the same VO2MAX were compared, boys were more active. The difference in physical activity between the sexes was higher when sustained activity of higher intensity was compared. Conclusions: VO₂MAX is higher in boys than girls (+11%), even when related to body mass (+8%) and LBM (+2%). Most of the difference in VO2MAX relative to body mass was explained by the larger percentage body fat in girls. When boys and girls with the same VO₂MAX were compared, boys engaged in more minutes of exercise of at least moderate intensity.

596. Physique traits of lightweight rowers and their relationship to competitive success - Slater G.J., Rice A.J., Mujika I. et al. [G.J. Slater, Singapore Sports Council, National Stadium, 15 Stadium Road, Singapore 397718, Singapore] - *BR. J. SPORTS MED.* 2005 39/10 (736-741) - summ in ENGL

Objectives: Physique traits and their relationship to competitive success were assessed amongst lightweight rowers competing at the 2003 Australian Rowing Championships. Methods: Full anthropometric profiles were collected from 107 lightweight rowers (n = 65 males, n = 45 females) competing in the Under 23 and Open age categories. Performance assessments were obtained for 66 of these rowers based on results in the single sculls events. The relationship between physique traits and competitive success was then determined. Results: Lower body fat (heat time estimate -8.4 s kg⁻¹, p<0.01), greater total body mass (heat time estimate -4.4 s kg⁻¹, p=0.03), and muscle mass (heat time estimate -10.2 s kg⁻¹, p<0.01) were associated with faster 2000 m heat times. Conclusions: The more successful lightweight rowers were those who had lower body fat and greater total muscle mass.

597. Influence of acute vitamin C and/or carbohydrate ingestion on hormonal, cytokine, and immune responses to prolonged exercise - Davison G. and Gleeson M. [G. Davison, School of Sport and Exercise Sciences, Loughborough University, Leicestershire, LE11 3TU, United Kingdom] - *INT. J. SPORT NUTR. EXER. METABOL.* 2005 15/5 (465-479) - summ in ENGL

The aim of the present study was to investigate the effect of vitamin C with or without carbohydrate consumed acutely in beverages before and during prolonged cycling on immunoendocrine responses. In a single blind, randomized manner six healthy, moderately trained males exercised for 2.5 h at 60% VO 2max and consumed either placebo (PLA), carbohydrate (CHO, 6% w/v), vitamin C (VC, 0.15% w/v) or CHO+VC beverages before and during the bouts; trials were separated by 1 wk. CHO and CHO+VC significantly blunted the post-exercise increase in plasma concentrations of cortisol, ACTH, total leukocyte, and neutrophil counts and limited the decrease in plasma glucose concentration and bacteria-stimulated neutrophil degranulation. VC increased plasma antioxidant capacity (PAC) during exercise (P < 0.05) but had no effect on any of the immunoendocrine responses (P > 0.05). CHO+VC increased PAC compared to CHO but had no greater effects, above those observed with CHO alone, on any of the immunoendocrine responses. In conclusion, acute supplementation with a high dose of VC has little or no effect on the hormonal, interleukin-6, or immune response to prolonged exercise and combined ingestion of VC with CHO provides no additional effects compared with CHO alone. $\ @\ 2005$ Human Kinetics, Inc.

598. Exercise and mononuclear cell DNA damage: The effects of antioxidant supplementation - Davison G.W., Hughes C.M. and Bell R.A. [G.W. Davison, School of Health Sciences, University of Ulster Jordanstown, Newtownabbey, Co. Antrim, BT37 OQB, United Kingdom] - *INT. J. SPORT NUTR. EXER. METABOL.* 2005 15/5 (480-492) - summ in ENGL

The purpose of this investigation was to determine the effects of antioxidant supplementation on DNA damage following exercise. Fourteen subjects were randomly assigned to one of two groups and required to ingest either antioxidants (400 mg α -lipoic acid, 200 mg co-enzyme Q10, 12 mg manganese, 600 mg vitamin C, 800 mg N-acetyl cysteine, 400 μg selenium, and 400 IU α -tocopherol per day) or placebos for 7 d. Exercise increased DNA damage, PS, FRAP, and LDH (P < 0.05), but not selectively between groups. LDH and PS concentration decreased 1 h post-exercise (P < 0.05), while LH concentration decreased 1 h post-exercise in the antioxidant group only (P < 0.05). The antioxidant group had a higher concentration of LH (P < 0.05), perhaps due to a selective difference between groups post-exercise (P < 0.05). The main findings of this investigation demonstrate that exhaustive aerobic exercise induces DNA damage, while antioxidant supplementation does not protect against damage. © 2005 Human Kinetics, Inc.

599. Knowledge, attitudes, and behaviors regarding hydration and fluid replacement of collegiate athletes - Nichols P.E., Jonnalagadda S.S., Rosenbloom C.A. and Trinkaus M. [P.E. Nichols, Athletic Dept., Eagles Landing Christian Academy, McDonough, GA 30253, United States] - *INT. J. SPORT NUTR. EXER. METABOL.* 2005 15/5 (515-527) - summ in ENGL

The purpose of this study was to determine collegiate athletes' knowledge, attitudes, and behaviors concerning hydration and fluid replacement. A survey containing questions pertaining to demographics and knowledge, attitude, and behavior on hydration and fluid replacement was distributed to the athletes during team meetings and practices. A total of 139 out of 171 (81.3%) athletes participated in the study. The mean age of the athletes was 19.8 y. The mean score for knowledge, attitude, and behavior was 13.9 ± 1.8 , 9.8 ± 2.2 , and 12.4 ± 2.5 , respectively, with higher scores indicating positive hydration knowledge, attitudes, and behaviors. Significant positive correlation was observed between knowledge, attitude, and behavior scores (P < 0.05). Significant difference (P< 0.05) was observed in the reported hydration behaviors between skilled (11.79 \pm 2.08) and endurance (12.71 \pm 2.63) athletes. Most athletes correctly answered the general hydration questions on the survey, but the majority did not correctly answer statements in regards to National Athletic Trainers' Association (NATA) and the American College of Sports Medicine (ACSM) position stands and lacked knowledge regarding appropriate use of sports drink. The results of this study identify specific areas of education for athletes with regards to hydration. © 2005, Human Kinetics, Inc.

600. Muscle damage, fluid ingestion, and energy supplementation during recreational alpine skiing - Seifert J.G., Kipp R.W., Amann M. and Gazal O. [J.G. Seifert, Human Performance Laboratory, Saint Cloud State University, Saint Cloud, MN 56301, United States] - *INT. J. SPORT NUTR. EXER. METABOL.* 2005 15/5 (528-536) - summ in ENGL

This study examined energy and fluid supplementation on indices of muscle damage during alpine skiing. Skiers were assigned to a carbohydrate-protein (CP), placebo (PL), or no fluid (NF) group. CP and PL ingested 1.62 L during and after skiing. Myoglobin did not change from pre-skiing (PS) to 2 h post-skiing (2PS) for CP (24.8 \pm 1.4 and 25.6 \pm 1.6 ng/mL), but rose significantly from 26.4 \pm 1.3 to 40.0 \pm 2.8 ng/mL for PL and from 29.0 \pm 1.3 to 82.9 \pm 3.6 ng/mL for NF. Creatine kinase was maintained from PRE to 2 PS for CP, but increased significantly from 117 \pm 7.2 to 174 \pm 43.4 U/L for PL and from 126 \pm 23.2 to 243 \pm 34.3 U/L for NF. This study demonstrates that ingestion of a CP beverage minimized muscle damage indices during skiing compared to PL and NF and that ingesting fluids may also minimize muscle damage compared to a NF condition. © 2005, Human Kinetics, Inc.

601. A comparison of three methods of determination of energy density of elite figure skaters - Ziegler P.J., Nelson J.A., Tay C. et al. [P.J. Ziegler, Gerber Products Co., Parsippany, NJ 07054-0622, United States] - *INT. J. SPORT NUTR. EXER. METABOL.* 2005 15/5 (537-549) - summ in ENGL

Dietary energy density (kcal/g) is defined as available dietary energy per unit weight or volume of food. The consumption of energy-dense foods has been associated with increased obesity risk and with excessive weight gain. The objectives of this study were to compare how dietary energy density, calculated using three different methods relates to food choices and nutrient composition of the diets of elite figure skaters. Participants were 159 elite figure skaters attending training camps. Mean age was 18.4 y for boys (n = 79) and 15.9 y for girls (n = 80). Heights and weights were measured to calculate body-mass indices (BMI). Dietary intakes were based on 3-d food records analyzed using the Nutritionist IV program. Mean energy intakes were 2326 kcal/d for boys and 1545 kcal/d for girls. Dietary energy density, based on foods and caloric beverages only, was 1.0 kcal/g. Dietary ED was positively associated with percent energy from fat and negatively with percent energy from sugar. The main sources of dietary energy in this group were baked goods, cereals, regular soda, low-fat milk, fruit juices, bagels and pizza. Percent energy from fast foods was associated with higher dietary energy density, whereas percent energy from dairy products. soft drinks, vegetables, and fruit was associated with lower dietary energy density. These results are consistent with past observations; higher energy density diets were higher in fat. In contrast, there was a negative relationship between sugar content and energy density of the diet. © 2005, Human Kinetics, Inc.

602. The effect of exercise intensity on the response to exercise rehabilitation in patients with intermittent claudication - Gardner A.W., Montgomery P.S., Flinn W.R. and Katzel L.I. [Dr. A.W. Gardner, CMRI Metabolic Research Center, University of Oklahoma Health Sciences Center, ORI-W 1400, 1122 N.E. 13th Street, Oklahoma City, OK 73117, United States] - *J. VASC. SURG.* 2005 42/4 (702-709) - summ in ENGL

Purpose: The purpose of this randomized trial was to compare the efficacy of a low-intensity exercise rehabilitation program vs a high-intensity program in changing physical function, peripheral circulation, and health-related quality of life in peripheral arterial disease (PAD) patients limited by intermittent claudication. Methods: Thirty-one patients randomized to low-intensity exercise rehabilitation and 33 patients randomized to high-intensity exercise rehabilitation completed the study. The 6-month exercise rehabilitation programs consisted of intermittent treadmill walking to near maximal claudication pain 3 days per week at either 40% (lowintensity group) or 80% (high-intensity group) of maximal exercise capacity. Total work performed in the two training regimens was similar by having the patients in the low-intensity group exercise for a longer duration than patients in the high-intensity group. Measurements of physical function, peripheral circulation, and health-related quality of life were obtained on each patient before and after the rehabilitation programs. Results: After the exercise rehabilitation programs, patients in the two groups had similar improvements in these measures. Initial claudication distance increased by 109% in the low-intensity group (P < .01) and by 109% in the high-intensity group (P < .01), and absolute claudication distance increased by 61% (P < 0.01) and 63% (P < .01) in the low-intensity and highintensity groups, respectively. Furthermore, both exercise programs elicited improvements (P < .05) in peak oxygen uptake, ischemic window, and health-related quality of life. Conclusion: The efficacy of low-intensity exercise rehabilitation is similar to high-intensity rehabilitation in improving markers of functional independence in PAD patients limited by intermittent claudication, provided that a few additional minutes of walking is accomplished to elicit a similar volume of exercise. Copyright © 2005 by The Society for Vascular

603. The jump height in a jump shot does not correlate with results measured on a force platform. A study conducted with the Swiss Junior National Handball team (Germ) - HÖHE BEIM SPRUNGWURF KORRELIERT NICHT MIT TESTWERTEN DER KRAFTMES PLATTE. STUDIE MIT 19 HANDBALLERN DES U 21-NATIONALKADERS - HÜBNER K., Knoll K., Bronst A. and Marti B. J. K. Hübner. Bundesamt

für Sport, Eidgenössische Hochschule für Sport, 2532 Magglingen, Switzerland] - *SCHWEIZ. Z. SPORTMED. SPORTTRAUMATOL.* 2005 53/3 (101-104) - summ in ENGL, GERM

Coaches of team sports are often interested in vertical jump height and strength measurements that simulate performance in a game situation. Even tests to control for the progress of the fitness of the athlete are integrated and conducted during daily trainings, but there is doubt to which extent these types of results carry over into competition performance. Does a sport art specific test that measures vertical jump height supplement the examination of explosive strength of the lower extremity on a force platform and can the vertical jump height in a jump shot be predicted with the use of a nonspecific jump test on a force platform? Nineteen Swiss Junior National Handball team members completed two tests within 7 days. The first test being a standardized jump test, both single and double legged, on a force platform, where mechanical maximal height was measured in accordance to Swiss Olympic guidelines. The second test measured jump height by means of video analysis during a jump shot. There was a surprisingly weak correlation (maximal between 0.2-0.4) between jump height during the jump shot and mechanical jump height measured on the force platform. A number of factors may have influenced these findings. Even though our findings did not validate these two tests as compatible, it can not go without saying that both the standardized jump test on a force platform, which indicates the level of explosive strength of the athletes and can be utilized in training recommendations, and the video analysis, which gives advise on the technique and height of the athletes jump are valuable tools for the athlete and coach.

604. Can field-tests replace the use of force platforms in the measurement of explosive strength? A study conducted with the Swiss Junior National Handball team (Germ) - LASSEN SICH EXPLOSIVKRAFTMESSUNGEN AUF DER KRAFTMESSPLATTE DURCH EINFACHE FELDTESTS ERSETZEN? STUDIE MIT 19 HANDBALLERN DES U 21-NATIONALKADERS - Hübner K., Tschopp M., Buholzer O. and Clénin G.E. [K. Hübner, Bundesamt für Sport, Eidgenössische Hochschule für Sport, 2532 Magglingen, Switzerland] - SCHWEIZ. Z. SPORTMED. SPORTTRAUMATOL. 2005 53/3 (106-109) - summ in ENGL, GERM

In many sports the importance of explosive strength as performance predictor in fast acyclic and cyclic movements has grown. With this growing interest, there is a greater demand from coaches and athletes to use field-tests as a reliable comparison to the measurements of lower extremity explosive strength made in the lab with a force platform, and to use these field test to track individual training improvements and improve training planning. For this reason, the aim of this study was to compare these field-tests with the standard results of the laboratory test. 19 males from the Junior National Handball team completed within 2 days four field-tests (Standing long jump, 5 series long jump, 30-m-Sprint, Jump and Reach) and a vertical jump test on a force platform in the lab. The relationship between Standing long jump, 5 series long jump, 30m-Sprint (using the split times) and the results from the laboratory test were in general significant to highly significant, represented by the correlation coefficient of 0.6 to 0.8. The Jump and Reach test did not correlate with the two-legged vertical jump test on the force platform. The large standard error of estimate concludes that an individual prediction when using only the field-tests is inaccurate. For a general impression of the team's average ability, the use of the standing long jump test, 5 series long jump test, and the 30-m-Sprint splits are applicable. But even for this use the Jump and Reach test is not reliable. For a precise individual assessment of lower extremity explosive strength, and documentation of individual changes, the accuracy of these field-tests is not sufficient, and the use of a force platform is indicated.

605. Coordination training: Individually and specifically (Germ) - KOORDINATIONSTRAINING: INDIVIDUELL UND SPEZIFISCH - Baer C. and Kakebeeke T.H. [C. Baer, Schweizer Paraplegiker-Forschung, 6207 Nottwil, Switzerland] - SCHWEIZ. Z. SPORTMED. SPORTTRAUMATOL. 2005 53/3 (111-113) - summ in FNGL GERM

It is generally known that coordination is essential not only for sports but also for the daily life. A clear and scientifically proven theory for the training of coordination is not available. Coordination

is influenced by several factors. From the theories on coordination it is difficult to deduce generalised rules; it is even more difficult to transfer these rules into practical training. Therefore, trainers are guided by experiences gathered during their education, own practical skills and what they learnt from others. The training of coordination has to be planned individually and must consider the specific demands of the discipline. All people involved have to know the athlete and the needs of the sport very well. Experience and personal know-how play a crucial role. On the basis of examples, we will show the main difficulties of the theories and the dilemmas in transfering the theoretical findings into practical training.

606. Exercise training differentially affects intrinsic excitability of autonomic and neuroendocrine neurons in the hypothalamic paraventricular nucleus - Jackson K., Vieira Silva H.M., Zhang W. et al. [J.E. Stern, Dept. of Psychiatry, University of Cincinnati, 2170 E. Galbraith Rd., Cincinnati, OH 45237, United States] - J. NEUROPHYSIOL. 2005 94/5 (3211-3220) - summ in ENGL

Oxytocinergic and vasopressinergic brain stem projections have been shown to play an important role in mediating cardiovascular adjustments during exercise training (ET). The aim of the present work was to determine whether the intrinsic excitability of hypothalamic neurons giving rise to brain stem peptidergic projections is altered as a consequence of ET. Whole cell patch-clamp recordings were obtained from nucleus of the solitarii tract (NTS)-projecting paraventricular nucleus of the hypothalamus (PVN) neurons and from supraoptic nucleus (SON) and PVN magnocellular cells (MNCs), in hypothalamic slices obtained from sedentary (S) and ET rats. Our results indicate that intrinsic excitability of PVN neurons that innervate the NTS (PVN-NTS) is enhanced by ET, resulting in a more efficient input-output function (increase number of evoked actions potentials, steeper frequency/current relationships and slower decaying frequency/time relationships). Changes in input-output function were accompanied by smaller hyperpolarizing afterpotentials (HAPs) and afterhyperpolarizing potentials (AHPs), during and after trains of spikes, respectively. On the other hand, a decreased efficacy in the input-output function was observed in SON/PVN MNCs during ET. Altogether, our results indicate that ET differentially affects the intrinsic excitability of autonomic and neurosecretory SON and PVN neurons. Increased excitability in PVN-NTS neurons may contribute to enhanced release of OT and VP peptides in the dorsal brain stem, and cardiovascular fine-tuning during exercise training. Copyright © 2005 The American Physiological Society.

607. Dimethylarginine dimethylaminohydrolase and endothelial dysfunction in failing hearts - Chen Y., Li Y., Zhang P. et al. [Y. Chen, Division of Cardiology, Univ. of Minnesota, Mayo Mail Code 508, 420 Delaware St. SE, Minneapolis, MN 55455, United States] - *AM. J. PHYSIOL. HEART CIRC. PHYSIOL.* 2005 289/5 58-5 (H2212-H2219) - summ in ENGL

Congestive heart failure (CHF) is associated with impaired endothelium-dependent nitric oxide (NO)-mediated vasodilation (endothelial dysfunction). We hypothesized that coronary endothelial dysfunction in CHF may be due in part to decreased dimethylarginine dimethylaminohydrolase (DDAH), the enzyme that degrades endogenous inhibitors of NO synthase (NOS), including asymmetric dimethylarginine. Coronary blood flow and the endothelium-dependent vasodilator response to acetylcholine were studied in dogs in which CHF was produced by rapid ventricular pacing for 4 wk. Coronary flow and myocardial O2 consumption at rest and during treadmill exercise were decreased after development of CHF, and the vasodilator response to intracoronary acetylcholine (75 μ g/min) was decreased by 39 \pm 5%. DDAH activity and DDAH isoform 2 (DDAH-2) protein content were decreased by 53 \pm 13% and 58 \pm 14%, respectively, in hearts with CHF, whereas endothelial NOS and DDAH isoform 1 (DDAH-1) were increased. Caveolin-1 and protein arginine N-methyltransferase 1, the enzyme that produces asymmetric dimethylarginine, were unchanged. Immunohistochemical staining showed DDAH-1 strongly expressed in coronary endothelium and smooth muscle and in the sarcolemma of cardiac myocytes. In cultured human endothelial cells, DDAH-1 was uniformly distributed in the cytosol and nucleus, whereas DDAH-2 was found only in the cytosol. Decreased DDAH activity and DDAH-2 protein expression may cause accumulation of endogenous inhibitors of endothelial NOS, thereby contributing to endothelial dysfunction in the failing heart. Copyright © 2005 the American Physiological Society.

608. Changes in basal hypothalamo-pituitary-adrenal activity during exercise training are centrally mediated - Park E., Chan O., Li Q. et al. [M.C. Riddell, Bethune College, Kinesiology and Health Science, York Univ., 4700 Keele St., Toronto, Ont. M3J 1P3, Canada] - AM. J. PHYSIOL. REGUL. INTEGR. COMP. PHYSIOL. 2005 289/5 58-5 (R1360-R1371) - summ in ENGL

The effects of exercise training on hypothalamo-pituitary-adrenal (HPA) function are unclear. We investigated whether pituitaryadrenal adaptation during exercise training is mediated by changes in neuropeptide and corticosteroid receptor gene expression in the brain and pituitary. Sprague-Dawley rats were subject to either daily swimming (DS) or sham exercise (SE) for 45 min/day, 5 days/week, for 2 (2W), 4 (4W), or 6 wk (6W) (n = 7-10/group). Corticosterone (Cort) and catecholamine responses during swimming were robust at 6W compared with 2W and 4W, indicating that HPA response to exercise during training is not attenuated when absolute intensity is progressively increased. In DS, basal (morning) plasma ACTH and Cort levels increased from 2W to 4W but plateaued at 6W, whereas in SE, they increased from 4W to 6W, with 6W values higher than in DS. In DS, there was a transient decrease in glucocorticoid receptor (GR) mRNA in the paraventricular nucleus (PVN) and pituitary and a transient increase in corticotrophin-releasing hormone (CRH) mRNA. In contrast, hippocampal mineralocorticoid receptor mRNA and PVN GR mRNA decreased from 4W to 6W in SE, with 6W values lower than in DS. These findings suggest that exercise training prevents an elevation in basal pituitary-adrenal activity potentially via transient alterations in the gene transcription of PVN and pituitary GR as well as CRH to suppress central drive to the HPA axis. In contrast, the increase in basal pituitary-adrenal activity with repeated sham exercise appears to be associated with decreases in hippocampal MR and PVN GR mRNA expression. Copyright © 2005 the American Physiological Society.

609. Why do arms extract less oxygen than legs during exercise? - Calbet J.A.L., Holmberg H.-C., Rosdahl H. et al. [J.A.L. Calbet, Departamento de Educación Física, Campus Universitario de Tafira, 35017 Las Palmas de Gran Canaria, Spain] - *AM. J. PHYSIOL. REGUL. INTEGR. COMP. PHYSIOL.* 2005 289/5 58-5 (R1448-R1458) - summ in ENGL

To determine whether conditions for O2 utilization and O2 offloading from the hemoglobin are different in exercising arms and legs, six cross-country skiers participated in this study. Femoral and subclavian vein blood flow and gases were determined during skiing on a treadmill at $\sim 76\%$ maximal O_2 uptake (V_{O2max}) and at V_{O2max} with different techniques: diagonal stride (combined arm and leg exercise), double poling (predominantly arm exercise), and leg skiing (predominantly leg exercise). The percentage of O2 extraction was always higher for the legs than for the arms. At maximal exercise (diagonal stride), the corresponding mean values were 93 and 85% (n = 3; P < 0.05). During exercise, mean arm O_2 extraction correlated with the P $_{02}$ value that causes hemoglobin to be 50% saturated (P $_{50}$: r = 0.93, P < 0.05), but for a given value of P_{50} , O_2 extraction was always higher in the legs than in the arms. Mean capillary muscle O₂ conductance of the arm during double poling was 14.5 (SD 2.6) ml min-1 mmHg-1, and mean capillary P O2 was 47.7 (SD 2.6) mmHg. Corresponding values for the legs during maximal exercise were 48.3 (SD 13.0) ml min-1 mmHg -1 and 33.8 (SD 2.6) mmHg, respectively. Because conditions for O₂ offloading from the hemoglobin are similar in leg and arm muscles, the observed differences in maximal arm and leg O_2 extraction should be attributed to other factors, such as a higher heterogeneity in blood flow distribution, shorter mean transit time, smaller diffusing area, and larger diffusing distance, in arms than in legs. Copyright © 2005 the American Physiological Society.

610. Supramaximal exercise mobilizes hematopoietic progenitors and reticulocytes in athletes - Morici G., Zangla D., Santoro A. et al. [M.R. Bonsignore, Institute of Medicine and Pneumology, Univ. of Palermo, c/o Ospedale V. Cervello, Via Trabucco,

180, 90146 Palermo, Italy] - *AM. J. PHYSIOL. REGUL. INTEGR. COMP. PHYSIOL.* 2005 289/5 58-5 (R1496-R1503) - summ in FNGL.

Marathon runners show increased circulating CD34+ cell counts and postexercise release of interleukin-6 (IL-6), granulocyte-colony stimulating factor (G-CSF) and flt3-ligand (Bonsignore MR, Morici G, Santoro A, Pegano M, Cascio L, Bonnano A, Abate P, Mirabella F, Profita M, Insalaco G, Gioia M, Vignola AM, Majolino I, Testa U, and Hogg JC. J Appl Physiol 93: 1691-1697, 2002). In the present study we hypothesized that supramaximal ("all-out") exercise may acutely affect circulating progenitors and reticulocytes and investigated possible mechanisms involved. Progenitor release was measured by flow cytometry (n = 20) and clonogenic assays (n = 6) in 20 young competitive rowers (13 M, 7 F, age \pm SD: 17.1 \pm 2.1 yr, peak O_2 consumption: 56.5 \pm 11.4 ml min $^{-1}$ kg $^{-1}$) at rest and shortly after 1,000 m "all-out." Release of reticulocytes, cortisol, muscle enzymes, neutrophil elastase, and several cytokines/growth factors was measured. Supramaximal exercise doubled circulating CD34+ cells (rest: 7.6 ± 3.0 , all-out: 16.3 ± 9.1 cells/ μ l, P < 0.001), and increased immature reticulocyte fractions: AC133+ cells doubled, suggesting release of angiogenetic precursors. Erythrocyte burst forming units and colony forming units for granulocytes-monocytes and all blood series increased postexercise by 3.4-, 5.5-, and 4.8-fold, respectively (P < 0.01 for all). All-out rowing acutely increased plasma cortisol, neutrophil elastase, flt3ligand, hepatocyte growth factor, VEGF, and transforming growth factor- β 1, and decreased erythropoietin; K-ligand, stromal-derived factor-1, IL-6, and G-CSF were unchanged. Therefore, all-out exercise is a physiological stimulus for progenitor release in athletes. Release of reticulocytes and proangiogenetic cells and mediators suggests tissue hypoxia as possibly involved in progenitor mobilization. Copyright © 2005 the American Physiological Society.

611. Effect of moderate-intensity exercise, whole-body periodic acceleration, and passive cycling on nitric oxide release into circulation - Sackner M.A., Gummels E. and Adams J.A. [Dr. M.A. Sackner, 555 NE 34th St, Miami, FL 33137, United States] - CHEST 2005 128/4 (2794-2803) - summ in ENGL

Study objective: To determine if a 3-min bout of moderately intensive supine bicycle exercise, whole-body periodic acceleration (pGz), and passive motorized cycling cause nitric oxide (NO) release into the circulation, as detected by dicrotic notch descent on the diastolic limb of a finger pulse wave. Participants: Fourteen healthy adults underwent two levels of supine bicycle ergometry that caused heart rate to rise to 56% (light moderate exercise) and 67% (heavy moderate exercise) of maximum predicted heart rate, and a single bout of pGz. Several months later, 9 of the 14 subjects underwent passive motorized cycling. Methods: The ECG and finger pulse wave were recorded. The dicrotic notch position was computed from the amplitude of the digital pulse wave (a) divided by the height of the dicrotic notch above the end-diastolic level (b) and designated the a/b ratio. Increase of the a/b ratio due to dicrotic notch descent reflects the vasodilator action of NO on resistance vessels. The last 30 s of baseline, exercise or pGz, and recovery periods were analyzed. Results: Compared to baseline, light moderate exercise produced a nonsignificant rise of the a/b ratio. Both heavy moderate exercise and pGz produced statistically significant rises of peak and mean a/b ratios over baseline. Heavy moderate exercise produced a greater mean a/b ratio than pGz, but the peak a/b ratio did not differ between the two. Episodic rises and falls of a/b ratios were more common during pGz than exercise. Passive motorized cycling did not alter the a/b ratio. Conclusions: Dicrotic notch descent occurs during a brief bout of moderate cycling exercise, consistent with NO release into circulation. pGz produces comparable descent, but passive motorized cycling does not. In terms of the beneficial effects of NO, this suggests that pGz might serve as a substitute in subjects who are physically incapable of exercising.

612. Impact of the exercise mode on exercise capacity: Bicycle testing revisited - Maeder M., Wolber T., Atefy R. et al. [Dr. M. Maeder, Division of Cardiology, Department of Internal Medicine, Kantonsspital St. Gallen, Rorschacherstrasse 95, CH-9007 St. Gallen, Switzerland] - CHEST 2005 128/4 (2804-2811) - summ in ENICI

Study objective: To test the performance of a tool designed

to estimate functional capacity in order to select a bicycle ramp protocol yielding a test duration from 8 to 12 min in healthy individuals, and to assess differences in exercise responses between bicycle and treadmill tests. Participants and measures: Forty-one healthy and physically active volunteers (10 women; median age, 37 years; interquartile range [IQR], 29.5 to 41 years) performed an individualized ramp exercise protocol on a bicycle ergometer and a treadmill in random order. Prior to testing, the Veterans Specific Activity Questionnaire (VSAQ) combined with a modified variant of the VSAQ nomogram (metabolic equivalents [METs] derived from VSAQ and age with the modified nomogram, resulting in METs nomogram) was used to estimate exercise capacity and to select the treadmill protocol. The corresponding bicycle work capacity nomogram (in watts) was derived by the following equation: (METs nomogram - 1) \times body weight/3.486. Results: Using treadmill tests, all 41 participants (100%) achieved maximal exercise from 8 to 12 min, as compared to 33 participants (80%) for the bicycle tests (p = 0.003). Peak oxygen uptake ($\dot{V}O_2$) [bicycle: median, 49.7 mL/kg/min (IQR, 45.4 to 56.6 mL/kg/min); vs treadmill: median, 53.1 mL/kg/min (IQR, 47.3 to 57.7 mL/kg/min; p < 0.0001)] was lower using the bicycle compared to the treadmill. However, the difference in peak VO₂ values between the two exercise modes was lower (2.6 mL/kg/min; IQR, 1.1 to 4.3 mL/kg/min), corresponding to 4.6% (IQR, 2.4 to 8.5%) of the lower of both values than reported in previous studies, and seven participants (17%) even achieved a higher peak VO2 using the bicycle. Conclusions: A modified version of the VSAQ can be effectively used to select appropriate ramp rates for exercise testing using a bicycle ergometer in healthy individuals. Differences in maximal responses are less than those previously reported, suggesting that the bicycle ergometer is an appropriate alternative to the treadmill test in healthy volunteers.

613. Class I_A phosphoinositide 3-kinase regulates heart size and physiological cardiac hypertrophy - Luo J., McMullen J.R., Sobkiw C.L. et al. [L.C. Cantley, Division of Signal Transduction, Beth Israel Deaconess Medical Center, 77 Avenue Louis Pasteur, Boston, MA 02115, United States] - *MOL. CELL. BIOL.* 2005 25/21 (9491-9502) - summ in ENGL

Class I_A phosphoinositide 3-kinases (PI3Ks) are activated by growth factor receptors, and they regulate, among other processes, cell growth and organ size. Studies using transgenic mice overexpressing constitutively active and dominant negative forms of the p110 α catalytic subnnit of class I_A PI3K have implicated the role of this enzyme in regulating heart size and physiological cardiac hypertrophy. To further understand the role of class I_A PDK in controlling heart growth and to circumvent potential complications from the overespression of dominant negative and constitutively active proteins, we generated mice with muscle-specific deletion of the p85 α regulatory subunit and germ line deletion of the p85 β regulatory subunit of class I_A PDK. Here we show that mice with cardiac deletion of both p85 subunits exhibit attenuated Akt signaling in the heart, reduced heart size, and altered cardiac gene expression. Furthermore, exercise-induced cardiac hypertrophy is also attenuated in the p85 knockout hearts. Despite such defects in postnatal developmental growth and physiological hypertrophy, the p85 knockout hearts exhibit normal contractility and myocardial histology. Our results therefore provide strong genetic evidence that class I_A PI3Ks are critical regulators for the developmental growth and physiological hypertrophy of the heart. Copyright © 2005, American Society for Microbiology. All Rights Reserved.

614. Substrate oxidation during exercise at moderate and hard intensity in middle-aged and young athletes vs sedentary men
- Manetta J., Brun J.-F., Prefaut C. and Mercier J. [J.-F. Brun, Service Central de Physiologie Clinique, Centre d'Exploration et de Réadaptation des Anomalies Métaboliques et Musculaires, 34295
Montpellier Cedex 5, France] - METAB. CLIN. EXP. 2005 54/11
(1411-1419) - summ in ENGL

This study investigated the combined effects of endurance training and aging on substrate oxidation during exercise. Thirty-one healthy male subjects in 4 groups (8 middle-aged trained cyclists, 8 young trained cyclists, 7 middle-aged sedentary men, and 8 young sedentary men) performed 2 50-minute cycle ergometer exercise tests, below and above ($\pm 15\%$) their individual ventilatory thresh-

old (VT). Substrate oxidation was evaluated by indirect calorimetry during the steady-state tests. Aging decreased carbohydrate (CHO)use (P < .05) in all subjects regardless of fitness status or exercise intensity. However, it declined 2-fold less in the trained men (P < .05) and was associated with a stronger epinephrine response (P < .05). During hard-intensity exercise, endurance training increased by 100% CHO use in the older men (P < .05). In the younger men, training increased fat oxidation but did not change CHO oxidation, resulting in a marked decrease in the ratio between CHO and fat used at high-intensity exercise (-93%; P < .05). These data suggest an age-related decline in the use of CHO as an energy source in exercising men, independent of intensity level. This decline, however, is attenuated in well-trained men for exercise intensities above the VT. In view of these findings, we hypothesize that cycling training performed at a specific exercise intensity (ie, 15% above VT) may improve CHO mobilization and use in middle-aged men. © 2005 Elsevier Inc. All rights reserved.

615. The effect of nutritional manipulation on ultra-endurance performance: A case study - Robins A.L., Davies D.M. and Jones G.E. [A.L. Robins, Community, Health Sciences and Social Care, University of Salford, Allerton Building, Frederick Road, Salford M6 6PU, United Kingdom] - *RES. SPORTS MED.* 2005 13/3 (199-215) - summ in FNGL.

The Atlantic Rowing Race requires teams of two to cover 3,000 nautical miles over 40-90 days. During this ultra-endurance event, competitors require substantial energy intake to meet metabolic requirements; therefore, sufficient physiological and nutritional support is paramount. Two highly trained males (aged 46) engaged in two 14d dietary interventions, with a 14d recovery period in between, to investigate the effect of such interventions on physiological (cardiovascular, cardiorespiratory, and blood-based measures) and performance-based (distance and split time) parameters during an ultra-endurance (2h on 2h off, for 24h)laboratory-based rowing protocol at 60% VO _{2max}. Diet 1: high fat (HF) [60% fat, 30% carbohydrate and 10% protein] and Diet 2: high carbohydrate (HC) [20%, 70% and 10% respectively]. A greater distance was rowed by both subjects (155, 329m and 134, 797m vs 130, 089m and 122, 112m) with a concomitant reduced heart rate, volume of oxygen uptake, and respiratory exchange ratio, following the HF as opposed to HC dietary intervention. In summary, ultra-endurance performance was enhanced following a 14d HF diet, without apparent implications on liver function and overall lipid profile. Copyright © Taylor & Francis Inc.

616. Resting pulmonary ventilation in sports scuba divers -Muth T., Gams E. and Schipke J.D. [Dr. J.D. Schipke, Zentrum für Operative Medizin I, Forschungsgruppe Experimentelle Chirurgie, Universitätsklinikum Düsseldorf, Moorenstr. 5, D-40225, Düsseldorf, United States] - *RES. SPORTS MED.* 2005 13/3 (257-272) -summ in ENGL

It should be investigated whether the traditional dependency between respiratory and systemic measures is preserved during scuba diving, and whether the diving experience would affect respiration. Additionally, respiration data were analyzed for gender differences (118 sports divers). Respiratory variables were assessed at poolside and during diving in the pool. The respiration pattern at poolside was significantly different from the pattern during diving, where respiration rate (RR) decreased (11.8 \pm 3.8 vs. 7.8 \pm 2.9 min ⁻¹; -34%) and tidal volume increased (1.1 ± 0.5 vs. 1.6 ± 0.6L; +45%). This produced a decrease in respiratory minute volume (RMV)from 12.4 ± 4.7 to 11.2 ± 3.8 L/min (-10%). Respiratory Minute Volume and vital capacity correlated at poolside. This physiologic correlation was lost while diving. Instead, RMV and number of dives (=diver's experience) correlated negatively. Because RMV at both poolside and during diving correlates with RR, an increased RMV in diving beginners can be estimated via RR. Thus, close observation of RR could help improve safety during a regular dive, avoiding hazardous hyperventilation. Female divers, irrespective of body height and weight, need less air during diving. Copyright © Taylor & Francis Inc.

617. Liquid chromatographic screening test for some diuretics of doping interest in human urine - Moreira V. and Moreau R.L.M. [R.L.M. Moreau, College of Pharmaceutical Sciences, Laboratory

of Analytical Toxicology, University of São Paulo, Av. Prof. Lineu Prestes, 580, CEP 05508-900, Brazil] - *J. LIQ. CHROMATOGR. RELAT. TECHNOL.* 2005 28/17 (2753-2768) - summ in ENGL

Despite being considered ergolytic drugs, diuretics have been included on the lists of prohibited substances of the International Olympic Committee since 1986 due to their capacity of masking doping agents in urine. As diuretics are also prone to be misused regarding weight categories, screening procedures to check their presence in urine, whenever doping control is involved, are mandatory. A simple screening method using liquid-liquid extraction was validated for the compounds: acetazolamide, amiloride, bumetanide, chlorthalidone, clopamide, furosemide, hydrochlorothiazide, piretamide, spironolactone, and triamterene. samples were extracted in both acidic and basic media. analyses were performed with a Spherisorb ODS column and diode array UV detector, set at 260, 270, and 360 nm wavelengths. A gradient mobile phase was used. Limits of detection varied from 0.09 to $0.75 \mu g/mL$. Recoveries ranged from 55.26 to 94.82%. Inter and intra-assay precision tests showed good values. Copyright © Taylor & Francis, Inc.

618. NaHCO₃-induced alkalosis reduces the phosphocreatine slow component during heavy-intensity forearm exercise Forbes S.C., Raymer G.H., Kowalchuk J.M. and Marsh G.D. [G.D. Marsh, School of Kinesiology, Univ. of Western Ontario, London, Ont., Canada] - *J. APPL. PHYSIOL*. 2005 99/5 (1668-1675) - summ in FNGI.

During heavy-intensity exercise, the mechanisms responsible for the continued slow decline in phosphocreatine concentration ([PCr]-) (PCr slow component) have not been established. In this study, we tested the hypothesis that a reduced intracellular acidosis would result in a greater oxidative flux and, consequently, a reduced magnitude of the PCr slow component. Subjects (n = 10) performed isotonic wrist flexion in a control trial and in an induced alkalosis (Alk) trial (0.3g/kg oral dose of NaHCO₃, 90 min before testing). Wrist flexion, at a contraction rate of 0.5 Hz, was performed for 9 min at moderate-(75% of onset of acidosis; intracellular pH threshold) and heavy-intensity (125% intracellular pH threshold) exercise. ³¹P- magnetic resonance spectroscopy was used to measure intracellular [H +], [PCr], [Pi], and [ATP]. The initial recovery data were used to estimate the rate of ATP synthesis and oxidative flux at the end of heavy-intensity exercise. In repeated trials, venous blood sampling was used to measure plasma [H+], [HCO₃], and [Lac $\dot{}$]. Throughout rest and exercise, plasma [H+] was lower (P < 0.05) and [HCO $_3$] was elevated (P < 0.05) in Alk compared with control. During the final 3 min of heavy-intensity exercise, Alk caused a lower (P < 0.05) intracellular [H+] [246 (SD 117) vs. 291 nmol/l (SD 129)], a greater (P < 0.05) [PCr] [12.7 (SD 7.0) vs. 9.9 mmol/l (SD 6.0)], and a reduced accumulation of [ADP] [0.065 (SD 0.031) vs. 0.098 mmol/l (SD 0.059)]. Oxidative flux was similar (P > 0.05) in the conditions at the end of heavy-intensity exercise. In conclusion, our results are consistent with a reduced intracellular acidosis, causing a decrease in the magnitude of the PCr slow component. The decreased PCr slow component in Alk did not appear to be due to an elevated oxidative flux. Copyright © 2005 the American Physiological Society.

619. Leg crossing, muscle tensing, squatting, and the crash position are effective against vasovagal reactions solely through increases in cardiac output - Krediet C.T.P., De Bruin I.G.J.M., Ganzeboom K.S. et al. [C.T.P. Krediet, Academic Medical Center, Univ. of Amsterdam, Dept. of Internal Medicine, Meibergdreef 9, 1105AZ, Amsterdam, Netherlands] - *J. APPL. PHYSIOL.* 2005 99/5 (1697-1703) - summ in ENGL

Tensing of lower body muscles without or with leg crossing (L-BMT, LCMT), whole body tensing (WBT), squatting, and sitting with the head bent between the knees ("crash position," HBK) are believed to abort vasovagal reactions. The underlying mechanisms are unknown. To study these interventions in patients with a clinical history of vasovagal syncope and a vasovagal reaction during routine tilt table testing, we measured blood pressure (BP) continuously with Finapres and derived heart rate, stroke volume, cardiac output (CO), and total peripheral resistance using Modelflow. In series A (n = 12) we compared LBMT to LCMT. In series B (n = 9), WBT was compared with LCMT. In series C (n = 14) and D (n = 9), we

tested squatting and HBK. All maneuvers caused an increase in BP, varying from a systolic rise from 77 ± 8 to 104 ± 18 mmHg (P <0.05) in series A during LBMT to a rise from 70 ± 10 to 123 ± 9 mmHg (P <0.05) in series B during LCMT. In each maneuver, the BP increase started within 3-5 s from start of the maneuver. In all maneuvers, there was an increase in CO varying from $54\pm 12\%$ of baseline to $94\pm 21\%$ in WBT to a rise from $65\pm 17\%$ to $110\pm 22\%$ in LCMT in series A. No maneuver caused significant change in total peripheral resistance. We conclude that the mechanism underlying the effects of these maneuvers is exclusively an increase in CO. Copyright © 2005 the American Physiological Society.

620. Effects of moderate-velocity strength training on peak muscle power and movement velocity: Do women respond differently than men? - Delmonico M.J., Kostek M.C., Doldo N.A. et al. [B.F. Hurley, Dept. of Kinesiology, Univ. of Maryland, College Park, MD 20742, United States] - *J. APPL. PHYSIOL.* 2005 99/5 (1712-1718) - summ in ENGL

The effects of a 10-wk unilateral knee extension strength training (ST) program on peak power (PP) and peak movement velocity (PV), at given absolute (force load) and relative (same % of 1 repetition maximum) resistances (loads), were examined in 30 older men [64 yr (7 SD)] and 32 older women [62 yr (6 SD)], PP increased significantly in both men and women at the same absolute (P < 0.001) and relative loads (P < 0.01) with ST. Men had a significantly greater increase in relative PP than women with ST at 60% (P < 0.01) and 70% (P < 0.001) of 1 repetition maximum when covarying for baseline differences and age. However, when each subject was tested at the same absolute load and when PP was normalized for the muscle volume of the trained knee extensors (i.e., absolute muscle power quality), women increased by 9% (P < 0.05), whereas men did not change. Both men and women increased their absolute PV (P <0.001) but decreased their relative PV significantly with ST (P <0.05). However, when baseline values and age were covaried, women had significantly less of a decrease in relative PV quality with ST than men (P < 0.01), although the difference was small. These normalized data suggest that ST-induced increases in PP depend on muscular hypertrophy in men, but not in women, providing further support for the hypothesis developed from our previous report (Ivey FM, Tracy BL, Lemmer JT, NessAiver M, Metter EJ, Fozard JL and Hurley BF. J Gerontol A Biol Sci Med Sci 55: B152-B157, 2000) that improvements in muscle function with ST result from nonmuscle mass adaptations to a greater extent in women than men.

621. Arg16/Gly β_2 -adrenergic receptor polymorphism alters the cardiac output response to isometric exercise - Eisenach J.H., Barnes S.A., Pike T.L. et al. [J.H. Eisenach, Dept. of Anesthesiology, Mayo Clinic, 200 First St. SW, Rochester, MN 55905, United States] - *J. APPL. PHYSIOL*. 2005 99/5 (1776-1781) - summ in ENGI

Normotensive adults homozygous for glycine (Gly) of the Arg16/Gly β_2 -adrenergic-receptor polymorphism have 1) greater forearm β_2 -receptor mediated vasodilation and 2) a higher heart rate (HR) response to isometric handgrip than arginine (Arg) homozygotes. To test the hypothesis that the higher HR response in Gly16 subjects serves to maintain the pressor response [increased cardiac output (CO)] in the setting of augmented peripheral vasodilation to endogenous catecholamines, we measured continuous HR (ECG), arterial pressure (Finapres), and CO (transthoracic echocardiography) during isometric, 40% submaximal handgrip to fatigue in healthy subjects homozygous for Gly (n = 30; mean age \pm SE: 30 ± 1.2 , 13 women) and Arg (n = 17, age 30 ± 1.6 , 11 women)-Resting data were similar between groups. Handgrip produced similar increases in arterial pressure and venous norepinephrine and epinephrine concentrations; however, HR increased more in the Gly group (60.1 \pm 4.3% increase from baseline vs. 45.5 \pm 3.9%, P = 0.03), and this caused CO to be higher (Gly: 7.6 ± 0.3 l/m vs. Arg: 6.5 ± 0.3 l/m, P = 0.03), whereas the decrease in systemic vascular resistance in the Gly group did not reach significance (P = 0.09). We conclude that Gly16 homozygotes generate a higher CO to maintain the pressor response to handgrip. The influence of polymorphic variants in the $\hat{\beta}_2$ - adrenergic receptor gene on the cardiovascular response to sympathoexcitation may have important implications in the development of hypertension and heart failure. Copyright © 2005 the American Physiological Society.

622. Nonthermoregulatory control of cutaneous vascular conductance and sweating during recovery from dynamic exercise in women - Journeay W.S., Reardon F.D., McInnis N.H. and Kenny G.P. [G.P. Kenny, University of Ottawa, School of Human Kinetics, Montpetit Hall, PO Box 450 Station A, Ottawa, Ont. K1N 6N5, Canada] - *J. APPL. PHYSIOL.* 2005 99/5 (1816-1821) - summ in ENGL

The purpose of the study was to examine the effect of 1) active (loadless pedaling), 2) passive (assisted pedaling), and 3) inactive (motionless) recovery modes on mean arterial pressure (MAP), cutaneous vascular conductance (CVC), and sweat rate during recovery after 15 min of dynamic exercise in women. It was hypothesized that an active recovery mode would be most effective in attenuating the fall in MAP, CVC, and sweating during exercise recovery. Ten female subjects performed 15 min of cycle ergometer exercise at 70% of their predetermined peak oxygen consumption followed by 20 min of 1) active, 2) passive, or 3) inactive recovery. Mean skin temperature (T_{sk}), esophageal temperature (T_{es}), skin blood flow, sweating, cardiac output (CO), stroke volume (SV), heart rate (HR), total peripheral resistance (TPR), and MAP were recorded at baseline, end exercise, and 2, 5, 8, 12, 15, and 20 min postexercise. Cutaneous vascular conductance (CVC) was calculated as the ratio of laser-Doppler blood flow to MAP. In the active recovery mode, CVC, sweat rate, MAP, CO, and SV remained elevated over inactive values (P < 0.05). The passive mode was equally as effective as the active mode in maintaining MAP. Sweat rate was different among all modes after 12 min of recovery (P < 0.05). TPR during active recovery remained significantly lower than during recovery in the inactive mode (P < 0.05). No differences in either T_{es} or T_{sk} were observed among conditions. The results indicate that CVC can be modulated by central command and possibly cardiopulmonary baroreceptors in women. However, differences in sweat rate may be influenced by factors such as central command, mechanoreceptor stimulation, or cardiopulmonary baroreceptors. Copyright © 2005 the American Physiological Society.

623. Kinetics of O₂ uptake, leg blood flow, and muscle deoxygenation are slowed in the upper compared with lower region of the moderate-intensity exercise domain - MacPhee S.L., Shoemaker J.K., Paterson D.H. and Kowalchuk J.M. [J.M. Kowalchuk, Canadian Centre for Activity and Aging, School of Kinesiology, Univ. of Western Ontario, London, Ont. N6A 3K7, Canada] - J. APPL. PHYSIOL. 2005 99/5 (1822-1834) - summ in ENGL

Six male subjects [23 yr (SD 4)] performed repetitions (6-8) of two-legged, moderate-intensity, knee-extension exercise during two separate protocols that included step transitions from 3 W to 90% estimated lactate threshold (θ_L) performed as a single step (S3) and in two equal steps (S1, 3 W to \sim 45% θ_L ; S2, \sim 45% θ_L to \sim 90% $\theta_{\rm L}$). The time constants (τ) of pulmonary oxygen uptake ($\dot{\rm V}{\rm O}_2$), leg blood flow (LBF), heart rate (HR), and muscle deoxygenation (HHb) were greater (P < 0.05) in S2 ($\tau\dot{V}O_2$, \sim 52 s; τLBF , \sim 39 s; τ HR, \sim 42 s; τ HHb, \sim 33 s) compared with S1 ($\tau\dot{V}O_2$, \sim 24 s; τ LBF, \sim 21 s; τ HR, \sim 21 s; τ HHb, \sim 16 s), while the delay before an increase in HHb was reduced (P < 0.05) in S2 (\sim 14 s) compared with S1 (\sim 20 s). The VO₂ and HHb amplitudes were greater (P < 0.05) in S2 compared with S1, whereas the LBF amplitude was similar in S2 and S1. Thus the slowed $\dot{V}O_2$ response in S2 compared with S1 is consistent with a mechanism whereby VO2 kinetics is limited, in part, by a slowed adaptation of blood flow and/or O2 transport when exercise was initiated from a baseline of moderateintensity exercise. Copyright © 2005 the American Physiological Society.

624. Prolonged muscle vibration increases stretch reflex amplitude, motor unit discharge rate, and force fluctuations in a hand muscle - Shinohara M., Moritz C.T., Pascoe M.A. and Enoka R.M. [M. Shinohara, 354 UCB, Dept. of Integrative Physiology, Univ. of Colorado, Boulder, CO 80309-0354, United States] - *J. APPL. PHYSIOL.* 2005 99/5 (1835-1842) - summ in ENGL

The purpose of this study was to compare the influence of prolonged vibration of a hand muscle on the amplitude of the stretch

reflex, motor unit discharge rate, and force fluctuations during steady, submaximal contractions. Thirty-two young adults performed 10 isometric contractions at a constant force (5.0 \pm 2.3% of maximal force) with the first dorsal interosseus muscle. Each contraction was held steady for 10 s, and then stretch reflexes were evoked. Subsequently, 20 subjects had vibration applied to the relaxed muscle for 30 min, and 12 subjects received no vibration. The muscle vibration induced a tonic vibration reflex. The intervention (vibration or no vibration) was followed by 2 sets of 10 constantforce contractions with applied stretches (After and Recovery trials). The mean electromyogram amplitude of the short-latency component of the stretch reflex increased by 33% during the After trials (P < 0.01) and by 38% during the Recovery trials (P < 0.01). The standard deviation of force during the steady contractions increased by 21% during the After trials (P<0.05) and by 28% during the Recovery trials (P<0.01). The discharge rate of motor units increased from 10.3 \pm 2.7 pulses/s (pps) before vibration to 12.2 \pm 3.1 pps (P < 0.01) during the After trials and to 11.9 \pm 2.6 pps during the Recovery trials (P < 0.01). There was no change in force fluctuations or stretch reflex magnitude for the subjects in the Control group. The results indicate that prolonged vibration increased the short-latency component of the stretch reflex, the discharge rate of motor units, and the fluctuations in force during contractions by a hand muscle. These adjustments were necessary to achieve the target force due to the vibration-induced decrease in the force capacity of the muscle. Copyright © 2005 the American Physiological Society.

625. Impact of glutamine supplementation on glucose homeostasis during and after exercise - Iwashita S., Williams P., Jabbour K. et al. [P.J. Flakoll, Food Science and Human Nutrition, 1127 Human Nutritional Sciences Bldg., Iowa State Univ., Ames, IA 50011, United States] - *J. APPL. PHYSIOL*. 2005 99/5 (1858-1865) - summ in ENGL

The interaction of glutamine availability and glucose homeostasis during and after exercise was investigated, measuring whole body glucose kinetics with [3-3H]glucose and net organ balances of glucose and amino acids (AA) during basal, exercise, and postexercise hyperinsulinemic-euglycemic clamp periods in six multicatheterized dogs. Dogs were studied twice in random treatment order: once with glutamine (12 μ mol kg ⁻¹ min⁻¹; Gln) and once with saline (Con) infused intravenously during and after exercise. Plasma glucose fell by 7 mg/dl with exercise in Con(P < 0.05), but it did not fall with Gln. Gln further stimulated whole body glucose production and utilization an additional 24% above a normal exercise response (P < 0.05). Net hepatic uptake of glutamine and alanine was greater with Gln than Con during exercise (P < 0.05). Net hepatic glucose output was increased sevenfold during exercise with Gln (P < 0.05) but not with Con. Net hindlimb glucose uptake was increased similarly during exercise in both groups (P < 0.05). During the postexercise hyperinsulinemic-euglycemic period, glucose production decreased to near zero with Con, but it did not decrease below basal levels with Gln. Gln increased glucose utilization by 16% compared with Con after exercise (P < 0.05). Furthermore, net hindlimb glucose uptake in the postexercise period was increased approximately twofold vs. basal with Gln (P < 0.05) but not with Con. Net hepatic uptake of glutamine during the postexercise period was threefold greater for Gln than Con (P < 0.05). In conclusion, glutamine availability modulates glucose homeostasis during and after exercise, which may have implications for postexercise recovery. Copyright © 2005 the American Physiological Society.

626. Exercise hyperemia and vasoconstrictor responses in humans with cystic fibrosis - Schrage W.G., Wilkins B.W., Dean V.L. et al. [W.G. Schrage, Dept. of Anesthesiology, Mayo Clinic, Joseph 4-184W, Rochester, MN 55905, United States] - *J. APPL. PHYSIOL.* 2005 99/5 (1866-1871) - summ in ENGL

ATP released from circulating erythrocytes is a potential signal regulating muscle blood flow during exercise (exercise hyperemia), and intravascular ATP appears to blunt sympathetic vasoconstriction during exercise. Erythrocytes from patients with cystic fibrosis (CF) do not release ATP. The goal of the present study was to determine whether increases in forearm blood flow during exercise are blunted in CF patients and whether CF patients exhibit greater vasoconstrictor responsiveness during exercise. Nine control subjects

and 10 CF patients who were free of other disease complications (~96% O₂ saturation) performed incremental rhythmic forearm exercise at 5, 10, and 15% of maximum handgrip strength for 21 min (7 min at each workload). We used a cold pressor test to evoke sympathetic vasoconstriction under resting conditions and at each exercise workload. As a control, subjects performed a second exercise bout without the cold pressor test. Continuous brachial artery blood velocity was monitored beat-to-beat, and vessel diameter was assessed by Doppler ultrasound. Artery diameter, as well as blood pressure, heart rate, and O 2 saturation, was measured at steadystate exercise and at 1 min into the cold pressor stimulus. Blood pressure and heart rate responses to the forearm exercise and each cold pressor test were similar in both groups (P > 0.05). Contrary to our hypothesis, forearm blood flow (P = 0.91) and forearm vascular conductance (P = 0.82) were similar at rest and at each level of exercise between CF patients and controls. Additionally, there was no difference in the degree of sympathetic vasoconstriction between groups at rest and at each level of exercise (P = 0.22). Our results suggest that ATP released from the deformation of erythrocytes is not an obligatory signal for exercise hyperemia in human skeletal muscle. Copyright © 2005 the American Physiological Society.

627. Lower capillarization, VEGF protein, and VEGF mRNA response to acute exercise in the vastus lateralis muscle of aged vs. young women - Croley A.N., Zwetsloot K.A., Westerkamp L.M. et al. [T.P. Gavin, 363 Ward Sports Medicine Bldg., East Carolina Univ., Greenville, NC 27858, United States] - *J. APPL. PHYSIOL.* 2005 99/5 (1872-1879) - summ in ENGL

In humans, the majority of studies demonstrate an age-associated reduction in the number of capillaries surrounding skeletal muscle fibers; however, recent reports in rats suggest that muscle capillarization is well maintained with advanced age. In sedentary and trained men, aging lowers the number of capillaries surrounding type II, but not type I, skeletal muscle fibers. The fiber type-specific effect of aging on muscle capillarization is unknown in women. Vascular endothelial growth factor (VEGF) is important in the basal maintenance of skeletal muscle capillarization, and lower VEGF expression is associated with increased age in nonskeletal muscle tissue of women. Compared with young women (YW), we hypothesized that aged women (AW) would demonstrate 1) lower muscle capillarization in a fiber type-specific manner and 2) lower VEGF and VEGF receptor expression at rest and in response to acute exercise. Nine sedentary AW (70 + 8 yr) and 11 YW (22 + 3 yr) had vastus lateralis muscle biopsies obtained before and at 4 h after a submaximal exercise bout for the measurement of morphometry and VEGF and VEGF receptor expression. In AW compared with YW, muscle capillary contacts were lower overall (YW: 2.36 + 0.32 capillaries; AW: 2.08 + 0.17 capillaries), specifically in type II (YW: 2.37 + 0.39 capillaries; AW: 1.91 + 0.36 capillaries) but not type I fibers (YW: 2.36 + 0.34 capillaries; AW: 2.26 + 0.24 capillaries). Muscle VEGF protein was 35% lower at rest, and the exerciseinduced increase in VEGF mRNA was 50% lower in AW compared with YW. There was no effect of age on VEGF receptor expression. These results provide evidence that, in the vastus lateralis of women, 1) capillarization surrounding type II muscle fibers is lower in AW compared with YW and 2) resting VEGF protein and the VEGF mRNA response to exercise are lower in AW compared with YW. Copyright © 2005 the American Physiological Society.

628. Training with unilateral resistance exercise increases contralateral strength - Munn J., Herbert R.D., Hancock M.J. and Gandevia S.C. [J. Munn, School of Physiotherapy, Univ. of Sydney, PO Box 170, Lidcombe, NSW 1825, Australia] - *J. APPL. PHYSIOL.* 2005 99/5 (1880-1884) - summ in ENGL

Evidence that unilateral training increases contralateral strength is inconsistent, possibly because existing studies have design limitations such as lack of control groups, lack of randomization, and insufficient statistical power. This study sought to determine whether unilateral resistance training increases contralateral strength. Subjects (n = 115) were randomly assigned to a control group or one of the following four training groups that performed supervised elbow flexion contractions: 1) one set at high speed, 2) one set at low speed, 3) three sets at high speed, or 4) three sets at low speed. Training was 3 times/wk for 6 wk with a six- to eight-repetition maximum load. Control subjects attended sessions but

did not exercise. Elbow flexor strength was measured with a one-repetition maximum arm curl before and after training. Training with one set at slow speed did not produce an increase in contralateral strength (mean effect of -1% or -0.07 kg; 95% confidence interval: -0.42-0.28 kg; P=0.68). However, three sets increased strength of the untrained arm by a mean of 7% of initial strength (additional mean effect of 0.41 kg; 95% confidence interval: 0.06-0.75 kg; P=0.022). There was a tendency for training with fast contractions to produce a greater increase in contralateral strength than slow training (additional mean effect of 5% or 0.31 kg; 95% confidence interval: -0.03-0.66 kg; P=0.08), but there was no interaction between the number of sets and training speed. We conclude that three sets of unilateral resistance exercise produce small contralateral increases in strength. Copyright © 2005 the American Physiological Society.

629. NADPH oxidase p22phox gene variants are associated with systemic oxidative stress biomarker responses to exercise training - Park J.-Y., Ferrel R.E., Park J.-J. et al. [M.D. Brown, Dept. of Kinesiology, Univ. of Maryland, College Park, MD 20742-2611, United States] - *J. APPL. PHYSIOL*. 2005 99/5 (1905-1911) - summ in FNGI.

Systemic oxidative stress plays a role in many degenerative diseases. Although regular physical activity has been known as the most effective nonpharmacological intervention to alleviate the oxidative stress, the beneficial effect varies between individuals. We investigated whether NADPH oxidase p22phox gene C242T and A640G polymorphisms are associated with systemic oxidative stress level response to exercise training (ExTr). Fifty-nine sedentary middle-aged to older Caucasians with relatively high cardiovascular disease risk factors underwent a 6-mo standardized ExTr program. Body mass index, plasma lipoprotein-lipid profiles, cardiovascular fitness, and plasma thiobarbituric acid reactive substances (TBARS) were measured before and after ExTr. Demographic and initial levels of cardiovascular disease risk factors were similar among genotype groups for both polymorphisms. Overall, TBARS was decreased by 16% with ExTr in the entire group (P < 0.001). There was no significant difference in TBARS changes with ExTr among the C242T genotype groups. However, A allele carriers showed greater reduction in TBARS than noncarriers at the A640G locus (P = 0.05). There was a significant interaction (P = 0.05). 0.05) between ExTr and A640G polymorphism in TBARS changes with ExTr. This interaction remained after accounting for age and baseline TBARS level. Furthermore, diplotype analysis showed that TBARS was decreased to a greater extent in the C242/A640 haplotype carriers compared with the noncarriers (P < 0.05). We found that p22phox polymorphisms, especially A640G, were associated with differential changes in systemic oxidative stress with aerobic exercise training. Copyright © 2005 the American Physiological

630. Exercise flow-volume loops in prepubescent aerobically trained children - Nourry C., Deruelle F., Fabre C. et al. [C. Nourry, UFR des STAPS de Liévin, Laboratoire d'Analyse Multidisciplinaire des Pratiques et Sportives, Chemin du Marquage, 62800 Liévin, France] - *J. APPL. PHYSIOL.* 2005 99/5 (1912-1921) - summ in ENGL

We studied mechanical ventilatory constraints in 13 aerobically trained (Tr) and 11 untrained (UT) prepubescent children by plotting the exercise flow-volume (F-V) loops within the maximal F-V loop (MFVL) measured at rest. The MFVL allowed to determine forced vital capacity (FVC) and maximal expiratory flows. Expiratory and inspiratory reserve volumes relative to FVC (ERV/FVC and IRV/FVC, respectively) were measured during a progressive exercise test until exhaustion. Breathing reserve (BR) and expiratory flow limitation (expFL), expressed in percentage of tidal volume (VT) and defined as the part of the tidal breath meeting the boundary of the MFVL, were measured. Higher FVC and maximal expiratory flows were found in Tr than UT (P < 0.05) at rest. Our results have shown that during exercise, excepting one subject, all Tr regulated their VT within FVC similarly during exercise, by breathing at low lung volume at the beginning of exercise followed breathing at high lung volume at strenuous exercise. In UT, ERV/FVC and IRV/FVC were regulated during exercise in many ways. The proportion of children who presented an expFL was nearly the same in both groups (\sim 70% with a range of 14 to 65% of VT), and no significant difference was found during exercise concerning expFL. However, higher ventilation (VE), ERV/FVC, and dyspnea associated with lower BR, IRV/FVC, and Sa $_{02}$ were reported at peak power in Tr than UT (P < 0.05). These results suggest that, because of their higher VE level, trained children presented higher ventilatory constraints than untrained. These may influence negatively the Sa $_{02}$ level and dyspnea during strenuous exercise. Copyright © 2005 the American Physiological Society.

631. Signs of muscle thixotropy during human ballistic wrist joint movements - Axelson H.W. [H.W. Axelson, Clinical Neurophysiology, Dept. of Neuroscience, Uppsala Univ. Hospital, S-751 85 Uppsala, Sweden] - *J. APPL. PHYSIOL*. 2005 99/5 (1922-1929) - summ in ENGL

A study was conducted on healthy subjects to determine whether voluntary ballistic wrist flexion movements are influenced by immediately preceding conditioning of the forearm muscles. Single rapid wrist flexion movements were made in response to an auditory "Go" signal. Rectified surface EMG was recorded from wrist flexors and extensors, and joint position was measured by a goniometer. The movements were preceded (2-3 s) by four different conditioning routines: 40-s rest (Rest), 10-s voluntary alternating wrist joint flexion and extension movements (Osc), and 10 s of 25° weak isometric wrist extensor (Ext) or flexor contractions (Flex). When subjects made ballistic movements after Osc compared with Rest. peak velocity was higher (P = 0.02) and movement time shorter (P = 0.02)0.06), but there was no difference (P = 0.83) in motor reaction time (time between the onset of the first agonist burst and movement onset). If the movements were preceded by Ext compared with Flex, motor reaction time was longer (P = 0.01), indicating a longer electromechanical delay. There were no indications that postconditioning differences in agonist or antagonist muscle activity could explain the results. It was also demonstrated that, after Rest, peak velocity was lower (P < 0.01) for the first than for the second of a series of repetitive ballistic movements. The observations corresponded to results from passive experiments in which the median nerve was electrically stimulated. In conclusion, history-dependent (thixotropic) changes in skeletal muscle resistance seem to have implications for voluntary ballistic wrist movements. The study also provided evidence that muscle conditioning influences the central nervous reaction time preceding ballistic contractions. Copyright © 2005 the American Physiological Society.

632. No effect of short-term testosterone manipulation on exercise substrate metabolism in men - Braun B., Gerson L., Hagobian T. et al. [B. Braun, Dept. of Exercise Science, 106 Totman Bldg., Univ. of Massachusetts, Amherst, MA 01003, United States] - *J. APPL. PHYSIOL.* 2005 99/5 (1930-1937) - summ in ENGL

Compared with women, men use proportionately more carbohydrate and less fat during exercise at the same relative intensity. Estrogen and progesterone have potent effects on substrate use during exercise in women, but the role of testosterone (T) in mediating substrate use is unknown. The purpose of this investigation was to assess how large variations in the concentration of blood T would impact substrate use during exercise in men. Nine healthy, active men were studied in three distinct hormonal conditions: physiological T (no intervention), low T (pharmacological suppression of endogenous T with a gonadotrophin-releasing hormone antagonist), and high T (supplementation with transdermal T). Total carbohydrate oxidation, blood glucose rate of disappearance, and estimated muscle glycogen use were assessed by using stable isotope dilution and indirect calorimetry at rest and while bicycling at $\sim 60\%$ of peak O₂ consumption for 90 min. Relative to the physiological condition $(T = 5.5 \pm 0.5 \text{ ng/ml})$, total plasma T was considerably suppressed in low T (0.8 \pm 0.1) and elevated in high T (10.9 \pm 1.1). Despite the large changes in plasma T, carbohydrate oxidation, glucose rate of disappearance, and estimated muscle glycogen use were very similar across the three conditions. There were also no differences in plasma concentrations of glucose, insulin, lactate, or free fatty acids. Plasma estradiol (E) concentrations were elevated in high T. but correlations between substrate use and plasma concentrations of T, E, or the T-to-E ratio were very weak ($r^2 < 0.20$). In conclusion, unlike the effect of acute elevation in E to constrain carbohydrate

use in women, acute changes in circulating T concentrations do not appear to alter substrate use during exercise in men. Copyright @ 2005 the American Physiological Society.

633. Hypohydration impairs endurance exercise performance in temperate but not cold air - Cheuvront S.N., Carter III R., Castellani J.W. and Sawka M.N. [S.N. Cheuvront, US Army Research Institute of Environmental Medicine, Thermal and Mountain Medicine Division, Kansas St., Natick, MA 01760-5007, United States] - *J. APPL. PHYSIOL.* 2005 99/5 (1972-1976) - summ in ENGL

This study compared the effects of hypohydration (HYP) on endurance exercise performance in temperate and cold air environments. On four occasions, six men and two women (age = $24 \pm$ 6 yr, height = 170 \pm 6 cm, weight = 72.9 \pm 11.1 kg, peak O₂ consumption = 48 \pm 9 ml \cdot kg⁻¹ \cdot min⁻¹) were exposed to 3 h of passive heat stress (45°C) in the early morning with [euhydration (EÜH)] or without (HYP; 3% body mass) fluid replacement. Later in the day, subjects sat in a cold (2°C) or temperate (20°C) environment with minimal clothing for 1 h before performing 30 min of cycle ergometry at 50% peak O_2 consumption followed immediately by a 30-min performance time trial. Rectal and mean skin temperatures, heart rate, and ratings of percieved exertion measurements were made at regular intervals. Performance was assessed by the total amount of work (kJ) completed in the 30-min time trial. Skin temperature was significantly lower in the cold compared with the temperate trial, but there was no independent effect of hydration. Rectal temperature in both HYP trials was higher than EUH after 60 min of exercise. but the difference was only significant within the temperate trials (P < 0.05). Heart rate was significantly higher at 30 min within the temperate trial (HYP > EUH) and at 60 min within the cold trial (HYP > EUH) (P < 0.05). Ratings of percieved exertion increased over time with no differences among trials. Total work performed during the 30-min time trial was not influenced by environment but was less (P < 0.05) for HYP than EUH in the temperate trials. The corresponding change in performance (EUH - HYP) was greater for temperate (-8%) than for cold (-3%) (P < 0.05). These data demonstrate that 1) HYP impairs endurance exercise performance in temperate but not cold air but 2) cold stress per se does not.

634. An open-circuit method for determining lung diffusing capacity during exercise: Comparison to rebreathe - Snyder E.M., Johnson B.D. and Beck K.C. [B.D. Johnson, Division of Cardiovascular Disease, Gonda 5-369, Mayo Clinic and Foundation, 200 1st St. SW, Rochester, MN 55905, United States] - *J. APPL. PHYSIOL.* 2005 99/5 (1985-1991) - summ in ENGL

To avoid limitations associated with the use of single-breath and rebreathe methods for assessing the lung diffusing capacity for carbon monoxide (DL CO) during exercise, we developed an open-circuit technique. This method does not require rebreathing or alterations in breathing pattern and can be performed with little cognition on the part of the patient. To determine how this technique compared with the traditional rebreathe (DL_{CO,RB}) method, we performed both the open-circuit (DL_{CO,OC}) and the DL _{CO,RB} methods at rest and during exercise (25, 50, and 75% of peak work) in 11 healthy subjects [mean age = 34 yr (SD 11)]. Both DL_{CO,OC} and DL_{CO,RB} increased linearly with cardiac output and external There was a good correlation between DL_{CO,OC} and DLCO,RB for rest and exercise (mean of individual $r^2 = 0.88$, overall $r^2 = 0.69$, slope = 0.97). $DL_{CO,OC}$ and $DL_{CO,RB}$ were similar at rest and during exercise [e.g., rest = 27.2 (SD 5.8) vs. 29.3 (SD 5.2), and 75% peak work = 44.0 (SD 7.0) vs. 41.2 ml min ⁻¹ mmHg⁻¹ (SD 6.7) for DL_{CO,OC} vs. DL_{CO,RB}]. The coefficient of variation for repeat measurements of DL_{CO,OC} was 7.9% at rest and averaged 3.9% during exercise. These data suggest that the DL_{CO,OC} method is a reproducible, well-tolerated alternative for determining DL_{CO}, particularly during exercise. The method is linearly associated with cardiac output, suggesting increased alveolar-capillary recruitment, and values were similar to the traditional rebreathe method. Copyright © 2005 the American Physiological Society.

635. Effects of creatine supplementation on aerobic power and cardiovascular structure and function - Murphy A.J., Watsford M.L., Coutts A.J. and Richards D.A.B. [A.J. Murphy, Human Performance Laboratory, University of Technology, Sydney, NSW,

Australia] - *J. SCI. MED. SPORT* 2005 8/3 (305-313) - summ in ENGL

This project aimed to determine 1) whether creatine (Cr) supplementation affects cardiovascular structure and function and 2) to examine its effect on aerobic power. Eighteen males undertook aerobic testing on a cycle ergometer and echocardiographic assessment of the heart. The experimental group (N=9) ingested 20g day-1 of Cr for seven days followed by 10g day-1 for a further 21 days. The control group (N=9) followed an identical protocol ingesting a placebo for the same period. Assessment was performed pre-, mid- (seven days) and post-testing (28 days). A MANOVA with repeated measures was used to test for group differences before and after supplementation. The Cr group demonstrated a significant increase in body mass for the pre-mid (1.0±0.6 kg) and the prepost (1.5±0.7 kg) testing occasions. Submaximal VO2 decreased significantly from the pre-mid and pre-post testing occasions by between 4.8% to 11.4% with Cr supplementation at workloads of 75 W and 150 W. Other oxygen consumption measures and exercise time to exhaustion, for the Cr group, showed decreasing trends that approached significance. Additionally, there was a significant pre-post decrease in maximum heart rate of 3.7%. There were no changes in any of the echocardiographic or blood pressure measures for either group. The present results suggest short term Cr supplementation has no detectable negative effect on cardiac structure or function. Additionally, Cr ingestion improves submaximal cycling efficiency. These results suggest that the increase in efficiency may be related to peripheral factors such an increase in muscle phosphocreatine, rather than central changes.

636. The detraining and retraining of an elite rower: A case study - Godfrey R.J., Ingham S.A., Pedlar C.R. and Whyte G.P. [R.J. Godfrey, Brunel University, Uxbridge, Middlesex, United Kingdom] - *J. SCI. MED. SPORT* 2005 8/3 (314-320) - summ in FNGI

A heavyweight male rower, and current Olympic champion, undertook a laboratory-based incremental rowing test on four separate occasions; eight weeks prior to the Sydney Olympics (Pre OG), after eight weeks of inactivity (Post-IA), after 8 weeks of retraining (Post 8) and after a further 12 weeks of training (Post 20). Following the period of inactivity, peak oxygen uptake (VO2peak) declined by 8%, power at reference blood lactate concentrations declined by approximately 100 W (25%), and power at VO 2 peak was 20% lower. With eight weeks of retraining, rapid improvements were seen. For most parameters, however, the rate of improvement slowed and after 20 weeks of retraining the individual was approaching pre-Olympic levels. VO₂ at lactate threshold as a percentage of VO₂peak remained unchanged. These results show that detraining in the elite athlete can be pronounced, with rapid improvements upon retraining which slow, so that retraining takes considerably longer to achieve than detraining did. Complete cessation of training should be limited to short periods only in the preparation of the elite heavyweight rower. Any break should, if possible, include 'maintenance training'. In this way any decrements in those physiological parameters associated with 2000 m rowing performance will be minimised.

637. Fitness testing and career progression in AFL football - Pyne D.B., Gardner A.S., Sheehan K. and Hopkins W.G. [D.B. Pyne, Department of Physiology, Australian Institute of Sport, Canberra, ACT, Australia] - *J. SCI. MED. SPORT* 2005 8/3 (321-332) - summ in ENGL

Relationships between fitness testing and career progression in the Australian Football League (AFL) are under-explored. This study investigated relationships between anthropometric and fitness tests conducted at the annual AFL National Draft Camp and subsequent career progression of players. A total of 283 players was tested over three consecutive camps (1999-2001). The anthropometric and fitness measures were: height, mass, sum of skinfolds, 20-m sprint test, vertical jump (standing and bilateral running), agility run and a multi-stage incremental shuttle run. The five outcome variables were: drafted (yes/no), AFL debut (yes/no), number of AFL games played to the end of 2003, and subjective ratings of career potential and career value (5-point scale). Of 205 players (72%) subsequently drafted, 166 (59%) eventually made their AFL

debut. Players drafted to AFL clubs were faster over 5m, 10m and 20 m, ran further in the shuttle run and ran marginally faster in the agility test than players not drafted. Multi-regression analysis showed small to moderate correlations (r=0.27-0.31) between the designated outcome variables and selected fitness tests: 20-m sprint time (faster), agility run test (faster), and running vertical jump (higher absolute height and smaller difference between left and ride sides). Regression analysis for the standing vertical jump relative to standing reach height showed a counterintuitive negative correlation with positive outcomes, possibly reflecting non-compliance with testing procedures by the less successful athletes. We conclude that the 20-m sprint, jump, agility and shuttle run tests have a small but important association with career progression of AFL footballers.

638. Physiological and anthropometric characteristics of starters and non-starters and playing positions in elite Australian Rules football: A case study - Young W.B., Newton R.U., Doyle T.L.A. et al. - *J. SCI. MED. SPORT* 2005 8/3 (333-345) - summ in ENGI.

A purpose of this study was to determine if pre-season anthropometric and physiological measures were significantly different for the players from one Australian Football League (AFL) club selected to play in the first game of the season compared to the players not selected. Another purpose was to compare fitness test results for defenders, forwards and mid-fielders in the same AFL club. Thirty-four players were tested for isolated quadriceps and hamstrings strength, leg extensor muscle strength and power, upper body strength, sprinting speed, vertical jump (VJ), endurance, skinfolds and hamstring flexibility. The starters who were selected to play the first game were a significantly older and more experienced playing group, and were significantly better (p<0.05) in measures of leg power, sprinting speed and the distance covered in the Yo Yo intermittent recovery test compared to the non-starters. Although there were trends for the superiority of the starters, the differences in lower and upper body strength, VJ and predicted VO₂max were non-significant. The forwards generally produced the worst fitness scores of the playing positions with the midfielders having significantly lower skinfolds and the defenders possessing better hamstring strength and VJ compared to the forwards. It was concluded that some fitness qualities can differentiate between starters and non-starters, at least in one AFL club. Comparisons of playing positions and the development of fitness norms for AFL players require further research.

639. Development of a psychometrically valid and reliable sports nutrition knowledge questionnaire - Zinn C., Schofield G. and Wall C. [C. Zinn, Massey University, Auckland, New Zealand] - *J. SCI. MED. SPORT* 2005 8/3 (346-351) - summ in ENGL

The present range of sports nutrition knowledge questionnaires have inadequate psychometric validation, and few are up to date in a rapidly changing discipline. The purpose of this study was to design a sports nutrition questionnaire that satisfied acceptable psychometric criteria of validity (content and construct) and reliability (test-retest). The questionnaire was designed by an expert panel of six sports dietitians and distributed to five groups, selected for their expected variation in sports nutrition knowledge. Dietitians, university business staff and nutrition students received questionnaires via e-mail. The response rates obtained were 21.3% (n=49), 34.4% (n=33), and 72.0% (n=18), respectively. University business and fitness students completed questionnaires during class time. Response rates were 52.3% (n=23) and 75.4% (n=49), respectively. The questionnaire was administered a second time to the business staff and the dietitians to assess test-retest reliability. Two methods were used: 1, Pearson's product-moment correlation; and 2, a percentage calculation of questions answered in an identical manner on both test occasions. Reliability was acceptable with Method 1 yielding acceptable values (r=0.74-0.93), aside from the fluid subcategory (r=0.52). Method 2 showed good test-retest concordance with 81.2% duplication of responses of all questions. Construct validity was high, as indicated by significant mean knowledge score differences between the groups (p=0.0001). Dietitians and nutrition students achieved significantly greater mean scores than the remaining groups. The findings of this study indicate that the questionnaire is suitably valid and reliable to be used in research and practice to determine sports nutrition knowledge.

640. Do squash players accurately report use of appropriate protective eyewear? - Eime R., Finch C., Owen N. and McCarty C. [C. Finch, NSW Injury Risk Management Research Centre, University of New South Wales, Kensington, NSW, Australia] - *J. SCI. MED. SPORT* 2005 8/3 (352-356) - summ in ENGL

Self-report surveys are a common method of collecting data on protective equipment use in sport. The aim of this study was to assess the validity of self-reported use of appropriate protective eyewear by squash players. Surveys of squash players' appropriate protective evewear behaviours were conducted over two consecutive years (2002 and 2003) at randomly-selected squash venues in Melbourne, Australia. Over the two years, 1219 adult players were surveyed (response rate of 92%). Trained observers also recorded the actual on-court appropriate protective eyewear behaviours of all players during the survey sessions. Eyewear use rates calculated from both data sources were compared. The self-reported appropriate protective eyewear use rate (9.4%; 95% CI 7.8, 11.0) was significantly higher (1.6 times more) than the observed rate (5.9%; 95% CI 4.6, 7.2). This suggests that players may over-report their use of appropriate protective equipment, though some may have incorrectly classified their eyewear as being appropriate or suitably protective. Studies that rely only on self-report data on protective equipment use need to take into account that this could lead to biased estimates

SUBJECT INDEX

(figures refer to item numbers)

- acetazolamide, amiloride, bumetanide, chlortalidone, clopamide, diuretic agent, doping, high performance liquid chromatography, 617
- **acetylcholine**, Aplysia, motoneuron, neuromodulation, temperature sensitivity, 422
 - avoidance behavior, cholinergic system, enzyme inhibition, memory, mitogen activated protein kinase, signal transduction, 350
- acetylsalicylic acid 3 (nitroxymethyl)phenyl ester, celecoxib, cyclooxygenase 2 inhibitor, hypertension, nonsteroid antiinflammatory agent, 546
- actin, CD2 associated protein, docking protein, green fluorescent protein, podocyte, 549
 - diacetyl oxime, muscle force, muscle stiffness, muscle stretching, 467
- acute heart infarction, clusterin, 497
- adaptation, auditory nervous system, nerve cell plasticity, 410 adenosine A1 receptor agonist, 2 chloro 6 n
 - cyclopentyladenosine, delta opiate receptor agonist, heart infarction, inducible nitric oxide synthase, nitric oxide, 503
- adenosine diphosphate ribosyl cyclase, angiotensin, calcium signaling, reactive oxygen metabolite, vascular smooth muscle, 540
- adenosine triphosphatase (potassium sodium), aorta, endothelium derived relaxing factor, sodium calcium exchange, 570
 - cyclic AMP dependent protein kinase, kidney collecting tubule, sodium channel, sodium transport, 542
- adenosine triphosphate, aging, creatine kinase, creatine phosphate, high energy phosphate, muscle metabolism, phosphate metabolism, skeletal muscle, 466
- cystic fibrosis, exercise, hyperemia, vasoconstriction, 626
 adenylate cyclase, blood vessel tone, diabetes mellitus, diabetic angiopathy, 501
- adrenergic activity, alpha 1A adrenergic receptor, alpha 1 adrenergic receptor, artery, messenger RNA, receptor subtype, 480
- adrenergic receptor, adrenergic system, alpha 1 adrenergic receptor, heat shock protein 72, stress, 380
- adrenergic system, adrenergic receptor, alpha 1 adrenergic receptor, heat shock protein 72, stress, 380
- melanocortin 4 receptor, messenger RNA, nucleotide sequence, protein expression, white adipose tissue, 426
- **adrenomedullin,** nerve cell, oxytocin, oxytocin blood level, oxytocin release, 358
- **aerobic capacity,** cardiovascular function, creatinine, diet supplementation, 635
 - shorebird, succinate dehydrogenase, 579
- aerobic metabolism, exercise, 630
- aggressiveness, fear, maternal behavior, newborn care, 428 aging, adenosine triphosphate, creatine kinase, creatine phosphate,
- high energy phosphate, muscle metabolism, phosphate metabolism, skeletal muscle, 466
- androgen, androgen receptor, cardiovascular disease, chronic kidney disease, endothelin, hormone action, testosterone, 534
- body weight, heart rate variability, systolic blood pressure, 477
- capillary density, exercise, messenger RNA, vasculotropin, vasculotropin receptor, vastus lateralis muscle, 627
- diffusion weighted imaging, helium, lung structure, 521
- exercise, oxidation, 614
- hand movement, muscle strength, 418
- muscle strength, muscle training, sex difference, 473 **alkalosis,** arm exercise, bicarbonate, 618
- alpha 1A adrenergic receptor, adrenergic activity, alpha 1 adrenergic receptor, artery, messenger RNA, receptor subtype, 480
- alpha 1 adrenergic receptor, adrenergic activity, alpha 1A adrenergic receptor, artery, messenger RNA, receptor subtype, 480

- adrenergic receptor, adrenergic system, heat shock protein 72, stress, 380
- amiloride, acetazolamide, bumetanide, chlortalidone, clopamide, diuretic agent, doping, high performance liquid chromatography, 617
- **amino acid,** brain, carbohydrate, carbohydrate intake, exercise,
- 4 aminobutyric acid, brain maturation, chloride, chloride transport, GABAergic transmission, spinal nerve, 408
 - GABAergic system, interneuron, spinal cord nerve cell, 359
- 4 aminobutyric acid A receptor, brain development, vestibular nucleus, 389
- 4 aminobutyric acid A receptor stimulating agent, arterial pressure, muscimol, pressor response, solitary tract nucleus, 507
- electroencephalography, muscimol, somatosensory cortex, 402
- 4 aminobutyric acid receptor stimulating agent, muscimol, periaqueductal gray matter, sympathetic blocking, sympathetic innervation, 406
- aminopeptidase, cell compartmentalization, insulin response, 566 amino terminal sequence, heart muscle, muscle force, myosin light chain, 459
- **ammonia**, carrier protein, glycoprotein, rhesus antigen, 324 **amygdaloid nucleus**, arousal, autonomic nervous system, fear, 376
 - auditory cortex, crying, hemispheric dominance, insula, nonverbal communication, 444
 - brain injury, fear, 442
- facilitation, fear, learning, synaptic transmission, 437
- flavor, learning, taste preference, 436
- gene function, genetic variability, tryptophan hydroxylase, 357
 androgen, aging, androgen receptor, cardiovascular disease, chronic kidney disease, endothelin, hormone action, testosterone, 534
- androgen receptor, aging, androgen, cardiovascular disease, chronic kidney disease, endothelin, hormone action, testosterone, 534
- angiotensin, adenosine diphosphate ribosyl cyclase, calcium signaling, reactive oxygen metabolite, vascular smooth muscle. 540
- ankle, brain, limb movement, sensorimotor function, 343 annexin, kidney, lipocortin 1, lipocortin 2, lipocortin 4, lipocortin 5, 535
- **anterior hypothalamus,** exercise, nerve cell excitability, 606 **anthropometry,** football, physiology, 638
- antioxidant, cell DNA, diet supplementation, DNA damage, exercise, mononuclear cell, 598
- anxiety, circadian rhythm, light exposure, memory, 429aorta, adenosine triphosphatase (potassium sodium), endothelium derived relaxing factor, sodium calcium exchange, 570
- Aplysia, acetylcholine, motoneuron, neuromodulation, temperature sensitivity, 422
- apoptosis, granzyme B, 322
 - heart infarction, heart muscle cell, 494
- **aquaporin 2,** hypertension, kidney collecting tubule, sodium channel, 536
- arachidonic acid, blood pressure, 20 hydroxyicosatetraenoic acid, icosanoid, kidney function, nitric oxide, n(g) nitroarginine methyl ester, pregnancy, 557
 - B lymphocyte, calcium signaling, diacylglycerol, 5 hydroperoxy 6,8,11,14 icosatetraenoic acid, 20 hydroxyicosatetraenoic acid, inflammation, inositol 1,4,5 trisphosphate, phospholipase C, 326
- **arginine**, beta 2 adrenergic receptor, genetic polymorphism, glycine, heart output, isometric exercise, 621
- aristolochic acid, phenanthrene derivative, plant extract, 551 arm exercise, alkalosis, bicarbonate, 618
- hemoglobin, leg exercise, oxygen, oxygen consumption, 609 **arousal**, amygdaloid nucleus, autonomic nervous system, fear, 376 **arterial pressure**, 4 aminobutyric acid A receptor stimulating

agent, muscimol, pressor response, solitary tract nucleus,

artery, adrenergic activity, alpha 1A adrenergic receptor, alpha 1 adrenergic receptor, messenger RNA, receptor subtype,

ascorbic acid, carbohydrate, carbohydrate intake, cytokine, exercise, immune response, vitamin intake, 597

assisted ventilation, helmet, 519

asthma, carbon dioxide, chemical analysis, ovalbumin, oxygen, protein analysis, 527

expiratory flow, smooth muscle, 529

atherosclerosis, collagen, elastin, percutaneous transluminal angioplasty, 500

athlete, attitude, fluid therapy, hydration, 599

- blood pressure regulation, computer prediction, hemodynamic monitoring, 512
- caloric intake, sport, 601
- CD34 antigen, exercise, Flt3 ligand, granulocyte colony stimulating factor, hematopoietic stem cell, interleukin 6, reticulocyte, 610
- coordination, training, 605
- eye protective device, self report, 640

- sport, training, 636 atrial natriuretic factor, atrial natriuretic factor receptor, calcineurin, cariporide, hypertension, sodium proton exchange protein 1, 475

- coronary blood vessel, endothelium cell, glycocalyx, 486 atrial natriuretic factor receptor, atrial natriuretic factor, calcineurin, cariporide, hypertension, sodium proton exchange protein 1, 475

attention, auditory discrimination, working memory, 337

- depth perception, genetic polymorphism, nicotinic receptor,
- lateral geniculate nucleus, motor performance, 416
- rotation, touch, vestibular system, visual orientation, 412 transcranial magnetic stimulation, vision, visual adaptation,

attitude, athlete, fluid therapy, hydration, 599

auditory cortex, amygdaloid nucleus, crying, hemispheric dominance, insula, nonverbal communication, 444

- auditory stimulation, sensory stimulation, tactile stimulation,
- depression, 405
- hearing impairment, sign language, visual cortex, 411
- somatosensory cortex, 386
- visual system, 383

auditory discrimination, attention, working memory, 337

spatial orientation, tactile discrimination, 356

auditory memory, music, musician, 447

auditory nervous system, adaptation, nerve cell plasticity, 410 auditory stimulation, auditory cortex, sensory stimulation, tactile stimulation, 349

- hemispheric dominance, right hemisphere, 392
- inferior colliculus, stereotypy, stimulus response, 403

auditory system, memory, vision, 397

autonomic nervous system, amygdaloid nucleus, arousal, fear, 376

autonomic nervous system function, cholinergic receptor, heart automaticity, receptor sensitivity, sympathetic tone, 485 aversion, fear, heart rate, 431

avoidance behavior, acetylcholine, cholinergic system, enzyme inhibition, memory, mitogen activated protein kinase, signal transduction, 350

bacterium lipopolysaccharide, thermoregulation, 582 ballistics, joint function, thixotropy, wrist, 631

beta 2 adrenergic receptor, arginine, genetic polymorphism, glycine, heart output, isometric exercise, 621

bicarbonate, alkalosis, arm exercise, 618

binaltorphimine, kappa opiate receptor, kappa opiate receptor antagonist, kidney function, sodium urine level, 553

binding protein, cyclic AMP dependent protein kinase, kidney collecting tubule, SNARE protein, sodium channel, water absorption, 537

biological marker, evoked brain stem auditory response, hearing, speech analysis, speech perception, 441

blood brain barrier, cell membrane permeability, endothelium cell, hypoxia, protein kinase C, 488

blood pressure, arachidonic acid, 20 hydroxyicosatetraenoic acid, icosanoid, kidney function, nitric oxide, n(g) nitroarginine methyl ester, pregnancy, 557

pulse wave, 476

blood pressure regulation, athlete, computer prediction, hemodynamic monitoring, 512

- heart rate variability, pressoreceptor reflex, 483
- hydrogen peroxide, vasomotor reflex, 478

portal vein blood flow, 592

blood vessel tone, adenylate cyclase, diabetes mellitus, diabetic angiopathy, 501

blood viscosity, hypotension, shear stress, vascular resistance, 492 blood volume, carbon monoxide, diagnostic error, erythropoietin, oxygen, 513

B lymphocyte, arachidonic acid, calcium signaling, diacylglycerol, 5 hydroperoxy 6,8,11,14 icosatetraenoic acid. 20 hydroxyicosatetraenoic acid. inflammation. inositol 1,4,5 trisphosphate, phospholipase C, 326

- B lymphocyte receptor, transient receptor potential channel,

B lymphocyte receptor, B lymphocyte, transient receptor potential channel, 334

body growth, dietary intake, exploratory behavior, 384 body image, spatial orientation, tactile discrimination, 355 body movement, tactile discrimination, visual orientation, 351 body position, hip, walking, 423

body posture, perceptive discrimination, proprioception, touch, 353

body size, clutch size, 560

- heart function, 489

body weight, aging, heart rate variability, systolic blood pressure,

brain, amino acid, carbohydrate, carbohydrate intake, exercise, 373

- ankle, limb movement, sensorimotor function, 343

brain blood flow, Doppler echography, 505

brain computer interface, 420

brain cortex, brain function, hippocampus, theta rhythm, 366

- hand function, magnetoencephalography, median nerve, 385
- mesencephalon, sensory cortex, 395
- thalamus, 342

brain development, 4 aminobutyric acid A receptor, vestibular nucleus, 389

brain function, brain cortex, hippocampus, theta rhythm, 366 brain injury, amygdaloid nucleus, fear, 442 brain maturation, 4 aminobutyric acid, chloride, chloride

transport, GABAergic transmission, spinal nerve, 408 brain metabolism, glutamate transporter, superior colliculus,

visual stimulation, 565 brain natriuretic peptide, kidney function, protein analysis, 556 brain vasospasm, 20 hydroxyicosatetraenoic acid, subarachnoid

hemorrhage, 498 breast epithelium, gene expression, gene product, protein protein interaction, 587

breath holding, lung volume, multidetector computed tomography, 520

breathing muscle, forced expiratory volume, lung flow volume curve, muscle stretching, 523

- inspiratory reserve volume, locomotion, lung pressure, 528
- periaqueductal gray matter, respiration control, 515

breathing rate, extensor digitorum longus muscle, mitochondrial respiration, muscle cell, soleus muscle, 464

bumetanide, acetazolamide, amiloride, chlortalidone, clopamide, diuretic agent, doping, high performance liquid chromatography, 617

calcineurin, atrial natriuretic factor, atrial natriuretic factor receptor, cariporide, hypertension, sodium proton exchange protein 1, 475

- calcitonin gene related peptide receptor, fetus circulation, nitric oxide, 479
- calcitriol, fibroblast growth factor 23, phosphate, phosphate metabolism, vitamin D metabolism, vitamin D receptor, 563
- calcium, calcium cell level, calcium transport, heart muscle cell, sarcoplasmic reticulum, 474
 - calcium transport, morphine, opiate receptor, 332
 - crypt cell, membrane transport, potassium, potassium transport, 328
 - diastole, heart muscle contractile force, heart ventricle, sodium, sodium calcium exchange, 510
- calcium activated potassium channel, heme oxygenase 2,
 oxygen sensing, voltage gated potassium channel, 413
 progesterone, smooth muscle contractility, 531
- calcium cell level, calcium, calcium transport, heart muscle cell, sarcoplasmic reticulum, 474
- **calcium ion,** calcium signaling, glucose, mesangium cell, phospholipase C beta3, protein kinase C, 547
 - cation, cation transport, cyclopiazonic acid, trachea muscle, 526
 - honeybee, mushroom body, smelling, 401
- calcium mobilization, chemokine receptor CCR2, monocyte chemotactic protein 1, nerve cell, 338
- calcium signaling, adenosine diphosphate ribosyl cyclase, angiotensin, reactive oxygen metabolite, vascular smooth muscle, 540
 - arachidonic acid, B lymphocyte, diacylglycerol, 5 hydroperoxy 6,8,11,14 icosatetraenoic acid, 20 hydroxyicosatetraenoic acid, inflammation, inositol 1,4,5 trisphosphate, phospholipase C, 326
 - calcium ion, glucose, mesangium cell, phospholipase C beta3, protein kinase C, 547
 - kidney collecting tubule, kidney polycystic disease, 538
 - mechanotransduction, plasticity, skeletal muscle, slow muscle fiber, 465
- calcium transport, calcium, calcium cell level, heart muscle cell, sarcoplasmic reticulum, 474
 - calcium, morphine, opiate receptor, 332
- metabolic acidosis, osteoclast differentiation factor, osteolysis, tumor necrosis factor alpha, 562
- caloric intake, athlete, sport, 601
- capillary, hydraulic conductivity, shear rate, 491
- capillary density, aging, exercise, messenger RNA, vasculotropin, vasculotropin receptor, vastus lateralis muscle, 627
- **carbohydrate**, amino acid, brain, carbohydrate intake, exercise, 373
 - ascorbic acid, carbohydrate intake, cytokine, exercise, immune response, vitamin intake, 597
- carbohydrate metabolism, carbon dioxide, oxidation, 574 **carbohydrate intake,** amino acid, brain, carbohydrate, exercise, 373
 - ascorbic acid, carbohydrate, cytokine, exercise, immune response, vitamin intake, 597
- **carbohydrate metabolism,** carbohydrate, carbon dioxide, oxidation, 574
- **carbon dioxide,** asthma, chemical analysis, ovalbumin, oxygen, protein analysis, 527
- carbohydrate, carbohydrate metabolism, oxidation, 574
 carbon monoxide, blood volume, diagnostic error, erythropoietin, oxygen, 513
- heart output, muscle tone, syncope, 619
- **cardiopulmonary hemodynamics,** geographic elevation, nitric oxide, oxygen, 591
- cardiovascular disease, aging, androgen, androgen receptor, chronic kidney disease, endothelin, hormone action, testosterone, 534
 - diabetes mellitus, inducible nitric oxide synthase, nitric oxide, 493
- **cardiovascular function,** aerobic capacity, creatinine, diet supplementation, 635
- cardiovascular response, emotion, facial expression, hypothalamus hypophysis adrenal system, stress, 454 - hormone substitution, mental stress, naloxone, 490
- **cariporide**, atrial natriuretic factor, atrial natriuretic factor

- receptor, calcineurin, hypertension, sodium proton exchange protein 1, 475
- carnosine, muscle contraction, 561
- carotid artery, endothelial nitric oxide synthase, shear strength, 499
 - potassium channel, 502
- carrier protein, ammonia, glycoprotein, rhesus antigen, 324 catecholamine, corticosteroid receptor, corticosterone,
- glucocorticoid receptor, hypophysis adrenal system, mineralocorticoid receptor, neuropeptide, training, 608
- cation, calcium ion, cation transport, cyclopiazonic acid, trachea muscle, 526
- cation transport, calcium ion, cation, cyclopiazonic acid, trachea muscle, 526
- **CD2 associated protein,** actin, docking protein, green fluorescent protein, podocyte, 549
- CD34 antigen, athlete, exercise, Flt3 ligand, granulocyte colony stimulating factor, hematopoietic stem cell, interleukin 6, reticulocyte, 610
- celecoxib, acetylsalicylic acid 3 (nitroxymethyl)phenyl ester, cyclooxygenase 2 inhibitor, hypertension, nonsteroid antiinflammatory agent, 546
- cell adhesion molecule, membrane protein, synapse, 348 cell compartmentalization, aminopeptidase, insulin response, 566 cell DNA, antioxidant, diet supplementation, DNA damage, exercise, mononuclear cell, 598
- cell function, cell viability, dendritic cell, electroporation, 335 cell membrane permeability, blood brain barrier, endothelium cell, hypoxia, protein kinase C, 488
- cell structure, heart muscle cell, protein kinase C epsilon, 481 cell viability, cell function, dendritic cell, electroporation, 335 chemical analysis, asthma, carbon dioxide, ovalbumin, oxygen, protein analysis, 527
- chemokine, mitosis inhibition, monocyte, 484
- **chemokine receptor CCR2,** calcium mobilization, monocyte chemotactic protein 1, nerve cell, 338
- **chloride**, 4 aminobutyric acid, brain maturation, chloride transport, GABAergic transmission, spinal nerve, 408
- **chloride transport,** 4 aminobutyric acid, brain maturation, chloride, GABAergic transmission, spinal nerve, 408
- 2 chloro 6 n cyclopentyladenosine, adenosine A1 receptor agonist, delta opiate receptor agonist, heart infarction, inducible nitric oxide synthase, nitric oxide, 503
- **chlortalidone**, acetazolamide, amiloride, bumetanide, clopamide, diuretic agent, doping, high performance liquid chromatography, 617
- cholinergic receptor, autonomic nervous system function, heart automaticity, receptor sensitivity, sympathetic tone, 485
- cholinergic system, acetylcholine, avoidance behavior, enzyme inhibition, memory, mitogen activated protein kinase, signal transduction, 350
- chromaffin cell, exocytosis, beta galactosidase, green fluorescent protein, virus DNA, 360
- chronic kidney disease, aging, androgen, androgen receptor, cardiovascular disease, endothelin, hormone action, testosterone, 534
- circadian rhythm, anxiety, light exposure, memory, 429
- gene, oncogene c fos, suprachiasmatic nucleus, 363
- gene function, nucleotide sequence, opsin, 344
- **cisplatin,** hypoxia inducible factor 1, kidney tubule, nephrotoxicity, 548
- clopamide, acetazolamide, amiloride, bumetanide, chlortalidone, diuretic agent, doping, high performance liquid chromatography, 617
- clusterin, acute heart infarction, 497
- clutch size, body size, 560
- cocaine, cocaine dependence, connexin 36, gap junction, synaptic transmission, 432
- cocaine dependence, cocaine, connexin 36, gap junction, synaptic transmission, 432
- cognition, language, 448
- **collagen**, atherosclerosis, elastin, percutaneous transluminal angioplasty, 500
- **complementary DNA**, gill, protein analysis, sodium proton exchange protein 3, vertebrate, 518

complex formation, hippocampus, initiation factor 4E binding protein, initiation factor 4F, memory, nerve cell plasticity, protein function, translation regulation, 367

computer assisted tomography, lung mechanics, lung ventilation, X ray, 522

computer prediction, athlete, blood pressure regulation, hemodynamic monitoring, 512

connexin 36, cocaine, cocaine dependence, gap junction, synaptic transmission, 432

coordination, athlete, training, 605

copper, metal, 321

coronary blood vessel, atrial natriuretic factor, endothelium cell, glycocalyx, 486

corpus striatum, learning, prefrontal cortex, 336

corticosteroid, diclofenac, fever, lipopolysaccharide, nitric oxide, n(g) nitroarginine methyl ester, prostaglandin, thermoregulation, 584

corticosteroid receptor, catecholamine, corticosterone, glucocorticoid receptor, hypophysis adrenal system, mineralocorticoid receptor, neuropeptide, training, 608

corticosterone, catecholamine, corticosteroid receptor, glucocorticoid receptor, hypophysis adrenal system, mineralocorticoid receptor, neuropeptide, training, 608 creatine kinase, adenosine triphosphate, aging, creatine

phosphate, high energy phosphate, muscle metabolism, phosphate metabolism, skeletal muscle, 466

creatine phosphate, adenosine triphosphate, aging, creatine kinase, high energy phosphate, muscle metabolism, phosphate metabolism, skeletal muscle, 466

creatinine, aerobic capacity, cardiovascular function, diet supplementation, 635

crying, amygdaloid nucleus, auditory cortex, hemispheric dominance, insula, nonverbal communication, 444

crypt cell, calcium, membrane transport, potassium, potassium transport, 328

cyclic AMP dependent protein kinase, adenosine triphosphatase (potassium sodium), kidney collecting tubule, sodium channel, sodium transport, 542

 binding protein, kidney collecting tubule, SNARE protein, sodium channel, water absorption, 537

cyclic GMP dependent protein kinase, nitric oxide, skin conductance, 333

cyclooxygenase 1, cyclooxygenase 2, fever, lipopolysaccharide, thermoregulation, 583

cyclooxygenase 2, cyclooxygenase 1, fever, lipopolysaccharide, thermoregulation, 583

 fever, immunoglobulin enhancer binding protein, lipopolysaccharide, mitogen activated protein kinase 1, mitogen activated protein kinase 3, pregnancy, STAT5 protein, 585

cyclooxygenase 2 inhibitor, acetylsalicylic acid 3 (nitroxymethyl)phenyl ester, celecoxib, hypertension, nonsteroid antiinflammatory agent, 546

cyclopiazonic acid, calcium ion, cation, cation transport, trachea muscle, 526

cyclosporin A, immunosuppressive treatment, kidney transplantation, nephrotoxicity, spironolactone, 541

cystic fibrosis, adenosine triphosphate, exercise, hyperemia, vasoconstriction, 626

cytokine, ascorbic acid, carbohydrate, carbohydrate intake, exercise, immune response, vitamin intake, 597

cytokine release, diaphragm muscle, malnutrition, muscle growth, nucleotide sequence, tumor necrosis factor alpha, 525

dehydration, endurance, exercise, 633

- neurohypophysis hormone, sodium ion, vasopressin, vasopressin release, 588

delta opiate receptor agonist, adenosine A1 receptor agonist, 2 chloro 6 n cyclopentyladenosine, heart infarction, inducible nitric oxide synthase, nitric oxide, 503

dendritic cell, cell function, cell viability, electroporation, 335 **depolarization,** pyramidal nerve cell, sodium channel, spike, 369 **depression,** auditory cortex, 405

depth perception, attention, genetic polymorphism, nicotinic receptor, 372

- hearing, time perception, vision, 430

developmental stage, Drosophila melanogaster, 578 **diabetes mellitus,** adenylate cyclase, blood vessel tone, diabetic

angiopathy, 501
- cardiovascular disease, inducible nitric oxide synthase, nitric oxide, 493

diabetic angiopathy, adenylate cyclase, blood vessel tone, diabetes mellitus, 501

diabetic nephropathy, kidney tubule cell, peroxisome proliferator activated receptor agonist, phenylacetic acid derivative, pioglitazone, 2,4 thiazolidinedione derivative, 550

diacetyl oxime, actin, muscle force, muscle stiffness, muscle stretching, 467

diacylglycerol, arachidonic acid, B lymphocyte, calcium signaling, 5 hydroperoxy 6,8,11,14 icosatetraenoic acid, 20 hydroxyicosatetraenoic acid, inflammation, inositol 1,4,5 trisphosphate, phospholipase C, 326

diagnostic error, blood volume, carbon monoxide, erythropoietin, oxygen, 513

diaphragm muscle, cytokine release, malnutrition, muscle growth, nucleotide sequence, tumor necrosis factor alpha, 525

diastole, calcium, heart muscle contractile force, heart ventricle, sodium, sodium calcium exchange, 510

diclofenac, corticosteroid, fever, lipopolysaccharide, nitric oxide, n(g) nitroarginine methyl ester, prostaglandin, thermoregulation 584

dietary intake, body growth, exploratory behavior, 384 diet supplementation, aerobic capacity, cardiovascular function, creatinine, 635

 antioxidant, cell DNA, DNA damage, exercise, mononuclear cell, 598

exercise, glucose, glucose homeostasis, glutamine, 625
 diffusion weighted imaging, aging, helium, lung structure, 521
 dimethylargininase, endothelial nitric oxide synthase, exercise, heart failure, nitric oxide, nitric oxide synthase inhibitor,

dipalmitoylphosphatidylcholine, lung alveolus surface tension, lung surfactant, phospholipid, phospholipid metabolism, 516

dipeptidyl carboxypeptidase, endothelium cell, enzyme regulation, nicotine, 487

diuretic agent, acetazolamide, amiloride, bumetanide, chlortalidone, clopamide, doping, high performance liquid chromatography, 617

diving, lung ventilation, sport, 616

dizocilpine, food intake, ion transport, n methyl dextro aspartic acid, n methyl dextro aspartic acid receptor, sensory nerve, solitary tract nucleus, vagus nerve, 365

DNA, gene expression regulation, gill, hypoxia, 517

DNA damage, antioxidant, cell DNA, diet supplementation, exercise, mononuclear cell, 598

docking protein, actin, CD2 associated protein, green fluorescent protein, podocyte, 549

dopamine, dopamine release, potentiometry, reward, striate cortex, 435

neurotensin, neurotransmission, nucleus accumbens, 339
 dopamine release, dopamine, potentiometry, reward, striate cortex, 435

dopaminergic nerve cell, ventral tegmentum, 424 doping, acetazolamide, amiloride, bumetanide, chlortalidone, clopamide, diuretic agent, high performance liquid chromatography, 617

Doppler echography, brain blood flow, 505 Drosophila melanogaster, developmental stage, 578 drowsiness, lung ventilation, sleep, 530

dynamic exercise, leg blood flow, muscle blood flow, oxygen, oxygen consumption, 623

echography, pleura cavity, 524 **education,** neuropsychological test, reading, 452

elastin, atherosclerosis, collagen, percutaneous transluminal angioplasty, 500

electroencephalogram, 378 419

electroencephalography, 4 aminobutyric acid A receptor stimulating agent, muscimol, somatosensory cortex, 402

electromyography, hand movement, spike wave, 461 electroporation, cell function, cell viability, dendritic cell, 335

emotion, cardiovascular response, facial expression, hypothalamus hypophysis adrenal system, stress, 454 prefrontal cortex, 443

endothelial nitric oxide synthase, carotid artery, shear strength,

- dimethylargininase, exercise, heart failure, nitric oxide, nitric oxide synthase inhibitor, 607

endothelin, aging, androgen, androgen receptor, cardiovascular disease, chronic kidney disease, hormone action, testosterone, 534

endothelium cell, atrial natriuretic factor, coronary blood vessel, glycocalyx, 486 - blood brain barrier, cell membrane permeability, hypoxia,

protein kinase C. 488

- dipeptidyl carboxypeptidase, enzyme regulation, nicotine, 487 endothelium derived relaxing factor, adenosine triphosphatase (potassium sodium), aorta, sodium calcium exchange, 570

endotracheal intubation, flight, laryngoscope, 590 **endurance**, dehydration, exercise, 633

 nutrition, physical performance, 615
 enteric feeding, glucose, glucose transport, intralipid, liver metabolism, nutritional support, total parenteral nutrition, travasol, 571

enzyme activation, epidermal growth factor, estrone sulfate, kidney proximal tubule, mitogen activated protein kinase, organic cation transporter, phosphatidylinositol 3 kinase, protein tyrosine kinase, 544

enzyme activity, heart hypertrophy, heart size, phosphatidylinositol 3 kinase, signal transduction, 613

enzyme analysis, exercise, oxidative stress, reduced nicotinamide

adenine dinucleotide phosphate oxidase, 629
enzyme inhibition, acetylcholine, avoidance behavior, cholinergic system, memory, mitogen activated protein kinase, signal transduction, 350

enzyme regulation, dipeptidyl carboxypeptidase, endothelium cell, nicotine, 487

epidermal growth factor, enzyme activation, estrone sulfate, kidney proximal tubule, mitogen activated protein kinase, organic cation transporter, phosphatidylinositol 3 kinase, protein tyrosine kinase, 544

erythropoietin, blood volume, carbon monoxide, diagnostic error, oxygen, 513

estrogen, estrogen activity, sex difference, thalamus ventral nucleus, 346

estrogen activity, estrogen, sex difference, thalamus ventral nucleus, 346

estrone sulfate, enzyme activation, epidermal growth factor, kidney proximal tubule, mitogen activated protein kinase, organic cation transporter, phosphatidylinositol 3 kinase, protein tyrosine kinase, 544

event related potential, 449

information processing, magnetoencephalography, motor system, somatosensory system, 421

language, music, 446

evoked brain stem auditory response, biological marker, hearing, speech analysis, speech perception, 441 evoked response, 391

Hoffmann reflex, muscle contractility, muscle isometric contraction, 462

evoked somatosensory response, 457

excitation contraction coupling, heart muscle contractility, sarcomere, 495

exercise, 612

- adenosine triphosphate, cystic fibrosis, hyperemia, vasoconstriction, 626

- aerobic metabolism, 630

- aging, capillary density, messenger RNA, vasculotropin, vasculotropin receptor, vastus lateralis muscle, 627

- aging, oxidation, 614

- amino acid, brain, carbohydrate, carbohydrate intake, 373

- anterior hypothalamus, nerve cell excitability, 606

- antioxidant, cell DNA, diet supplementation, DNA damage, mononuclear cell, 598

- ascorbic acid, carbohydrate, carbohydrate intake, cytokine, immune response, vitamin intake, 597

- athlete, CD34 antigen, Flt3 ligand, granulocyte colony stimulating factor, hematopoietic stem cell, interleukin 6, reticulocyte, 610

- dehydration, endurance, 633

- diet supplementation, glucose, glucose homeostasis, glutamine, 625

- dimethylargininase, endothelial nitric oxide synthase, heart failure, nitric oxide, nitric oxide synthase inhibitor, 607

- enzyme analysis, oxidative stress, reduced nicotinamide adenine dinucleotide phosphate oxidase, 629

- functional magnetic resonance imaging, nuclear magnetic resonance spectroscopy, 375 - intermittent claudication, 602

- lung diffusion capacity, rebreathing, 634

- muscle strength, muscle training, 628

- nitric oxide, 611

- oxygen, skin blood flow, sweating, thermoregulation, 622

- testosterone, testosterone release, 632 **exocytosis**, chromaffin cell, beta galactosidase, green fluorescent protein, virus DNA, 360

expiratory flow, asthma, smooth muscle, 529

exploratory behavior, body growth, dietary intake, 384 extensor digitorum longus muscle, breathing rate, mitochondrial

respiration, muscle cell, soleus muscle, 464 extraocular muscle, eye movement control, nuclear magnetic resonance imaging, 460

eve movement control, extraocular muscle, nuclear magnetic resonance imaging, 460

eye protective device, athlete, self report, 640

face, recognition, 438

facial expression, cardiovascular response, emotion, hypothalamus hypophysis adrenal system, stress, 454 facilitation, amygdaloid nucleus, fear, learning, synaptic

transmission, 437 fast muscle, inhibitor of differentiation 2, protein analysis, protein p53, skeletal muscle, slow muscle, 469

fast muscle fiber, limb girdle muscular dystrophy, protein deficiency, sarcoglycan, slow muscle fiber, 463

fatigue, sports medicine, 594

fatty acid oxidation, fatty acid synthase, fatty acid synthase inhibitor, hypothalamus, skeletal muscle, 564

fatty acid synthase, fatty acid oxidation, fatty acid synthase inhibitor, hypothalamus, skeletal muscle, 564

fatty acid synthase inhibitor, fatty acid oxidation, fatty acid synthase, hypothalamus, skeletal muscle, 564

fear, aggressiveness, maternal behavior, newborn care, 428

amygdaloid nucleus, arousal, autonomic nervous system, 376

- amygdaloid nucleus, brain injury, 442

- amygdaloid nucleus, facilitation, learning, synaptic transmission, 437

- aversion, heart rate, 431

feeding behavior, neuropeptide, protein isolation, 368 fetus circulation, calcitonin gene related peptide receptor, nitric oxide, 479

fever, corticosteroid, diclofenac, lipopolysaccharide, nitric oxide, n(g) nitroarginine methyl ester, prostaglandin, thermoregulation, 584

- cyclooxygenase 1, cyclooxygenase 2, lipopolysaccharide, thermoregulation, 583

- cyclooxygenase 2, immunoglobulin enhancer binding protein, lipopolysaccharide, mitogen activated protein kinase 1, mitogen activated protein kinase 3, pregnancy, STAT5 protein, 585

fibroblast growth factor 23, calcitriol, phosphate, phosphate metabolism, vitamin D metabolism, vitamin D receptor, finger, hand movement, motor activity, sequential analysis, 379 fitness, football, 637

leukocyte count, 575

flavor, amygdaloid nucleus, learning, taste preference, 436 flight, endotracheal intubation, laryngoscope, 590

Flt3 ligand, athlete, CD34 antigen, exercise, granulocyte colony stimulating factor, hematopoietic stem cell, interleukin 6, reticulocyte, 610

fluid therapy, athlete, attitude, hydration, 599

food, taste, 415

food intake, dizocilpine, ion transport, n methyl dextro aspartic acid, n methyl dextro aspartic acid receptor, sensory nerve, solitary tract nucleus, vagus nerve, 365

football, anthropometry, physiology, 638

fitness, 637

forced expiratory volume, breathing muscle, lung flow volume curve, muscle stretching, 523

functional magnetic resonance imaging, exercise, nuclear magnetic resonance spectroscopy, 375

- illusion, learning, perception, 445

- signal transduction, spatial discrimination, visual cortex, 439

GABAergic system, 4 aminobutyric acid, interneuron, spinal cord nerve cell 359

GABAergic transmission, 4 aminobutyric acid, brain maturation, chloride, chloride transport, spinal nerve, 408

beta galactosidase, chromaffin cell, exocytosis, green fluorescent protein virus DNA 360

gap junction, cocaine, cocaine dependence, connexin 36, synaptic transmission, 432

gap junction protein, thalamocortical tract, 340

gene, circadian rhythm, oncogene c fos, suprachiasmatic nucleus, 363

gene expression, breast epithelium, gene product, protein protein interaction, 587

gene expression regulation, DNA, gill, hypoxia, 517

glucocorticoid receptor, hypothalamus hypophysis adrenal system, leukemia inhibitory factor, 329

gene function, amygdaloid nucleus, genetic variability, tryptophan hydroxylase, 357

- circadian rhythm, nucleotide sequence, opsin, 344

gene overexpression, immediate early gene, intestine absorption, obesity, 568

gene product, breast epithelium, gene expression, protein protein interaction, 587

genetic polymorphism, arginine, beta 2 adrenergic receptor, glycine, heart output, isometric exercise, 621

- attention, depth perception, nicotinic receptor, 372 genetic variability, amygdaloid nucleus, gene function, tryptophan hydroxylase, 357

geographic elevation, cardiopulmonary hemodynamics, nitric oxide, oxygen, 591

gill, complementary DNA, protein analysis, sodium proton exchange protein 3, vertebrate, 518

DNA, gene expression regulation, hypoxia, 517

glucocorticoid receptor, catecholamine, corticosteroid receptor, corticosterone, hypophysis adrenal system, mineralocorticoid receptor, neuropeptide, training, 608

- gene expression regulation, hypothalamus hypophysis adrenal system, leukemia inhibitory factor, 329

glucose, calcium ion, calcium signaling, mesangium cell, phospholipase C beta3, protein kinase C, 547

- diet supplementation, exercise, glucose homeostasis, glutamine, 625

- enteric feeding, glucose transport, intralipid, liver metabolism, nutritional support, total parenteral nutrition, travasol, 571

glucose homeostasis, diet supplementation, exercise, glucose, glutamine, 625

glucose transport, enteric feeding, glucose, intralipid, liver metabolism, nutritional support, total parenteral nutrition, travasol, 571

glucose transporter, insulin release, lacrimal gland, 586 glucose transporter 4, guanosine triphosphatase activating protein, protein kinase B, 325

glutamate transporter, brain metabolism, superior colliculus, visual stimulation, 565

glutamic acid, neurotransmission, 433

glutamine, diet supplementation, exercise, glucose, glucose homeostasis, 625

glycine, arginine, beta 2 adrenergic receptor, genetic

polymorphism, heart output, isometric exercise, 621 glycocalyx, atrial natriuretic factor, coronary blood vessel, endothelium cell, 486

glycolysis, muscle isometric contraction, 569

glycoprotein, ammonia, carrier protein, rhesus antigen, 324 gonadorelin, hypophysis, 573

granulocyte colony stimulating factor, athlete, CD34 antigen, exercise, Flt3 ligand, hematopoietic stem cell, interleukin 6, reticulocyte, 610

granzyme B, apoptosis, 322

green fluorescent protein, actin, CD2 associated protein, docking protein, podocyte, 549

- chromaffin cell, exocytosis, beta galactosidase, virus DNA, 360 guanosine triphosphatase activating protein, glucose transporter 4, protein kinase B. 325

hand, proprioception, spatial discrimination, time perception, vision, 352

hand function, brain cortex, magnetoencephalography, median nerve, 385

hand movement, aging, muscle strength, 418

- electromyography, spike wave, 461

- finger, motor activity, sequential analysis, 379 hand muscle, muscle force, muscle stretching, vibration, 624 hearing, biological marker, evoked brain stem auditory response, speech analysis, speech perception, 441

- depth perception, time perception, vision, 430 - magnetoencephalography, 377

hearing aid, noise reduction, 390

hearing impairment, auditory cortex, sign language, visual cortex, 411

heart automaticity, autonomic nervous system function, cholinergic receptor, receptor sensitivity, sympathetic tone,

heart failure, dimethylargininase, endothelial nitric oxide synthase, exercise, nitric oxide, nitric oxide synthase inhibitor, 607

heart function, body size, 489

heart hypertrophy, enzyme activity, heart size,

phosphatidylinositol 3 kinase, signal transduction, 613 heart infarction, adenosine A1 receptor agonist, 2 chloro 6 n

cyclopentyladenosine, delta opiate receptor agonist, inducible nitric oxide synthase, nitric oxide, 503

- apoptosis, heart muscle cell, 494

heart left ventricle pressure, heart left ventricle volume, 509 heart left ventricle volume, heart left ventricle pressure, 509 heart mitochondrion, peroxisome proliferator activated receptor

alpha, thyroid gland, thyroid hormone, 504 heart muscle, amino terminal sequence, muscle force, myosin light chain, 459

- Purkinje fiber, 458

heart muscle cell, apoptosis, heart infarction, 494

- calcium, calcium cell level, calcium transport, sarcoplasmic reticulum, 474

- cell structure, protein kinase C epsilon, 481

heart muscle contractile force, calcium, diastole, heart ventricle, sodium, sodium calcium exchange, 510

heart muscle contractility, excitation contraction coupling, sarcomere, 495

- sarcomere, 496

heart output, arginine, beta 2 adrenergic receptor, genetic polymorphism, glycine, isometric exercise, 621

- carbon monoxide, muscle tone, syncope, 619

heart rate, aversion, fear, 431

heart rate variability, aging, body weight, systolic blood pressure, 477

- blood pressure regulation, pressoreceptor reflex, 483

heart size, enzyme activity, heart hypertrophy,

phosphatidylinositol 3 kinase, signal transduction, 613 ventricle, calcium, diastole, heart muscle contractile force,

sodium, sodium calcium exchange, 510

heat sensation, pain, sensory stimulation, stimulus response, 580 heat shock, heat shock protein 70, larval development, 581 heat shock protein 70, heat shock, larval development, 581

heat shock protein 72, adrenergic receptor, adrenergic system, alpha 1 adrenergic receptor, stress, 380

helium, aging, diffusion weighted imaging, lung structure, 521

helmet, assisted ventilation, 519 hematopoietic stem cell, athlete, CD34 antigen, exercise, Flt3 ligand, granulocyte colony stimulating factor, interleukin 6, reticulocyte, 610

heme oxygenase 2, calcium activated potassium channel, oxygen sensing, voltage gated potassium channel, 413

hemispheric dominance, amygdaloid nucleus, auditory cortex, crying, insula, nonverbal communication, 444

- auditory stimulation, right hemisphere, 392 hemodynamic monitoring, athlete, blood pressure regulation, computer prediction, 512

hemodynamics, perfusion pressure, vasoconstriction, vein blood flow, 506

hemoglobin, arm exercise, leg exercise, oxygen, oxygen consumption, 609

Henle loop, ion transport, kidney tubule, reduced nicotinamide adenine dinucleotide phosphate oxidase, sodium proton exchange protein, 543

hibernation, swimming, turtle, 576 high energy phosphate, adenosine triphosphate, aging, creatine kinase, creatine phosphate, muscle metabolism, phosphate metabolism, skeletal muscle, 466

high performance liquid chromatography, acetazolamide, amiloride, bumetanide, chlortalidone, clopamide, diuretic agent, doping, 617

hip, body position, walking, 423

hippocampus, brain cortex, brain function, theta rhythm, 366 complex formation, initiation factor 4E binding protein, initiation factor 4F, memory, nerve cell plasticity, protein function, translation regulation, 367

Hoffmann reflex, evoked response, muscle contractility, muscle isometric contraction, 462

honeybee, calcium ion, mushroom body, smelling, 401

hormone action, aging, androgen, androgen receptor, cardiovascular disease, chronic kidney disease, endothelin, testosterone, 534

hormone substitution, cardiovascular response, mental stress, naloxone, 490

hostility, stress, testosterone, 451

hydration, athlete, attitude, fluid therapy, 599

hydraulic conductivity, capillary, shear rate, 491

hydrocortisone, stress, 450

hydrogen peroxide, blood pressure regulation, vasomotor reflex,

5 hydroperoxy 6,8,11,14 icosatetraenoic acid, arachidonic acid, B lymphocyte, calcium signaling, diacylglycerol, 20 hydroxyicosatetraenoic acid, inflammation, inositol 1,4,5 trisphosphate, phospholipase C, 326

20 hydroxyicosatetraenoic acid, arachidonic acid, blood pressure, icosanoid, kidney function, nitric oxide, n(g) nitroarginine methyl ester, pregnancy, 557

- arachidonic acid, B lymphocyte, calcium signaling, diacylglycerol, 5 hydroperoxy 6,8,11,14 icosatetraenoic acid, inflammation, inositol 1,4,5 trisphosphate, phospholipase C, 326

- brain vasospasm, subarachnoid hemorrhage, 498

hyperemia, adenosine triphosphate, cystic fibrosis, exercise, vasoconstriction, 626 - hypervolemia, splanchnic blood flow, tachycardia, Valsalva

maneuver, 482 hypertension, acetylsalicylic acid 3 (nitroxymethyl)phenyl ester,

celecoxib, cyclooxygenase 2 inhibitor, nonsteroid antiinflammatory agent, 546

- aquaporin 2, kidney collecting tubule, sodium channel, 536

- atrial natriuretic factor, atrial natriuretic factor receptor,

calcineurin, cariporide, sodium proton exchange protein 1,

hypervolemia, hyperemia, splanchnic blood flow, tachycardia, Valsalva maneuver, 482

hypophysis, gonadorelin, 573

hypophysis adrenal system, catecholamine, corticosteroid receptor, corticosterone, glucocorticoid receptor, mineralocorticoid receptor, neuropeptide, training, 608

hypotension, blood viscosity, shear stress, vascular resistance, 492 hypothalamus, fatty acid oxidation, fatty acid synthase, fatty acid synthase inhibitor, skeletal muscle, 564

hypothalamus hypophysis adrenal system, cardiovascular response, emotion, facial expression, stress, 454

gene expression regulation, glucocorticoid receptor, leukemia inhibitory factor, 329

hypothalamus hypophysis system, neurokinin 1 receptor, neurokinin 2 receptor, vasopressin, 374

hypoxia, blood brain barrier, cell membrane permeability,

endothelium cell, protein kinase C, 488 - DNA, gene expression regulation, gill, 517

hypoxia inducible factor 1, cisplatin, kidney tubule,

nephrotoxicity, 548
hypoxic lung vasoconstriction, lung artery pressure, lung structure, 514

icosanoid, arachidonic acid, blood pressure, 20 hydroxyicosatetraenoic acid, kidney function, nitric oxide, n(g) nitroarginine methyl ester, pregnancy, 557

illusion, functional magnetic resonance imaging, learning,

perception, 445
immediate early gene, gene overexpression, intestine absorption, obesity, 568

immobilization stress, 347

immune response, ascorbic acid, carbohydrate, carbohydrate intake, cytokine, exercise, vitamin intake, 597

immunoglobulin enhancer binding protein, cyclooxygenase 2, fever, lipopolysaccharide, mitogen activated protein kinase 1, mitogen activated protein kinase 3, pregnancy, STAT5 protein, 585

immunosuppressive treatment, cyclosporin A, kidney transplantation, nephrotoxicity, spironolactone, 541

inducible nitric oxide synthase, adenosine A1 receptor agonist, 2 chloro 6 n cyclopentyladenosine, delta opiate receptor agonist, heart infarction, nitric oxide, 503

cardiovascular disease, diabetes mellitus, nitric oxide, 493

inferior colliculus, auditory stimulation, stereotypy, stimulus response, 403

inflammation, arachidonic acid, B lymphocyte, calcium signaling, diacylglycerol, 5 hydroperoxy 6,8,11,14 icosatetraenoic acid, 20 hydroxyicosatetraenoic acid, inositol 1,4,5 trisphosphate, phospholipase C, 326

information processing, event related potential, magnetoencephalography, motor system, somatosensory

inhibitor of differentiation 2, fast muscle, protein analysis, protein p53, skeletal muscle, slow muscle, 469

inhibitory guanine nucleotide binding protein, kidney collecting tubule, prostaglandin receptor, water absorption, 552

initiation factor 4E binding protein, complex formation, hippocampus, initiation factor 4F, memory, nerve cell plasticity, protein function, translation regulation, 367

initiation factor 4F, complex formation, hippocampus, initiation factor 4E binding protein, memory, nerve cell plasticity, protein function, translation regulation, 367

inositol 1,4,5 trisphosphate, arachidonic acid, B lymphocyte, calcium signaling, diacylglycerol, 5 hydroperoxy 6,8,11,14 icosatetraenoic acid, 20 hydroxyicosatetraenoic acid, inflammation, phospholipase C, 326

inspiratory reserve volume, breathing muscle, locomotion, lung pressure, 528

insula, amygdaloid nucleus, auditory cortex, crying, hemispheric dominance, nonverbal communication, 444

insulin, iontophoresis, skin blood flow, vasodilatation, 472

insulin release, glucose transporter, lacrimal gland, 586

insulin response, aminopeptidase, cell compartmentalization, 566 **insulin sensitivity,** liver X receptor, 567

interhemispheric transfer, split brain, 399 400

interleukin 6, athlete, CD34 antigen, exercise, Flt3 ligand, granulocyte colony stimulating factor, hematopoietic stem cell, reticulocyte, 610

intermittent claudication, exercise, 602

intermittent positive pressure ventilation, positive end expiratory pressure, swallowing, 533

interneuron, 4 aminobutyric acid, GABAergic system, spinal cord nerve cell, 359

intestine absorption, gene overexpression, immediate early gene, obesity, 568

intralipid, enteric feeding, glucose, glucose transport, liver metabolism, nutritional support, total parenteral nutrition, travasol, 571

iontophoresis, insulin, skin blood flow, vasodilatation, 472 ion transport, dizocilpine, food intake, n methyl dextro aspartic acid, n methyl dextro aspartic acid receptor, sensory nerve, solitary tract nucleus, vagus nerve, 365

- Henle loop, kidney tubule, reduced nicotinamide adenine dinucleotide phosphate oxidase, sodium proton exchange protein, 543

isometric exercise, arginine, beta 2 adrenergic receptor, genetic polymorphism, glycine, heart output, 621 **isoprotein**, osteoblast, transcription factor, 330

joint function, ballistics, thixotropy, wrist, 631 · limb movement, motor control, 417

jumping, muscle strength, 604

sports medicine, 603

juxtaglomerular apparatus, kidney, prostaglandin E2, prostaglandin E receptor, renin, renin release, 539

kappa opiate receptor, binaltorphimine, kappa opiate receptor antagonist, kidney function, sodium urine level, 553

kappa opiate receptor antagonist, binaltorphimine, kappa opiate receptor, kidney function, sodium urine level, 553

kidney, annexin, lipocortin 1, lipocortin 2, lipocortin 4, lipocortin

- juxtaglomerular apparatus, prostaglandin E2, prostaglandin E receptor, renin, renin release, 539

kidney blood flow, natriuresis, sodium chloride, 555

kidney collecting tubule, adenosine triphosphatase (potassium sodium), cyclic AMP dependent protein kinase, sodium channel, sodium transport, 542

aquaporin 2, hypertension, sodium channel, 536

- binding protein, cyclic AMP dependent protein kinase, SNARE protein, sodium channel, water absorption, 537

- calcium signaling, kidney polycystic disease, 538

- inhibitory guanine nucleotide binding protein, prostaglandin receptor, water absorption, 552

- mineralocorticoid, potassium channel, potassium ion, protein tyrosine kinase, sodium channel, sodium ion, 545

kidney function, arachidonic acid, blood pressure, 20 hydroxyicosatetraenoic acid, icosanoid, nitric oxide, n(g) nitroarginine methyl ester, pregnancy, 557

- binaltorphimine, kappa opiate receptor, kappa opiate receptor antagonist, sodium urine level, 553

- brain natriuretic peptide, protein analysis, 556

kidney polycystic disease, calcium signaling, kidney collecting tubule, 538

kidney proximal tubule, enzyme activation, epidermal growth factor, estrone sulfate, mitogen activated protein kinase, organic cation transporter, phosphatidylinositol 3 kinase, protein tyrosine kinase, 544

kidney transplantation, cyclosporin A, immunosuppressive treatment, nephrotoxicity, spironolactone, 541

kidney tubule, cisplatin, hypoxia inducible factor 1, nephrotoxicity, 548

- Henle loop, ion transport, reduced nicotinamide adenine dinucleotide phosphate oxidase, sodium proton exchange protein, 543

kidney tubule cell, diabetic nephropathy, peroxisome proliferator activated receptor agonist, phenylacetic acid derivative, pioglitazone, 2,4 thiazolidinedione derivative, 550 kinetics, metabolism, sulfate, 572

lacrimal gland, glucose transporter, insulin release, 586 alpha lactalbumin, lysozyme, male genital system, molecular cloning, 559

language, cognition, 448

- event related potential, music, 446

larval development, heat shock, heat shock protein 70, 581 laryngoscope, endotracheal intubation, flight, 590

lateral geniculate nucleus, attention, motor performance, 416 learning, amygdaloid nucleus, facilitation, fear, synaptic transmission, 437

- amygdaloid nucleus, flavor, taste preference, 436

- corpus striatum, prefrontal cortex, 336

- functional magnetic resonance imaging, illusion, perception,

- mitogen activated protein kinase, nerve cell plasticity, oncogene H ras, presynaptic membrane, synapsin I, 370 - nerve cell plasticity, positive feedback, 345

leg blood flow, dynamic exercise, muscle blood flow, oxygen, oxygen consumption, 623

leg exercise, arm exercise, hemoglobin, oxygen, oxygen

consumption, 609
leukemia inhibitory factor, gene expression regulation, glucocorticoid receptor, hypothalamus hypophysis adrenal system, 329

leukocyte count, fitness, 575

light exposure, anxiety, circadian rhythm, memory, 429 limb girdle muscular dystrophy, fast muscle fiber, protein deficiency, sarcoglycan, slow muscle fiber, 463

limb movement, ankle, brain, sensorimotor function, 343 - joint function, motor control, 417

lipocortin 1, annexin, kidney, lipocortin 2, lipocortin 4, lipocortin

lipocortin 2, annexin, kidney, lipocortin 1, lipocortin 4, lipocortin 5, 535

lipocortin 4, annexin, kidney, lipocortin 1, lipocortin 2, lipocortin

lipocortin 5, annexin, kidney, lipocortin 1, lipocortin 2, lipocortin 4, 535

lipopolysaccharide, corticosteroid, diclofenac, fever, nitric oxide, n(g) nitroarginine methyl ester, prostaglandin, thermoregulation, 584

- cyclooxygenase 1, cyclooxygenase 2, fever, thermoregulation,

cyclooxygenase 2, fever, immunoglobulin enhancer binding protein, mitogen activated protein kinase 1, mitogen activated protein kinase 3, pregnancy, STAT5 protein, 585

liver metabolism, enteric feeding, glucose, glucose transport, intralipid, nutritional support, total parenteral nutrition, travasol, 571

liver X receptor, insulin sensitivity, 567

locomotion, breathing muscle, inspiratory reserve volume, lung

lung alveolus surface tension, dipalmitoylphosphatidylcholine, lung surfactant, phospholipid, phospholipid metabolism, 516

lung artery pressure, hypoxic lung vasoconstriction, lung structure, 514

lung diffusion capacity, exercise, rebreathing, 634 lung flow volume curve, breathing muscle, forced expiratory

volume, muscle stretching, 523 lung mechanics, computer assisted tomography, lung ventilation, X ray, 522

lung pressure, breathing muscle, inspiratory reserve volume, locomotion, 528

lung structure, aging, diffusion weighted imaging, helium, 521 hypoxic lung vasoconstriction, lung artery pressure, 514

lung surfactant, dipalmitoylphosphatidylcholine, lung alveolus surface tension, phospholipid, phospholipid metabolism, **lung ventilation,** computer assisted tomography, lung mechanics, X ray, 522

- diving, sport, 616

- drowsiness, sleep, 530

lung volume, breath holding, multidetector computed tomography, 520

lymph vessel, pump, 508

lysozyme, alpha lactalbumin, male genital system, molecular cloning, 559

magnetoencephalography, brain cortex, hand function, median nerve. 385

 event related potential, information processing, motor system, somatosensory system, 421

- hearing, 377

male genital system, alpha lactalbumin, lysozyme, molecular cloning, 559

malnutrition, cytokine release, diaphragm muscle, muscle growth, nucleotide sequence, tumor necrosis factor alpha, 525

maternal behavior, aggressiveness, fear, newborn care, 428 mechanotransduction, calcium signaling, plasticity, skeletal muscle, slow muscle fiber, 465

median nerve, brain cortex, hand function, magnetoencephalography, 385

melanocortin 4 receptor, adrenergic system, messenger RNA, nucleotide sequence, protein expression, white adipose tissue, 426

membrane protein, cell adhesion molecule, synapse, 348 membrane transport, calcium, crypt cell, potassium, potassium transport, 328

memory, 453

 acetylcholine, avoidance behavior, cholinergic system, enzyme inhibition, mitogen activated protein kinase, signal transduction, 350

- anxiety, circadian rhythm, light exposure, 429

- auditory system, vision, 397

 complex formation, hippocampus, initiation factor 4E binding protein, initiation factor 4F, nerve cell plasticity, protein function, translation regulation, 367

- motor performance, task performance, 434

mental stress, cardiovascular response, hormone substitution, naloxone, 490

mesangium cell, calcium ion, calcium signaling, glucose, phospholipase C beta3, protein kinase C, 547

mesencephalon, brain cortex, sensory cortex, 395

messenger RNA, adrenergic activity, alpha 1A adrenergic receptor, alpha 1 adrenergic receptor, artery, receptor subtype, 480

- adrenergic system, melanocortin 4 receptor, nucleotide sequence, protein expression, white adipose tissue, 426

 aging, capillary density, exercise, vasculotropin, vasculotropin receptor, vastus lateralis muscle, 627

metabolic acidosis, calcium transport, osteoclast differentiation factor, osteolysis, tumor necrosis factor alpha, 562

metabolism, kinetics, sulfate, 572

metal, copper, 321

n methyl dextro aspartic acid, dizocilpine, food intake, ion transport, n methyl dextro aspartic acid receptor, sensory nerve, solitary tract nucleus, vagus nerve, 365

n methyl dextro aspartic acid receptor, dizocilpine, food intake, ion transport, n methyl dextro aspartic acid, sensory nerve, solitary tract nucleus, vagus nerve, 365

microanalysis, skeletal muscle, 470

microtubule protein, spermatogenesis, 558

microvascularization, muscle metabolism, muscle perfusion, serotonin, vasoconstriction, 471

micturition, sex difference, 554

mineralocorticoid, kidney collecting tubule, potassium channel, potassium ion, protein tyrosine kinase, sodium channel, sodium ion. 545

mineralocorticoid receptor, catecholamine, corticosteroid receptor, corticosterone, glucocorticoid receptor, hypophysis adrenal system, neuropeptide, training, 608

mitochondrial respiration, breathing rate, extensor digitorum longus muscle, muscle cell, soleus muscle, 464

mitogen activated protein kinase, acetylcholine, avoidance behavior, cholinergic system, enzyme inhibition, memory, signal transduction, 350

 enzyme activation, epidermal growth factor, estrone sulfate, kidney proximal tubule, organic cation transporter, phosphatidylinositol 3 kinase, protein tyrosine kinase, 544

 learning, nerve cell plasticity, oncogene H ras, presynaptic membrane, synapsin I, 370

mitogen activated protein kinase 1, cyclooxygenase 2, fever, immunoglobulin enhancer binding protein, lipopolysaccharide, mitogen activated protein kinase 3, pregnancy, STAT5 protein, 585

mitogen activated protein kinase 3, cyclooxygenase 2, fever, immunoglobulin enhancer binding protein, lipopolysaccharide, mitogen activated protein kinase 1, pregnancy, STAT5 protein, 585

mitosis inhibition, chemokine, monocyte, 484

molecular cloning, alpha lactalbumin, lysozyme, male genital system, 559

monocyte, chemokine, mitosis inhibition, 484

monocyte chemotactic protein 1, calcium mobilization, chemokine receptor CCR2, nerve cell, 338

mononuclear cell, antioxidant, cell DNA, diet supplementation, DNA damage, exercise, 598

morphine, calcium, calcium transport, opiate receptor, 332 motoneuron, acetylcholine, Aplysia, neuromodulation, temperature sensitivity, 422

motor activity, finger, hand movement, sequential analysis, 379 - sensory nerve, 427

motor control, joint function, limb movement, 417

motor cortex, vascularization, 511

motor performance, attention, lateral geniculate nucleus, 416 - memory, task performance, 434

motor system, event related potential, information processing, magnetoencephalography, somatosensory system, 421

multidetector computed tomography, breath holding, lung volume, 520

muscimol, 4 aminobutyric acid A receptor stimulating agent, arterial pressure, pressor response, solitary tract nucleus, 507

 4 aminobutyric acid A receptor stimulating agent, electroencephalography, somatosensory cortex, 402

 4 aminobutyric acid receptor stimulating agent, periaqueductal gray matter, sympathetic blocking, sympathetic innervation, 406

muscle blood flow, dynamic exercise, leg blood flow, oxygen, oxygen consumption, 623

muscle cell, breathing rate, extensor digitorum longus muscle, mitochondrial respiration, soleus muscle, 464

muscle contractility, evoked response, Hoffmann reflex, muscle isometric contraction, 462

muscle contraction, carnosine, 561

muscle fatigue, skeletal muscle, 455

muscle force, actin, diacetyl oxime, muscle stiffness, muscle stretching, 467

- amino terminal sequence, heart muscle, myosin light chain, 459 - hand muscle, muscle stretching, vibration, 624

muscle growth, cytokine release, diaphragm muscle, malnutrition, nucleotide sequence, tumor necrosis factor alpha, 525

muscle injury, skiing, supplementation, 600

muscle isometric contraction, evoked response, Hoffmann reflex, muscle contractility, 462

- glycolysis, 569

muscle metabolism, adenosine triphosphate, aging, creatine kinase, creatine phosphate, high energy phosphate, phosphate metabolism, skeletal muscle, 466

- microvascularization, muscle perfusion, serotonin, vasoconstriction, 471

muscle perfusion, microvascularization, muscle metabolism, serotonin, vasoconstriction, 471

muscle spindle afferent nerve, pressoreceptor reflex, static exercise, tendon, 468

muscle stiffness, actin, diacetyl oxime, muscle force, muscle stretching, 467

muscle strength, aging, hand movement, 418

aging, muscle training, sex difference, 473

- exercise, muscle training, 628

- jumping, 604

- muscle training, sex difference, 620

muscle stretching, actin, diacetyl oxime, muscle force, muscle stiffness, 467

- breathing muscle, forced expiratory volume, lung flow volume curve, 523

- hand muscle, muscle force, vibration, 624

muscle tone, carbon monoxide, heart output, syncope, 619 muscle training, aging, muscle strength, sex difference, 473

exercise, muscle strength, 628

- muscle strength, sex difference, 620

mushroom body, calcium ion, honeybee, smelling, 401 music, auditory memory, musician, 447

event related potential, language, 446

musician, auditory memory, music, 447

myosin light chain, amino terminal sequence, heart muscle, muscle force, 459

naloxone, cardiovascular response, hormone substitution, mental

natriuresis, kidney blood flow, sodium chloride, 555 **nephrotoxicity**, cisplatin, hypoxia inducible factor 1, kidney tubule, 548

cyclosporin A, immunosuppressive treatment, kidney transplantation, spironolactone, 541

nerve cell, adrenomedullin, oxytocin, oxytocin blood level,

oxytocin release, 358

calcium mobilization, chemokine receptor CCR2, monocyte chemotactic protein 1, 338

nerve cell excitability, anterior hypothalamus, exercise, 606

nerve cell plasticity, adaptation, auditory nervous system, 410

- complex formation, hippocampus, initiation factor 4E binding protein, initiation factor 4F, memory, protein function, translation regulation, 367

- learning, mitogen activated protein kinase, oncogene H ras, presynaptic membrane, synapsin I, 370

- learning, positive feedback, 345

- somatosensory system, visual system, 382

nerve conduction, 425

nerve excitability, pressoreceptor reflex, sympathetic nerve, 364 nerve potential, stimulus response, superior colliculus, 362 nervous system, temporal cortex, 440

neurohypophysis hormone, dehydration, sodium ion, vasopressin, vasopressin release, 588

neuroimaging, sensory cortex, 394

sensory cortex, sensory system, 393

neurokinin 1 receptor, hypothalamus hypophysis system, neurokinin 2 receptor, vasopressin, 374

neurokinin 2 receptor, hypothalamus hypophysis system, neurokinin 1 receptor, vasopressin, 374

neuromodulation, acetylcholine, Aplysia, motoneuron, temperature sensitivity, 422

neuropeptide, catecholamine, corticosteroid receptor, corticosterone, glucocorticoid receptor, hypophysis adrenal system, mineralocorticoid receptor, training, 608

- feeding behavior, protein isolation, 368

neurophysiology, reading, 371

neuropsychological test, education, reading, 452

neurotensin, dopamine, neurotransmission, nucleus accumbens,

neurotransmission, dopamine, neurotensin, nucleus accumbens,

glutamic acid, 433

newborn care, aggressiveness, fear, maternal behavior, 428 nicotine, dipeptidyl carboxypeptidase, endothelium cell, enzyme regulation, 487

nicotinic receptor, attention, depth perception, genetic polymorphism, 372

nitric oxide, adenosine A1 receptor agonist, 2 chloro 6 n

cyclopentyladenosine, delta opiate receptor agonist, heart infarction, inducible nitric oxide synthase, 503

- arachidonic acid, blood pressure, 20 hydroxyicosatetraenoic acid, icosanoid, kidney function, n(g) nitroarginine methyl ester, pregnancy, 557

- calcitonin gene related peptide receptor, fetus circulation, 479 - cardiopulmonary hemodynamics, geographic elevation,

oxygen, 591

- cardiovascular disease, diabetes mellitus, inducible nitric oxide synthase, 493

- corticosteroid, diclofenac, fever, lipopolysaccharide, n(g) nitroarginine methyl ester, prostaglandin, thermoregulation, 584

- cyclic GMP dependent protein kinase, skin conductance, 333

- dimethylargininase, endothelial nitric oxide synthase, exercise, heart failure, nitric oxide synthase inhibitor, 607 - exercise, 611

nitric oxide synthase inhibitor, dimethylargininase, endothelial nitric oxide synthase, exercise, heart failure, nitric oxide,

n(g) nitroarginine methyl ester, arachidonic acid, blood pressure. 20 hydroxyicosatetraenoic acid, icosanoid, kidney function, nitric oxide, pregnancy, 557

- corticosteroid, diclofenac, fever, lipopolysaccharide, nitric oxide, prostaglandin, thermoregulation, 584

noise reduction, hearing aid, 390

nonsteroid antiinflammatory agent, acetylsalicylic acid 3 (nitroxymethyl)phenyl ester, celecoxib, cyclooxygenase 2 inhibitor, hypertension, 546

nonverbal communication, amygdaloid nucleus, auditory cortex, crying, hemispheric dominance, insula, 444

nuclear magnetic resonance imaging, extraocular muscle, eye movement control, 460

nuclear magnetic resonance spectroscopy, exercise, functional magnetic resonance imaging, 375 nucleotide sequence, adrenergic system, melanocortin 4 receptor,

messenger RNA, protein expression, white adipose tissue,

- circadian rhythm, gene function, opsin, 344

- cytokine release, diaphragm muscle, malnutrition, muscle growth, tumor necrosis factor alpha, 525

nucleus accumbens, dopamine, neurotensin, neurotransmission,

nutrition, endurance, physical performance, 615 - psychometry, sport, 639

nutritional support, enteric feeding, glucose, glucose transport, intralipid, liver metabolism, total parenteral nutrition, travasol, 571

obesity, gene overexpression, immediate early gene, intestine absorption, 568

olfactory receptor, smelling, 381

oncogene c fos, circadian rhythm, gene, suprachiasmatic nucleus,

oncogene H ras, learning, mitogen activated protein kinase, nerve cell plasticity, presynaptic membrane, synapsin I, 370

opiate receptor, calcium, calcium transport, morphine, 332 opsin, circadian rhythm, gene function, nucleotide sequence, 344 optokinetic stimulation, otolith, 361

organic cation transporter, enzyme activation, epidermal growth factor, estrone sulfate, kidney proximal tubule, mitogen activated protein kinase, phosphatidylinositol 3 kinase, protein tyrosine kinase, 544

osteoblast, isoprotein, transcription factor, 330

osteoclast differentiation factor, calcium transport, metabolic acidosis, osteolysis, tumor necrosis factor alpha, 562

osteolysis, calcium transport, metabolic acidosis, osteoclast differentiation factor, tumor necrosis factor alpha, 562 otolith, optokinetic stimulation, 361

ovalbumin, asthma, carbon dioxide, chemical analysis, oxygen, protein analysis, 527

oxidation, aging, exercise, 614

carbohydrate, carbohydrate metabolism, carbon dioxide, 574

oxidative stress, enzyme analysis, exercise, reduced nicotinamide adenine dinucleotide phosphate oxidase, 629

oxygen, arm exercise, hemoglobin, leg exercise, oxygen consumption, 609

- asthma, carbon dioxide, chemical analysis, ovalbumin, protein analysis, 527
- blood volume, carbon monoxide, diagnostic error, erythropoietin, 513
- cardiopulmonary hemodynamics, geographic elevation, nitric oxide, 591
- dynamic exercise, leg blood flow, muscle blood flow, oxygen consumption, 623
- exercise, skin blood flow, sweating, thermoregulation, 622
 oxygen consumption, arm exercise, hemoglobin, leg exercise, oxygen, 609
 - dynamic exercise, leg blood flow, muscle blood flow, oxygen, 623
- physical activity, 595
- **oxygen sensing,** calcium activated potassium channel, heme oxygenase 2, voltage gated potassium channel, 413
- oxytocin, adrenomedullin, nerve cell, oxytocin blood level, oxytocin release, 358
- oxytocin blood level, adrenomedullin, nerve cell, oxytocin, oxytocin release, 358
- **oxytocin release,** adrenomedullin, nerve cell, oxytocin, oxytocin blood level, 358
- pain, heat sensation, sensory stimulation, stimulus response, 580 perception, functional magnetic resonance imaging, illusion, learning, 445
- **perceptive discrimination,** body posture, proprioception, touch, 353
- **percutaneous transluminal angioplasty,** atherosclerosis, collagen, elastin, 500
- **perfusion pressure**, hemodynamics, vasoconstriction, vein blood flow. 506
- **periaqueductal gray matter,** 4 aminobutyric acid receptor stimulating agent, muscimol, sympathetic blocking, sympathetic innervation, 406
 - breathing muscle, respiration control, 515
- peroxisome proliferator activated receptor agonist, diabetic nephropathy, kidney tubule cell, phenylacetic acid derivative, pioglitazone, 2,4 thiazolidinedione derivative, 550
- peroxisome proliferator activated receptor alpha, heart mitochondrion, thyroid gland, thyroid hormone, 504 pethidine, shivering, thermal analysis, water immersion, 589 phenanthrene derivative, aristolochic acid, plant extract, 551 phenylacetic acid derivative, diabetic nephropathy, kidney tubule cell, peroxisome proliferator activated receptor agonist,
- pioglitazone, 2,4 thiazolidinedione derivative, 550 **phosphatase**, phosphatidic acid, sphingosine 1 phosphate, 323 **phosphate**, calcitriol, fibroblast growth factor 23, phosphate metabolism, vitamin D metabolism, vitamin D receptor, 563
- phosphate metabolism, adenosine triphosphate, aging, creatine kinase, creatine phosphate, high energy phosphate, muscle metabolism, skeletal muscle, 466
 - calcitriol, fibroblast growth factor 23, phosphate, vitamin D metabolism, vitamin D receptor, 563
- phosphatidic acid, phosphatase, sphingosine 1 phosphate, 323 phosphatidylinositol 3 kinase, enzyme activation, epidermal growth factor, estrone sulfate, kidney proximal tubule, mitogen activated protein kinase, organic cation transporter, protein tyrosine kinase, 544
 - enzyme activity, heart hypertrophy, heart size, signal transduction. 613
- phospholipase C, arachidonic acid, B lymphocyte, calcium signaling, diacylglycerol, 5 hydroperoxy 6,8,11,14 icosatetraenoic acid, 20 hydroxyicosatetraenoic acid, inflammation, inositol 1,4,5 trisphosphate, 326
- phospholipase C beta3, calcium ion, calcium signaling, glucose, mesangium cell, protein kinase C, 547
- phospholipid, dipalmitoylphosphatidylcholine, lung alveolus

- surface tension, lung surfactant, phospholipid metabolism, $516\,$
- phospholipid metabolism, dipalmitoylphosphatidylcholine, lung alveolus surface tension, lung surfactant, phospholipid, 516
- physical activity, oxygen consumption, 595
- physical performance, endurance, nutrition, 615
- physiology, anthropometry, football, 638
- pioglitazone, diabetic nephropathy, kidney tubule cell, peroxisome proliferator activated receptor agonist, phenylacetic acid derivative, 2,4 thiazolidinedione derivative, 550
- plant extract, aristolochic acid, phenanthrene derivative, 551 plasticity, calcium signaling, mechanotransduction, skeletal muscle, slow muscle fiber, 465
- pleura cavity, echography, 524
- podocyte, actin, CD2 associated protein, docking protein, green fluorescent protein, 549
- portal vein blood flow, blood pressure regulation, 592
- **positive end expiratory pressure,** intermittent positive pressure ventilation, swallowing, 533
- positive feedback, learning, nerve cell plasticity, 345
- potassium, calcium, crypt cell, membrane transport, potassium transport, 328
- potassium channel, carotid artery, 502
- kidney collecting tubule, mineralocorticoid, potassium ion, protein tyrosine kinase, sodium channel, sodium ion, 545
- potassium current, potassium ion, thiopental, 331 potassium ion, kidney collecting tubule, mineralocorticoid, potassium channel, protein tyrosine kinase, sodium channel, sodium ion, 545
 - potassium current, thiopental, 331
- potassium transport, calcium, crypt cell, membrane transport, potassium, 328
- **potentiometry**, dopamine, dopamine release, reward, striate cortex, 435
- **prefrontal cortex,** corpus striatum, learning, 336 emotion, 443
- pregnancy, arachidonic acid, blood pressure, 20
 - hydroxyicosatetraenoic acid, icosanoid, kidney function, nitric oxide, n(g) nitroarginine methyl ester, 557
 - cyclooxygenase 2, fever, immunoglobulin enhancer binding protein, lipopolysaccharide, mitogen activated protein kinase 1, mitogen activated protein kinase 3, STAT5 protein, 585
- pressoreceptor reflex, blood pressure regulation, heart rate variability, 483
- muscle spindle afferent nerve, static exercise, tendon, 468
- nerve excitability, sympathetic nerve, 364
- pressor response, 4 aminobutyric acid A receptor stimulating agent, arterial pressure, muscimol, solitary tract nucleus, 507
- **presynaptic membrane**, learning, mitogen activated protein kinase, nerve cell plasticity, oncogene H ras, synapsin I, 370
- **progesterone,** calcium activated potassium channel, smooth muscle contractility, 531
- **proprioception,** body posture, perceptive discrimination, touch, 353
- hand, spatial discrimination, time perception, vision, 352 **prostaglandin,** corticosteroid, diclofenac, fever,
 - lipopolysaccharide, nitric oxide, n(g) nitroarginine methyl ester, thermoregulation, 584
- **prostaglandin E2,** juxtaglomerular apparatus, kidney, prostaglandin E receptor, renin, renin release, 539
- prostaglandin E receptor, juxtaglomerular apparatus, kidney, prostaglandin E2, renin, renin release, 539
- prostaglandin receptor, inhibitory guanine nucleotide binding protein, kidney collecting tubule, water absorption, 552
- protein analysis, asthma, carbon dioxide, chemical analysis, ovalbumin, oxygen, 527
 - brain natriuretic peptide, kidney function, 556
- complementary DNA, gill, sodium proton exchange protein 3, vertebrate, 518
- fast muscle, inhibitor of differentiation 2, protein p53, skeletal muscle, slow muscle, 469

protein deficiency, fast muscle fiber, limb girdle muscular dystrophy, sarcoglycan, slow muscle fiber, 463

protein expression, adrenergic system, melanocortin 4 receptor, messenger RNA, nucleotide sequence, white adipose tissue, 426

protein function, complex formation, hippocampus, initiation factor 4E binding protein, initiation factor 4F, memory, nerve cell plasticity, translation regulation, 367

protein inhibitor, sodium calcium exchange protein, 456 protein isolation, feeding behavior, neuropeptide, 368

protein kinase B, glucose transporter 4, guanosine triphosphatase activating protein, 325

protein kinase C, blood brain barrier, cell membrane

permeability, endothelium cell, hypoxia, 488

- calcium ion, calcium signaling, glucose, mesangium cell, phospholipase C beta3, 547

protein kinase C epsilon, cell structure, heart muscle cell, 481 protein p53, fast muscle, inhibitor of differentiation 2, protein analysis, skeletal muscle, slow muscle, 469 protein protein interaction, breast epithelium, gene expression,

gene product, 587

protein tyrosine kinase, enzyme activation, epidermal growth factor, estrone sulfate, kidney proximal tubule, mitogen activated protein kinase, organic cation transporter, phosphatidylinositol 3 kinase, 544

- kidney collecting tubule, mineralocorticoid, potassium channel, potassium ion, sodium channel, sodium ion, 545

psychometry, nutrition, sport, 639

pulse wave, blood pressure, 476 pump, lymph vessel, 508

Purkinje fiber, heart muscle, 458

pyramidal nerve cell, depolarization, sodium channel, spike, 369

reactive oxygen metabolite, adenosine diphosphate ribosyl cyclase, angiotensin, calcium signaling, vascular smooth muscle, 540

reading, education, neuropsychological test, 452 neurophysiology, 371

rebreathing, exercise, lung diffusion capacity, 634 receptor sensitivity, autonomic nervous system function,

cholinergic receptor, heart automaticity, sympathetic tone,

receptor subtype, adrenergic activity, alpha 1A adrenergic receptor, alpha 1 adrenergic receptor, artery, messenger RNA, 480

recognition, face, 438

reduced nicotinamide adenine dinucleotide phosphate oxidase, enzyme analysis, exercise, oxidative stress, 629

Henle loop, ion transport, kidney tubule, sodium proton exchange protein, 543

renin, juxtaglomerular apparatus, kidney, prostaglandin E2, prostaglandin E receptor, renin release, 539

renin release, juxtaglomerular apparatus, kidney, prostaglandin E2, prostaglandin E receptor, renin, 539

respiration control, breathing muscle, periaqueductal gray matter,

reticulocyte, athlete, CD34 antigen, exercise, Flt3 ligand, granulocyte colony stimulating factor, hematopoietic stem cell, interleukin 6, 610

retina cone, 409

reward, dopamine, dopamine release, potentiometry, striate cortex, 435

rhesus antigen, ammonia, carrier protein, glycoprotein, 324 right hemisphere, auditory stimulation, hemispheric dominance,

rotation, attention, touch, vestibular system, visual orientation,

sarcoglycan, fast muscle fiber, limb girdle muscular dystrophy, protein deficiency, slow muscle fiber, 463

sarcomere, excitation contraction coupling, heart muscle contractility, 495

- heart muscle contractility, 496

sarcoplasmic reticulum, calcium, calcium cell level, calcium transport, heart muscle cell, 474

self report, athlete, eye protective device, 640 sensorimotor cortex, superior colliculus, 396 sensorimotor function, ankle, brain, limb movement, 343 sensory cortex, brain cortex, mesencephalon, 395

neuroimaging, 394

- neuroimaging, sensory system, 393

sensory nerve, dizocilpine, food intake, ion transport, n methyl dextro aspartic acid, n methyl dextro aspartic acid receptor, solitary tract nucleus, vagus nerve, 365

motor activity, 427

sensory stimulation, auditory cortex, auditory stimulation, tactile stimulation, 349

- heat sensation, pain, stimulus response, 580

sensory system, neuroimaging, sensory cortex, 393 sequential analysis, finger, hand movement, motor activity, 379 serotonin, microvascularization, muscle metabolism, muscle

perfusion, vasoconstriction, 471 sex difference, aging, muscle strength, muscle training, 473

- estrogen, estrogen activity, thalamus ventral nucleus, 346
- micturition, 554

- muscle strength, muscle training, 620

shear rate, capillary, hydraulic conductivity, 491

shear strength, carotid artery, endothelial nitric oxide synthase,

shear stress, blood viscosity, hypotension, vascular resistance, 492 shivering, pethidine, thermal analysis, water immersion, 589 shorebird, aerobic capacity, succinate dehydrogenase, 579 signal transduction, acetylcholine, avoidance behavior,

cholinergic system, enzyme inhibition, memory, mitogen activated protein kinase, 350

- enzyme activity, heart hypertrophy, heart size, phosphatidylinositol 3 kinase, 613

- functional magnetic resonance imaging, spatial discrimination, visual cortex, 439

sign language, auditory cortex, hearing impairment, visual cortex,

skeletal muscle, adenosine triphosphate, aging, creatine kinase, creatine phosphate, high energy phosphate, muscle metabolism, phosphate metabolism, 466

- calcium signaling, mechanotransduction, plasticity, slow muscle fiber, 465
- fast muscle, inhibitor of differentiation 2, protein analysis, protein p53, slow muscle, 469
- fatty acid oxidation, fatty acid synthase, fatty acid synthase inhibitor, hypothalamus, 564
- microanalysis, 470
- muscle fatigue, 455

skiing, muscle injury, supplementation, 600

skin blood flow, exercise, oxygen, sweating, thermoregulation,

insulin, iontophoresis, vasodilatation, 472

skin conductance, cyclic GMP dependent protein kinase, nitric

sleep, drowsiness, lung ventilation, 530

slow muscle, fast muscle, inhibitor of differentiation 2, protein analysis, protein p53, skeletal muscle, 469

slow muscle fiber, calcium signaling, mechanotransduction, plasticity, skeletal muscle, 465

- fast muscle fiber, limb girdle muscular dystrophy, protein deficiency, sarcoglycan, 463

smelling, 414

calcium ion, honeybee, mushroom body, 401

- olfactory receptor, 381

smooth muscle, asthma, expiratory flow, 529

smooth muscle contractility, calcium activated potassium channel, progesterone, 531

SNARE protein, binding protein, cyclic AMP dependent protein kinase, kidney collecting tubule, sodium channel, water absorption, 537

sodium, calcium, diastole, heart muscle contractile force, heart ventricle, sodium calcium exchange, 510

sodium calcium exchange, adenosine triphosphatase (potassium sodium), aorta, endothelium derived relaxing factor, 570

- calcium, diastole, heart muscle contractile force, heart ventricle, sodium, 510

sodium calcium exchange protein, protein inhibitor, 456 sodium channel, adenosine triphosphatase (potassium sodium), cyclic AMP dependent protein kinase, kidney collecting tubule, sodium transport, 542

- aquaporin 2, hypertension, kidney collecting tubule, 536

- binding protein, cyclic AMP dependent protein kinase, kidney collecting tubule, SNARE protein, water absorption, 537

- depolarization, pyramidal nerve cell, spike, 369

- kidney collecting tubule, mineralocorticoid, potassium channel, potassium ion, protein tyrosine kinase, sodium ion, 545

sodium chloride, kidney blood flow, natriuresis, 555

sodium ion, dehydration, neurohypophysis hormone, vasopressin, vasopressin release, 588

- kidney collecting tubule, mineralocorticoid, potassium channel, potassium ion, protein tyrosine kinase, sodium channel, 545

sodium proton exchange protein, Henle loop, ion transport, kidney tubule, reduced nicotinamide adenine dinucleotide phosphate oxidase, 543

sodium proton exchange protein 1, atrial natriuretic factor, atrial natriuretic factor receptor, calcineurin, cariporide, hypertension, 475

sodium proton exchange protein 3, complementary DNA, gill,

protein analysis, vertebrate, 518
sodium transport, adenosine triphosphatase (potassium sodium), cyclic AMP dependent protein kinase, kidney collecting tubule, sodium channel, 542

sodium urine level, binaltorphimine, kappa opiate receptor, kappa opiate receptor antagonist, kidney function, 553

soleus muscle, breathing rate, extensor digitorum longus muscle, mitochondrial respiration, muscle cell, 464

solitary tract nucleus, 4 aminobutyric acid A receptor stimulating agent, arterial pressure, muscimol, pressor response, 507

- dizocilpine, food intake, ion transport, n methyl dextro aspartic acid, n methyl dextro aspartic acid receptor, sensory nerve, vagus nerve, 365

somatosensory cortex, 387

4 aminobutyric acid A receptor stimulating agent, electroencephalography, muscimol, 402

- auditory cortex, 386

somatosensory system, event related potential, information processing, magnetoencephalography, motor system, 421 nerve cell plasticity, visual system, 382

spatial discrimination, functional magnetic resonance imaging, signal transduction, visual cortex, 439

- hand, proprioception, time perception, vision, 352

spatial orientation, auditory discrimination, tactile discrimination, 356

- body image, tactile discrimination, 355

species distribution, species richness, 577

species richness, species distribution, 577

speech analysis, biological marker, evoked brain stem auditory response, hearing, speech perception, 441

speech perception, biological marker, evoked brain stem auditory response, hearing, speech analysis, 441

spermatogenesis, microtubule protein, 558

sphingosine 1 phosphate, phosphatase, phosphatidic acid, 323 spike, depolarization, pyramidal nerve cell, sodium channel, 369

spike wave, electromyography, hand movement, 461 spinal cord nerve cell, 4 aminobutyric acid, GABAergic system, interneuron, 359

spinal nerve, 4 aminobutyric acid, brain maturation, chloride, chloride transport, GABAergic transmission, 408 spironolactone, cyclosporin A, immunosuppressive treatment,

kidney transplantation, nephrotoxicity, 541 splanchnic blood flow, hyperemia, hypervolemia, tachycardia,

Valsalva maneuver, 482

split brain, interhemispheric transfer, 399 400 sport, athlete, caloric intake, 601

- athlete, training, 636

- diving, lung ventilation, 616

nutrition, psychometry, 639

sports medicine, 596

fatigue, 594

jumping, 603

STAT5 protein, cyclooxygenase 2, fever, immunoglobulin enhancer binding protein, lipopolysaccharide, mitogen activated protein kinase 1, mitogen activated protein kinase 3, pregnancy, 585

static exercise, muscle spindle afferent nerve, pressoreceptor reflex, tendon, 468

stereotypy, auditory stimulation, inferior colliculus, stimulus response, 403

stimulus response, auditory stimulation, inferior colliculus, stereotypy, 403

- heat sensation, pain, sensory stimulation, 580

- nerve potential, superior colliculus, 362

- visual cortex, 404

stress, adrenergic receptor, adrenergic system, alpha 1 adrenergic receptor, heat shock protein 72, 380

- cardiovascular response, emotion, facial expression, hypothalamus hypophysis adrenal system, 454 - hostility, testosterone, 451

- hydrocortisone, 450

striate cortex, dopamine, dopamine release, potentiometry, reward, 435

stromelysin 3, 327

subarachnoid hemorrhage, brain vasospasm, 20

hydroxyicosatetraenoic acid, 498

succinate dehydrogenase, aerobic capacity, shorebird, 579 suicide, 593

sulfate, kinetics, metabolism, 572

sulfotransferase, 532

superior colliculus, brain metabolism, glutamate transporter, visual stimulation, 565

- nerve potential, stimulus response, 362

- sensorimotor cortex, 396

supplementation, muscle injury, skiing, 600

suprachiasmatic nucleus, circadian rhythm, gene, oncogene c fos. 363

swallowing, intermittent positive pressure ventilation, positive end expiratory pressure, 533

sweating, exercise, oxygen, skin blood flow, thermoregulation,

swimming, hibernation, turtle, 576

sympathetic blocking, 4 aminobutyric acid receptor stimulating agent, muscimol, periaqueductal gray matter, sympathetic innervation, 406

sympathetic innervation, 4 aminobutyric acid receptor stimulating agent, muscimol, periaqueductal gray matter, sympathetic blocking, 406

sympathetic nerve, nerve excitability, pressoreceptor reflex, 364 sympathetic tone, autonomic nervous system function, cholinergic receptor, heart automaticity, receptor sensitivity, 485

synapse, cell adhesion molecule, membrane protein, 348

- thalamocortical tract, wakefulness, 341

synapsin I, learning, mitogen activated protein kinase, nerve cell plasticity, oncogene H ras, presynaptic membrane, 370 synaptic transmission, amygdaloid nucleus, facilitation, fear,

learning, 437

- cocaine, cocaine dependence, connexin 36, gap junction, 432 syncope, carbon monoxide, heart output, muscle tone, 619

systolic blood pressure, aging, body weight, heart rate variability,

tachycardia, hyperemia, hypervolemia, splanchnic blood flow, Valsalva maneuver, 482

tactile discrimination, auditory discrimination, spatial orientation, 356

- body image, spatial orientation, 355

- body movement, visual orientation, 351

tactile stimulation, auditory cortex, auditory stimulation, sensory stimulation, 349

- time perception, visual stimulation, 354

task performance, memory, motor performance, 434

taste, food, 415

taste preference, amygdaloid nucleus, flavor, learning, 436 temperature sensitivity, acetylcholine, Aplysia, motoneuron, neuromodulation, 422

temporal cortex, nervous system, 440

tendon, muscle spindle afferent nerve, pressoreceptor reflex, static exercise, 468

testosterone, aging, androgen, androgen receptor, cardiovascular disease, chronic kidney disease, endothelin, hormone action, 534

exercise, testosterone release, 632

- hostility, stress, 451

testosterone release, exercise, testosterone, 632

thalamocortical tract, gap junction protein, 340 synapse, wakefulness, 341

thalamus, brain cortex, 342

vibrissa, 388

thalamus ventral nucleus, estrogen, estrogen activity, sex difference, 346

thermal analysis, pethidine, shivering, water immersion, 589 thermoregulation, bacterium lipopolysaccharide, 582 - corticosteroid, diclofenac, fever, lipopolysaccharide, nitric

oxide, n(g) nitroarginine methyl ester, prostaglandin, 584

 cvclooxygenase 1, cvclooxygenase 2, fever. lipopolysaccharide, 583

exercise, oxygen, skin blood flow, sweating, 622

theta rhythm, brain cortex, brain function, hippocampus, 366 2,4 thiazolidinedione derivative, diabetic nephropathy, kidney tubule cell, peroxisome proliferator activated receptor agonist, phenylacetic acid derivative, pioglitazone, 550

thiopental, potassium current, potassium ion, 331 thixotropy, ballistics, joint function, wrist, 631

thyroid gland, heart mitochondrion, peroxisome proliferator activated receptor alpha, thyroid hormone, 504

thyroid hormone, heart mitochondrion, peroxisome proliferator activated receptor alpha, thyroid gland, 504

time perception, depth perception, hearing, vision, 430 - hand, proprioception, spatial discrimination, vision, 352

- tactile stimulation, visual stimulation, 354

total parenteral nutrition, enteric feeding, glucose, glucose transport, intralipid, liver metabolism, nutritional support, travasol, 571

touch, attention, rotation, vestibular system, visual orientation, 412 - body posture, perceptive discrimination, proprioception, 353

trachea muscle, calcium ion, cation, cation transport, cyclopiazonic acid, 526

training, athlete, coordination, 605

- athlete, sport, 636

- catecholamine, corticosteroid receptor, corticosterone, glucocorticoid receptor, hypophysis adrenal system, mineralocorticoid receptor, neuropeptide, 608

transcranial magnetic stimulation, attention, vision, visual adaptation, 407

transcription factor, isoprotein, osteoblast, 330

transient receptor potential channel, B lymphocyte, B lymphocyte receptor, 334

translation regulation, complex formation, hippocampus, initiation factor 4E binding protein, initiation factor 4F, memory, nerve cell plasticity, protein function, 367

travasol, enteric feeding, glucose, glucose transport, intralipid, liver metabolism, nutritional support, total parenteral nutrition, 571

tryptophan hydroxylase, amygdaloid nucleus, gene function, genetic variability, 357

tumor necrosis factor alpha, calcium transport, metabolic acidosis, osteoclast differentiation factor, osteolysis, 562 - cytokine release, diaphragm muscle, malnutrition, muscle

growth, nucleotide sequence, 525 turtle, hibernation, swimming, 576

vagus nerve, dizocilpine, food intake, ion transport, n methyl dextro aspartic acid, n methyl dextro aspartic acid receptor, sensory nerve, solitary tract nucleus, 365

Valsalva maneuver, hyperemia, hypervolemia, splanchnic blood flow, tachycardia, 482

vascularization, motor cortex, 511

vascular resistance, blood viscosity, hypotension, shear stress,

vascular smooth muscle, adenosine diphosphate ribosyl cyclase, angiotensin, calcium signaling, reactive oxygen metabolite, 540

vasculotropin, aging, capillary density, exercise, messenger RNA, vasculotropin receptor, vastus lateralis muscle, 627

vasculotropin receptor, aging, capillary density, exercise, messenger RNA, vasculotropin, vastus lateralis muscle, 627

vasoconstriction, adenosine triphosphate, cystic fibrosis, exercise, hyperemia, 626

- hemodynamics, perfusion pressure, vein blood flow, 506

- microvascularization, muscle metabolism, muscle perfusion, serotonin, 471

vasodilatation, insulin, iontophoresis, skin blood flow, 472 vasomotor reflex, blood pressure regulation, hydrogen peroxide,

vasopressin, dehydration, neurohypophysis hormone, sodium ion, vasopressin release, 588

- hypothalamus hypophysis system, neurokinin 1 receptor, neurokinin 2 receptor, 374

vasopressin release, dehydration, neurohypophysis hormone, sodium ion, vasopressin, 588
vastus lateralis muscle, aging, capillary density, exercise,

messenger RNA, vasculotropin, vasculotropin receptor,

vein blood flow, hemodynamics, perfusion pressure, vasoconstriction, 506

ventral tegmentum, dopaminergic nerve cell, 424

vertebrate, complementary DNA, gill, protein analysis, sodium proton exchange protein 3, 518

vestibular nucleus, 4 aminobutyric acid A receptor, brain development, 389

vestibular system, attention, rotation, touch, visual orientation,

vibration, hand muscle, muscle force, muscle stretching, 624 vibrissa, thalamus, 388

virus DNA, chromaffin cell, exocytosis, beta galactosidase, green fluorescent protein, 360

vision, attention, transcranial magnetic stimulation, visual adaptation, 407

- auditory system, memory, 397

- depth perception, hearing, time perception, 430

- hand, proprioception, spatial discrimination, time perception,

- touch, 398

visual adaptation, attention, transcranial magnetic stimulation, vision, 407

visual cortex, auditory cortex, hearing impairment, sign language,

- functional magnetic resonance imaging, signal transduction, spatial discrimination, 439

stimulus response, 404

visual orientation, attention, rotation, touch, vestibular system,

- body movement, tactile discrimination, 351

visual stimulation, brain metabolism, glutamate transporter, superior colliculus, 565

- tactile stimulation, time perception, 354

visual system, auditory cortex, 383

nerve cell plasticity, somatosensory system, 382

vitamin D metabolism, calcitriol, fibroblast growth factor 23, phosphate, phosphate metabolism, vitamin D receptor, 563

vitamin D receptor, calcitriol, fibroblast growth factor 23, phosphate, phosphate metabolism, vitamin D metabolism,

vitamin intake, ascorbic acid, carbohydrate, carbohydrate intake, cytokine, exercise, immune response, 597

voltage gated potassium channel, calcium activated potassium channel, heme oxygenase 2, oxygen sensing, 413

wakefulness, synapse, thalamocortical tract, 341 walking, body position, hip, 423

water absorption, binding protein, cyclic AMP dependent protein kinase, kidney collecting tubule, SNARE protein, sodium channel, 537

- inhibitory guanine nucleotide binding protein, kidney collecting tubule, prostaglandin receptor, 552

water immersion, pethidine, shivering, thermal analysis, 589 white adipose tissue, adrenergic system, melanocortin 4 receptor,

messenger RNA, nucleotide sequence, protein expression, 426

working memory, attention, auditory discrimination, 337 wrist, ballistics, joint function, thixotropy, 631

X ray, computer assisted tomography, lung mechanics, lung ventilation, 522

AUTHOR INDEX

(figures refer to item numbers)

Abe A.S. 514 Ache B.W. 381 Adams J.A. 611 Addad F. 500 Adolphs R. 443 Afkhami M. 329 Akhmanova A. 558 Albanese M.-C. 580 Alberts J.L. 418 Alexeeva V. 368 Almeida R. 440 Altes T.A. 521 Alway S.E. 469 Amann M. 600 Andersen J.L. 555 Andrade D.V. 514 Andreescu C.E. 361 Ang C.W. 366 Anglada-Figueroa D. 442 Anson J.G. 434 Antonelli M. 519 Arbeille P.P. 592 Arendshorst W.J. 540 Argaud L. 494 Arshavsky Y.I. 427 Arteaga G.M. 496 Ashton-Rickardt P.G. 322 Atefy R. 612 Augath M. 349 Aukland K. 508 Axelson H.W. 631

Babilonia E. 545 Baer C. 605 Bal M.P. 509 Balakrishnan S. 510 Banisadr G. 338 Banko J.L. 367 Barakat M.T. 363 Barnes S.A. 621 Barth D.S. 386 Barton M.J. 376 Başar E. 453 Baum A.L. 593 Beck K. 520 Beck K.C. 634 Befroy D.E. 466 Begum G. 561 Bell R.A. 598 Beneka A. 473 Bentivegna F. 576 Bergan J.F. 410 Berman R.A. 399, 400 Bers D.M. 474 Besle J. 397 Besnard S.S. 592 Bezdudnaya T. 341 Bharathi A.V. 477 Bie P. 555 Blanco J.A. 541 Blankertz B. 419 Blitek A. 573 Blomstrand E. 373 Bohman Q.C. 498 Bonath B. 430 Borg L.K. 488 Boudreau D. 408 Boyman L. 456 Boynton G.M. 411

Brandeis D. 371 Brasselet C. 500 Braun B. 632 Brem S. 371 Brette F. 474 Brevard M.E. 347 Brezina V. 422 Brimacombe J. 590 Bristow G.K. 589 Bronst A. 603 Bruegger D. 486 Brun J.-F. 614 Bucher K. 371 Buholzer O. 604 Burge C.M. 513 Burguillos L. 328 Burns G.A. 365 Bushinsky D.A. 562 Bustamante M. 542

Butterworth M.B. 537

Byrd D.A. 452

Cağlar E. 375 Calbet J.A.L. 609 Campisi J. 380 Canli T. 357 Cao V.H. 363 Carlson G.C. 366 Carmosino M. 552 Carneiro E.M. 586 Carpentier B. 492 Carpi A. 472 Carroll J. 409 Carter III R. 633 Casagrande V.A. 416 Castellani J.W. 633 Castro J.P.M.V. 429 Cha S.H. 564 Chabicovsky M. 321 Chan O. 608 Chantler P.D. 489 Chatsudthipong V. 544 Chavanis N. 494 Chen G. 346 Chen J. 531 Chen S. 337 Chen S.-S. 571 Chen X. 550 Chen Y. 607 Cheuvront S.N. 633 Choe K.P. 518 Chohnan S. 564 Chon D. 520 Chu D. 581 Ciccarelli O. 343 Cillessen S.A.G.M. 497 Clark R.A. 460 Clarke S. 396 Clements R.E. 489 Clemmesen O. 556 Clénin G.E. 604 Colby C.L. 399, 400 Congdon E. 357 Connors B.W. 340

Croley A.N. 627 Cruikshank S.J. 340 Cruz Y. 554 Cunha D.A. 586 Cunliffe A. 561 Curio G. 419

Da Silva S.P. 428 Da X. 525 Dahl R.E. 454 Dajani H.R. 391 Dallinger R. 321 Dalsgaard M.K. 556 Dalton N.D. 591 D'Ambrosio A.-M. 324 Danieli-Betto D. 463 Danoff J.V. 470 Dantzler W.H. 544 Darlington C.L. 389 Darroch P. 323 Davatzikos C. 378 Davenport P.W. 515 Davies D.M. 615 Davis T.P. 488 Davison G. 597 Davison G.W. 598 De Alves M.C. 586 De Azevedo M.S. 428 De Bruin I.G.J.M. 619 De Jeu M.T.G. 361 De Oliveira M. 483 De Ruiter M.M. 361 De Vries W.B. 509 De Windt L.J. 475 De Zeeuw C.I. 361 Dean C. 406 Dean V.L. 626 Deco G. 440 Del Castillo J.R. 328 Delacuisine B. 396 Delmonico M.J. 620 Demer J.L. 460 Dempsey J.A. 528 Derive S. 541 Deruelle F. 630 Deschênes M. 388 Despa S. 474 DeWeese M.R. 383 Dias Da Silva V.J. 483 Ditzen M. 401 Dobkins K.R. 411 Doldo N.A. 620 Donelan J.M. 423 Dougherty K.J. 359 Dounskaia N. 417 Downie J.W. 554 Doyle T.L.A. 638 Driver J. 407

Ebner F.F. 402 Eiberg S. 595 Eime R. 640 Eisenach J.H. 621 El-Husseini A. 348

Du W. 560

Duan Y. 538

Dubois A. 565

Duclay J. 462

Durand E. 500

Dufresne C. 388

Duncan G.H. 580

Elgersma Y. 370 Ellis S. 585 Elston-Güttler K.E. 448 Endlich N. 549 Engineer N.D. 405 Enoka R.M. 624 Erzurum S.C. 591 Escartin C. 565 Esposito A. 463 Evans K.L. 577 Evans P.R. 579

Fabre C. 630 Fain S.B. 521 Fan Y. 378 Faraci F. 502 Fatouros I. 473 Fazan Jr. R. 483 Fellner S.K. 540 Fendrich R. 430 Ferrel R.E. 629 Figliozzi F. 412 Finch C. 640 Fine I. 411 Finney E.M. 411 Finucane C. 420 Finucane C.M. 351 Fleegal M.A. 488 Flinn W.R. 602 Folch N. 574 Foley C.M. 364 Forbes S.C. 618 Fort A. 397 Fossella J.A. 372 Fournier M. 525 Fox K. 382 Foxe J.J. 394 Frecker H. 547 Freedman B.D. 326 Frick K.K. 562 Friederici A.D. 449 Friedrich M. 449 Friis U.G. 539 Frizzell R.A. 537 Frussa-Filho R. 429 Fu Q. 506 Fujioka T. 447 Fukushiro D.F. 429 Fuster J. 440 Fyhrquist F. 487

Galfano G. 355 Galkin A. 401 Galkina E. 484 Gallez A. 580 Gams E. 616 Gandevia S.C. 628 Ganzeboom K.S. 619 Gao R. 559 Gardner A.S. 637 Gardner A.W. 602 Garelick T.S. 347 Gaston K.J. 577 Gazal O. 600 Gerber L.H. 470 Gerke V. 535 Germinario E. 463 Gerson L. 632 Giard M.-H. 397 Giesbrecht G.G. 589

Gillespie B.R. 365

1

Corbetta M. 439

Cordingley J.J. 530

Corin G. 455 Coscarella E. 511 Costa R. 519

Coull J.A.M. 408

Coulter D.A. 366

Cordero-Erausquin M. 408

Giovannini M.G. 350 Giovenardi M. 428 Giussani D.A. 479 Glaister M. 594 Glaubic-Latka M. 505 Gleeson M. 597 Gliddon C.M. 389 Godfrey R.J. 636 Goeritz M.L. 425 Gökce G. 549 Gokhale K. 578 Gomez L. 494 Gonzalez Andino S.L. 394 Gonzalez R.M. 454 Goodchild A.K. 485 Gore C.L. 513 Gosselin R.-D. 338 Gottlieb H.B. 553 Gratze G. 512 Gray D.A. 584 Greenwood J.J.D. 577 Greenwood P.M. 372 Grefhorst A. 567 Groemer G.E. 590 Grønfeldt V. 595 Guariglia P. 412 Gummels E. 611 Gunter T.C. 446 Guo Y. 503 Gusev A.G. 341 Gutknecht L. 357

Haas T. 590 Hagobian T. 632 Hamade M.W. 499 Hamadeh M.J. 572 Hamby S.M. 432 Hammer A. 567 Hancock M.J. 628 Harrar V. 398 Harré E.-M. 585 Harris C. 353 Harris L.R. 398 Harris N.R. 491 Harris R.B.S. 426 Hashimoto H. 358 Hasselstrom H. 595 Hasser E.M. 364 Hayes H. 587 Hayes S.G. 468 Hays G.C. 576 Hayward L.F. 515 Hébert R.L. 552 Heesch C.M. 364 Heimel J.A. 404 Heiser A. 335 Heiser L.M. 399, 400 Heistad D. 502 Helli P.B. 526 Henderson G. 332 Herard A.-S. 565 Herbert R.D. 628 Hertrich I. 377 Herzog W. 467 Hiller R. 456 Hilpert F. 335 Hiraumi H. 392 Hirose S. 518 Hochman S. 359 Hochscheid S. 576 Hödl E. 321 Hofer E. 458 Hofer H. 409 Hoffer L.J. 572

Hoffmann M.L. 588

Hoit B.D. 591 Holmberg H.-C. 609 Holmer H.K. 433 Holmes N.P. 352 Holstein-Rathlou N.-H. 555 Hom S. 488 Hopkins W.G. 513, 637 Hosein N. 571 Hou J.C. 566 Hou L. 367 Hromádka T. 383 Hu Z. 564 Huang H. 557 Huang Y.-F. 330 Hübner K. 603, 604 Huelsing D.J. 458 Hughes C.M. 598 Hung J. 407 Huo Y. 484 Hyland B.I. 434 Hyodo S. 358

Ikeda K. 450 Iliescu R. 534 Ingham S.A. 636 Inui K. 421 Iordanov H. 568 Ishii T. 384 Ishikawa M. 450 Itou T. 384 Iwashita S. 625 Izumiyama S. 327

Jabbour K. 625 Jackson K. 606 Jackson R.M. 426 Jacob M. 486 Jacques A.J. 528 Janssen L.J. 526 Jemel B. 438 Ji X. 560 Johns E.J. 546 Johnson B.D. 634 Johnson J.D. 380 Johnson J.P. 537 Johnson K.L. 441 Jones G.E. 615 Jonnalagadda S.S. 599 Jordan K. 434 Journeay W.S. 622 Juliano S.L. 387 Juszczak M. 374 Jyoti T. 510

Kaczmarek M. 573 Kahilogullari G. 511 Kakebeeke T.H. 605 Kakigi R. 457 Kamata K. 501 Kamerman P.R. 584 Kane S. 325 Kang M. 481 Kansaku K. 379 Kapusta D.R. 553 Kariagina A. 329 Kato A. 518 Katzel L.I. 602 Kaufman M.P. 468 Kawasaki H. 443 Kawasaki M. 358 Kayser C. 349 Keil A. 431 Kelly S.P. 420 Kemp A.H. 376 Kemp P.J. 413

Kenny G.P. 622 Kent-Braun J.A. 466, 569 Kerbeci P.P. 592 Keskin T. 375 Kida T. 457 Kilic A. 475 Kim D.-J. 575 Kim M.-H. 491 Kim M.Y. 570 Kim S. 333 Kim S.W. 536 Kindig A.E. 468 King J.A. 347, 451 Kipp R.W. 600 Kitagawa N. 356 Klose M.K. 581 Knight S. 546 Knoll K. 603 Knudsen E.I. 410 Kobayashi T. 501 Kochman K. 573 Kocijančič I. 524 Kocijančič K. 524 Koelsch S. 446 Kojima I. 548 Kostek M.C. 620 Kotz S.A. 448 Kowalchuk J.M. 618, 623 Kraus N. 441 Kream B.E. 330 Krediet C.T.P. 619 Krijnen P.A.J. 497

Kumpf S. 478

Kushner S.A. 370

Kwon T.-H. 536

Labelie E.F. 326 Lalor E.C. 420 Lambert R.K. 529 Landesberg A. 495 Landisman C.E. 340 Landry J.C. 339 Lane M.D. 564 Lang C.J. 516 Lanza I.R. 466, 569 LaPlante K. 562 Latka M. 505 Laubach M. 336 Lauer N. 478 Laurienti P.J. 393 Lavallée P. 388 Ledberg A. 440 Lee B.-W. 575 Lee L.-Y. 527 Lemm S. 419 Lerner J.S. 454 Leveritt M. 561 Levi R. 427 Levinson J.N. 348 Lewis M.I. 525 Ley K. 484 Li H. 403, 525 Li L. 402 Li N. 543 Li Q. 608 Li W.-H. 344 Li Y. 607 Liang G.H. 570 Lievremont J.-P. 334 Lim I. 333 Litschauer B. 490 Liu F. 330 Liu G. 566 Liu W. 538 Liu X. 326

Liu Y. 465 Lockhart T.L. 589 Logothetis N.K. 349 Long J. 323 Luo J. 613

Ma Y. 451

MacLean J.N. 425 MacLeod K.M. 493 MacPhee S.L. 623 Maeder M. 612 Maertens M. 445 Magometschnigg D. 476 Maj J.-B. 390 Malliou P. 473 Malmberg-Aiello P. 350 Maloney S.K. 584 Mancilla J.G. 340 Mandros C. 523 Manetta J. 614 Manly J.J. 452 Manoe R. 497 Markoff A. 535 Marsden J.F. 343 Marsh G.D. 618 Marti B. 603 Martí D. 480 Martin A. 462 Martini E.R. 506 Martini J. 492 Mathiak K. 377 Matsumoto T. 501 Maurer U. 371 Maurizio S. 472

Mausset-Bonnefont A.-L. 558 McCarty C. 640 McClure T.D. 504 McCracken C.B. 432 McGregor A.H. 455 McInnis N.H. 622 McLaughlin D.F. 387 McMullen J.R. 613 McNeill J.H. 493 McVea D.A. 423 Mechighel P. 338 Medow M.S. 482 Melara R.D. 337 Menendez R.G.D.P. 394 Menzel R.R. 386 Mercier J. 614 Mîinea C.P. 325 Miller J.D. 528 Miller M.S. 459 Milutinovic S. 496 Miquel R. 480 Mogensen M. 464 Møller K. 373 Momoi N. 331 Montgomery L.D. 482 Montgomery P.S. 602 Monty D.M. 592 Moonen M. 390 Moore C. 433 Moratti S. 431 Mordasini D. 542

Moreau R.L.M. 617

Moreira T.S. 507

Moreira V. 617

Morici G. 610

Morita T. 392 Moritz C.T. 624

Morrell M.I. 530

Mouihate A. 585

Mueller P.J. 364

Mouro-Chanteloup I. 324

Mujika I. 596 Müller K.-R. 419 Munk S. 547 Munn J. 628 Muraki S. 379 Murcia N.S. 538 Murphy A.J. 635 Murphy G.G. 370 Murray M.M. 394 Muth T. 616

Nagamine T. 392 Nagareddy P.R. 493 Nakata H. 421, 457 Nakazato T. 435 Navalesi P. 519 Negrete A.C. 492 Neitz J. 409 Nelson J.A. 601 Nelson S.B. 404 Newell F.N. 351 Newman J.M.B. 471 Newton R.U. 638 Nichols P.E. 599 Nicol TG 441 Nishimura M. 384 Noesselt T. 430 Noh J.-H. 575 Norwich K.H. 572 Nourry C. 630 Nsegbe E. 533 Numaga T. 334 Nybo L. 373

Oberecker R. 449 Odaka C. 327 O'Hara B.F. 363 Ohashi M. 502 Ohse T. 548 Okazaki K. 506 Ono T. 331 Orchard C.H. 474 Orgeig S. 516 Otis T.S. 345 Overstreet D.H. 485 Own N. 640 Oya H. 443

Nyman T. 487

Padley J.R. 485 Pallas S.L. 362 Palmer B.M. 459 Panchapakesan U. 550 Panth S.R. 521 Parasuraman R. 372 Park E. 608 Park J.-J. 629 Park J.-Y. 629 Pascoe M.A. 624 Pasqualotto A. 351 Patel K.M. 432 Paterson D.H. 623 Paulmann S. 448 Pauloin A. 587 Pavani F. 355 Pazzagli M. 350 Péan M. 574 Pearson K.G. 423 Pedlar C.R. 636 Pegelow D.F. 528 Percaccio C.R. 405 Pérez-Rojas J.M. 541 Péronnet F. 574 Perrault T.J. 393 Pertens E. 526

Pessin J.E. 566 Peters M.J. 385 Petkov C.I. 349 Pfaff D.W. 346 Phillips T.M. 470 Pike T.L. 621 Pilowsky P.M. 485 Pisani M. 438 Pittman Q.J. 585 Pollmann S. 445 Pollock C.A. 550 Postle A.D. 516 Poulin F. 367 Poussin K. 587 Prasad N.G. 578 Prefaut C. 614 Probst A. 396 Proekt A. 368 Pruette A.L. 405 Purcell D. 391 Pyne D.B. 637

Quirk G.J. 442

Rainville P. 580 Raju V.T. 557 Randall W.R. 465 Rassier D.E. 467 Raymer G.H. 618 Razak K.A. 362 Reardon F.D. 622 Reckelhoff J.F. 534 Reed G.W. 451 Rehm M. 486 Rema V. 402 Remy S. 369 Renic M. 498 Rice A.J. 596 Richards D.A.B. 635 Richards S.M. 471 Ritter R.C. 365 Rivlis G. 461 Ro D. 410 Ro P. 410 Robbins J.M. 583 Robbins J.R. 582 Robia S.L. 481 Robins A.L. 615 Robitaille L. 572 Rosal M.C. 451 Rosdahl H. 609 Rosenbloom C.A. 599 Ross B. 447 Rossi M. 472 Rothman D. 569 Rousselle L. 438 Rousselot M. 542 Royackers L. 390 Royal D. 416 Ruch S. 459 Rudaya A.Y. 582, 583

Saba O.I. 520 Sabuncuoğlu H. 375 Sackner M.A. 611 Sahlin K. 464 Saijonmaa O. 487 Saito O. 552 Sammler D. 446 Samson N. 533 Samways D.S.K. 332

Rudnicki R. 512

Ruparel K. 378

Russ D.W. 569

Ruiz O. 416

Sanchez D. 452 Sander K. 444 Sandgaard N.C.F. 555 Sano H. 325 Santoro A. 610 Sáry G. 416 Sato M.A. 507 Saunders R.C. 399, 400 Sawchuk M.A. 359 Sawka M.N. 633 Schafferhofer-Steltzer I. 458 Schaller G. 490 Scheich H. 444 Schieber M.H. 461 Schipke J.D. 616 Schneider M.F. 465 Schofield G. 639 Schou M. 556

Schrage W.G. 626 Schroeder B.W. 437 Sclafani A. 436 Scott K. 415 Secher N.H. 373 Seifert J.G. 600 Seko A. 532 Selman C. 579 Semple S.J. 530 Seol G.H. 570 Shah J.P. 470 Shakarad M. 578 Shakil S.S. 433 Sharkey C.M. 380 Sharp L. 489 Sheehan K. 637 Shen T. 465 Sherman S.M. 342 Shi W.-X. 424 Shimada T. 563 Shine R. 560 Shinnick-Gallagher P. 437 Shinohara M. 624

Shoemaker J.K. 623

Shore D.I. 354

Shpak B. 456

Siami K. 499

Silvetti M. 412 Simic N. 354 Simon B.A. 522 Sinex D.G. 403 Siu P.M. 469 Skovgaard N. 514 Slater G.J. 596 Smith D.F. 484 Smith P.F. 389 Smith S.L. 345 Snyder E.M. 634 Sobel N. 414 Sobkiw C.L. 613 Song C.K. 426 Soodvilai S. 544 Spence C. 352, 353, 356 St.Hilaire M. 533 Stanford T.R. 393 Stanley C.M. 439 Stein A.B. 503

Stein B.E. 395 Steiner A.A. 582, 583 Steinman A.M. 589 Sterling H. 545 Stewart J.M. 482 Stowe Z.N. 339 Stricker E.M. 588 Strutton P.H. 455 Stubbe J. 539

Su H. 369

Su T. 551 Subramani S. 510 Sucharita S. 477 Sumiya J.-I. 532 Sumual S. 550 Suvorava T. 478 Suzuki H. 331 Swadlow H.A. 341 Swietlicki E.A. 568 Szyszka P. 401

Tachibana A. 423 Taegtmeyer H. 504 Takahashi M. 563 Takahashi T. 450 Takakura A.C.T. 507 Takeuchi K. 498 Tan Y. 344 Tanaka T. 548 Tang Z. 339 Tansy A.P. 439 Tarbell J.M. 491 Tardif E. 396 Tay C. 601 Tchaicheeyan O. 495 Tewolde T. 360 Thakor A.S. 479 Theuvenet P.J. 385 Thiagarajan R. 360 Thomson S. 530 Timofeeva E. 388 Toosy A.T. 343 Torres-Sanchez C.J. 571 Touzani K. 436 Trainor L.J. 447 Trinkaus M. 599 Tschopp M. 604 Turalska M. 505 Tzelepis G.E. 523

Ugur H.C. 511 Uhrenholt T.R. 539 Umeyama S. 379 Urban W. 512

Van Cappellen W. 558 Van Den Thillart G.E.E.J.M. Van Der Leij F.R. 509 Van Der Meer D.L.M. 517 Van Dijk B.W. 385 Van Dijk T.H. 567 Van Hooser S.D. 404 Varona P. 427 Vaz M. 477 Vazquez G. 334 Velenovsky D.S. 403 Velic A. 475 Vidmar G. 524 Vieira Silva H.M. 606 Vilim F.S. 368 Voelcker-Rehage C. 418

Wakabayashi K. 501 Walker J.W. 481 Wall C. 639 Walsh V. 407 Wan K.F. 323 Wang H. 337, 547 Wang T. 514 Wang W. 536 Wang X. 551 Wang Y. 568 Warren C.M. 496 Wasaka T. 421, 457

Zhang W. 515, 606 Zhang Y. 425 Zhou J. 346 Zhou T. 527 Zhou Y. 557 Zhu P. 326 Zhuang J. 527 Zhurov Y. 422 Ziani K. 480 Zidi-Yahiaoui N. 324 Ziegler P.J. 601 Zinn C. 639 Zonis S. 329 Zvyagintsev M. 377 Young J.M. 381 Young M.E. 504 Young W.B. 638 Yu B. 531 Yue C. 369 Yun J. 333 Wolzt M. 490 Wong R.O.L. 382 Watsford M.L. 635 Watson R.T. 566 Wei Y. 545 Welsch T. 549 Wong W. 391 Wouters J. 390 Wright S.H. 544 Welsch T. 549
Westerkamp L.M. 627
White C.R. 499
Whiteside C. 547
Whyte G.P. 636
Wickens J.R. 434
Wieckhorst W. 335
Wilhelm J. 360
Wilkins B.W. 626
Williams L.M. 376
Williams P. 625
Wilson T.A. 529
Wite F. 517
Wittfoth M. 446
Wolber T. 612 Wu W.-J. 503 Xia Z. 493 Zador A.M. 383 Zador A.M. 383 Zakynthinos S. 523 Zampini M. 353, 356 Zangla D. 610 Zelano C. 414 Zhang C.-Y. 551 Zhang G. 543 Zhang H. 559 Zhang K. 559 Zhang L. 471 Zhang P. 607 Xiao C. 581 Xu F. 527 Xu L. 531 Yamashita K. 532 Yamashita N. 344 Zvyagintsev M. 377 Zwetsloot K.A. 627 Yamazaki Y. 563 Yanes L.L. 534 Yi F.-X. 543 Yoder A.D. 344